Universidade de Aveiro
2011

Departamento de Engenharia Cerâmica e do Vidro

Rejini Rajamma

Incorporação de cinzas volantes de biomassa em materiais cimentíceos
Biomass fly ash incorporation in cement based materials

Universidade de Aveiro
2011

Departamento de Engenharia Cerâmica e do Vidro

Rejini Rajamma

Incorporação de cinzas volantes de biomassa em materiais cimentíceos

Tese submetida à Universidade de Aveiro para cumprimento dos requisitos necessários à obtenção do grau de Doutor em Ciência e Engenharia de Materiais, realizada sob a orientação científica do Prof. Doutor Victor Miguel Carneiro de Sousa Ferreira, Professor Associado do Departamento de Engenharia Civil da Universidade de Aveiro e a co-orientação do Prof. Doutor João António Labrincha Batista, Professor Associado com Agregação do Departamento de Engenharia Cerâmica e do Vidro da Universidade de Aveiro.

texto Apoio financeiro da FCT e do FSE no âmbito do III Quadro Comunitário de Apoio.

Universidade de Aveiro
2011

Departamento de Engenharia Cerâmica e do Vidro

Rejini Rajamma

Biomass fly ash incorporation in cement based materials

Thesis submitted to University of Aveiro in partial fulfillment of the requirements for obtaining the degree of Doctor of Philosophy in Materials Science Engineering, held under the scientific guidance of Prof. Dr. Victor Miguel Carneiro de Sousa Ferreira, Associate Professor, of Department of Civil Engineering, University of Aveiro and the co-supervision of Prof. Dr. João António Labrincha Batista, Associate Professor with Aggregation Department of Ceramics and Glass Engineering, University of Aveiro

texto Apoio financeiro da FCT e do FSE no âmbito do III Quadro Comunitário de Apoio.

Dedicated to the people of Portugal

o júri

presidente

Doutora Nilza Maria Vilhena Nunes da Costa
Professora Catedrática da Universidade de Aveiro

Doutor Jorge Manuel Caliço Lopes de Brito
Professor Catedrático da Universidade Técnica de Lisboa

Doutor João António Labrincha Batista
Professor Associado com Agregação da Universidade de Aveiro

Doutor Victor Miguel Carneiro de Sousa Ferreira
Professor Associado da Universidade de Aveiro

Doutor Luís António da Cruz Tarelho
Professor Auxiliar da Universidade de Aveiro

Doutora Maria Cãndida Lobo Guerra Vilarinho
Professora Auxiliar da Universidade do Minho

Doutor António Manuel dos Santos Silva
Investigador Auxiliar do Laboratório Nacional de Engenharia Civil

Acknowledgements

First of all I thank my creator for providing me strength to endure and to hope for the good always.

I would like to thank my supervisors, Prof. Victor M. Ferreira and Prof. João A. Labrincha for guiding me throughout the research and in writing the thesis. I thank for their valuable supports in making this thesis.

I use this occasion to thank Foundation of Science and Technology (FCT), Portugal for providing me a PhD grant (SRFH/BD/32500/2006) with which it was possible to do this work.

It is acknowledged the financial support from Fundação para a Ciência e a Tecnologia (FCT), Portugal, through the project with reference PTDC/AAC-AMB/098112/2008 (Bias-to-soil - Biomass ash: Characteristics in relation to its origin, treatment and application to soil.).

I express my sincere gratitude to Prof. Luís Tarelho, Dept of Environmental Engineering, UA for giving valuable support in the collection and characterisation of biomass fly ashes.

I acknowledge and am greatly thankful for the support provided by Dr. A. Santos Silva, Materials Department, LNEC, Lisbon in doing the internal expansion tests in the mortar and concretes.

I would also thank Prof Geoffrey Allen and Dr. Richard Ball, IAC Bristol, UK for their assistance in this work especially by helping with the Environmental scanning electron microscopy.

Sincere thanks to Regina M. and Dora S. who helped me in an extensive way during the work.

Much thanks to Prof. Ribeiro M. (Polytechnic Institute, Viana do Castelo), Luis P., Luciano S., Lina M., Sofia S., Ana C., Teresa E. and all those technicians and researchers in the Dept. of Civil Engineering, Dept. of Ceramics and Glass Engineering, Interface Analysis centre (IAC) Bristol, and National Laboratory of Civil Engineering (LNEC), Lisbon who helped me directly and indirectly in doing this work. I express my sincere gratitude to all including those whose names are not mentioned here but have helped me in one way or the other in making this thesis possible.

And I thank my beloved family who always gives me all courage and support by standing with me both in my ups and downs.

palavras-chave

cinzas volantes de biomassa; resíduos; reciclagem; cimentos, betões e argamassas

resumo

Recentemente, as pressões ao nível da segurança, do ambiente e da energia conduziram a uma procura crescente de fontes de energia renováveis, e à diversificação das fontes de energia da Europa. Entre estes recursos a biomassa pode ter um papel importante, uma vez que é considerada como um recurso renovável e neutra em termos de CO2 pois a taxa do consumo é mais baixa do que a taxa de crescimento e pode potencialmente fornecer energia para calor, eletricidade e transportes a partir da mesma instalação. Atualmente, a maioria da cinza de biomassa produzida em unidades industriais é disposta em aterro ou reciclada na floresta ou na agricultura e, na maioria das vezes, isto sucede sem grande controlo. Contudo, considerando que o custo da eliminação de cinzas de biomassa vem crescendo, e que os volumes da cinza de biomassa estão a aumentar, uma gestão sustentável das cinzas tem de ser implementada.

O objetivo principal deste trabalho é o estudo do efeito de cinzas volantes de biomassa em argamassas e betões com base em cimento de modo a serem usadas como um material cimentíceo suplementar. Os resíduos analisados no estudo foram colhidos de caldeiras de leito fluidizado e caldeiras de grelha disponíveis em unidades de produção elétrica e em unidades industriais de produção de pasta e papel em Portugal. As caracterizações físicas e químicas das cinzas volantes de biomassa foram efetuadas. O cimento foi substituído pelas cinzas de biomassa a fim de investigar o efeito nas propriedades no estado fresco bem com nas propriedades no estado endurecido de formulações de argamassa e betão. Reações expansivas tais como a reação alcali-sílica (ASR) e as reações sulfáticas (externas e internas) foram estudadas a fim verificar a durabilidade das argamassas e betões de cimento contendo cinzas volantes de biomassa. As aplicações alternativas tais como a incorporação de cinzas em argamassas de cal e a ativação alcalina foram também estudadas.

As partículas da cinza de biomassa eram irregulares na forma e finas. A caracterização química revelou que as cinzas eram similares a uma cinza volante da classe C. Os resultados em argamassas mostraram viabilidade para o uso de cinzas de biomassa como materiais cimentíceos suplementares em teores baixos (<20%). A trabalhabilidade, o conteúdo orgânico, o teor de alcalinos, cloretos e sulfatos são razões para impedir maiores incorporações de cinza de biomassa nas argamassas de cimento. Os resultados dos testes da durabilidade mostraram uma redução na expansão para argamassas e betões contendo cinzas de biomassa especialmente quando se misturou cinzas (20%) com metacaulino (10%). A incorporação da cinza de biomassa em argamassas de cal não melhorou as propriedades significativamente embora a carbonatação fosse maior quando da incorporação de 15 ou 20%. A mistura do metacaulino com a cinza de biomassa funcionou bem na aplicação envolvendo a ativação alcalina. Ligantes sem cimento Portland com resistência à compressão de 30-40 MPa foram obtidas pela ativação alcalina das cinzas de biomassa (60-80%) misturadas com o metacaulino (20-40%).

keywords biomass fly ashes, wastes, recycling, cement, mortar and concrete

abstract

In recent years, pressures on global environment and energy security have led to an increasing demand on renewable energy sources, and diversification of Europe's energy supply. Among these resources the biomass could exert an important role, since it is considered a renewable and CO_2 neutral energy resource once the consumption rate is lower than the growth rate, and can potentially provide energy for heat, power and transports from the same installation. Currently, most of the biomass ash produced in industrial plants is either disposed of in landfill or recycled on agricultural fields or forest, and most times this goes on without any form of control. However, considering that the disposal cost of biomass ashes are raising, and that biomass ash volumes are increasing worldwide, a sustainable ash management has to be established.

The main objective of the present study is the effect of biomass fly ashes in cement mortars and concretes in order to be used as a supplementary cementitious material. The wastes analyzed in the study were collected from the fluidized bed boilers and grate boilers available in the thermal power plants and paper pulp plants situated in Portugal. The physical as well as chemical characterisations of the biomass fly ashes were investigated. The cement was replaced by the biomass fly ashes in 10, 20 and 30% (weight %) in order to investigate the fresh properties as well as the hardened properties of biomass fly ash incorporated cement mortar and concrete formulations. Expansion reactions such as alkali silica reaction (ASR), sulphate attack (external and internal) were conducted in order to check the durability of the biomass fly ash incorporated cement mortars and concretes. Alternative applications such as incorporation in lime mortars and alkali activation of the biomass fly ashes were also attempted.

The biomass fly ash particles were irregular in shape and fine in nature. The chemical characterization revealed that the biomass fly ashes were similar to a class C fly ash. The mortar results showed a good scope for biomass fly ashes as supplementary cementitious materials in lower dosages (<20%). The poor workability, concerns about the organic content, alkalis, chlorides and sulphates stand as the reasons for preventing the use of biomass fly ash in high content in the cement mortars. The results obtained from the durability tests have shown a clear reduction in expansion for the biomass fly ash mortars/concretes and the binder blend made with biomass fly ash (20%) and metakaolin (10%) inhibited the ASR reaction effectively. The biomass fly ash incorporation in lime mortars did not improve the mortar properties significantly though the carbonation was enhanced in the 15-20% incorporation. The biomass fly ash metakaolin blend worked well in the alkali activated complex binder application also. Portland cement free binders (with 30-40 MPa compressive strength) were obtained on the alkali activation of biomass fly ashes (60-80%) blended with metakaolin (20-40%).

CONTENTS

CHAPTER 5. DURABILITY: EXPANSIVE REACTIONS: ALKALI SILICA REACTIONS AND SULPHATE REACTIONS 164

TABLES

FIGURES

CHAPTER 1. INTRODUCTION

1.1. Cement industry and the current environmental issues

In booming economies from Asia to Eastern Europe, cement is literally the glue of progress. Despite the effects of the global crisis and a poor economic growth, the graph of world cement production is ever increasing especially in developing countries. But making cement means making pollution, in the form of carbon dioxide emissions. Cement plants account for around 5% of global emissions of carbon dioxide, the main cause of global warming [source:-WBCSD 2005] [Figure 1.1].

Table 1 shows the Portland cement production till the year of 2010 in million tonnes [Hardjito, 2007]. The continued growth of key world economies results in an increasing demand for construction materials. As a consequence, the global production of cement in 2030 is projected to grow to a level roughly five times higher than its level in 1995, with close to 5 billion tonnes worldwide [OECD/IEA 2003]. This has a significant impact on the overall level of anthropogenic greenhouse gas (GHG) emissions. Currently the production of one ton of cement commonly results in the release of 0.65 to 0.95 tonnes of CO_2 depending on the efficiency of the process, the fuels used, and the specific type of cement product. As a consequence, the emissions of the global cement sector alone are very likely to surpass the total amount of CO_2 emissions of the EU before 2030 [source: Nicolas et al. 2007].

This is particularly visible in emerging economies. The global cement industry is facing the challenge to sustain its business while decreasing its carbon intensity, from production processes, fuel uses and its product end use. Energy production using traditional fossil fuel sources is the major factor responsible for climatic global changes, through emission of greenhouse gases and global warming of this planet. Science tells that the world must reduce its emissions of greenhouse gases by at least 80% below 1990 levels by 2050 [source:-Nicolas et al. 2007].

Carbon dioxide emissions from a cement plant are divided into two source categories: combustion and calcinations. Combustion accounts for approximately 40% and calcinations 60% of the total CO_2 emissions from a cement manufacturing facility.

Table 1.1. Regional and world cement production to year 2010 (in million tonnes) (Hardjito 2007)

	1995	*2000*	*2005*	*2010*	*% of total 1995*	*% of total 2010*
European Union	168.1	187.9	194.1	189.3	12.1	9.7
Other Europe	65.8	80.0	90.2	94.7	4.7	4.9
Former Soviet Union	58.1	80.3	110.1	128.2	4.2	6.6
North America	92.9	94.9	94.8	94.7	6.6	4.9
C/S America	89.4	106.6	127.4	145.0	6.4	7.5
Africa	64.8	74.3	80.7	85.5	4.6	4.4
Middle East	63.5	75.6	76.9	73.4	4.6	3.8
East Asia	623.4	732.7	798.8	844.3	44.6	43.4
S/SE Asia	161.2	219.1	255.0	279.2	11.6	14.4
Oceania	8.0	10.6	11.1	11.8	0.6	0.6
World totals	1396.1	1662.1	1839.1	1946.1	100.0	100.0

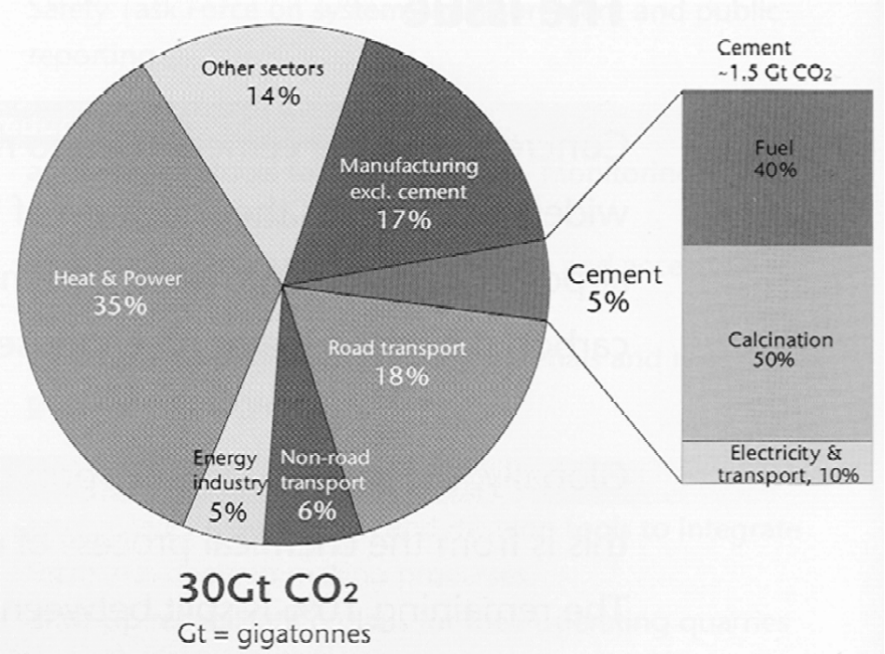

Figure 1.1. Global CO_2 production *(Source:*. WBCSD 2005*)*

This is the basic problem the cement production faces in reducing the CO_2 emission as it is the chemical reaction that creates it that releases large amounts of carbon dioxide. The remainder is

produced from the fuels used in production, although those emissions may be mitigated with the use of greener technology.

The chemical composition of a typical Portland cement clinker is almost entirely just four oxides: calcium oxide or lime (CaO), about 65%; silica (SiO_2), about 22%; alumina (Al_2O_3), about 6%; and iron oxide (Fe_2O_3), about 3%. In cement industry shorthand, these four oxides are written in as C, S, A, and F, respectively, and most clinkers do not show deviations in these oxide proportions of more than 2 to 4 percentage points. The remaining 4% or so of the clinker composition is divided among oxides of magnesium, potassium, sodium, sulphur, and others. Clinker is primarily made up of four clinker minerals, denoted in shorthand as tricalcium silicate; $(CaO)_3\ SiO_2$ or C_3S, dicalcium silicate ;$(CaO)_2\ SiO_2$ or C_2S, tricalcium aluminate; $(CaO)_3Al_2O_3$ or C_3A, and tetracalcium aluminoferrite $(CaO)_4Al_2O_3Fe_2O_3$ or C_4AF. The C_3S and C_2S are the main contributors to the performance of Portland cement and together make up about 70% to 80% of the weight of the clinker. During their hydration, C_3S and C_2S combine with water by similar reaction paths to form calcium silicate hydrate (its variable composition is denoted as "C-S-H") plus calcium hydroxide $(CaOH)_2$; the C-S-H is a colloidal gel that is the actual binding agent in the concrete. The bulk of the C_3S hydrates rapidly (hours to days) and provides most of the early strength of the concrete, whereas the C_2S hydrates slowly (days to weeks) and is responsible for most of the concrete's long-term strength. The lime by-product of hydration activates any pozzolans that may be present in the concrete mix. The manufacture of clinker involves the thermo chemical processing of large quantities of limestone and other raw materials, typically about 1.7 t/t clinker, and requires enormous kilns and related equipment, sustained very high kiln temperatures (the materials reach temperatures of about 1450ºC in order to form the key C_3S mineral), and the consumption of large amounts of energy (fuels and electricity). Clinker manufacture results in significant emissions, particularly of carbon dioxide (CO_2).

Considering the scale of the worldwide cement production, even a slight decrease in the average global emissions per ton has a large CO_2 reduction potential. Every 10% decrease in the cement CO_2 intensity by 2050 could save around 0.4 Gt CO_2, and substantially contribute to slowing climate change. But the cement industry´s problems are not stopped with the global warming effect; it also makes drastic consequences in the natural raw materials availability. And also because as cement requires so many raw materials such as rock, sand and water, the consumption of energy required to mine the rock and sand as well as transport the material to the factory is high. Transporting and using these resources can also put a strain on the earth.

The clear need of reducing the CO_2 emission in the present world climate situations and conservation of the non-renewable natural resources of raw materials has led to the research on finding effective solutions, among which two of them are significant in the present work of the thesis. They are,

1. **Increasing the share of biomass in the combustion process in the cement kiln as well as in other industries where the energy is produced by fuel combustion.**

Natural fuels like coal are not neutral whereas biomass is considered as a renewable and CO_2 neutral energy resource, once when the consumption rate is lower than the growth rate, and can potentially provide energy for heat, power and transports from the same installation. It would require a long term sustainable supply chain for biomass fuels originating from forestry, biological wastes or crops.

2. Expanding the use of additives (chemical and materials added to cement slurry to modify the characteristics) and substitutes to cement.

Conventional and advanced alternatives to Portland cement can lead to substantial CO_2 reductions ranging from 20 to 80% depending on the case. Until now, the use of additives and substitutes to Ordinary Portland Cement (OPC) clinker has been one of the most successful measures in decreasing the specific CO_2 emissions from making cements. A long term clinker ratio as low as 0.75 is desirable. Such a target is still challenging since the availability of additives will not necessarily grow at the same rate as the cement demand. The alternative materials are selected on a supplementary basis to make up for chemical deficiencies of the primary limestone feed. These supplementary materials may, replace nearly all of the alumina or silica, or they may be added as "sweeteners" to boost one oxide or another. Examples of sweeteners include high-purity limestone, or calcite itself, to boost the lime content; silica sand, silica fume, or diatomite to boost silica; alumina or aluminium dross to supply alumina; or mill scale for iron. Apart from the oxide content of a proposed alternative material, plant operators consider the material's thermochemical accessibility [Mishulovich 2003]. For example, silica sand is a commonly used supplementary silica source, yet it is hard to grind (thus increasing electricity consumption) and the component quartz (SiO_2) requires high temperatures and a long exposure in the kiln to activate the silica. If available, a more easily grindable and/or more reactive silica source might be preferable; examples include diatomite, ferrous slag, or a material containing amorphous silica, such as coal fly ash. Although many of the supplementary materials are mined products, any number of other materials, including wastes, are potentially suitable, especially if they are of low cost. Some materials contribute both oxides and energy, for example, deinking sludge from recycling and shredder fines from paper plants. Some of these materials offer process advantages; for example, certain

aluminium smelter by-products (pot liners, catalysts) not only contribute alumina, but also sufficient fluorine or calcium fluoride to act as a flux [Mishulovich 2003]. Fly ash and bottom ash from coal power plants, as well as ferrous slags, are consumed in large quantities as supplementary silica, alumina, and lime sources for clinker. Noncarbonated lime sources are of particular interest in an environmental context because they reduce the calcinations CO_2 component of the process; this is discussed in more detail later. The criteria for selecting waste materials for the kiln include appropriate chemistry (composition and reactivity), resulting cement quality, material availability, material costs (base, transportation, storage, handling, and preparation, regulatory compliance and general environmental, and public and government acceptance.

1.2. Objective and scope of the work

The present study has been conducted in the framework of a Portuguese research project (PTDC/AAC-AMB/098112/2008 (Bias-to-soil - Biomass ash: Characteristics in relation to its origin, treatment and application to soil) aiming at widening the knowledge of the use of biomass fly ash wastes in cement formulations.

The solid biomass combustion is a proven technology for heat and power production, where the technologies of fluidised bed and grate combustion are mainly used [Loo and Koppejan 2003, Yin et al. 2008]. One of the problems associated to biomass combustion is related with the ash, in the thermal conversion process itself (for example, slagging and fouling phenomena), and also its environmental management.

Bio fuels represent an area of diversification in the supply of fuel to the transport sector which has recorded the highest growth rates in terms of energy consumption. In Portugal, the transport sector's energy dependency on oil, which is responsible for 42% of total imported oil consumption, is very high. The replacement of more than 300 million litres of fuel by 2010, comprising the incorporation of 10% in road fuels, bringing the EU's objective forward by 10 years, promotes the creation of industrial plants and development of energy based agriculture. The government set the quantity of bio fuels to be exempted from ISP (tax on oil products) at 205000 tonnes in 2007. Of this amount, 4973 tonnes derive from national agricultural production. However, this figure should rise to 405000 tonnes by 2010 in light of the forecast increase of the incorporation percentage. The fiscal exemptions (ISP) have been designed to promote the use of bio fuels in the transport sector, to reduce Portuguese energy dependency and comply with the community directive establishing the replacement of 10% of conventional fuels used in the transport sector, by alternative fuels by 2020.

Small dedicated producers are entitled to total exemption from ISP up to a maximum global amount of 40 thousand tonnes per year.

Currently, most of the biomass ash produced in thermal power plants is either disposed of in landfill or recycled on agricultural fields or forest, and most times this goes on without any form of control. However, considering that the disposal cost of biomass ashes are raising, and that biomass ash volumes are increasing worldwide, a sustainable ash management has to be established. Besides, for a sustainable biomass to energy strategy it is essential to close the material fluxes and to integrate the biomass ashes within the natural cycles [Obernberger et al. 1997, Loo and Koppejan 2003].

The wastes analyzed in the study are collected from the fluidized bed boilers and grate boilers available in the thermal power plants and paper pulp plants situated in Portugal. An attempt was made to answer the following questions in explaining the various possibilities of the use of these wastes in the cement industry.

1. The effect and limitations of the use of biomass fly ashes in terms of cement quality and durability.
2. The benefits in the sector and country environmentally and economically by the use of biomass fly ashes.

The second chapter is a literature review of the various fine ash waste materials used in the construction and about the biomass combustion in Portugal. The current energy situation in Portugal is discussed along with the emerging possibility of the use of biomass as a renewable energy source in industrial plants in Portugal. It is preceded by the research done so far on the use of various industrial waste ashes as additives in cement. The survey on the industrial byproducts includes coal fly ashes and the biomass ashes such as the municipal solid waste (MSW), rice husk ash, bagass ash (RHA), and wood ash (forest residues), which is the focus of the present work.

The third chapter details the characterizations techniques and methods used to analyze the biomass fly ash samples. The physical as well as chemical characterisation of the biomass fly ashes were investigated. For the convenience of a detailed investigation, two types of biomass fly ashes available in Portugal were used based on the combustion processes that influence the chemical nature of the biomass fly ashes. These ashes were the representatives of biomass fly ash collected from 1) a grate furnace and 2) a fluidised bed furnace.

The fourth chapter is mainly concentrated on the effect of biomass fly ashes in the cement mortars. An evaluation of the potential of biomass fly ashes as a substitute for the ordinary Portland cement in mortar applications is carried out. The behaviour of biomass fly ash incorporated cement mortars were discussed in terms of impact on fresh as well as on the hardened properties. Cement pastes and cement mortars were prepared by replacing an ordinary Portland cement -Type I 42.5 R, by different amounts of biomass fly ashes (10%, 20% and 30% by weight of cement) in dry conditions. The fresh properties of the mortars were investigated using various methods such as flow table, initial and final setting by Vicat, and rheological studies. The hydration behavior and phase analysis were studied using quasi adiabatic calorimetry thermal analysis, X-Ray diffraction and impedance spectroscopy. The hardened properties were studied using strength measurements and porosimetry methods. The microstructure of the cement pastes were evaluated using electron microscopy. The overall performance of biomass fly ash incorporated cement pastes and mortars for a duration of two years was evaluated and a discussion on the potential use of biomass fly ashes in the replacement of cement was carried out.

The fifth chapter addresses the potential role of biomass fly ash in controlling the durability of concretes containing biomass fly ashes against expansive reactions. Alkali Silica Reaction (ASR), External Sulphate Reaction (ESR) and Internal Sulphate Reaction (ISR) tests were conducted in the biomass incorporated mortar and/or concretes. The influence of biomass fly ash in mortars as well as concrete specimens to mitigate ASR was determined. Accelerated mortar-bar tests were conducted according to ASTM C 1260/ASTM C 1567 to evaluate the behaviour of the biomass fly ash in the ASR inhibition mechanism. The concrete prism expansion tests according the RILEM AAR-3 and RILEM AAR-4 methods were also performed on selected composition to confirm the response of biomass fly ash in mortar-bar tests. The microstructures of the specimens were investigated by SEM/EDS analysis. The expansion rates and microstructures observed were compared with control specimens. The ESR tests were conducted in mortars soaked in a mixture solution of 5% sodium sulphate and 5% magnesium sulphate. The expansion and strength of mortars at different curing period upto one year were compared with that of the reference mortar. ISR reaction test was carried out on a selected composition of biomass fly ash incorporated concrete. The ISR occurring due to the delayed ettringite formation (DEF) was analyzed. The experimental procedure was in accordance to the French concrete performance test- MLPC No. 66 test method, for DEF accelerated concrete performance.

The sixth chapter is about other potential application of biomass fly ashes. The alkali solution activated biomass fly ash as an alternative for geopolymers production is studied. The influence of biomass fly ashes in the strength development of lime mortars was also investigated. The possibilities of the use of biomass fly ash in other industrial applications based on its physical chemical characterisation werare discussed to propose the future of biomass fly ash wastes in the industry.

The seventh chapter starts with the conclusions including the major findings in the research and the fure work. This investigation also provides a comprehensive database of biomass fly ash impacts on concrete applications.

CHAPTER 2 A LITERATURE REVIEW

2.1. Introduction

Considerable research is being conducted worldwide on the use of waste materials in order to avert an increasing toxic threat to the environment, or to streamline present waste disposal techniques by making them more affordable. It follows that an economically viable solution to this problem should include utilization of waste materials for new products rather than land disposal. The pozzolanic and hydraulic properties of the industrial waste ashes obtained by combustion processes make them useful for the manufacture of cement, building materials concrete and concrete-admixed products. This chapter will review the characteristics of industrial fine ash wastes such as coal fly ash, various biomass ashes such as municipal solid waste ash (MSW), sugar cane bagasse ash, rice husk ash (RHA), palm oil fuel ash, wood fly ash, their application in cement industry as cement replacement materials and the significance of biomass fly ashes in the current energy and environmental framework in Portugal.

2.2. Coal fly ash

Since wide scale coal firing for power generation began in the 1920s, many millions of tons of ash and related by-products have been generated. The worldwide production of coal fly ash in the early 21st century was between 480 Mt [Feuerborn et al. 2009] and 660 Mt [Malhotra et al. 1999]. Thus, the amount of coal waste (fly ash), released by factories and thermal power plants [Figure 2.1] has been increasing throughout the world, and the disposal of the large amount of fly ash has become a serious environmental problem. The present day utilization of ash on worldwide basis varied widely from a minimum of 3% to a maximum of 57%, yet the world average only amounts to 16% of the total ash [Joshi et al. 1997]. Fly ash can be considered as the world's fifth largest raw material resource [Mukherjee et al. 2008]. A substantial amount of ash is still disposed of in landfills and/or lagoons at a significant cost to the utilizing companies and thus to the consumers.

Worldwide, coal-fired power generation presently accounts for roughly 38% of total electricity production [OECD/IEA publications 2003]. While coal use in some of the more developed countries remains static or is in decline, significant increases in coal-fired generation capacity are taking place in many of the developing nations and large capacity increases are planned. As a consequence of the extensive investments being made in many parts of the world, and because coal

resources are far more abundant than other fossil fuel resources, and also because power plants having a long working life, coal will remain an important source of energy for many years.

During coal-fired electric power generation three types of coal combustion by-products (CCBs) are obtained. These by-products can be classified according to the zone where it is recovered from. Thus two kinds of ashes are distinguished: fly ash and bottom ash.

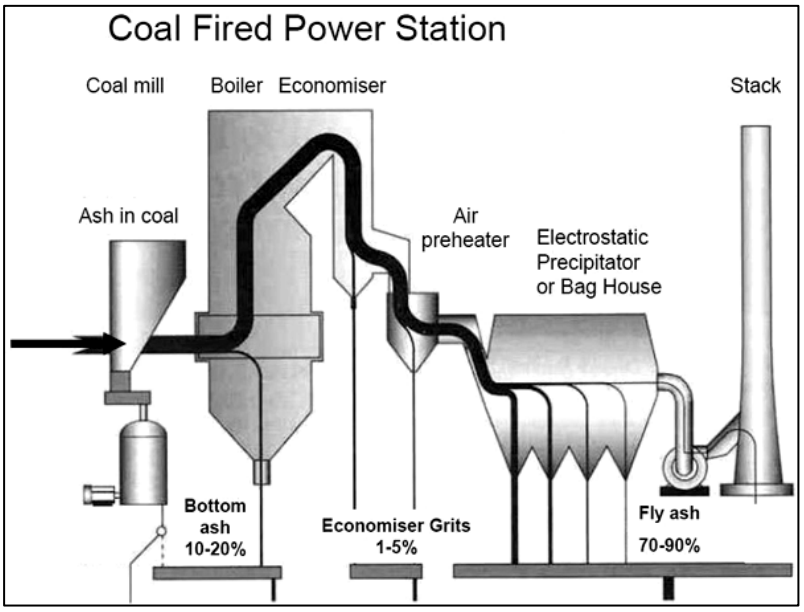

Figure 2.1. Illustration of fly ash generation in coal fired thermal power plant(Source www.flyashaustralia.com.au/WhatIsFlyash.aspx).

About 80% of the ash is entrained in the gas flow and it is captured and recovered as fly ash. The remaining 20% ash is the bottom ash and the economiser grits which are collected in a hopper at the bottom of the furnace. Utilization of all power plant wastes in construction industry in large quantities seems to be a reasonable solution for these environmental and economic problems. One of the main areas to utilize power plant wastes is manufacturing building materials [Ahmaruzzaman 2010].

2.2.1. Physical properties

Coal fly ash consists of inorganic matter present in the coal that has been fused during coal combustion. This material is solidified while suspended in the exhaust gases and is collected from the exhaust gases by electrostatic precipitators. Since the particles solidify while suspended in the exhaust gases, fly ash particles are generally spherical in shape either solid or hollow, and mostly

glassy (amorphous) in nature [Feuerborn et al. 2009]. The carbonaceous material in the fly ash is composed of angular particles. Fly ash particles that are collected in electrostatic precipitators are usually silt size (0.074 - 0.005mm). Although sub-bituminous coal fly ash is also silt-sized, it is generally slightly coarser than bituminous coal fly ash. The specific gravity of fly ash usually ranges from 2.1 to 3.0, while its specific surface area may vary from 170 to 1000 m^2/kg [Ahmaruzzaman 2010]. The colour of fly ash can vary from tan to gray to black, depending on the amount of unburned carbon in the ash.

2.2.2. Chemical properties

The properties of fly ash are influenced to a great extent by the properties of the coal being burned and the techniques used for handling and storage. There are basically four types, or ranks, of coal, each vary in heating value, chemical composition, ash content, and geological origin. The four types (ranks) of coal are anthracite, bituminous, sub-bituminous and lignite. In addition to being handled in a dry, conditioned, or wet form, fly ash is also sometimes classified according to the type of coal from which the ash was derived. Bituminous coal is the most common coal and is used for generating electricity, making coke, and space heating. The principal components of bituminous coal fly ash are silica, alumina, iron oxide, and calcium, with varying amounts of carbon, as measured by the loss on ignition (LOI). Lignite is more like soil than a rock and tends to disintegrate when exposed to the weather. Sub-bituminous coal is used for generating electricity and space heating. Lignite and sub-bituminous coal fly ashes were characterized by higher concentrations of calcium and magnesium oxide and reduced percentages of silica and iron oxide, as well as lower carbon content, compared with bituminous coal fly ash. Often referred to as hard coal, anthracite is hard, black and lustrous. Anthracite is low in sulphur and high in carbon. It is the highest rank of coal. Very little anthracite coal is burned in utility boilers, so there are only small amounts of anthracite coal fly ash. Table 2.1 compares the normal range of the chemical constituents of bituminous coal fly ash with those of lignite coal fly ash and sub-bituminous coal fly ash.

Table 2.1. Normal range of chemical composition for fly ash produce from different coal types (expressed as percent by weight) (*Source: HRC, US DOT)*

Component	*Bituminous*	*Sub bituminous*	*Lignite*
SiO_2	20-60	40-60	15-45
Al_2O_3	5-35	20-30	10-25
Fe_2O_3	10-40	4-10	4-15
CaO	1-12	5-30	15-40
MgO	0-5	1-6	3-10
SO_3	0-4	0-2	0-10
Na_2O	0-4	0-2	0-6
K_2O	0-3	0-4	0-4
LOI	0-15	0-3	0-5

From the table, it is evident that lignite and sub-bituminous coal fly ash has a higher calcium oxide content and lower loss on ignition than fly ash from bituminous coals. Lignite and sub-bituminous coal fly ash may have a higher concentration of sulphate compounds than bituminous coal fly ash. **Table 2.2** explains the current limit values of chemical compositions of the fly ash for construction purposes according to the American Society for Testing Materials (ASTM C 618) and European Standard 450 (EN 450).

Table 2.2. Current chemical requirements for fly ash classification ASTM C 618 and EN 450.(limit values).

Properties	*ASTM C 618*		*EN 450*
	Class F	Class C	
Silicon dioxide (SiO_2) plus aluminum oxide (Al_2O_3) plus iron oxide (Fe_2O_3), min, %	70.0	50.0	>70.0
Sulfur trioxide (SO_3), max, %	5.0	5.0	3.0
Moisture Content, max, %	3.0	3.0	-
Na_2O	1.5	1.5	< 5.0
Loss on ignition, max, %	6.0*	6.0	5.0

** The use of class F fly ash containing up to 12% loss of ignition may be approved by the user if acceptable performance results are available.*

Briefly, the high-calcium Class C fly ash is normally produced from the burning of low-rank coals (lignites or sub-bituminous coals) and have cementitious properties (self-hardening when reacted with water) and usually contains significant amount of calcium oxide (CaO) or lime [Cockrell et al. 1970]. This class of fly ash, in addition to having pozzolanic properties, also has some cementitious properties. On the other hand, the low-calcium Class F fly ash is commonly produced from the burning of higher-rank coals (bituminous coals or anthracites) that are pozzolanic in nature. This fly ash has siliceous or siliceous and aluminous material, which itself possesses little or no cementitious value but will, in finely divided form and in the presence of moisture, chemically

react with calcium hydroxide at ordinary temperature to form cementitious compound [Chu et al. 1993]. The chief difference between Class F and Class C fly ash is in the amount of calcium and the silica, alumina, and iron content in the ash. Color is one of the important physical properties of fly ash in terms of estimating the lime content qualitatively. It is suggested that lighter color indicate the presence of high calcium oxide and darker colors suggest high organic content [Cockrell et al. 1970].

In Class F fly ash, total calcium typically ranges from 1 to 12%, mostly in the form of calcium hydroxide, calcium sulphate, and glassy components, in combination with silica and alumina. In contrast, Class C fly ash may have reported calcium oxide contents as high as 30–40% (Table 2.3). Another difference between Class F and Class C is that the amounts of alkalis (combined sodium and potassium), and sulphates (SO_4), are generally higher in the Class C fly ash than in the Class F fly ash. The mineralogical composition of fly ash, which depends on the geological factors related to the formation and deposition of coal, its combustion conditions, can be established by X-ray diffraction (XRD) analysis. The dominant mineral phases in the fly ashes are quartz (SiO_2), kaolinite $Al_2Si_2O_5(OH)_4$, ilite $(K,H_3O)(Al,Mg,Fe)_2(Si,Al)_4O_{10}[(OH)_2,(H_2O)]$, and siderite ($FeCO_3$) [Stanislav et al. 2003]. The less predominant minerals in the unreacted coals include calcite ($CaCO_3$), pyrite (FeS_2) and hematite (Fe_2O_3). Quartz and mullite ($3Al_2O_3.2SiO_2$) are the major crystalline constituents of low-calcium ash, whereas high-calcium fly ash consists of quartz, Tricalcium aluminate (C_3A or $Ca_3Al_2O_4$), Tetra calcium aluminoferrite (C_4AF or$Ca_4Al_nFe_{2-n}O_7$) etc [Stanislav et al. 2003].

The several distinct end uses of fly ash differ considerably among themselves in the stringency of the properties required in the fly ash for its successful utilization. The success of fly ash in structural fill applications rests primarily on the ability of the material to be compacted to a reasonably strong layer of low unit weight. This is primarily a function of particle size distribution, and to some extent of the content of spherical particles. The chemical characteristics of fly ash are secondary, although the post compaction cementation provided by some high-calcium fly ash is likely to prove beneficial [Ahmaruzzaman, 2010]. With highway bases chemical considerations come into play, although not in an important way. Stabilization of some base courses (and stabilized sub grades) may rest on lime fly ash chemical reactions, i.e. the classical ‘‘pozzolanic’’ reaction, with lime. Low-calcium fly ash may be entirely satisfactory or even preferred, especially where sufficient time is available for these slow reactions to take place. The only real chemical requirement is that fly ash has a sufficient content of glass that eventually will react with added lime [Diamond, 1984]. Some road base applications of fly ash depend on the physical effects of fly

ash incorporation rather than its reaction with lime. The cement and concrete end-use areas are by far the most demanding of the fly ash in terms of adherence to strict criteria and requirements. However, the requirements differ considerably depending on the specific end use involved.

Table 2.3. Typical chemistry of the coal fly ashes in wt %, as per ASTM C 618 Standard.

Elements	*Class F*	*Class F*	*Class C*	*Class C*
	Low Fe	High Fe	High- Ca	Low- Ca
SiO_2	46-57	42-54	25-42	46-59
Al_2O_3	18-29	16.5-24	15-21	14-22
Fe_2O_3	**6-16**	**16-24**	5-10	5-13
CaO	1.8-5.5	1.3-3.8	**17-32**	**8-16**
MgO	0.7-2.1	0.3-1.2	4-12.5	3.2-4.9
K_2O	1.9-2.8	2.1-2.7	0.3-1.6	0.6-1.1
Na_2O	0.2-1.1	0.2-0.9	0.8-6.0	1.3-4.2
SO_3	0.4-2.9	0.5-1.8	0.4-5.0	0.4-2.5
LOI	0.6-4.8	1.2-5.0	0.1-1.0	0.1-2.3
TiO_2	1-2	1-1.5	<1	<1

Fly ash for use as a raw material in cement manufacture is sold and used primarily on the basis of its chemical composition, as expressed in the usual oxide convention. Such factors as glass content, the type of crystalline matter present, size distribution, etc., are relatively immaterial. Even high carbon content, which may be limiting in most other end uses, may actually be beneficial in cement raw material use, since it provides a definite (although modest) proportion of the fuel needed. Uniformity and chemical consistency from day to day and week to week is the prime necessity. Fly ash, as a blended cement component shares some of the requirements for both raw material and direct concrete admixture use [Diamond 1984]. Since such fly ash eventually is incorporated in concrete, its chemical and physical characteristics must be suitable for that purpose. However, since little or no adjustment can be provided at the concrete mixing stage, fly ash for use in blended cements must be of consistent and uniform chemical and physical characteristics, the consistency and predictability being as important as the numerical values of the various parameters involved. Since the blended cement manufacturer has little control over the concurrent use of chemical admixtures or of mixing and curing conditions, the fly ash used should be relatively insensitive to such variations. Especially to be considered here are rheological effects, strength development characteristics, and possibilities for developing efflorescence. The colour of the ash and its effect on the colour of the final concrete to be produced by the blended cement may also be of importance.

Because of the presence of cementitious compounds of calcium and a reactive glass, the high-calcium fly ash is also proposed suitable in Portland cement products [Oscar 1998]. Several studies are being conducted and review reports are published to better understand the complexities of alkali

aggregate reactivity and sulphate resistance with respect to fly ash in concrete [Bouzoubaâ et al. 2003, Detwiler 2002, Thomas 1996, Docter 2009, Oscar 1999, Wang et al. 2004].The availability of high-lime fly ash containing compounds found in cement has led to high-strength concretes produced by the addition of fly ash and plasticizers. High-strength and high-performance concrete can also be made with Class F fly ash. The ball bearing effect produced by the spherical fly ash particles has resulted in better pumpability of concrete and easier finishing with trowels and other tools [Oscar 1999]. The utilization of fly ash in concrete produces less permeability because of the spherical particles, and therefore improved packing, i.e. more dense paste and pozzolanic reaction. In mass concrete, with high-percentage replacement of cement with fly ash, there is a lower heat of hydration compared to straight Portland cement concrete, particularly when Class F fly ash is used. Class C fly ash may not lower the heat of hydration. Traditionally, with bituminous-type fly ash, 15–25% of the cement was replaced. The advent of cementitious, high-lime fly ash has permitted normal replacements of 25–40% and up to 75% for parking lots, driveways, and streets. A fly ash concrete mix, designed for equivalent performance to conventional concrete at normal ages, will generally gain strength more slowly at early ages. After about seven days, the rate of strength gain of fly ash concrete exceeds that of conventional concrete, enabling equivalence at the desired age. This higher rate of strength gain continues over time, enabling fly ash concrete to produce significantly higher ultimate strength than can be achieved with conventional concrete.

2.2.3. Hydration of fly ash cement

From the researches, it is known that the hydration of fly ash cement includes two processes:

1. Hydration of cement clinker and
2. The pozzolanic reaction between fly ash and $Ca(OH)_2$ which is released in the hydration of the cement clinker [Wang et al. 2004].

Formation of cementitious material by the reaction of $Ca(OH)_2$ with the pozzolans (Al_2O_3, SiO_2, Fe_2O_3) is known as pozzolanic reaction. The hydrated calcium silicate gel or calcium aluminate gel (cementitious material) can bind inert material together. For class C fly ash, the calcium oxide (lime) of the fly ash can react with the siliceous and aluminous materials (pozzolans) of the fly ash itself. Since the lime content of class F fly ash is relatively low, addition of lime is necessary for hydration reaction with the pozzolans of the fly ash. The pozzolanic reactions are as follows [Helmuth 1987]:

$$\mathbf{Ca(OH)_2 \Rightarrow Ca^{++} + 2[OH]^-}$$

$$Ca^{++} + 2[OH]^- + SiO_2 \Rightarrow CSH$$

$$Ca^{++} + 2[OH]^- + Al2O_3 \Rightarrow CAH$$

Hydration of tricalcium aluminate in the ash provides one of the primary cementitious products in many ashes. The rapid rate at which hydration of the tricalcium aluminate occurs results in the rapid setting of these materials, and is the reason why delays in compaction result in lower strengths of the stabilized materials. As well as CSH, other important hydration products may include carboaluminate hydrate ($C_3A.CC.H_{12}$ C_4AH_{13} solid solution) and other calcium aluminate hydrates such as hydrogarnet (C_2AH_8) [Takemoto & Uchikawa 1980].

2.2.4. Fly ash applications

Coal fly ash can be utilized in the following ways [Dunstan et al. 1980].

i) High Volume Uses

High volume utilization of fly ash includes

- as structural fills in embankments, dams, dikes and leves, and
- as sub-base and base courses in road way construction.

ii) Medium Volume Uses

This includes the use of fly ash

- as raw material in cement production
- as an admixture in blended cements and
- as replacement of cement or as a mineral admixture in concrete.
- used as partial replacement of fine aggregate in concrete.
- for production of lightweight aggregates for concrete and many other applications.

iii) Low Volume Uses

This includes the coal ash utilization

- in high value added applications such as metal extractions. High value metal recovery of Aluminum (Al), Gold (Au), Silver (Ag), Vanadium (Va) and Strontium (Sr) fall in this category.
- Fly ash has potential uses for producing light weight refractory material and exotic high temperature resistant tiles.
- Cenospheres or floaters in fly ash are used as special refractory material and also as additives in forging to produce high strength alloys.

iv) Miscellaneous Uses

Based upon its physical properties, coal ash is used

- as landfill for land reclamations for residential, commercial and recreational development projects.
- as filler in asphalt, plastics, paints and rubber products.
- in water treatment and as absorbent for oil and chemical spills.

2.2.5. Major research findings on coal fly ash applications in the cement/concrete industry

Exhaustive research has been conducted on fly ash admixture concrete and its properties [Singh et al. 1999, Oner et al. 2005, Gao et al. 2007, Zhang et al. 1999, Dunstan et al. 1980, Mehta et al. 1986, Siddique 2004, Naik et al. 1994, Naik et al. 1998, Hwang et al. 1998, Dhir et al. 1999, Lupu et al. 2006, Antiohos et al. 2008, Shi et al. 2003]. Research showed that fly ash used as an additive to Portland cement has a number of positive effects on the resulting concrete. A decrease in water demand, decreasing the water/cement ratio. An improvement of the packing of particle size decreases air entrainment in the concrete. Fly ash increases resistance to corrosion, and ingress of corrosive liquids by reacting with calcium hydroxide in cement into a stable, cementitious compound of calcium silicate hydrate. The original calcium hydroxide is soluble, whereas the calcium silicate hydrate is less soluble in fly ash concrete, thereby reducing the possibility of leaching of calcium hydroxide from the concrete. In addition to calcium silicate hydrate being less soluble, reaction products tend to the filling of capillary voids in the concrete mixture, thereby reducing permeability of the concrete [Barry and Russel 1998]. Singh et al. (1999) studied the cementitious binder from fly ash. The study suggested that the binders are eminently suitable for partial replacement (up to 25% of the cement in concrete) without any detrimental effect on the strength. Fly ash can be used in the range from 45% to 70% in formulating these binders along with other industrial wastes to help in mitigating environmental pollution. Oner et al. (2005) conducted a study on strength development of concrete containing fly ash, and optimum usage of fly ash in concrete. The utilization of fly ash in the construction of concrete dams was investigated [Gao et al. 2007]. The compressive strengths of dam concrete with 50% of fly ash in 90 days are higher than those with 30% of fly ash or without fly ash. This is because fly ash may decrease the deformation of dam concrete with 50% of fly ash, and the shrinkage and expansive strain was reduced significantly about 33% and 40% less than the specimens without fly ash, respectively. Zhang et al. (1999) studied the leachability of trace metal elements from fly ash concrete. They studied the effect of leaching conditions, and found that none of the trace metals analyzed (As, Cd, Cr, Cu, Pb,

Se and Zn) in the leachates from fly ash concrete exceeded the regulated concentration levels specified in the toxicity characteristic leaching procedure (TCLP) test. Dunstan et al. (1980) and Mehta et al. (1986) have discussed the factors that contribute to attack of sulphates on fly ash concrete. Siddique (2004) reported that Class F fly ash can be suitably used up to 50% of cement replacement in concrete for use in precast elements, and reinforced cement concrete construction.

High volumes of Class C and Class F fly ash can be used to produce high-quality pavements in concrete with excellent performance [Naik et al. 1994]. Blending of Class C fly ash with Class F fly ash showed either comparable or better results than either of the control mixture without fly ash or the unblended Class C fly ash [Naik et al. 1998]. Hwang et al. (1998) examined the effects of fine aggregate replacement on the rheology, compressive strength, and carbonation properties of fly ash and mortar. Test results showed that rheological constants increased with higher replacement level of fly ash and that, when water/cement ratio was maintained, the strength development and carbonation properties were improved. The low-lime fly ash was used to develop chloride-resistant concrete by improving its physical resistance to the ingress of chlorides and binding capacity of these ions in the cover zone [Dhir et al. 1999]. Researchers have modified fly ash to increase the setting properties of cement by chemical treatment [Lupu et al. 2006, Antiohos et al. 2008, Shi et al. 2003]. These results in decreased setting time, accelerated strength development, and increased strength of materials containing fly ash, especially with a high percentage of fly ash. Thus, chemical activation of reactivity of fly ash is an effective method to increase the use of fly ash in concrete.

There are some disadvantages also associated with the use of fly ashes though the advantages of using fly ash far outweigh the disadvantages, The quality of fly ash is important–but it can vary. Poor-quality fly ash can have a negative effect on concrete. The principle advantage of fly ash is reduced permeability at a low cost, but fly ash of poor quality can actually increase permeability. Some fly ash, such as that produced in a power plant, is compatible with concrete. Other types of fly ash must be beneficiated, and some types cannot be improved sufficiently for use in concrete.

Some concrete will set slowly when fly ash is used. Though this might be perceived as a disadvantage, it can actually be a benefit by reducing thermal stress. Certain fly ash can be used to keep the temperature from rising too high (< 45 ºC). However, concrete with fly ash can set up normally or even rapidly, since many other factors control the set and strength development.

Freeze-thaw durability may not be acceptable with the use of fly ash in concrete. The amount of air entrained in the concrete controls the freeze-thaw durability, and the high carbon content in certain

fly ash products absorbs some air entraining agents, reducing the amount of air produced in the concrete, making the concrete susceptible to frost damage. High-carbon fly ash materials tend to use more water and darken the concrete as well. It is not recommended to use a high-carbon (greater than 5 percent) content fly ash, but if it must be used, the proper air content can be reached by increasing the dosage of an air-entraining agent.

Slow set and low early strength need not be consequences of using fly ash. Most of the time, high-fineness and low-carbon fly ash will result in high early strength. Sometimes, additional lime, an accelerator or a superplasticizer will be needed. Fly ash also can be mixed with a small amount of condensed silica fume (CSF) to improve set or early-strength properties. Certainly, careful attention to the mix design and water content is always necessary to obtain proper set and early strength development.

2.2.6. Fly ash for sustainable construction materials

Besides the benefits associated to the synergistic action of fly ash with cement which leads to the improvement of the properties of concrete in certain applications, the incorporation of fly ash in the construction material shows definitive advantages in the environment and contributes to different parameters of sustainability. The scheme in Figure 2.2 summarizes the gain to the environment from each utilized ton of fly ash.

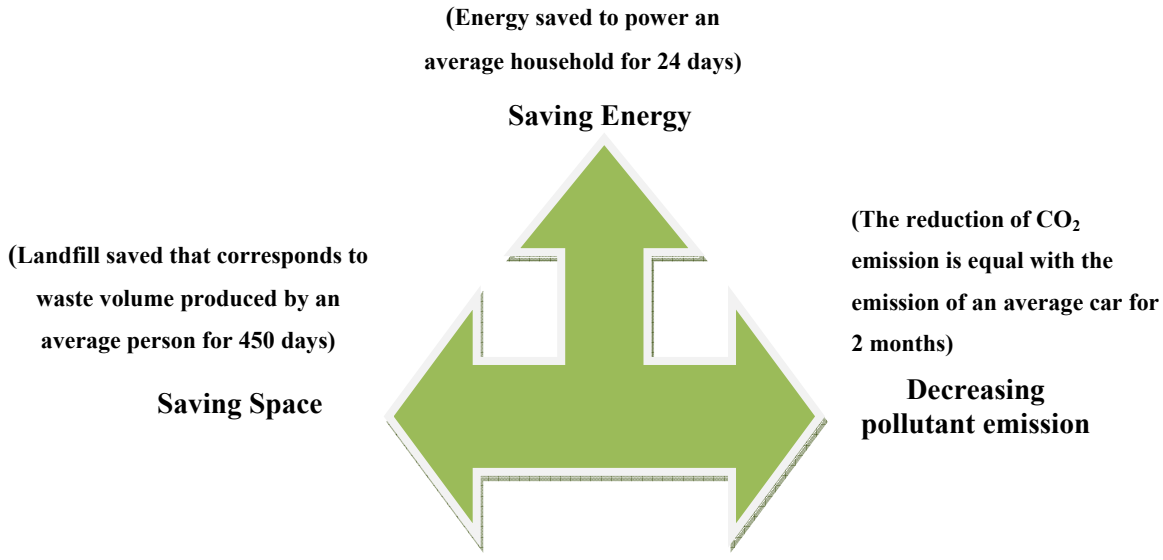

Figure 2. 2. Environmental gain for each ton of fly ash utilized [Tsimas 2010]

More specifically the use of fly ash as a supplementary cementing material (SCM) leads to a substantial energy saving by reducing the amount of Portland cement, which is an energy intensive

product [Worrell et al. 2000, Bentur et al. 2002, Bijen et al. 1996]. It contributes also to the reduction of CO_2 emissions produced during cement manufacture [Bentur et al. 2002, Bijen et al. 1996]. Apart from assisting sustainable development, utilizing such a by-product contributes to the protection of the environment since, when not recycled, fly ash is land filled or disposed to inappropriate sites [Bijen et al. 1996, Cheerarot et al. 2004]. Reductions of the amount of residues to be land filled along with partial substitution of common raw materials used in cement making are the major beneficial effects of the recycling process.

Analysing the CO_2 emissions reduction gain the contribution of fly ash incorporation in blended cements and the relevant substitution of clinker leads to a significant reduction of CO_2 emissions and therefore is of major importance especially for the cement industry. Additionally, except for blended cements, the use of both bottom and fly ash as raw mix constituents for partial replacement of limestone, contribute to a small (max 4%, Table 2.4) but remarkable CO_2 reduction during the burning process in the cement industry [Tsimas et al. 2008]. According to EN 197-1 [EN 197-1 (2000)], clinker participates in different percentages in cement depending on the cement type. For the case of fly ash substitution, apart from the specifications in the above standard, the exact percentage of fly ash depends also on its composition and especially on the percentage of some constituents (as are e.g. sulphates:SO_3) which limit their participation.

It is important to remember that landfill avoidance plays a key role in the need to beneficiate fly ash. However, research attempts were done on disposed fly ash also as a replacement of cement and it could be concluded that ground disposed fly ashes were excellent pozzolanic materials and could be used as a partial replacement of cement in concrete, even though they were exposed to the weather for 24 months [Cheerarot and Jaturapitakkul 2004] It's no surprise that fly ash is more widely available than ever before. The use of processed fly ash in concrete continues to positively impact performance characteristics. In 2006, fly ash accounted for 20 per cent of coal combustion products worldwide as more than 15 million tons were used in the production of concrete. Despite its increasing popularity in the ready mix industry, not all fly ash is created equal. Ultimately, it is up to concrete users to ensure their products are manufactured with consistent, high quality fly ash that can stand the test of time.

Table 2.4. Emission reduction data in cement manufacture (Tsimas et al. 2008)

Fly ash in blended cements and raw mix constituent	*emission reduction based on max possible substitution (EN 197-1)*
CEM IIa	21 %
CEM IIb	37 %
CEM IVa	37 %
CEM IVb	58 %
Fly ash	0.5 – 4 %
Bottom ash	0.5 – 4 %

2.3. Biomass ashes

Biomass ashes differ from coal ashes, in particular in what concerns its chemistry and mineralogy [Werther et al. 2000, Loo and Koppejan 2003, Demirbas 2005, Masiá et al. 2007]. As a class, biomass fuels exhibit more variation in both composition and amount of inorganic material than is typical of coal. The characteristics of ashes from biomass combustion are influenced by: i) biomass characteristics (for example, herbaceous material, wood or bark), ii) combustion technology (for example, fixed bed or fluidised bed), iii) the location where the ashes are collected (for example, bottom ashes or fly ashes) [Obernberger et al. 1997, Loo and Koppejan 2003, Yin et al. 2008].

2.3.1. Process and mechanisms of ash formation

The process of biomass combustion involves a number of physical/chemical aspects of high complexity. The nature of the combustion process depends both on the fuel properties and the combustion application [Loo and Koppejen 2008]. The combustion process can be divided into several general processes: drying, pyrolysis, gasification and combustion. The relative importance of these steps will vary, depending on the combustion technology implemented, the fuel properties and the combustion process conditions. In large-scale biomass combustion applications with continuous fuel feeding, such as moving grates, these processes will occur in various sections of the grate. Figure 2.3 shows qualitatively the combustion process for a small biomass particle. For larger particles, there will be a certain degree of overlap between the phases, while in batch combustion processes, as in wood log combustion in wood-stoves and fireplaces, there will be a large degree of overlap between the phases.

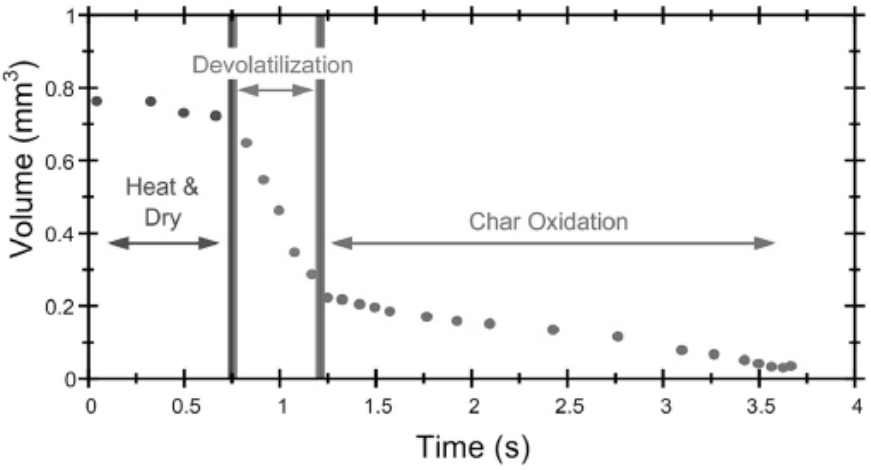

Figure 2.3. The combustion of a small biomass particle proceeds in distinct stages

Source: [Loo and Koppejan 2008].

Ash-forming elements are present in biomass as salts, bound in the carbon structure (inherent ash) or they are attendant as mineral particles from dirt and clay introduced into the biomass fuel during harvest or transport (entrained ash). The compounds in inherent ash are homogeneously dispersed in the fuel and are much more mobile than the compounds in entrained ash and, therefore, are readily volatile and available for reactions in burning char (Figure 2.4) [Musil et al. 2005]. During combustion, a fraction of the ash-forming compounds in the fuel is volatilized and released to the gas phase. The volatilized fraction depends on the fuel characteristics, the gas atmosphere, and the combustion technology in use. For example, high combustion temperatures and a reducing atmosphere have been reported to enhance the volatilization of the environmentally relevant heavy metals Zn, Pb and Cd [Obernberger 2002]. In the reducing gas conditions and the high temperatures inside and on the surface of burning char, even a small fraction present as refractory oxides, such as SiO_2, CaO and MgO, may convert to more volatile SiO, Ca and Mg and volatilize. Depending on the furnace temperature, Cd and Pb will pass through the boundary layer and enter the surrounding furnace environment in their gaseous state, together with other volatile elements such as Cl, S and K [Good et al. 2004]. Primary particles formed by vaporization and subsequent nucleation in the boundary layer are very small in size, about 5–10 nm, but on their way in the flue gas they grow by coagulation, agglomeration and condensation [Johansson et al. 2005]. These particles form the basis for the fine mode of the fly ash, characterized by a particle size of < 1 μm. The non-volatile ash compounds remaining in the char may melt and coalesce inside and on the surface of the char, depending on the temperature and chemical composition of the particles. This results in residual ash particles with a wide range of compositions, shapes and sizes, related to the characteristic of the parent mineral particles. Depending on the density and size of the residual ash

particles, the combustion technology and the flue gas velocity, a fraction of the residual ash will be entrained with the flue gas and form the coarse part of fly ash, while the other fraction will stay on the grate and form bottom ash. In contrast to the fine-mode fly-ash particles from volatilized ash compounds, coarse fly-ash particles are larger, typically exceeding 5 µm. Upon cooling of the flue gas in the convective heat exchanger section, vapours of volatilized compounds condense or react on the surface of pre-existing ash particles in the flue gas. Due to the much larger specific surface of the fine-mode particles compared to the coarse fly-ash particles, the concentrations of condensing or reacting ash-forming elements increase with decreasing particle size. This explains some of the very high heavy-metal concentrations found in aerosol particles from combustion plants [Obernberger 2002, Merckx 2005].

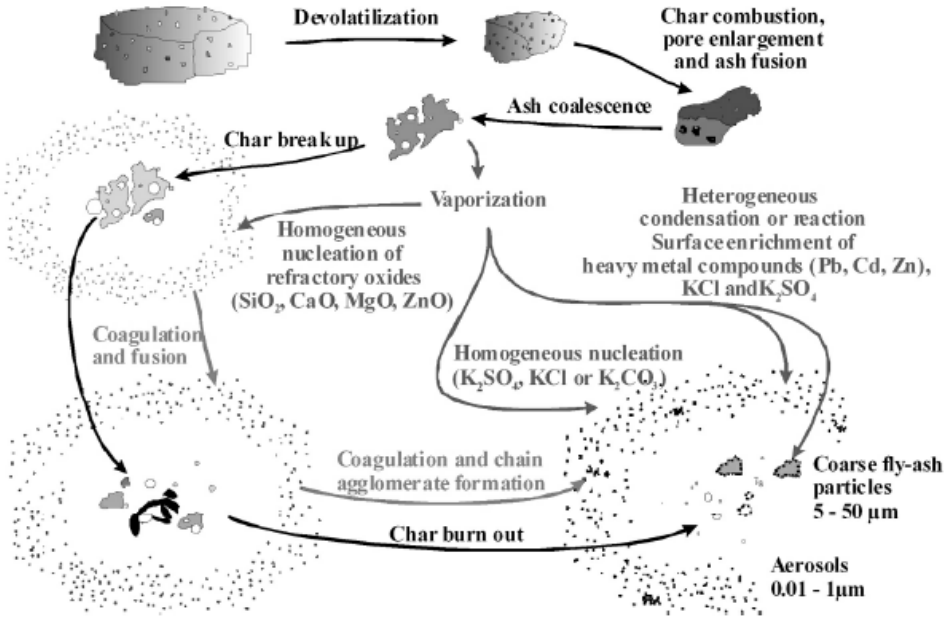

Figure 2.4. Mechanism involved in biomass fly ash formation: Ash fractions formed in biomass combustion plants (Loo and Koppejan 2008)

According to the ash formation process explained, in biomass combustion plants three different ash fractions must normally be distinguished

The bottom ash: Ash fraction produced on the grate and bottom bed and in the primary combustion chamber; often mixed with mineral impurities contained in the biomass fuel like sand, stones and clay or with bed material in fluidized bed combustion plants. These mineral impurities can, especially in bark-fired fixed-bed combustion plants, cause slag formation (due to a lowering of the melting point) and sintered ash particles in the bottom ash.

The cyclone fly ash: Fine, mainly inorganic, ash particles carried with the flue gas and precipitated in the secondary combustion zone, in the boiler and especially in multicyclones placed after the combustion unit. This ash fraction mainly consists of coarse fly ash particles.

The filter fly ash: Second and finer fly-ash fraction precipitated in electrostatic filters, fibrous filters or as condensation sludge in flue gas condensation units (normally placed after the multi-cyclone). In small-scale biomass combustion plants without efficient particulate matter removal technology, this ash fraction is emitted with the flue gas. A small part of the fly ash remains in the flue gas anyway and causes dust emissions (depending on the efficiency of the particulate matter removal technology used). This ash fraction mainly consists of aerosols (sub-micron ash particles).

2.3.2. Biomass characteristics

The quantity and quality of ashes produced in a biomass power plant are strongly influenced by the characteristics of the biomass used: agriculture wastes or herbaceous biomass, wood or bark [Loo and Koppejan 2003, Masiá et al. 2007]. The major biomass materials of industrial interest on a worldwide basis are shown in Table 2.5. Typical ash elemental analysis data (major elements) for a number of industrial important biomass materials are shown in Table 2.6.

Furthermore, even for the same type of biomass, the properties of its fly ash depends also on some growth and production factors including weather, season, storage and geographic origins [Bridgeman et al. 2007, Wiselogel et al. 1996]. In general, the major ash forming inorganic elements in biomass fuels are Ca, K, Na, Si and P and some of these act as important nutrients for the biomass [Masiá et al. 2007]. However, some agro waste or herbaceous biomass fuels have high silicon content (rice husk ash) while some have high alkali metal content (wood ash).

Table 2.5. The major biomass materials of industrial interest on a worldwide basis [Demirbas 2005]

Agricultural products	*Forestry products*	*Domestic and municipal wastes*	*Energy crops*
Harvesting Residues	**Harvesting residues**	**Domestic/industrial**	**Wood**
Cereal straws Oil seed rape and linseed oil straws Flax straw Corn stalks	Forestry residues	Municipal solid waste (MSW) Refuse-derived fuelsConstruction and demolition wood wastes Scrap tyres Waste pallets	Willow Poplar Cottonwood
Processing residues	**Primary processing wastes**	**Urban green wastes**	**Grasses and other crops**
Rice husks Sugarcane bagasse Olive residues Palm oil residues Citrus fruit residues	Sawdusts Bark Offcuts	Leaves Grass and hedge cuttings	Switchgrass Reed canary grass Miscanthus
Animal wastes	**Secondary processing wastes**		
Poultry litter Tallow Meat/bone meal	Sawdusts Offcuts		

Table 2.6. Typical ash elemental analysis data (major elements) for a number of biomass materials (in weight %).

Element (wt.%)	*Wood ash (Wang et.al 2008)*	*Municipal solid waste ash (Remond et al. 2002)*	*Sugar cane Bagasse ash (Ganesan et al.2007)*	*Rice husk Ash (Zerbino 2011)*	*Wheat straw ash (Hasan et al. 2000)*	*Palm oil fuel ash Tangchirapat et al. 2007)*
SiO_2	48.9	27.2	64.2	95.0	20.6	57.7
Al_2O_3	12.5	11.7	9.1	0.3	6.1	4.6
Fe_2O_3	5.4	1.8	5.5	0.4	3.7	3.3
CaO	13.6	16.8	8.1	1.3	63.6	6.6
MgO	3.2	2.5	2.9	0.5	1.3	4.2
Na_2O	1.7	5.9	0.9	0.1	--	0.5
K_2O	3.4	5.8	1.4	1.4	--	8.3
LOI	7.8	13.0	4.9	0.5	1.4	10.5
SO_3	1.3	3.0	--	--	2.6	0.3

2.3.3. Types of biomass combustion technology and their influence on the fly ash characteristics

The type of combustion equipment is relevant to the ash behaviour, since the combustion conditions are significantly different. The majority of the laboratory and industrial scale experimental work on these processes have recognised this, and these have generally been aimed specifically at one or the other of these types of combustion.

In principle, the following combustion technologies can be distinguished: [Loo and Koppejan 2008],

• fixed bed combustion;

• fluidized bed combustion;

• pulverized fuel combustion.

The basic principles of these three technologies are shown in Figure 2.5.

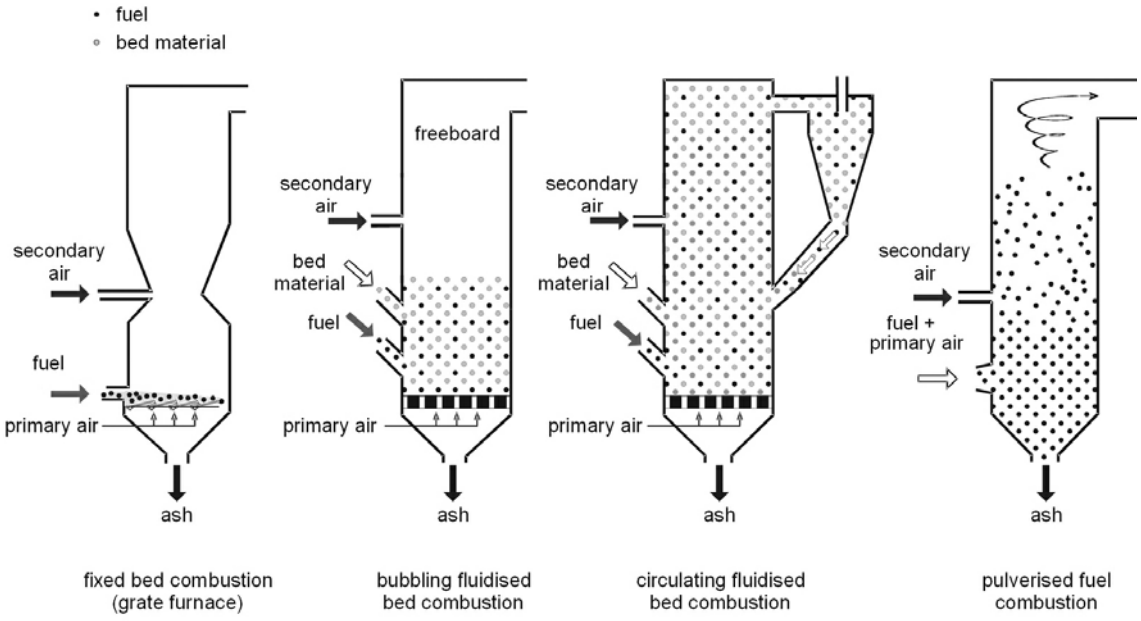

Figure 2.5 Principal combustion technologies for biomass (Loo and Koppejan, 2008).

Fixed bed combustion systems include grate furnaces and underfeed stokers. Primary air passes through a fixed bed, in which drying, gasification and char combustion take place. The combustible gases produced are burned after secondary air addition has taken place, usually in a combustion zone separated from the fuel bed.

Within a fluidized bed furnace, biomass fuel is burned in a self-mixing suspension of gas and solid-bed material into which combustion air enters from below. Depending on the fluidization velocity, bubbling fluidized bed (BFB) and circulating fluidized bed (CFB) combustion can be distinguished.

Pulverized fuel (PF) combustion is suitable for fuels available as small particles (average diameter smaller than 2mm). A mixture of fuel and primary combustion air is injected into the combustion chamber. Combustion takes place while the fuel is in suspension and gas burnout is achieved after secondary air addition. Variations of these technologies are available. Examples are combustion systems with spreader stokers and cyclone burners.

The biomass combustion technology used influences the amount and characteristics of the ash produced in a power plant. For example, in a grate furnace the biomass ashes are subjected to higher temperatures (the maximum fuel bed temperature can be as high as 1000-1200ºC) in comparison to a fluidised bed (less than 900ºC). In consequence, this influences the amount of organic species that volatilise in the furnace, and consequently the relative composition of bottom and fly ashes. This difference in operating temperature in the furnace also influences the degree of slagging and fouling in the furnace and boiler, because of the relatively low melting temperature characteristic of biomass ashes [(Werther et al. 2000, Loo and Koppejan 2003, Demirbas 2005], and consequently the composition of slag formed. Also, the hydrodynamics of the furnace influences the biomass ash fractions collected. In a grate furnace the amount of bottom ashes is dominant compared to multi-cyclone or filter (bag filter or electrostatic precipitator) fraction, whereas in the case of a fluidised beds the fly ash is quantitatively dominant. The concentration of ecological relevant heavy metals (for example, Zn, Cd, Pb, Hg) and organic contaminants (Polychlorinated Dibenzodioxin and Dibenzofuran PCDD/F, Polycyclic aromatic hydrocarbons (PAHs)) increase from the bottom to the fly ash (Loo and Koppejan 2003, Demirbas 2005). Consequently it is not recommended the mix of those ashes fluxes, in particular the filter fly ashes with bottom ashes, since they must follow distinct management strategies, in order to minimize environmental impacts.

2.3.4. Research on biomass ash in construction materials

Compared to coal fly ash, where significant research has already taken place and high utilisation figures are already reported in several countries [Bridgeman et al. 2007, Lewandowski et al. 2000], commercial utilisation of biomass ash is not widely reported except in very few countires like in

India (ricehuskash.com). However, several research efforts are underway for applications such as adsorbent, raw material for ceramics, cement and concrete additive, material recovery, etc., based on its characteristics. The composition, surface area, and presence of unburnt material play an important role in determining the application.

2.3.4.1. Municipal solid waste ash

Thousands of millions of tons of municipal solid waste (MSW) are produced every year. Incineration is a common technique for treating waste, as it can reduce waste mass by 70% and volume by up to 90%, as well as providing recovery of energy from waste to generate electricity. Generally, municipal solid waste incineration (MSWI) produces two main types of ash, which can be grouped as bottom ashes (BA) and fly ashes (FA). The waste generated from MSWI usually ends up in two ways, disposed as landfill or for reuse as secondary raw materials. Although the ashes contain high concentrations of heavy metals, salts, chloride and organic pollutants, which may limit the applications of reuse, the treatment of ashes will improve the environmental characteristics and enhance the possibility for reuse [Charles et al. 2010].

The incineration process is separated into three main parts: incineration, energy recovery and air pollution control. The MSW is fed into the furnace continually for incineration. The temperature for incineration should be at least 850 ºC with a flu gas residence time of more than two seconds. During the process, the air supply must be sufficient to ensure complete combustion of waste and to prevent the formation of dioxins and carbon monoxide.

Since MSWI ash contains CaO, SiO_2, Fe_2O_3, and Al_2O_3, and the fact that a considerable amount of cement was used for the production of mortar and concrete, the composition of fly ash and bottom ash is similar to the composition of raw materials for cement production. Thus, it could be a possible replacement of raw material in Portland cement production [Pan et al. 2008, Huang and Chu 2003]. Pre-treatment of fly ash is recommended to remove the chloride and heavy metals content, also the quantities of MSWI ash added to the process should be carefully controlled in order to ensure the process safety as well as product quality. For the hydration behaviour of cement clinker, it is found that alkali metal content enhances hydration and contents of Zn, Pb and Cd retards the rate of hydration of cement. After washing, pre-treatment of MSWI ash, the alkali metal content is reduced and the hydration rate of washed MSW ash containing clinkers is lower than the raw MSWI ash containing clinkers [Saikia et al. 2007]. Fly ash contains chloride and sulphate content, which reveal the formation of a ettringite phase in the hydration period, thus the hydration

reaction slows down with the increasing fly ash content [Ubbriaco et al. 2000]. Internal sulfate ions are the main cause of delayed ettringite formation, which leads to expansive damage of cement concretes. On the other hand, the exposure of cementitious systems to chloride ions causes corrosion of reinforcement bars that finally seriously shortens the service life of reinforced concrete structures. It has been found that, when concomitantly present in cementitious systems, chlorides interact with sulfate ions. Particularly, for a given concentration of sulfate ions present, low to moderate concentrations of chloride ions bring about serious deterioration of concretes due to high amount of ettringite formed, while higher contents of chlorides tend to reduce and even completely eliminate ettringite formation [Palmane et al. 2008].

Based on Solidification/Stabilization (S/S) technology, the MSWI fly ash can be potentially applied as a replacement of cement or as an aggregate [Rashid et al. 1992]. The addition of up to 50% treated fly ash will not affect the strength and hardness, and the leaching property is acceptable for the use in road construction. However, the long-term durability has not yet been determined [Aubert et al. 2004, Aubert et al. 2006].

It is possible to use MSWI bottom ash as concrete aggregate. The results show that treated (immersion in sodium hydroxide for 15 days) bottom ash can replace up to 50% of gravel in concrete without affecting the durability. The aggregates passing the 20 mm sieve and retained on the 4 mm sieve were considered for investigation. The leaching problem is the major environmental concern of this application. Although many results show that the heavy metal leaching is not significant, unexpected heavy metal leaching may occur when the structure is demolished or comes in contact with rain. Several road sections have utilized MSWI bottom ash in road construction [Aberg 2006, Bruder-Hubscher 2001, Francois 2009].

Eco-Cement is a brand-name for a type of cement which incorporates reactive magnesia (sometimes called caustic calcined magnesia or magnesium oxide, MgO), another hydraulic cement such as Portland cement, and optionally pozzolans and industrial by-products, to reduce the environmental impact relative to conventional cement [TecEco 2009]. Wastes such as fly and bottom ash, slags MSWI etc can be included, without incurring problems such as delayed reactions. Typically about half of the traditional cement raw materials are replaced with ash and other solid waste by-products. The resultant product absorbs CO_2, with absorption varying with the degree of porosity and the amount of magnesia (FHWA 2005). Moreover, the reactive magnesia in Eco-Cement uses a lower kiln temperature (about 750 °C), whereas conventional PCC requires a kiln temperature of around 1450 °C), which reduces energy requirements and hence fossil fuel usage and CO_2 emissions (TecEco 2009). Eco-Cement has the following characteristics (FHWA 2005):

- Rapid hardening, similar to high-early-strength cement.
- Short initial setting time (approximately 20 to 40 minutes).
- Handling time that can be adjusted to suit particular applications.

MSWI is incorporated in limestone and clay to produce the Ecocement. This new cement is designed to use municipal waste incinerator ashes in amounts up to 50% of the raw materials. The manufacturing process of ecocement [Shimoda et al. 1999] is almost the same as Ordinary Portland cement (OPC). The first type of ecocement produced is designed to take advantage of chlorides in the incinerator ashes to make rapid-hardening cement. During the sintering process, chloride combines with calcium aluminate to form calcium chloroaluminate ($C_{11}A_7\_CaCl_2$) in place of tri-calcium aluminate (C_3A) [Shimoda et al. 1999]. The performance of this type of ecocement is similar to the rapid hardening cement, which develops that performance because of $C_{11}A_7\_CaF_2$. This type of ecocement, however, contains relatively large amounts of chlorides. One problem with the commercialization of this cement, other than the conservatism of the building industry, is that the feedstock magnesite is rarely mined.

2.3.4.2. Rice husk ash (RHA)

Rice-husk (RH) is an agricultural by-product material. Rice milling industry generates a lot of rice husk during milling of paddy which comes from the fields. This rice husk is mostly used as a fuel in the boilers for processing of paddy. Rice husk is also used as a fuel for power generation. Rice husk ash (RHA) is about 25% by weight of rice husk when burnt in boilers. It is estimated that about 70 million tonnes of RHA is produced annually worldwide. This RHA is a great environment threat causing damage to the land and the surrounding area in which it is dumped.

During milling of paddy about 78% of weight is received as rice, broken rice and bran. The remaining 22% of the weight of paddy is received as husk. This husk is used as fuel in the rice mills to generate steam for the parboiling process. It constitutes about 20% of the weight of rice. It contains about 50% cellulose, 25–30% lignin, and 15–20% of silica. When rice-husk is burnt rice-husk ash (RHA) is generated. On burning, cellulose and lignin are removed leaving behind silica ash. During firing process the organic volatile matter which is about 75% in total is burnt and the balance 25% of the weight of this husk is converted into ash is known as rice husk ash (RHA). This RHA in turn contains around 85% - 95% amorphous silica [Ou et al. 2007].

So for every 1000 kgs of paddy milled, about 220 kgs (22%) of husk is produced, and when this husk is burnt in the boilers, about 55 kgs (25%) of RHA is generated. The controlled temperature and environment of burning yields better quality of rice-husk ash as its particle size and specific surface area are dependent on burning condition. Completely burnt rice-husk is grey to white in color, while partially burnt rice-husk ash is blackish. The form of silica obtained after combustion of rice husk depends on the temperature and duration of combustion of rice husk. Essentially amorphous silica can be produced by maintaining the combustion temperature below 500 ºC under oxidizing conditions for prolonged periods or up to 680 ºC with a hold time less than 1 min. However, Yeoh et al. (1979) reported that RHA can remain in the amorphous form at combustion temperatures of up to 900 ºC if the combustion time is less than 1 h, while crystalline silica is produced at 1000 ºC with combustion time greater than 5min. Using X-ray diffraction, Chopra et al. (1981) observed that at burning temperatures up to 700 ºC, the silica was in an amorphous form. The effect of different burning temperatures and the chemical composition of rice husk and the effect of different burning temperature on it were studied by Hwang and Wu (1989). It was observed that at 400 ºC, polysaccharides begin to depolymerise. Above 400 ºC, dehydration of sugar units occurs. At 700 ºC, the sugar units decompose. At temperatures above 700 ºC, unsaturated products react together and form a highly reactive carbonic residue.

The X-ray data and chemical analyses of RHA produced under different burning conditions given by Hwang and Wu (1989) showed that the higher the burning temperature, the greater the percentage of silica in the ash. K, S, Ca, Mg as well as several other components were found to be volatile.

Rice-husk ash (RHA) is a very fine pozzolanic material. The utilization of rice husk ash as a pozzolanic material in cement and concrete provides several advantages, such as improved strength and durability properties, reduced materials costs due to cement savings, and environmental benefits related to the disposal of waste materials and to reduced carbon dioxide emissions. Reactivity of RHA is attributed to its high content of amorphous silica, and to its very large surface area governed by the porous structure of the particles [Cook 1984, Mehta 1992]. Generally, reactivity is favoured also by increasing fineness of the pozzolanic material. Della et al. (2002) reported that a 95% silica powder could be produced afterheat-treatment at 700 ºC for 6 hours. And specific surface area of particles was increased after wet milling from 54 to 81 m^2/g.

Many researches were done to evaluate the influence of rice husk ash in the strength properties of cement mortars and concretes [Zhang and Malhotra 1996, Singh et al. 2002, Nehdi et al. 2003, Jaturapitakkul and Roongreung 2003, Bui et al. 2005]. Zhang et al. (1996) studied the effect of

incorporation of RHA on the hydration, microstructure and interfacial zone between the aggregate and paste. Based on the investigation, they concluded that: (i) calcium hydroxide ($Ca(OH)_2$) and calcium silicate hydrates (C-S-H) were the major hydration and reaction products in the RHA paste. Because of the pozzolanic reaction, the paste incorporating RHA had lower $Ca(OH)_2$ content than the control Portland cement paste; and (ii) incorporation of the RHA in concrete reduced the porosity and the $Ca(OH)_2$, amount in the interfacial zone; the width of the interfacial zone between the aggregate and the cement paste compared with the control Portland cement composite was also reduced. Yu et al. (1999) reported that improvement of concrete properties up on addition of RHA may be attributed to the formation of more C-S-H gel and less portlandite in concrete due to the reaction between RHA and the Ca^{2+}, OH^- ions or $Ca(OH)_2$. It was concluded that RHA is highly effective in cement formulations because of its pozzolanic nature.

2.3.4.3. Sugar cane bagasse ash

Bagasse ash is the by-product from burning sugar cane (or bagasse) as a fuel to heat steam for electricity generation as well as the sugar extraction process. In general, bagasse ash is disposed of in landfills and is now becoming an environmental burden. Every year millions of tonnes of bagasse ash is produced, and this increases annually. The study of bagasse ash for potential application in concrete production was introduced by Martirena et al. (1998) who used different waste ashes from the sugar industry as pozzolanic materials in lime-pozzolan binders. They found that the sugar cane bagasse ash produced in the boilers of the sugar industry could be classified as a pozzolanic material. Subsequently, Singh et al. (2000) found that the presence of 10% bagasse ash in concrete gave a higher compressive strength than that of their control concrete at all ages, and the chemical deterioration of the blended cement was less than that of the control concrete due to the pozzolanic reaction that produced more hydrated cementitious materials which in turn induced permeability reduction of bagasse ash. Paya et al. (2002) have reported that combustion yields ashes containing high amount of unburnt matter, silicon and aluminium oxides as main components. They have indicated that the bagasse ashes have to be chemically, physically and mineralogically characterized, in order to evaluate the possibility of their use as a cement replacement material in concrete. Ganesan et al. (2007) studied the effects of bagasse ash content as a partial replacement for cement on the physical and mechanical properties of hardened concrete. They found that the bagasse ash is an effective mineral admixture, with 20% constituting an optimal cement replacement ratio. Raw bagasse ash has a large particle size and a high porosity, so it needs more water content in the concrete mixture and thus results in a lower compressive strength of concrete. However, when bagasse ash is ground up into small particles, the compressive strength of concrete containing this ground bagasse ash improves significantly [Cordeiro 2008].

The optimum proportion of bagasse ash was found to be in the range of 10–20 wt% of binder. Recently, Nuntachai et al. (2009) reported that concrete containing up to 30% ground bagasse ash had a higher compressive strength and lower water permeability than the control concrete, both at ages of 28 and 90 days. The results show the beneficial application of ground bagasse ash in concrete.

2.3.4.4. Wood ash

Wood ash (WA) is the residue generated due to combustion of wood and wood products (chips, saw dust, bark, etc.). It is the inorganic and organic residue remaining after the combustion of wood or unbleached wood fiber. The physical and chemical properties of wood ash vary significantly depending on many factors. The physical and chemical properties of wood ash, which determine its beneficial uses, are dependent upon the species of the wood and the combustion methods that include combustion temperature, efficiency of the boiler, and supplementary fuels used. It is reported that the ash content yield decreases with increasing combustion temperature [Etiegni and Campbell 1991].

Hardwoods usually produce more ash than softwoods and the bark and leaves generally produce more ash than the inner woody parts of the tree. On average, the burning of wood results in about 6–10% ashes. When ash is produced in industrial combustion systems, the temperature of combustion, cleanliness of the fuel wood, the collection location, and the process can also have profound effects on the nature of the ash material. Therefore, wood ash composition can be highly variable depending on geographical location and industrial processes. This makes testing the ash extremely important. Density of wood ash decreases with increasing carbon content. Typical wood burnt for fuel at pulp and paper mills and wood products industries may consist of saw dust, wood chips, bark, and saw mill scraps, hard chips rejected from pulping, excess screenings such as sheaves and primary residuals without mixed secondary residuals. Physical and chemical properties of wood ash are important in determining their beneficial uses. These properties are influenced by species of tree, tree growing regions and conditions, method and manner of combustion including temperature, other fuel used with wood fuel, and method of wood ash collection [Etiegni 1990, Etiegni and Campbell 1991, NCASI 1993]. Further quality variation in the wood ash properties occur when wood is co-fired with other supplementary fuels such as coal, coke, gas, and the relative quantity of wood versus such other fuels [NCASI 1993].

i). Physical and chemical properties

Etiegni and Campbell (1991) studied the effect of combustion temperature on yield and chemical properties of wood ash. The reduction in wood waste ash yielded up to 45% with a combustion temperature increase from 538 C to 1093°C. Combustion of wood waste at higher temperatures beyond 1000°C also resulted in a profound decrease in carbonate content due to the chemical decomposition of the aforesaid chemical compound at such temperatures. The reduction of carbonates and bicarbonates chemical species which contribute to alkalinity of wood ash at higher combustion temperatures resulted in a corresponding decrease in alkalinity of ash. Moreover, there was a decline in composition of light metallic elements such as potassium, sodium and zinc in wood waste ash with increasing temperature of combustion [Etiegni and Campbell 1991].

Naik (1999) determined the physical and chemical properties of wood ashes derived from different mills. Scanning Electron Microscopy (SEM) was used to determine shape of wood ash particles. The SEM micrographs showed wood ashes as a heterogeneous mixture of particles of varying sizes, which were generally angular in shape. The wood fly ash consisted of cellular particles, which were unburned, or partially burned wood or bark particles. The average moisture content values for the wood ash studied were about 13% for fly ash and 22% for bottom ash..In terms of fineness, average amount of wood fly ash passing sieve #200 (75 μm) and retained on sieve #325 (45 μm) were 50% and 31% respectively. The bulk density of wood fly ash was determined to be relatively low at 490 kg/m^3 with a specific gravity value of 2.48. Wood fly ash was found to have low average autoclaved expansion value of 0.2%. ASTM standards do not exist for wood ash. The nearest ASTM standard (ASTM C 618 2008), available is for coal ash and volcanic ash, was used for analysis of its properties.

Udoeyo et al. (2006) reported the physical properties of burnt (1000ºC) saw wood dust ash used as additive in concrete. A micrograph obtained from a scanning electron microscopy (SEM) analysis on residual ash produced from the incineration of wood waste ash at a temperature of 1000 °C indicated that wood waste ash consists of two dominating phases, namely a fibre-like continuous layer and particle like aggregates. The fibre like continuous layer is highly carbonaceous in nature with high carbon content. On the contrary, carbon content in the particle like aggregates' phase is low and consists mainly of silica and alumina compounds. The major minerals detected in the wood ash using XRD were lime (CaO), calcite ($CaCO_3$), portlandite ($Ca(OH)_2$) and calcium silicate (Ca_2SiO_4).

Several authors have reported that swelling of wood ash occurred due to the possible hydration of silicates and lime present in the ash [Etiegni 1990, Campbell 1991, Naik et al. 2003]. The LOI

obtained for the wood ashes ranged from 6.7 to 58.1%. Steenari and Lindqvist (1998) characterized fly ashes derived from co-combustion of wood chips and fossil fuels, and compared their properties with those obtained from combustion of wood ash alone. The fly ashes derived from the co-combustion of wood with coal or peat exhibited lower concentrations of calcium, potassium, and chlorine, and higher concentrations of aluminum ion and sulfur relative to pure wood ash. The pH of leachates obtained from the co-combustion ashes were lower compared to pure wood ash. The concentrations of trace metals in these ashes were similar to those observed in pure wood ashes. The predominant crystalline phase present in the wood ash sample was quartz (SiO_2). Additional trace amounts of crystalline phases detected in wood ash included gypsum ($CaSO_4H_2O$), magnetite (Fe_3O_4), microcline ($KAlSi_3O_8$), mullite ($Al_2O_3.SiO_2$), periclase (MgO), and plagioclase ($NaAlSi_3O_8$ – $CaAl_2Si_2O_8$) [Steenari and Lindqvist 1998]. The XRD analysis performed by Campbell (1990) and Etiegni and Campbell (1991) detected the presence of additional dominant phases, namely portlandite ($Ca(OH)^2$) and lime (CaO), in the wood waste ash samples examined.The mineralogical analysis also indicated large amounts of amorphous materials present in the wood ash (46.9%). The calcite, hematite, magnetite, microcline, mullite, plagioclase, and quartz present in the wood ash are generally not reactive when used in concrete [Naik et al. 2002].

XRF analysis performed by several researchers [Elinwa and Mahmood 2002, Elinwa and Mahmood 2002, Udoeyo and Dashibil 2002, Elinwa and Ejeh 2004, and Abdullahi 2006] found significant amounts of silica in the ash samples obtained from incinerated wood waste sawdust under an uncontrolled burning condition. A total chemical composition of pozzolanic essential compounds, namely silica, alumina and ferric, was reported to have a range from 62.14 to 80.67% with a mean value of 72.78% which is similar to those of class N and F coal fly ashes. In an effort to characterize the chemical composition of wood waste ash obtained from five distinct sources for use as a binder in a controlled low strength material, Naik et al. (2003) found a wider range of a total chemical composition of silica, alumina and ferric compounds between 18.6 and 59.3% for the wood ash samples examined. Chemical compositions of wood waste ash determined by several researchers above are summarized in Table 3. An evaluation of pozzolanicity wood waste ash by Elinwa and Mahmood (2002) indicated that wood waste ash is chemically reactive with the pozzolanic activity index (PAI) value of 75.9% when exceeding the minimum 70% specified by ASTM C618 for all classes of coal fly ash to be suitable as pozzolan [Chee et. al 2011].

Co-firing of 20% wood waste with 80% coal in the coal power plant was observed to yield a resulting fly ash with a similar chemical composition and organic matter content in comparison with class C fly ash [Chee et. al 2011]. Further evaluation on pozzolanicity using the 70:30 ash mixture-the portlandite ratio indicated wood waste-coal co-fired ash possesses similar pozolanic

reactivity in comparison to class C fly ash at a later age of tests, beyond 6 months, though the rate of pozzolanic reaction at early age were relatively lower in comparison to the class C fly ash [Wang and Baxter 2007].

ii). Use of wood ash as a construction material

Not much work has been reported relating to the application of wood ash as a construction material, particularly in cement-based materials. Based on the measured physical, chemical, morphological properties, Naik (1999) reported that wood ash has a substantial potential for use as a pozzolanic mineral admixture and an activator in cement-based materialsHe further indicated that wood ash has significant potential for use in numerous other materials including Controlled Low Strength Materials (CLSM), low and medium-strength concrete, masonry products, roller-compacted concrete pavements (RCCP), materials for road base, and blended cements. Several CLSM mixtures containing high volumes of wood fly ash were found to be appropriate for backfill of excavations, and/or for making low to medium-strength concrete [Naik 1999, Naik and Kraus 2000]. Air-entrained concrete, with up to 35% replacement of cementitious materials with wood ash, achieved compressive strengths of 35 MPa (5 ksi), which is suitable for many structural applications. Fehrs (1996) also reported that wood ash can be used in manufacture of low-strength concrete and controlled low-strength materials in construction materials.

Greater wood ash content in concrete requires greater water content to achieve a reasonable workability [Udoeyo et al. 2006, Abdullahi 2006]. Compressive strength generally increased with age but decreased with the increase in the wood ash content. Comparisons of the strength of wood ash concrete with those of the control (plain) concrete of corresponding ages showed that the strength of wood ash concrete was generally less than that of the plain concrete [Udoeyo et al. 2006, Abdullahi 2006, Wang et al. 2008]. A possible explanation for this trend is that the WWA acts more like filler in the matrix than as a binder. Tkaczewska et al (2009) reported that cement formulations containing coal-biomass fly ashes demonstrate a features like lower heat of hydration, higher $Ca(OH)_2$ content and lower rate of C_3S hydration in comparison to the ones containing fly ashes from bituminous coal. Wang et al. (2007, 2008) compared the properties of biomass fly ashes from co-fired (herbaceous with coal), pure wood combustion and blended (pure wood fly ash blended with coal fly ash) to those of coal fly ash in concrete. Their results imply that biomass fly ash with co-firing concentration within a certain blending ratio (25%) should be considered in concrete. Andrea et al. (2010) studied the mortar compositions made with two coal-biomass fly-ashes (CBFAs) which correspond to approximate mass ratios of 13:87 and 62:38 wood pellets and lignite coal. They reported that the compressive strength of mortars in which up to 40% of cement

is substituted by co-combustion fly-ash exceeded 75% that of ash free mortars by 28 days, and approached or even surpassed the compressive strength of ash-free mortars after 90 days of curing. Hence, all co-combustion fly-ashes met ASTM C 618 strength requirements. Fly-ash that contained a higher proportion of large (>50 μm) particles exhibited the lowest 28-day strength. However, for the time being, biomass fly ash is excluded from addition in concrete according to the standards because of its non-coal origin. Further investigations are needed on improving the biomass fly ashes applications in order to establish its firm position among the current usage of waste materials in cement concrete industry.

2.4. Biomass in Portugal

In Portugal, primary energy is obtained mainly from fossil fuels (heavy fuel oil, coal and natural gas), hydraulic resources (using high river flows) and power plants, either thermal or hydroelectric. The energy derived is transmitted and distributed through the electrical network to end-users. In 2005, 87% of the Portuguese energy needs were fulfilled by imported fossil fuels - oil, gas and coal [Renewable energy in Portugal, 2007]. The scarcity of natural non-renewable resources and the growing contamination of the environment, due to industrial activities, resulted in an incessant search for new alternative energy sources having, in the beginning, low efficiency which improved considerably gradually with the advancement of technology and the maintenance of high oil prices in the international market. The vast field of renewable energy sources under development and exploitation such as geothermal, hydroelectric, tidal, solar thermal and photovoltaic, wind and biomass, tends to be particularly beneficial in finding the solution for the energy resources problems.

Portugal has an important potential of renewable energy resources, namely, in terms of biomass – forest residues and wood waste. The use of biomass to produce energy has other advantages beyond the decrease of greenhouse gases from using fossil fuel emissions and the decrease of the external depedance on energy, namely those that are related with the reduction of fire risks by cleaning the forest, removing the combustible matters. To use this potential, the Portuguese Government, already in 1990, asked EDP [Energy of Portugal, S.A], the Portuguese utility, to build and manage a power plant, in which the input will be the forestry residues. CBE (Portuguese Centre for Biomass Energy) performed the studies and chose locations to implement the power plant, considering the region having thick forested areas. Another important reason to consider the locations, was the number of wood industries in the region, namely sawmills, which produce wood residues such as bark.

The commitment to renewable energies for electricity generation aims to meet 45% of the country's electricity requirements by 2010, 5% of which from forestry biomass. Energy, as an important growth factor for the Portuguese economy, represents a challenge for the country's sustainable development. The development of endogenous energy resources represents major potential for innovation and an important contribution to achieving the National Energy Strategy and Technological Plan. Forestry biomass is one of the priorities, given its impact on revitalising and boosting economic activity in the forestry strand, in addition to minimising fire risks. The issue of a tender for 15 new forestry biomass power stations represents an additional 100 MW and a total estimated investment of EUR 225 million. Preference has been given to two types of power station: [Energy of Portugal, S.A]

- Up to 12 MW, permitting economies of scale in electricity generation and ensuring a larger forestry bio mass collection area;
- Up to 6 MW, permitting the development of small local development units.

The location of the future power stations was pre-selected taking into account the availability of forestry biomass and structural fire risk. The new biomass power stations will make it possible to extract 1 million tonnes of wastes from national forests and create new dynamics of innovation in terms of forestry management and exploitation. The exploitation of forestry biomass for energy purposes is considered not only as a business opportunity and for its creation of employment in rural zones, but also as a fire-fighting instrument in the form of forest clearing operations. In environmental terms, the reduction in the emission of carbon dioxide (CO_2) by 700,000 tonnes will make it possible to converge with the targets defined in the Kyoto protocol. [Tarelho et al. 2011].

Currently Portugal has two thermal power plants dedicated to electricity production and connected to the national electric grid; both installations use forestry biomass as their main fuel. Most of the remaining plants are located in the center-north of Portugal in industries related with the wood and wood products sector and in the pulp and paper industry. The location of the main biomass to energy thermal plants existing in Portugal is shown in Figure 2.6(a).

In addition to these, nine cogeneration power plants are installed in forestry sector industries, which use biomass for combined heat and power production. There are also a wide range of other industrial consumers of biomass for heat production, although in at lower scale. In the very near future new biomass thermal power plants are scheduled to join with the existing ones, according to the energy policy of the Portuguese Government [Renewable energy in Portugal 2007] (Figure

2.6(b)). This will result in an increase of generation of several thousand of tonnes of biomass ashes per year requiring proper monitoring and management.

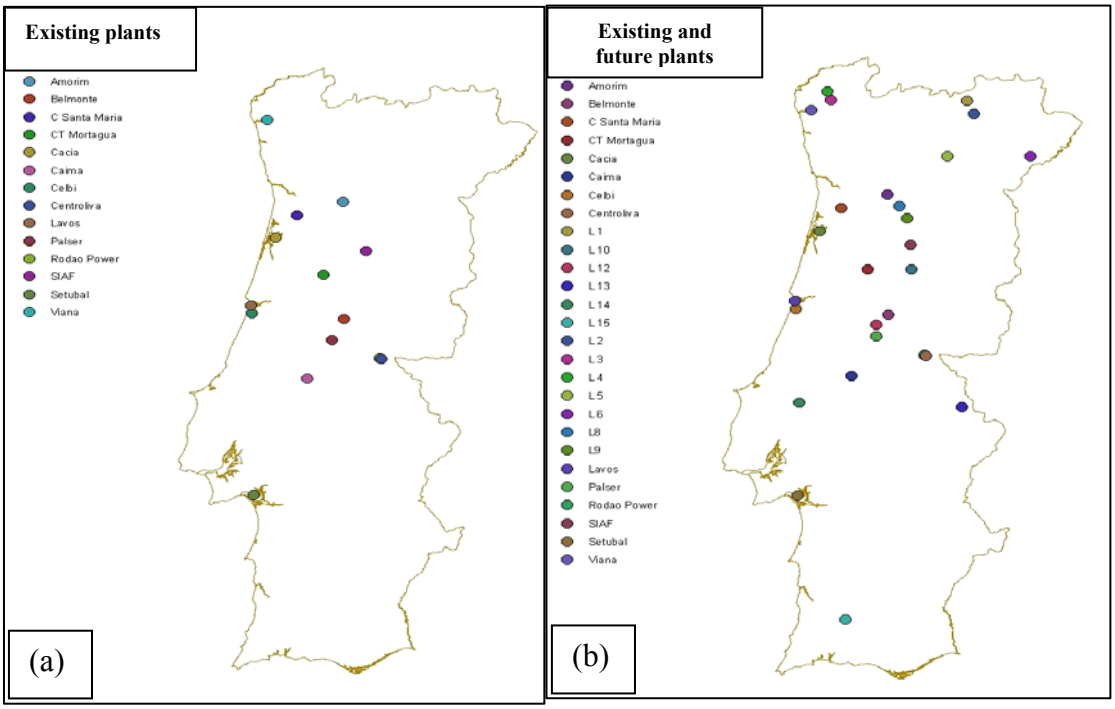

Figure 2.6: The main biomass thermal plants in Portugal. (a) Present (a) and (b) planned for the near future. (b) Main biomass thermal plants in Portugal. [Tarelho et al., 2011].

Still, there are no much detailed studies done so far on the estimation of biomass and the the ashes produced in Portugal. Based on a set of assumptions, namely, the estimated biomass needed to feed each plant based on its nominal thermal power, the biomass characteristics, and the thermochemical conversion technology used, the estimated amount of biomass ashes produced in Portugal nowadays, and in the future when the planned plants will be in operation, could be around 1.1×10^5 ton (dry)/year and 2.2×10^5 ton (dry)/year, respectively (Figure.2.7); and most of the ashes produced could be fly ashes [Tarelho et al. 2011].

The information about the management practices applied to that amount of ashes produced is also scarce. The biomass ashes from thermal power plants are classified as an industrial waste, with code 100101 or 100103 according to the European List of Wastes (Portaria nº 209/2004) [European list of waste 2000] and should be managed accordingly, and one common option is deposition in landfill. However, this practice brings considerable problems to the industrial plants owners, now looking for alternative options of biomass ash deposition on landfill.

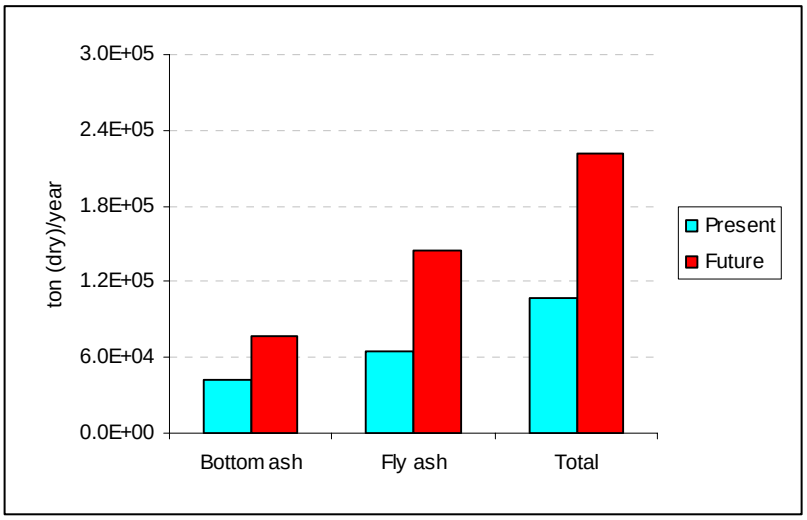

Figure 2.7. Estimated amount of (bottom and fly) ashes produced at present (estimated for the year 2010) in Portugal and in the future in biomass thermal plants and cogeneration plants. [Tarelho et al., 2011].

Nevertheless, some current practices include the utilization of biomass ashes in agriculture or in road construction. There are also some ongoing studies about the mixing of biomass ashes with other wastes, as for example sewage sludge and green parts of gardens maintenance, in order to produce a compost to be used in forestry and agriculture [Dias and Carvalho 2008].

There is a clear need for guidelines for a sustainable management of biomass ash especially biomass fly ash from thermal power plants and should be managed accordingly. In order to establish guidelines for a national practice of correct management of the diverse ash streams it is necessary to know the characteristics of the ash produced and the respective amount.This is very important considering the sustainability of the Portuguese biomass to energy policy also. .

CHAPTER 3 CHARACTERISATION OF BIOMASS FLY ASHES

3.1 Biomass fly ash - collection

Two types of biomass fly ashes were used for the characterisation analysis depending on the combustion technology used in the thermal plants. The biomass fly ash samples used were collected from the electrostatic precipitator of a biomass thermal power plant and of a co-generation plant; both located in Portugal and are named as BFA1 and BFA2 respectievely. Both the plants use forest wastes as main fuel (mainly eucalyptus wastes, resulting from logging and wood processing activities). The biomass fly ash samples were collected bimonthly during one year to monitor the trend of the physical and chemical variations in the fly ashes.

3.1.1. Biomass fly ash from grate combustion: - biomass fly ash BFA1

Grate furnaces are appropriate for biomass fuels with high moisture content, varying particle sizes (with a downward limitation concerning the amount of fine particles in the fuel mixture) and high ash content [Loo and Koppejan 2008]. The fly ash BFA1 was collected from a biomass thermal power plant dedicated to electricity production, which uses forest residues and grate combustion technology for energy production (Figure 3.1(a)).

The typical grate boiler was designed to burn (at full load) about 8.7 tonnes/h of residues with a LCV (low calorific value) of 13800 kJ/kg and 30% moisture content. The annual consumption of biomass is 109,000 tonnes. The annual generation of power at full load is 7.64 MW_{th}. Vibrating grate furnaces consist of an inclined finned tube wall placed on springs (Figure 3.1(b)). Fuel is fed into the combustion chamber by spreaders, screw conveyors or hydraulic feeders. Depending on the combustion process, two or more vibrators transport fuel and ash towards the ash removal. Primary air is fed through the fuel bed from below through holes located in the ribs of the finned tube walls. Due to the grate vibrating for short periods, the formation of larger slag particles is inhibited, which the reason why this grate technology is especially applied with fuels that are showing sintering and slagging tendencies (e.g. straw, waste wood). Vibrating grates causes high fly-ash emissions due to the vibrations of the grate. The thermal power plant from where BFA1 was collected uses forestry residues as the main fuel. The boiler uses natural gas as a start up and regulation fuel, burning the fuel mix. The combustion temperature is approximately 1000°C. In order to increase the total efficiency a fuel with 40% of pine bark and 60% of forest residues is

used. The boiler can produce a maximum steam flow of 11.1 kg/s at 42 bars and 422 °C. The generator is driven by a condensing turbine.

The biomass fly ashes were collected from the electrostatic precipitator. The biomass fly ashes used for the tests were collected fresh from the electrostatic precipitators.

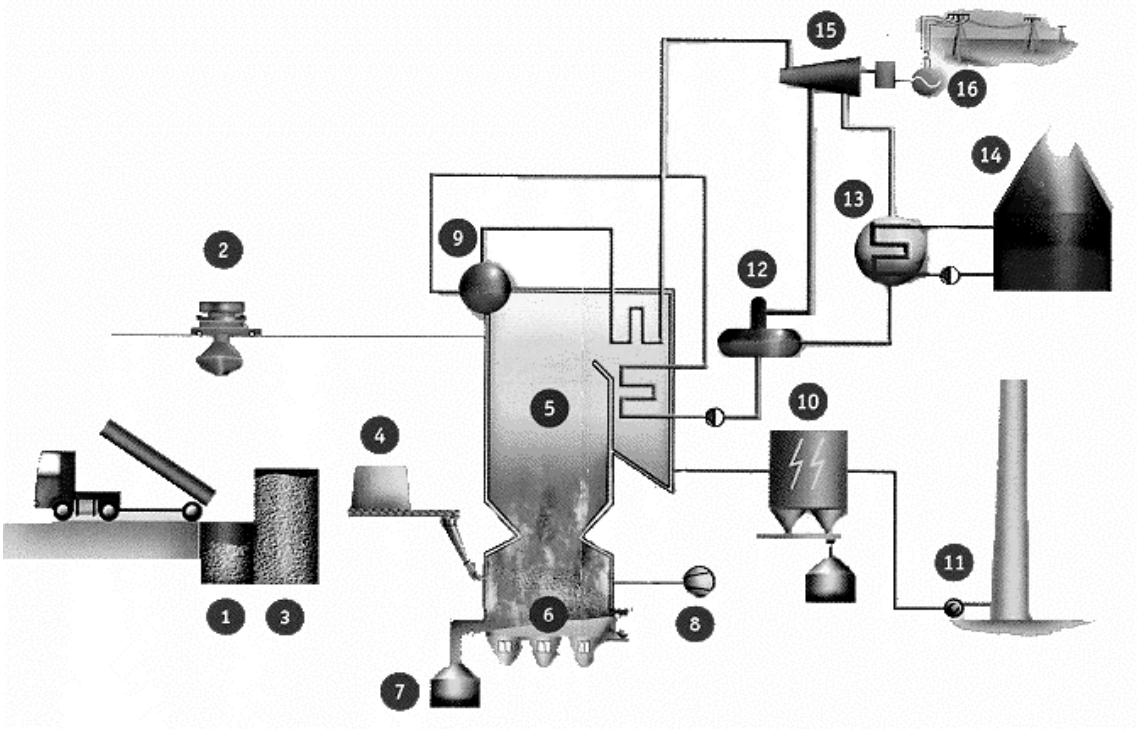

Figure 3.1(a). Schematic layout of a typical thermal power plant with grate furnace.

1 – Pit	7 – Bottom ash trays	12 – Degasifier
2 - Crane	8 – Fans	13 – Condenser
3 – Silo	9 – Holdfast	14 – Refrigerator Tower
4 – Hopper	10 – Electrostatic precipitator for fly ash	15 – Turbine
5 – Boiler	11 – Chimney	16 - Generator
6 – Grate		

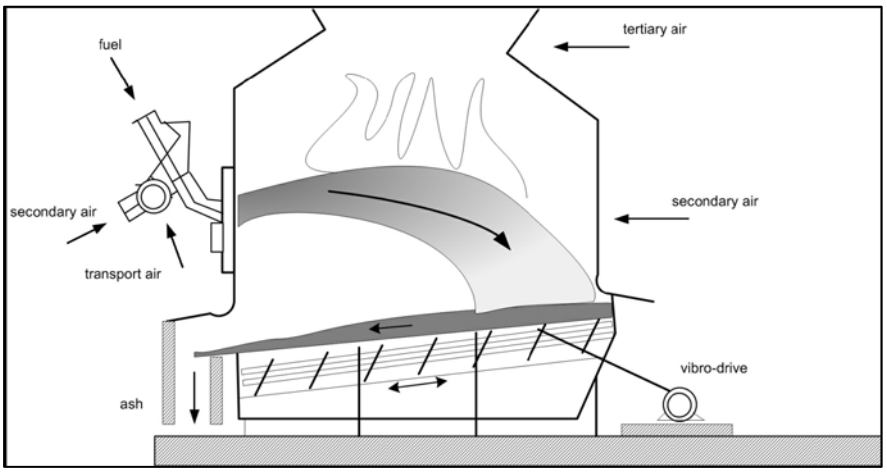

Figure 3.1(b). Vibrating grate fed by spreader stokers [Source:Loo and Koppejan 2008]

3.1.2. Biomass fly ash from fluidized bed combustion: - biomass fly ash BFA2

Fluidized bed combustion is an environmentally favourable, proven technology for disposal of solid wastes and generation of energy [Loo and Koppejan 2008]. Fluidized bed combustion systems use a heated bed of sand-like material, suspended (fluidized) within a rising column of air to burn many types and classes of fuel. This technique results in a vast improvement in combustion efficiency of high moisture content fuels, and is adaptable to a variety of waste type fuels. The scrubbing action of the bed material on the fuel particle enhances the combustion process by stripping away the carbon dioxide and char layers that normally form around the fuel particle. This allows oxygen to reach the combustible material much more readily and increases the rate and efficiency of the combustion process. The turbulence in the combustor vapour space (free board) combined with the tumultuous scouring effect and thermal inertia of the bed material provide for complete, controlled and uniform combustion. These factors are key to maximizing the thermal efficiency, minimizing char, and controlling emissions [Stratos 1991].

The high combustion efficiency of a fluidized bed results in a reduced amount of inorganic material as fine ash. The remaining larger material consists mainly of non-combustibles, such as rocks, and metallic strands brought in with the fuel, and coarse sand-like neutral particles. Low combustion temperatures in the fluidized bed minimize the formation of toxic materials that might go into the ash. The thermal "flywheel" effect of the bed material allows swings in moisture and heating content of the fuel to be absorbed by the system without negative impact [Stratos 1991].

The biomass fly ash BFA2 was collected from a co-generation plant - inside a pulp and paper industrial plant - where the fuel is burnt in a boiler with fluidized bed technology and a nominal thermal capacity of 90 MW_{th}. The paper pulp plant uses bubbling fluidized bed (BFB) combustion technology for fuel burning. The schematic diagram of a cogeneration power plant with BFB technology is shown in Figure 3.2(a). In BFB furnaces (3.2 (b)), bed material is located in the bottom part of the furnace. The primary air is supplied over a nozzle distributor plate from below and fluidizes the bed. The bed material is usually silica sand of about 0.5–1.0mm in diameter; the fluidization velocity of the air varies between 1.0 and 2.0m/s. The secondary air is introduced through several inlets in the form of groups of horizontally arranged nozzles at the beginning of the upper part of the furnace (called the freeboard) to ensure a staged-air supply to reduce NO_x emissions. In contrast to coal-fired BFB furnaces, the biomass fuel are not fed onto, but into, the bed by inclined chutes from fuel hoppers because of the higher reactivity of biomass in comparison to coal [Loo and Koppejan 2008]. The fuel amounts only to 1–2% (mass basis) of the bed material and the bed has to be heated (internally or externally) before the fuel is introduced. The advantage of BFB furnaces is their flexibility concerning particle size and moisture content of the biomass fuels. Furthermore, it is also possible to use mixtures of different kinds of biomass or to co-fire them with other fuels. In modern BFB furnaces a sub- stoichiometric bed operation is possible, which allows the bed temperature to be controlled in the range of 650–850 °C. Therefore, fuels with low ash-melting temperature can also be burned [Obernberger 1997].

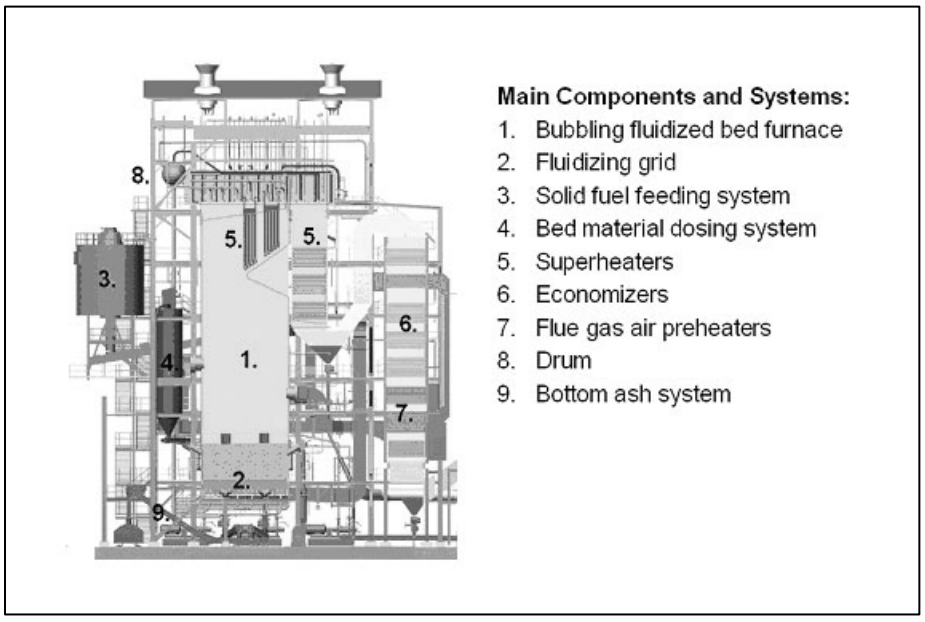

Figure 3.2 (a) Schematic diagram of bubbling fluidised bed boiler for biomass fuels.(Source:- http://www.tappsa.co.za/html_index_links/html_issue_Nov_09/biomass_boilers.html)

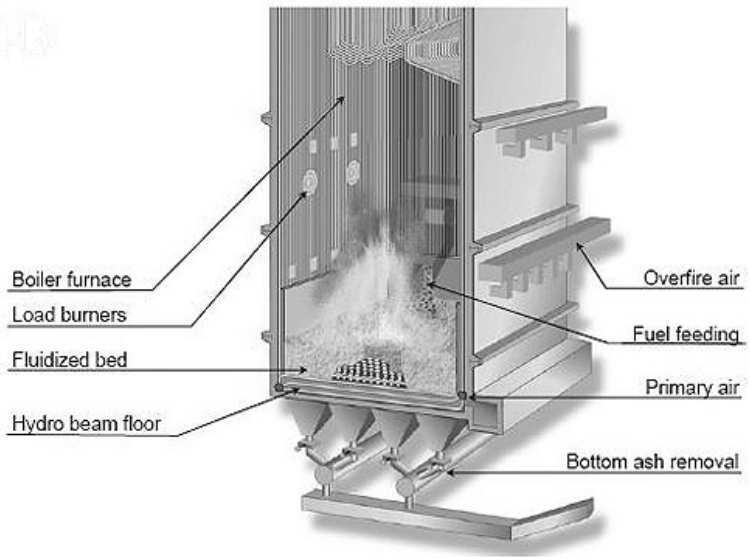

Figure 3.2 ((b) Inside of a BFB boiler: [Nussbaumer 1993]

3.2 Experimental techniques used for biomass fly ash characterization

3.2.1. Particle size distribution

The particle size distributions of the fly ashes were analysed by 1) sieving manually and 2) by a laser diffraction particle size analyser.

The manual sieving was done in 6 fractions with sieve number ranging from No4 –No 140. (4.75 mm, 2 mm, 850 µm, 425 µm, 250 µm, and 106 µm). Before the sieving process the fly ashes were subjected to a heating at 105ºC for overnight in order to remove the moisture content to prevent the agglomeration of the fine particles. A net content of 300g was used for the manual sieving for each sample. The amount retained in different sieves was weighed and was calculated for each size fraction.

In order to determine the particle size distribution of fly ashes below 1mm, a Coulter LS 230 (Coulter Electronics, Krefeld, Germany) equipped with PIDS technique (Polarization Intensity Differential Scattering) and running in Mie mode was used, as well as a Malvern Mastersizer Micro (Malvern, Herrenberg, Germany) running in Fraunhofer mode. The Coulter LS 230 uses a laser of 750 nm and a double Fourier lens setup for focussing the scattered light on the ring-shaped detector setup. The detection range (angles) for diffraction is claimed to be 40 nm - 2000 µm, thus theoretically covering the size range. The sieved fly ashes with a diameter <1mm (removing the coarse char particles) were used to find the particle sizes by laser interface.

3.2.2. Real density

The real density of a substance is the average mass per unit volume, exclusive of all voids that are not a fundamental part of the molecular packing arrangement. The real densities of the fly ash particles were determined using a gas pycnometer where Helium is used as the gas (ASTM D5550-06). The helium pycnometer allows measuring the volume and true density of solid objects, without damaging the samples.

The measured density is a volume-weighted average of the densities of individual powder particles. The biomass fly ash samples were dried in order to remove the moisture prior to the experiments. The mass of the volume was determined directly, and the volume was derived by the volume of helium displaced when the sample is introduced into the helium pycnometer. The ratio of the mass of the sample to the volume is reported as the real density. The test has a repeatability of 0.018 and reproducibility of 0.025 g/cm^3. Around 2 g of fly ash was used for each test. The real density was determined as the average of 3 test values.

3.2.3. Surface area

The surface area of the biomass fly ashes was measured by a BET ((Named after Stephen Brunauer, P.H. Emmet and Edward Teller developed in 1938) surface area analyser. The analyser was designed by Micromeritics Instrument Co Gemini which utilizes an adaptive rate, static volumetric technique. According to BET method the amount of gas adsorbed by the sample at a given pressure allows determining the surface area. Software is programmed to determine the specific surface area with the measured pressure differences. A sample weight of around 0.3 g is used in each measurement.

3.2.4. Mineral characterization

3.2.4.1. X-Ray Diffraction (XRD)

The mineral characterisation of the biomass fly ash samples were done using an X-ray diffractometer. RIGAKU-Geiger flex X-ray diffractometer was used for the diffraction analysis with a power 40 kV/30 mA, and scan mode continuous/speed-2◦ (/min). A C Series; CuKά radiation is used and the angle range 2Θ was 10º-80º. The fly ashes were dried to remove the moisture and were ground well in an agate mortar before the test was conducted.

3.2.4.2. Thermogravimetric and differential thermal analysis (TG/DTA)

Thermogravimetric and differential thermal analysis (TG/DTA) of the fly ashes were performed up to 1000°C with a heating rate of 10°C/min, in a simultaneous TG/DTA (STA 409 EP). The fly ashes were sieved to remove particles larger than 75 μm and dried at 120 ºC before performing the thermal analysis (TG/DTA) in order to remove the moisture content. The data were analyzed using software programs supplied with the instrument. The thermo gravimetric (TG) curve was corrected for buoyancy effect, and the differential thermal analysis (DTA) curve was corrected for baseline effect. Corrections for buoyancy and baseline effects were obtained in a blank run using empty crucibles that were later used to run the sample in a second run, but the two experimental runs were made under identical conditions.

3.2.5. Chemical characterization

3.2.5. 1. X-Ray Fluorescence Spectroscopy (XRF)

The chemical composition of the fly ashes was studied using X-ray fluorescence spectroscopy (XRF) a non-destructive spectroscopic method. The sample is irradiated by an intense X-ray beam (by a radioisotope source, or by an electron beam). The primary source "excites" the sample by removing/"knocking out" tightly bound electrons from the inner-shell orbital of the excited atom in the sample. Relaxation of the excited atom to the ground state is accompanied by the emission of fluorescent X-rays. The emitted X-rays are detected using an energy dispersive detector. The energies of the emitted X-rays are used to identify the elements present in the sample while the concentrations (how much) of the elements are determined by the intensity of the X-rays. The depth of sample analyzed varying from less than 1mm to 1cm depending on the energy of the emitted X-ray and the sample composition. The fly ashes were dried and ground and sieved through 100 μm for the analysis. During the analysis the samples were heated up to a temperature of 1000 ºC and the loss on Ignition was also determined.

3.2.5.2. X- Ray Photoelectron Spectroscopy (XPS)

VG Scientific Escascope X-Ray Photoelectron Spectroscopy (XPS), (Argon ion/neutral gun) was used for the analysis of surface chemistry of the biomass fly ashes. The low kinetic energy (0-1500 eV) of emitted photoelectrons limits the depth from which it can emerge so that XPS is a very surface-sensitive technique and the sample depth is in the range of few nanometers. Photoelectrons

are collected and analysed by the instrument to produce a spectrum of emission intensity verse electron binding energy. The elements present on the surface of the ash particles are quantified by measuring the kinetic energy and the number of electrons that escape from the top 1 to 10 nm of the material. Each element produces a characteristic set of XPS peaks at characteristic binding energy values that directly identify each element that exist in or on the surface of the material being analyzed. The number of detected electrons in each of the characteristic peaks is directly related to the amount of element within the area (volume) irradiated which is expressed is atomic volume percentage. XPS is performed under ultra-high vacuum (UHV) conditions. For XPS analysis the samples must be solid and vacuum compatible with a size range 4 mm to 20 mm in diameter. The dried fly ash samples were used for the XPS analysis.

3.2.5. 3. Raman Imaging Spectroscopy

Renishaw System 2000 micro Raman imaging spectrometer (632.8 nm red laser with integral Leica compound optical microscope, 5 accumulations, 10 second scan, 50x magnification lens) is used for the detection of Raman peaks in the biomass fly ash samples. The samples were used as such without any pre-treatment. Change in the molecular polarization potential or amount of deformation of the electron cloud with respect to the vibrational coordinate is required for a molecule to exhibit a Raman Effect. The amount of the polarizability change will determine the Raman scattering intensity. The pattern of shifted frequencies is determined by the rotational and vibrational states of the sample.

3.2.5. 4 Organic content

The ash content of the biomass fly ashes were characterised by the standard CEN/TS 14775. The ash content is determined by calculation from the mass of the residue remaining after the sample is heated in air under rigidly controlled conditions of time, sample weight and equipment specifications to a controlled temperature of 550 ±10ºC. This analysis allows the calculation of the ash, through the content of organic matter in the sample. It also allows inferring the combustion efficiency by assessing the amount of unburned material existing in the fly ash. The fly ashes are normally composed of inorganic materials (not fuel) and organic materials (fuel). If the combustion was 100% efficient, all organic material would be converted into CO_2 and H_2O (for example the carbon to CO_2 and the hydrogen to H_2O), with no combustible materials remaining in the fly ash (Bushnell et al., 1989). For this analysis samples should be used with a size less than 1mm in order to ensure complete burning. The as received fly ash samples were previously ground in agate mortar and then dried in an oven and weighed. They were then placed in the furnace and burned up

to 550ºC with a uniform increase for 50 min up to 250 ºC (heating rate of 5 ºC /min), soaked for 60 min, allowing volatilization of the samples before ignition, then followed another period of heating up by 10 °C/min to the temperature 550 ºC and remained at this temperature for about 4 hours. The samples were then removed from the furnace and weighed after cooling to constant weight. As in the determination of moisture content, also in the calculation of ash content was used a desiccator without desiccant material in cooling of the samples. When it is suspected that the samples were not completely burned were reintroduced into the furnace, in periods of 30 minutes, until confirmation of complete combustion. The ash content of the sample is determined using the equation 3.1

$$Z_{bs} = \frac{(m_3 - m_1)}{(m_2 - m_1)} \times 100 \longrightarrow \textbf{Eqn. 3.1}$$

where:

Z_{bs} - ash content in dry basis, expressed in percentage by weight

m_1 - mass of empty crucible (g);

m_2 - mass of empty crucible + sample (g);

m_3 - mass of empty crucible + ash (g);

During combustion at 550 ºC, organic matter is eliminated, leaving the mineral matter - the ash. Knowing the ash content, it is possible to know the content of unburned or organic carbon content, since the organic matter released during combustion is mostly carbon. The carbon content in dry basis (C_{bs}) is calculated using equation

$$C_{bs} = 100 - Z_{bs} \longrightarrow \textbf{Eqn. 3.2}$$

Around 2-4 g fly ash was taken for each experiment and a minimum of two determinations are carried out on each test sample.

3.2.5. 5. Determination of chlorides and sulphates

The chloride and sulphate contents of the fly ashes were determined by the Argentometric method (CHLORIDE, 4500-Cl^-; Standard Methods Committee 1997) and the Gravimetric method (SULFATE, 4500-SO_4^{-2}; ignition of residue, Standard Methods Committee 1997), respectively.

In order to make the sample for the analysis the 100 g of dried biomass fly ash is dissolved in 1 liter of double distilled water and stirred the solution for 24 hours keeping on a magnetic stirrer. When the stirring period is completed the solution is filtered and 100 ml from it is used for the titration purpose.

In the titration procedure the chlorides are titrated with the silver nitrate solution in the presence of chromate anions. The end point is signaled by the appearance of the red silver nitrate. In low pH silver chromate solubility grows due to the protonation of chromate anions, in high pH silver starts to react with hydroxide anions, precipitating in the form of AgOH and Ag_2O. Both processes interfere with the determination accuracy. So the PH of the solution is reduced to 7 by adding sulfuric acid. Potassium chromate solution was added as the indicator to the solution to give a slightly yellow colour and was titrated against 0.0141M Silver nitrate. After all the chloride has been precipitated as white silver chloride, the first excess of titrant results in the formation of a silver chromate precipitate, which signals the end point. The reactions are:

$$\mathbf{Ag + Cl \longrightarrow AgCl(\ s)}$$

$$\mathbf{2Ag^{+} + CrO_{4} \longrightarrow Ag_{2}CrO_{4}\ (s)}$$

By knowing the stoichiometry and moles consumed at the end point, the amount of chloride in an unknown sample can be determined.

In gravimetric method of determining the sulphate content, the fly ash sample is dried, weighed and dissolved in dilute HCl. Barium chloride solution is added in excess to precipitate barium sulphate, and the precipitate is digested in the hot solution. The precipitate is filtered through a paper filter which is then ignited and completely ashed. From the weight of the sample and weight of the precipitate, the percentage of sulphate in the sample is calculated. The precipitation reaction is the following:

$$\mathbf{Ba^{2+}\ (aq) + SO_4^{2-}\ (aq) \longrightarrow BaSO_4\ (s)}$$

3.2.6. Microstructural analysis

3.2.6. 1. Scanning electron microscopy (SEM) and Energy dispersive analysis (EDS)

The microstructure of the ash samples was studied using a scanning electron microscope (SEM) (Hitachi S2300 SEM with EDX25KV and SU70). The applied voltage was kept at 15kV. Samples were attached to aluminium stubs using carbon sticky pads and in some cases silver dag. A layer of gold was applied using a Edwards Scan coat 6 for duration of 90 seconds. During EDS, a sample is exposed to an electron beam inside a scanning electron microscope (SEM). These electrons collide with the electrons within the sample, causing some of them to be knocked out of their orbits. The vacated positions are filled by higher energy electrons which emit X-rays in the process. By analyzing the emitted X-rays, the elemental composition of the sample can be determined. The EDS count signal was kept for 3 and 5 minutes.

3.2.6. 2. Environmental scanning electron microscopy (ESEM)

The Environmental SEM retains all of the performance advantages of a conventional SEM, but removes the high vacuum constraint on the sample environment. Wet, oily, dirty, non-conductive samples may be examined in their natural state without modification or preparation.

For the present work a Phillips Electro Scan 2020 environmental scanning electron microscope (ESEM) equipped with a Peltier cooling stage was used for the studies. Images were obtained at an accelerating voltage of 20 kV and filament current of 2.5 A. The microscope was operated in wet mode, using water vapour as the imaging gas. A gaseous ion detector was used with a sample chamber pressure of 5 Torr for imaging and 15 Torr when flooding. The chamber was flooded 3 times after loading the sample. The images were obtained with a close up detector with a working distance of 1mm.

The difference in technology between the SEM and ESEM instruments is that instead of using a single pressure limiting aperture in conventional SEM, ESEM uses multiple Pressure Limiting Apertures (PLA's) to separate the sample chamber from the column. The ESEM offers high resolution secondary electron imaging in a gaseous environment of practically any composition, at pressures as high as 50 Torr, and temperatures as high as 1500°C. ESEM uses a proprietary Environmental Secondary Detector (ESD) which can function in non-vacuum environment. The ESD uses the principle of gas ionization (Figure 3.3). By applying a positive potential of a few

hundred volts to the detector, the secondary electron emitted by the sample when interacts with electron beam is attracted to detector. As the electrons accelerate in the detector field, they collide with gas molecules. The resulting ionizations create additional electrons, amplifying original secondary electron signal, and positive ions. The detector collects secondary electron signal and passes it directly to an electron amplifier. In nonconductive samples the positive ions created in gas ionization process are attracted to the sample surface and they effectively suppress charging artefacts.

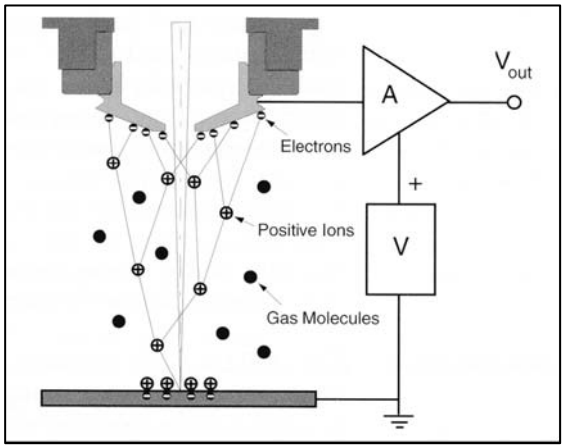

Figure 3. 3. The schematic diagram of the working of environmental scanning detector [Athene et al. 1998]

3.2.7. Leaching tests

Leaching of biomass fly ash was calculated using the German Standard DIN 38414-S4, with the aim of determining the soluble elements in water under the conditions of this method. Samples with a mass equivalent to 100 g dry were taken, and were placed in 2000 ml beakers along with 1 liter of distilled water, and been subjected to shaking using a mechanical rotary shaker (avoiding the reduction of particle size, for example due to abrasion). After 24 hours the samples were filtered through membrane filter of cellulose nitrate with 0.45μm. Then the volume of eluate obtained, the pH and conductivity, were measured using the equipment pH 211 Microprocessor pH Meter and EC 215 Conductivity Mete (Hanna Instruments). Samples were subjected to a second leaching, adding the same volume of distilled water, and then repeating the whole process. In order to preserve the eluates for analysis by Inductively Coupled Plasma - Mass Spectroscopy (ICP-MS) , the eluates were acidified with the addition of approximately 10 ml of nitric acid 65% (JTBaker) per liter sample.

From the quantities of each element in each eluate, the volume filtered and the initial mass of the sample leached determines the proportion of element leached in the initial sample, according to equation 3.3.

$$\omega_{ES} = \frac{\beta \times V_E}{m_S} \longrightarrow \textbf{Eqn. 3.3}$$

Where:

ω_{ES} – is the proportion by mass of a substance leached from the aqueous sludge sample (mg/kg);

β - mass concentration of leached substance in the eluate (mg / l);

V_E - filtered volume of eluate (l);

m_S– is the initial mass of the original sample of the aqueous sludge (in kg) (wet basis);

Since two leaching tests were performed for each ash, total ω_{ES} is the sum of each leaching values. The proportion by mass of the leached substance in the ash sample was then calculated on a dry basis, applying the equation 3.4.

$$\omega_{ET} = \frac{\omega_{ES} \times f}{\omega_T} \longrightarrow \textbf{Eqn. 3.4}$$

where: ω_{ET} –is the proportion by mass of the leached substance in the dry residue of the sample under examination, (in mg / kg);

ω_T – is the dry residue of the sample under examination (%);

f - conversion factor (f = 100%);

The ratio between the amount of each element leached and the total amount of the element in the dry residue is calculated according to equation 3.5

$$\omega_R = \frac{\omega_{ET} \times f}{\omega_{GT}} \longrightarrow \textbf{Eqn. 3.5}$$

Where: ω_R - the proportion by mass of element leached over the sample -(%);

ω_{GT} - mass of element in the sample (mg / kg);

f - conversion factor (f = 100%)

The elemental analysis of the solid biomass fly ashes were also studied using Inductively Coupled Plasma Mass Spectroscopy (ICP-MS) method, a widely used technique for multi element analysis, since it allows a single scan to evaluate qualitatively almost all elements of the periodic table. Digestion was performed based on a modification of the standard CEN / TS 15290:2006- Samples of 100 mg of materials subjected to microwave digestion in Teflon bombs adding 4 ml of nitric

acid HNO_3, 65% (m / m) and 1 ml of hydrofluoric acid HF 40% (m/m).The ICP-MS allows the use of the highly abrasive hydrofluoric acid. After the microwave digestion, the samples were taken in bottles, by adding ultrapure water of 250 ml. Then they were analyzed using the apparatus Thermo X Series.

3.2.8. Pozzolanicity

A pozzolan is defined (ASTM C125) as "a siliceous and aluminous material which, in itself, possesses little or no cementitious value but which will, in finely divided form in the presence of moisture, react chemically with calcium hydroxide at ordinary temperature to form compounds possessing cementitious properties". A wide range of test methods both direct and indirect for assessing pozzolanic activity have been reported in the literature. In this work three pozzolanic activity test methods have been used to assess the pozzolanic activity of the biomass fly ashes. The direct tests used among them were the Frattini test and the modified Chapelle test, and the indirect test used was the strength activity index test. The Frattini test and strength activity index test were selected because they have been widely reported and standard procedures exist (BS 3892, EN 196-5 and ASTM C311). The modified chapelle test method was selected because it is simpler than the Frattini test and provides quantitative results from a direct reaction of fly ash with the calcium hydroxide. [NF P 18-513, Annex A].

3.2.8.1 The Frattini Test

The Rio Frattini method is a commonly used direct method that involves a chemical titration to determine the dissolved Ca^{2+} and OH^- concentrations in a solution containing CEM-I and the test pozzolan. This method has been widely used to measure the pozzolanic activity of metakaolin, catalytic cracking residues, crushed bricks and fly ash. The pozzolanicity is assessed by comparing the quantity of calcium hydroxide in the aqueous solution in contact with the hydrated cement, after a fixed period of time, with the quantity of calcium hydroxide capable of saturating a solution of the same alkalinity. The material tested is considered to be pozzolanic if the concentration of calcium hydroxide in the solution is lower than the saturation concentration.The procedure is described in the Standard EN 196-5:2005. According to this standard, pozzolanicity was determined by measuring the concentration of CaO and OH^- ions in the reacted solution of the test material with high grade cement. The concentrations of ions were determined by titration methods. The appropriate amounts of the test material, high grade cement and double distilled water were mixed in a plastic bottle and were kept in an oven at about 40 ºC. After 14 days the solution was

filtered and titrated against HCl and EDTA solutions to find out the OH− and CaO concentrations, respectively.

3.2.8. 2. The modified Chapelle´s Test

According to Chapelle test [NF P 18-513, Annexe A], the pozzolanic reactivity is evaluated on the basis of the amount of $Ca(OH)_2$ consumed per gram of test material during the pozzolanic reaction. To carry out the Chapelle test, 1 g of biomass fly ash and 2 g of previously decarbonated CaO were added to 100 ml distilled water and kept for heating at 85 ± 5ºC, to provide a lime/ash ratio of 2:1. During reaction, in a continuous, agitated system which uses a magnetic stirrer, the volume of the solution was maintained constant using a refrigerant (Figure 3.4). After 16h the unreacted lime was dissolved by adding 60 g of sugar to the solution (by dissolving sugar in 250g of water) to form a calcium saccharate complex. Titration was performed using a 0.1 N HCl solution using phenolphthalein as an indicator, which changes from purple to colourless. The results are expressed in terms of mg of $Ca(OH)_2$ fixed by the biomass fly ash.The minimum amount of $Ca(OH)_2$ fixed by a material should be 650mg/g inorder to consider it as pozzolanic[Raverdy et. al 1980].

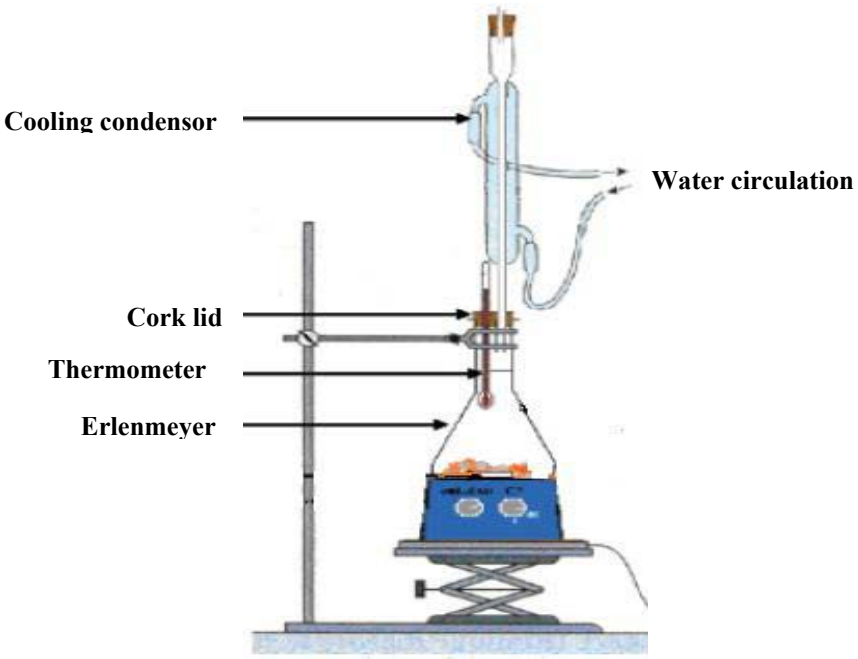

Figure 3. 4. The modified Chapelle´s Test apparatus (NF P 18-513, Annexe A).

3.2.8. 3 Pozzolanic activity index (Compressive strength of mortars)

The pozzolanic activity index (PAI) of biomass fly ashes were determined according to the European standard EN 450. PAI is the ratio of the compressive strength of standard mortar bars, prepared with 75% reference cement plus 25% ash by mass, to the compressive strength of standard mortar bars prepared with reference cement alone, when tested at the same age. If these indexes are higher than 0.75 at 28 days the tested material is considered as pozzolanic. Control mortar blocks were prepared by mixing 1200 g sand, 400 g CEM-I and 220ml water in a planetary orbital mixer for 4 min. Test samples were prepared in the same manner, except that 25% of the CEM-I was replaced with the test pozzolan. Mortar blocks were made with the dimensions of 16cmx4cmx4cm All blocks were de-moulded after 24 h and placed in a water bath at 40 ºC for 90 days. They were then removed from the bath, surface dried and tested for 28 days and 90 days compressive strength. Strength results reported are the averages of three tests and are presented as percentage strength relative to the control mortar with the strength activity index (PAI) therefore reported as

$$\text{PAI} = A/B \times 100 \longrightarrow \text{Eqn. 3.6}$$

where A is the unconfined compressive strength of the test pozzolan specimen (MPa) and B is the unconfined compressive strength of the control mortar (MPa)

3.3. Results and Discussions

3.3.1. Particle morphology

From **Figure 3.5.** it can be noted that the biomass fly ashes were significantly different in appearance in terms of colour. The colour of the fly ashes BFA1 and BFA2 were black and grey respectively. Presence of coarse char particles were visible in the fly ash BFA1 compared to BFA2 fly ash. Char is the coarse part of the fly ash, mostly made of partially burnt biomass particles and it is the prime reason for the colour difference in these biomass fly ashes.

in general the colour of the ashes is largely dependant on the amount of unburnt carbon present in the ashes. In the cases of coal fly ashes some researches showed that the colour of the fly ashes are controlled by some chemical components in the ashes also such as iron (Fe) and lime (CaO).

[Akhmad et al. 2010, Yufen et al. 2005, Cockrell et al. 1970]. Other studies indicate that only particle size and its shape determine the colour of fly ash [Akhmad et al. 2010, Yasuda et al. 1991 .

Figure 3.5. Biomass fly ashes (a) BFA1 and (b) BFA2.

The fly ashes were irregular in shape and sizes. The ESEM images taken for the ashes under finer fraction (< 75 μm) reveal that biomass fly ashes are largely heterogeneous with particles of varying shapes (Figure 3.6). It can be noticed that elongated char particles were present in BFA1 and the particle shape and size appears more irregular compared to biomass fly ash BFA2. The fly ash appearance is indicating the presence of particles, which were unburned, or partially burned wood or bark particles. Calcium carbonate crystals were also observed in BFA2 fly ash in significant portions (Figure 3.6. 2c).

It can be suggested that for BFA1 and BFA2, the major reason for the colour change is the difference in the unburnt carbon content. The fly ashes BFA1 and BFA2 were burnt at a grate furnace and fluidized bed furnace respectively at a temperature between 700-1000ºC. The burning technology used in the fluidized bed furnace is more efficient than in the grate furnace though the burning temperature is less than that of the grate furnace and it has naturally resulted into the difference in the carbon content in these biomass fly ashes [Stratos 1991].

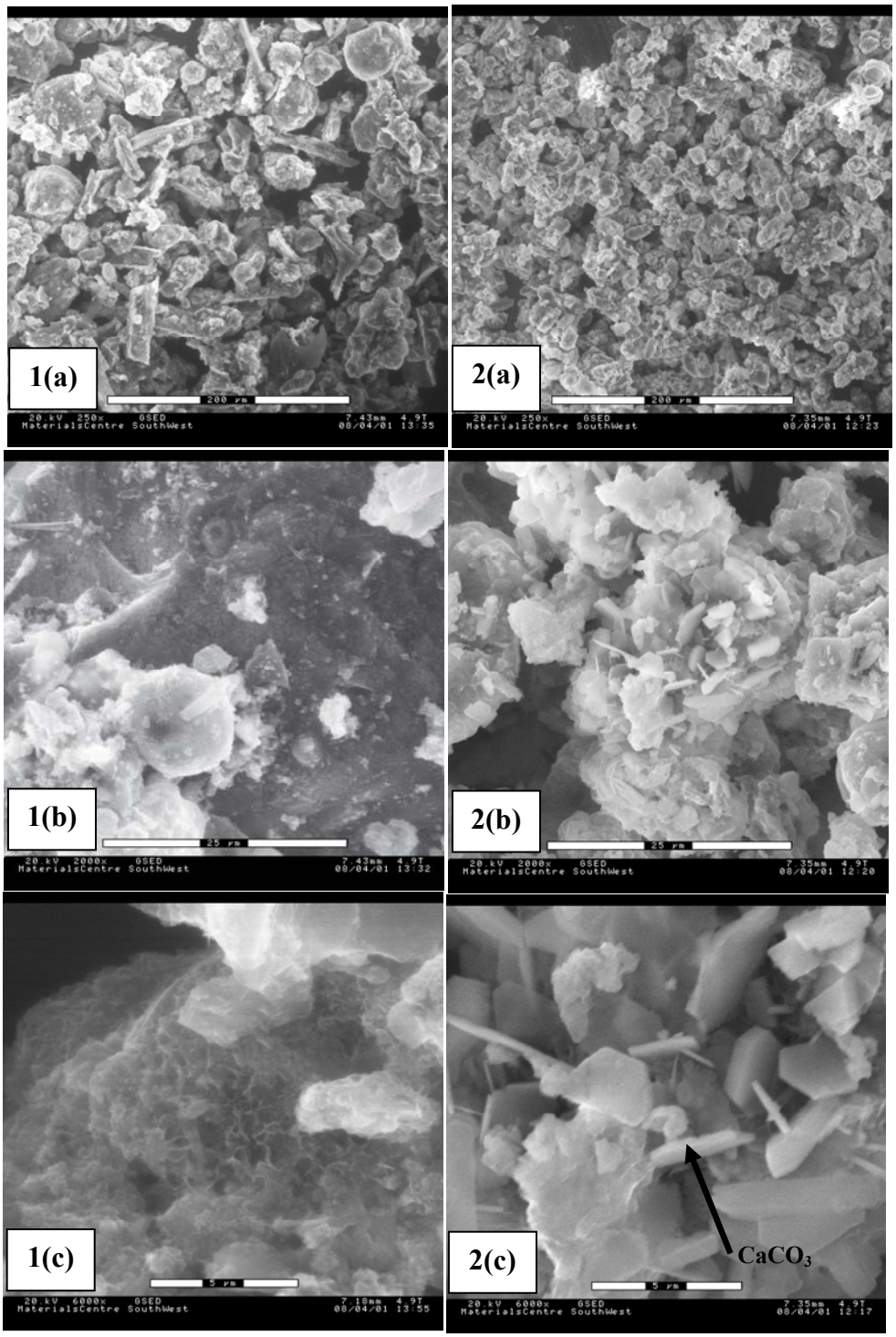

Figure 3.6. ESEM pictures of 1) Biomass fly ash BFA1 and 2) Biomass fly ash BFA2.

3.3.2 Fineness

The manual sieving method was used for the particle size distribution of biomass fly ash in the higher particle size range (>75 µm). A Colter particle size analyzer was used for the size distribution of fine fractions. The particle size distribution determined by the manual sieving is shown in Figure 3.7. It can be noticed that both the fly ashes are moderately fine in nature having a significant percentage of fine fractions below 75µm (-70%). Biomass fly ash BFA2 shows a slightly higher volume percentage under the size range 75µm. On physical observation it can be noticed that, the particles size greater than 1mm contained unburned fly ash in high amount. The particles in these size fractions are because of the unburnt or partially burnt wood particles that were captured in the electrostatic precipitator from where these fly ashes were collected. The fly ash distribution in both ashes show a similar trend of distribution at different volume fractions from 4.75 mm - 75 µm. The size of the biomass fly ash particle is determined by both the burning conditions and also the capturing conditions at the electrostatic precipitator.

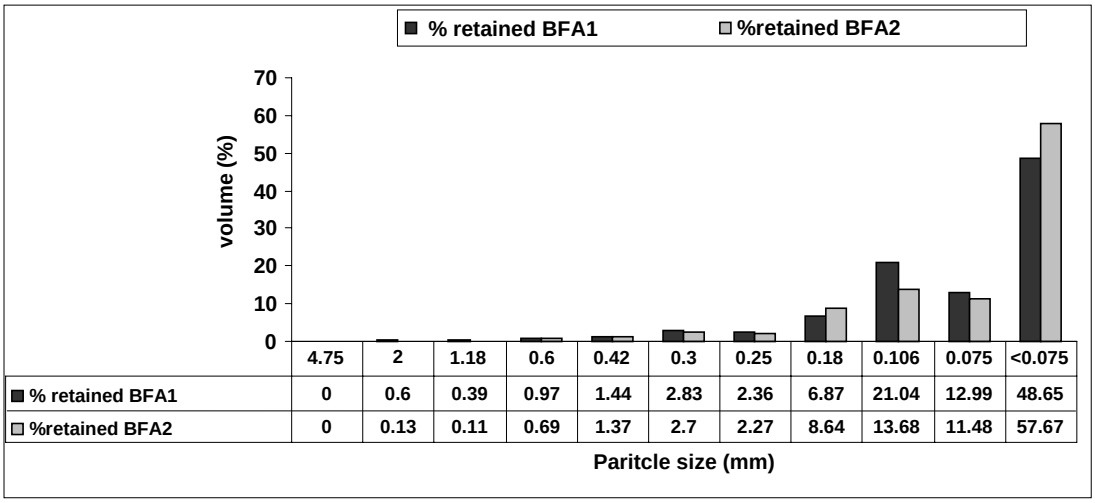

	4.75	2	1.18	0.6	0.42	0.3	0.25	0.18	0.106	0.075	<0.075
% retained BFA1	0	0.6	0.39	0.97	1.44	2.83	2.36	6.87	21.04	12.99	48.65
%retained BFA2	0	0.13	0.11	0.69	1.37	2.7	2.27	8.64	13.68	11.48	57.67

Figure 3.7. Particle size distribution of biomass fly ashes by manual sieving.

From the Colter particle size analyser it could be inferred that the overall particle size distribution of the ashes cut at 1 mm were typically below 100 µm with a mean particle size 52.9 µm and 16.0 µm for biomass fly ash BFA1 and BFA2 respectively. The particle size distribution of the fly ashes in terms of fly ash passed and retained are shown in Figure 3.8 - Figure 3.10. The distribution analysis shows that volume fraction between 1mm and 75µm are higher for BFA1 while BFA2 shows an increase in the volume fraction below 75 µm.

Table 3.1 gives a comparison study of the fly ashes. The results prove that the biomass fly ash BFA2 is no much different from BFA1 in particle size distribution. The slight increase in the content of finer fraction (<75 µm) compared to BFA1 which is an outcome of the difference in the efficiency of burning procedure as well the capture quality of the electrostatic precipitators.

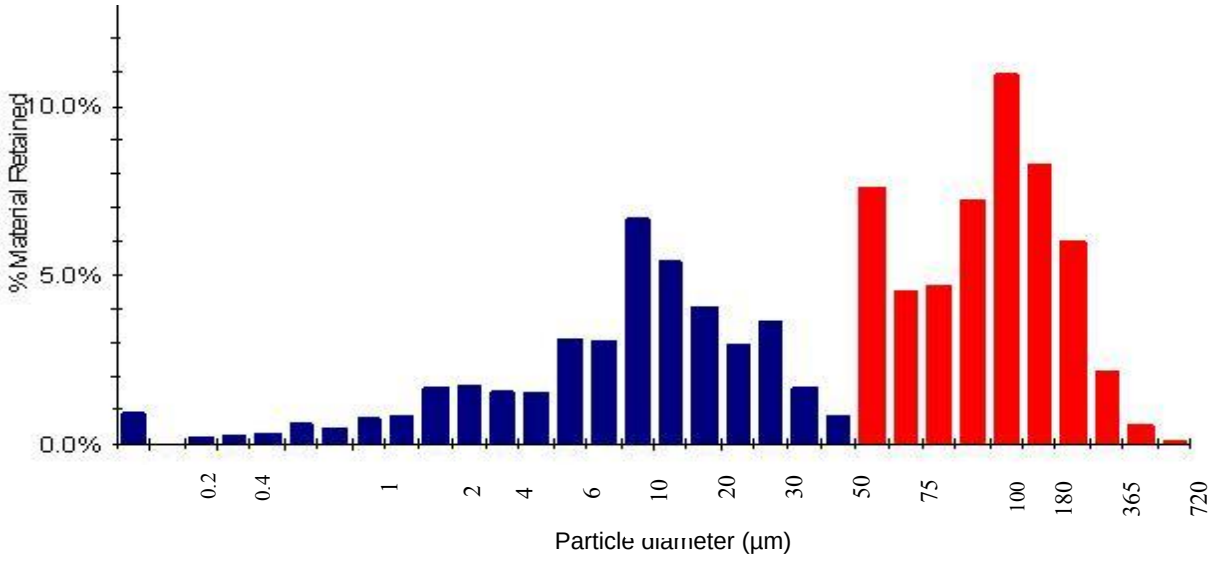

Figure 3.8. Particle size distribution (in volume) of biomass fly ash BFA1.

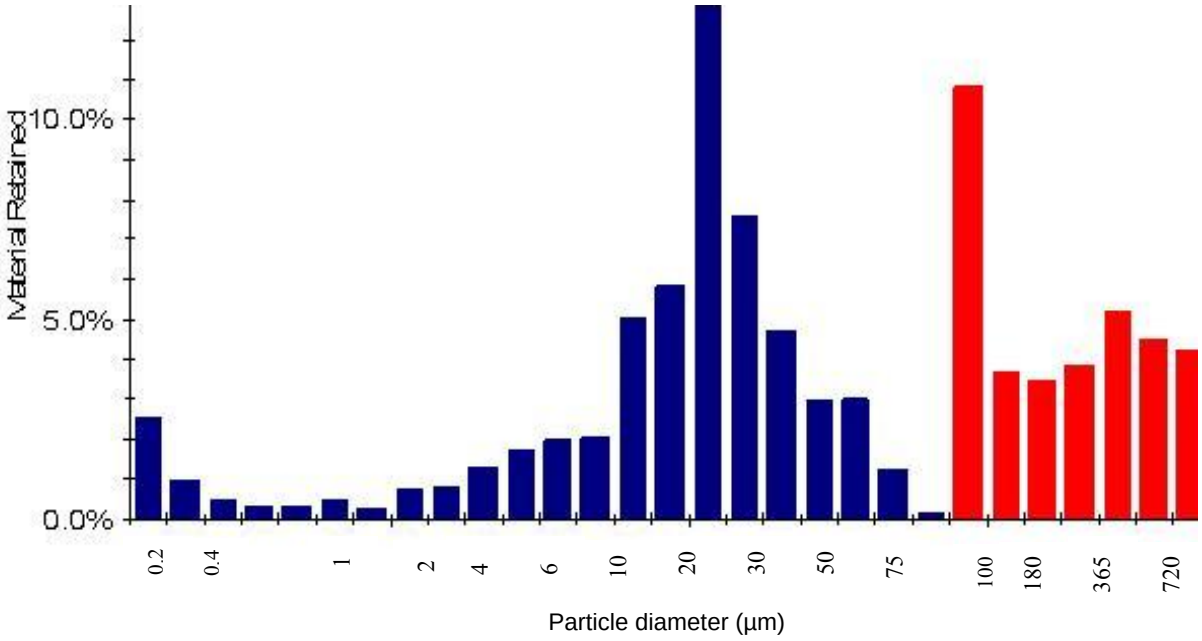

Figure 3.9. Particle size distribution of biomass fly ash BFA2.

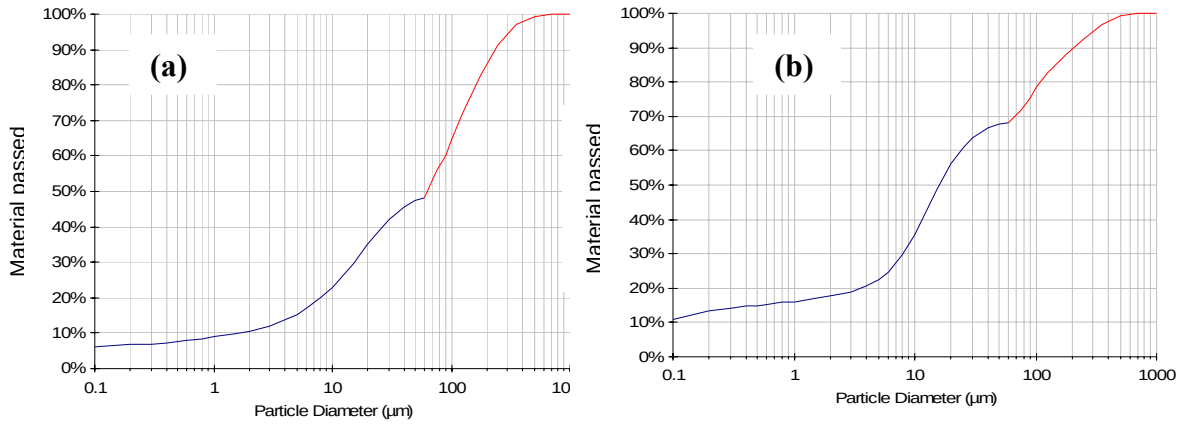

Figure 3.10. Cumulative particle size distribution of biomass fly ashes (a) BFA1 and (b) BFA2 in terms of the material passed through

Table 3.1. Particle size distribution (after sieving in 1mm mesh)

Fraction of particles	*Biomass Fly Ash BFA1 (%)*	*Biomass Fly Ash BFA2 (%)*
1mm - 500 µm	0.6	0.8
500 µm - 75 µm	44.3	28.4
75 µm – 2 µm	45.3	53.9
< 2 µm	10.4	17.7

A similar observation was made by Naik et al (1999) where he estimated that around 50% of the wood fly ash particles are under the size range 75 µm. Wang et al. (2008a) also suggested that most of the fly ash particles have diameter within the 30-130 µm. A recent research done on the fly ash characterisation of biomass fly ash collected from some other thermal power plants in Portugal also showed similar values [Tarelho et al. 2011]. The similarities in the results gives a standard data base for the size distribution and density of the biomass fly ashes, no matter the kind of wood is used or the combustion conditions.

3.3.3. Real density and surface area

The real densities of the ash particles below 75 µm (afterremoving the char content), BFA1 and BFA2 were determined as 2.59 and 2.54 g/cm^3, respectively after conducting three experiments for each ashes. Both fly ashes were significantly lighter than that of the cement powder which was 3.04 g/cm^3. The porous and irregular shapes of the biomass fly ashes are the reasons for the lightness.

Some other researches reported the real densities in the range 2.1- 2.6 g/ cm^3 [Naik et al.2003, Abdullahi 2006].

The surface area of fly ashes with 3 fractions were evaluated as shown in Table 3.2. Fineness of the ash particles and their irregular shapes play a significant role in the surface area. Theinterestingly higher value of surface area for fly ash BFA1 compared to that of fly ash BFA2 can be also explained as highly porous and adsorbing nature of the char present in the biomass fly ashes indicating an inefficient burning of the wood in the particular grate boiler. The suface area determined for the biomass fly ashes collected from some other Portuguese plants also showed similar values. (Tarelho et al. 2011). In that case both fly ashes from the grate and from the fluidized bed show the higher specific surface areas, with values between 13 and 14 m^2/g; yet the higher values are observed for the grate.

Table 3.2. Surface area of the typical fractions of the biomass fly ashes

Fly ash fractions	*Surface area (m^2/g)*	
	Fly ash BFA1	Fly ash BFA2
As received	52.97±0.07	7.21±0.02
< 500 μm	37.82±0.05	9.42±0.02
< 75 μm	40.29±0.04	7.92±0.03

3.3.4. Mineral Characterization

3.3.4.1 X - Ray Diffraction patterns

The X-Ray diffraction patterns shown in Figure 3.11. and Figure 3.12 suggest the presence of quartz (SiO_2) and Calcite ($CaCO_3$) as the major mineral components in both the biomass fly ashes;therese are the common minerals in biomass fly ashes [Elinwa and Mahmood(2002), Loo and Coppejan (2008)]. Portlandite ($Ca(OH)_2$), feldspar $K(AlSi_3O_8)$ and anhydrite ($CaSO_4$) were also present in the biomass fly ashes. In BFA2 a peak of calcium silicate (Ca_2SiO_4) was also observed. The possibility of the presence of minerals like magnetite (Fe_3O_4), microcline ($KAlSi_3O_8$), mullite ($Al_2O_3.SiO_2$), periclase (MgO), plagioclase (NaCa) etc are also expected [Udoeyo et al. 2006] though not identifiable in the present diagram. But these minerals do not have any reactive contributions in the cement formulations. The same trend of minerals are observed when samples from different batches of collection were tested.

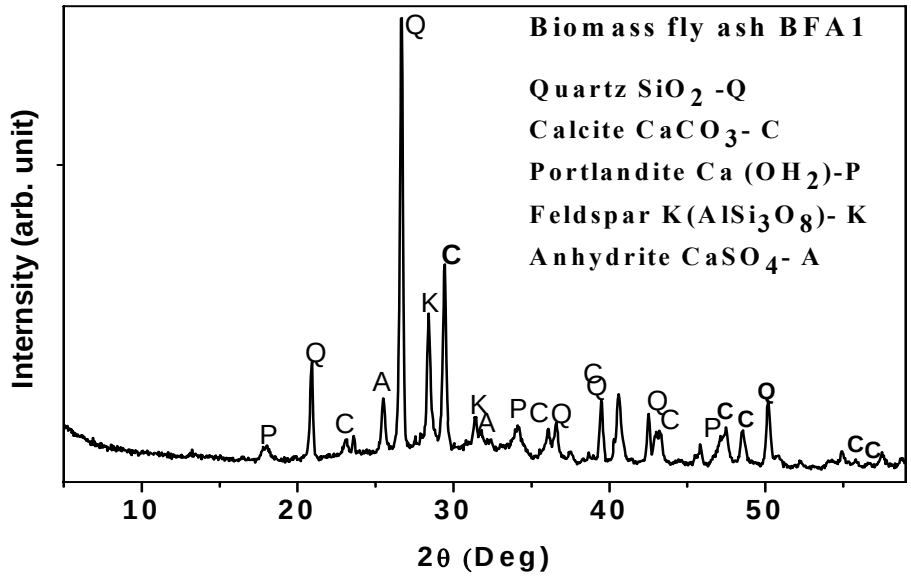

Figure 3.11. X-Ray diffraction patterns of biomass fly ahes BFA1

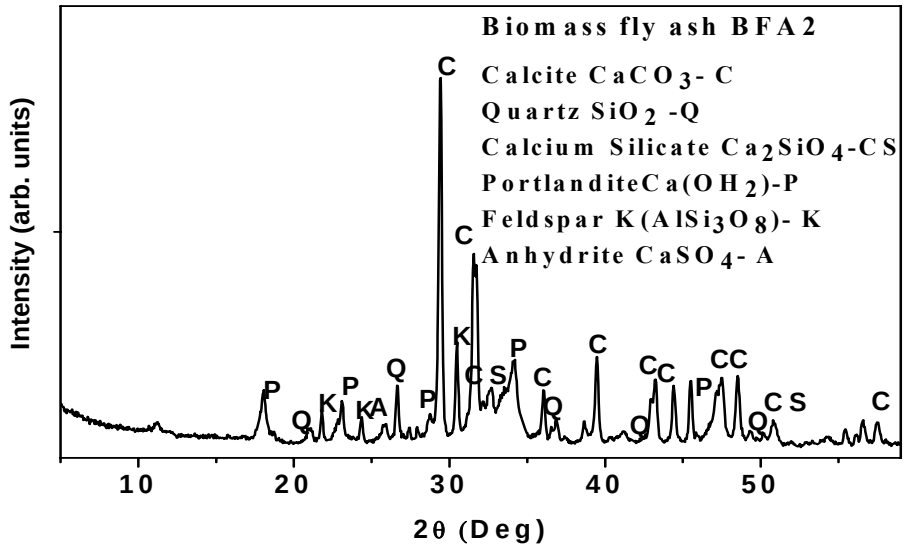

Figure 3.12. X-Ray diffraction patterns of biomass fly ash BFA2.

The XRD patterns give only slight indication of the amorphous content in the biomass fly ashes (a small hump around 30º 2Θ). The lower content of reactive pozzolans in the fly ashes will make the ashes less pozzolanic.

3.3.4.2. Thermo gravimetric/differential thermal Analysis (TG/DTA)

The TG/DTA curves of biomass fly ashes are shown in Figure 3.13 and Figure 3.14. Two major variations in temperature were seen in the TG/DTA in the range of 300 ºC - 600 ºC and at around 800 ºC in both ashes indicating the presence of organic matter and Calcite. The exothermic combustion of wood materials occurs in the range 300-600ºC and the end thermal decomposition of Calcite at 800ºC. The total loss on ignition was around 25% in BFA1 while it was around 18 % in

BFA2. The TG/DTA curves indicated that fly ash BFA1 contained more organic matter than fly ash BFA2, so explaining its higher loss on ignition. In fact, although the biomass is burned under sufficiently high temperature (750ºC-1000ºC) in the furnace, there is always some inefficiency on carbon conversion due to kinetic and mass transfer limitations. Consequently, the fly ashes present some amount of organic matter. The calcite decomposition in BFA1 is overlapped by the high organic content decomposition that disrupted the DTA of the BFA1 in the temperature range 600-800 making it difficult to determine the calcite content from the TG data. In BFA2 the calcite content is estimated to be more than 15% from the TG data in the temperature range 650-825ºC..

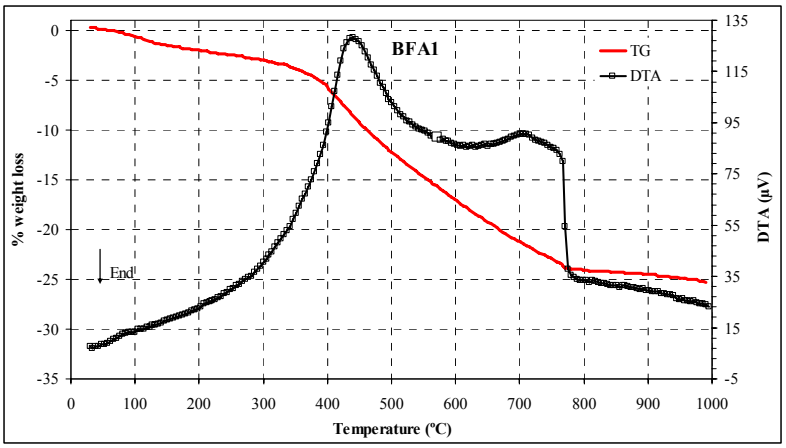

Figure 3.13. TG/DTA analysis of biomass fly ashes BFA1.

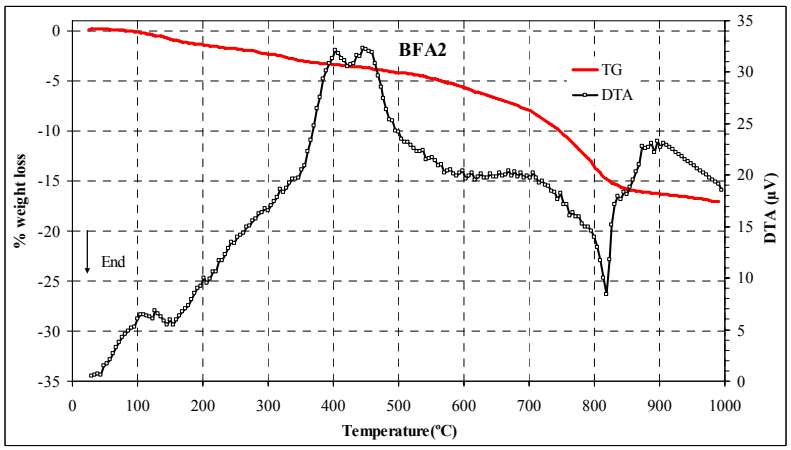

Figure 3.14. TG/DTA analysis of biomass fly ashes BFA2.

3.3. 5. Chemical Characterisation

3.3. 5. 1 X-Ray Fluorescence Spectroscopy (XRF)

The chemical composition of biomass fly ash is an important property to consider as a supplementary cementing material in blended cement and concrete. The major chemical analysis of

the fly ashes obtained using XRF is shown in Table 3.3**.** A loss on iginition of 25% and 20% were obtained for BFA1 and BFA2 respectively. The organic content as well as the decomposition of calcite is the reason for the high loss on ignition which is confirmed by the TG/DTA analysis. Fly ash BFA1 contained significantly higher amount of SiO_2, Al_2O_3 compared to BFA2 and Fe_2O_3. Fly ash BFA2 contained 25% CaO. Both fly ashes were similar to a class C material (ASTM C618) in terms of chemical composition. When the ash is produced in industrial combustion systems, the temperature of combustion, cleanliness of the biomass fuel, the collection location, and the technology used can also have profound effects on the characteristics of the ash. Therefore, the biomass composition can be highly variable depending on geographical locations and industrial processes and even batch to batch samples. In order to monitor the trend of variation of the elements in the biomass fly ashes, a number of samples were collected in several months along a period of one year and were analysed for chemical composition using XRF technique. The results are shown in Figure 3.15.

The vairations were comparatively significant in SiO_2, CaO as they are the main oxides in the fly ashes. The variations can be attributed to the variation in the operating conditions as well as the biomass fuels used for the combustion. Al_2O_3 was the third major oxide in both the fly ashes. A variation of an absolute maximum of around 10% is observed in the distributiton of major elements.

Table 3.3. XRF analysis of biomass fly ashes.

Element	*BFA1* *(Wt. %)*	*BFA2* *(Wt. %)*
Loss of ignition (at 1000ºC)	25	20
SiO_2	41	28
Al_2O_3	9.3	6.2
Fe_2O_3	2.6	2.2
CaO	11.4	25.4
MgO	2.3	5.0
Na_2O	0.9	3.3
K_2O	3.9	3.2
TiO_2	0.4	0.3
MnO	0.3	0.7
P_2O_5	0.9	0.9

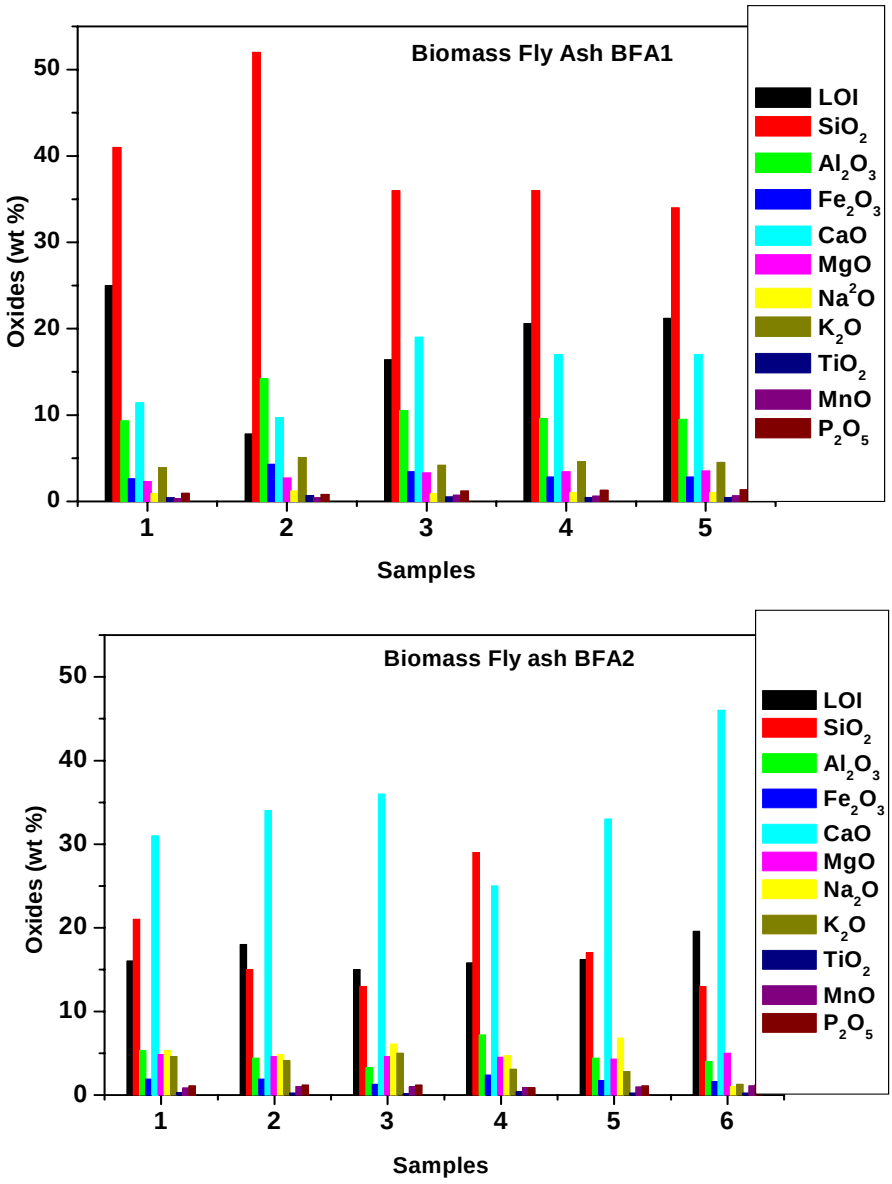

Figure 3.15.Variation of oxides in the biomass fly ashes in several samples collected in distinct months (bimonthly) along one year.

It can be noticed that BFA2 has CaO in higher amount compared to BFA1 whereas for BFA1 SiO_2 is the dominant oxide. As explained in chapter 2 the quantity and quality of ashes produced in a biomass power plant are strongly influenced by the characteristics of the biomass used: agriculture wastes or herbaceous biomass, wood or bark [Loo and Koppejan 2003, Masiá et al. 2007].

In the thermal power plant from where BFA1 was collected the fuel used was mainly forestry biomass wastes which comprises a variety of wood wastes. However in the pulp and paper plant mainly eucalyptus bark was used. The additional fuel used to control the combustion conditions such as fuel gas as starter also influences the chemical composition of biomass fly ashes. These are considered to be the reason for the composition difference especially in major oxides in the fly ashes examined here.

A wide range of variation in the chemical compositions of biomass is also observed in the reports by several other researchers also (Table 3.4). The major oxides such as SiO_2, Al_2O_3 , Fe_2O_3, CaO varies from 8 %-67%. 0.89%-28%, 0.85-14% and 0.58-25% respectively and this makes it difficult to obtain a general idea of the categorization of biomass fly ashes. These results strongely recommend that it is necessary to know the burning conditons and the source of biomass fly ashes to have an idea about the chemical composition of the fly ashes.

Table 3.4. Summary of chemical composition of wood waste ash (Cheah et al. 2011).(W1-W5= wood ashes)

Chemical compound	SiO_2	Al_2O_3	Fe_2O_3	CaO	MgO	TiO_2	K_2O	Na_2O	SO_3	C	P_2O_5	LOI (%)
Elinwa and Mahmood (2002)	67.20	4.09	2.26	9.98	5.80	–	–	0.08	0.45	–	0.48	4.67
Udoeyo and Dashibil (2002)	78.92	0.89	0.85	0.58	0.96	–	–	0.43	–	17.93	–	8.40
Elinwa and Ejeh (2004)	67.20	4.09	2.26	9.98	5.80	–	–	0.08	0.45	–	0.48	4.67
Abdullahi (2006)	31.80	28.00	2.34	10.53	9.32	–	10.38	6.50	–	–	–	27.00
Naik et al. (2003)												
W1	32.40	17.10	9.80	3.50	0.70	0.70	1.10	0.90	2.20	–	–	31.60
W2	13.00	7.80	2.60	13.70	2.60	0.50	0.40	0.60	0.90	–	–	58.10
W3	50.70	8.20	2.10	19.60	6.50	1.20	2.80	2.10	0.10	–	–	6.70
W4	30.00	12.30	14.20	2.20	0.70	0.90	2.00	0.50	2.10	–	–	35.30
W5	8.10	7.50	3.00	25.30	4.50	0.30	2.70	3.30	12.50	–	–	32.80

3.3. 5. 2 Raman Spectroscopy

The Raman Spectra of the fly ashes cut at 75 µmare shown in Figure 3.16. The vibrational Raman shifts corresponding to $[CO_3]^{2-}$ and $[SO_4]^{2-}$ bonds are detected. Broad shifts are detected peaking around 1300 cm^{-1} and 1600 cm^{-1} indicating the organic content present in the fly ashes. In biomass fly ash BFA1 the amorphous carbon peak is dominant that had suppressed the vibrational peaks of other bonds. The Raman spectroscopy tool did not seem to be effective for determining the chemical structure of these biomass fly ashes.

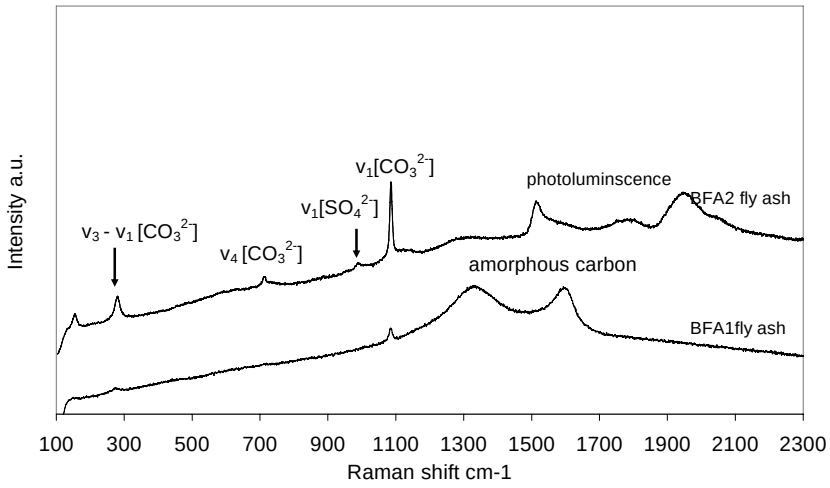

Figure 3.16. Raman spectra of biomass fly ashes BFA1 and BFA2

3.3. 5. 3 Organic content

For many biomass materials, however, a significant portion of the inorganic material is volatile at the conventional ashing temperatures for coal, and an ashing temperature of 550 ºC has been adopted as standard for ash content determination, to avoid underestimation of the ash content of the fuel, due to loss of the volatile inorganic components (CEN/TS 14775:2004).

The organic content of the samples was analysed for the as received fly ashes and the fly ashes cut at 75 µm. It was observed that the biomass fly ash BFA1 contained more organic content compared to BFA2. It was also noticed that the ash fractions sieved below 75 µm had less organic content present compared to the as received fly ashes (Table 3.5).These results in turn give a comparison of the biomass combustion efficiency inside the combustion chambers, showing the efficiency of fluidized bed boiler compared to the grate boiler and the influence of the combustion chamber in determining the quality of the biomass fly ashes.

Table 3.5 Organic content in the biomass fly ashes.

Material	*Organic content (%)*
Fly ash BFA1as received	23.33
Fly ash BFA1 <75 µm size	14.05
Fly ash F2 as received	10.45
Fly ash F2 <75 µm size	7.27

3.3. 5. 4 Chloride and sulphate contents

Much of the inherent inorganic material in biomass is in the form of simple inorganic salts, and principally as the oxides and hydroxides of silicon, and the nitrates, sulphates, chlorides, phosphates and oxalates of the alkali and alkaline earth metals [Thek et al. 2005 and Van et al. 2005]. The content of chloride and sulphate of the biomass fly ashes is shown in Table 3.6. It can be noticed that fly ash BFA2 had more Cl^- and SO_4^{2-}. This increase could be due to the contamination caused in the combustion chamber where natural gas is is used as fuel at times to trigger the burning and also wastes from paper pulp processing might also be adding to the boiler at times. Contaminants in natural gas include organometallic compounds such as those containing lead and mercury, as well as many other compounds which lead to the formation of hazardous air pollutants, including some halogenated compounds]. The variations of chlorides and sulphates

obtained in the leached solutions for samples collected biomontly for a duration of 1 year is shown in Figure 3.17. There were significant variations in the chloride as well as sulphate content between the sample collected at different months during a year.

Table 3.6. Chloride and Sulphate content in biomass fly ashes

Biomass fly ash	*Chloride (g/l) (Cl^-)*	*Sulphate (g/l) ($SO4^{2-}$)*
BFA1	1.42	1.30
BFA2	3.74	2.60

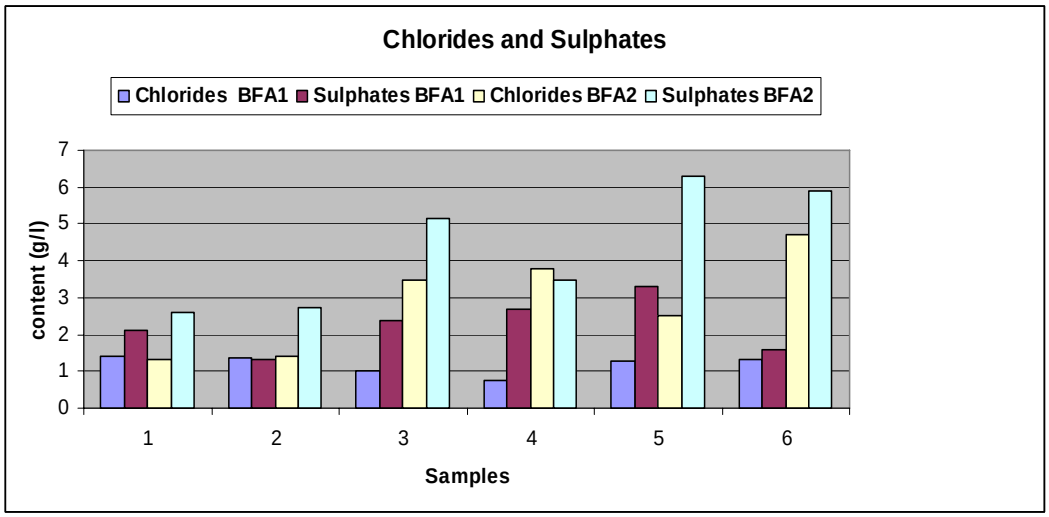

Figure. 3.17. Evaluation of the trend of variation of chlorides and sulphates in the biomass fly ash samples collected in distinct months (bimonthly) along one year.

3.3.6. Microstructural analysis and surface chemistry

According to the Energy Dispersion X -Ray spec^{tr}oscopy (EDX) analysis at the SEM of fly ash BFA1 and fly ash BFA2 75 µm (Figure 3.18 and Figure 3.19 respectively), the major elements in both fly ashes were Ca, Si and Al. The presence of Na, K, Cl and S was also evident in the ashes.

A quantitative elemental analysis of the ash particles (cut at along with cement using XPS is shown in Table 3.7. It is the surface of fly ash that reacts first in a matrix. Significant amounts of Ca, Si, Al and Mg were present on the ash surfaces compared to those of cement. The carbon

content was high for the fly ashes. The amount of chlorine as chloride was also high in the fly ashes: 1.9 and 3.0% for fly ash BFA1 and fly ash BFA2, respectively. A significant amount of alkali metals Na, K was also present in the fly ashes.

The EDS as well as the XPS analysis also reveals that biomass fly ashes have significant content of both chlorides and sulphates. The XPS results also shows the dominance of Si , Al and Ca elements along with the Carbon content. These results also agreeing well with the XRF results obtained for the biomass fly ashes indicating the homogenous distribuiton of the various elements in biomass fly ash particles.

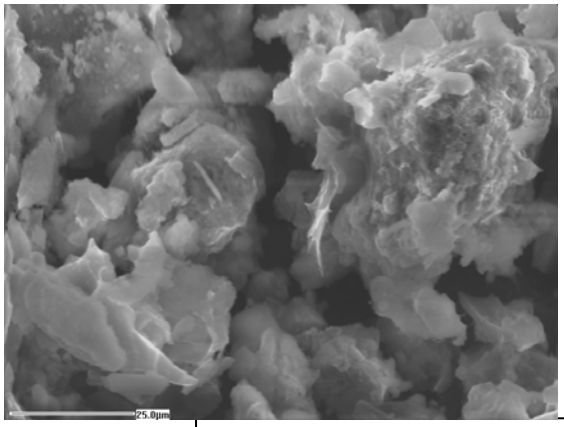

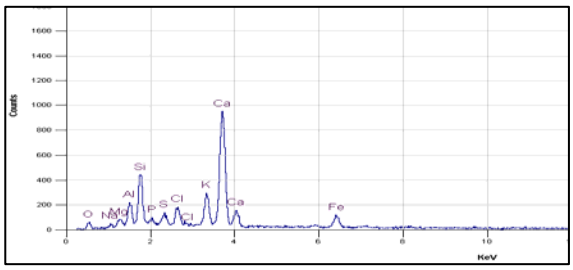

Element	Atoms%	Compound	Weight%	Error(±)	Norm%
Na	2.97	Na	2.38	0.03	2.38
Mg	3.09	Mg	2.62	0.03	2.62
Al	3.35	Al	3.15	0.04	3.15
Si	5.75	Si	5.63	0.05	5.63
S	2.10	S	2.35	0.07	2.35
Cl	4.56	Cl	5.64	0.07	5.64
K	5.40	K	7.37	0.09	7.37
Ca	30.90	Ca	43.18	0.19	43.18
Mn	0.77	Mn	1.48	0.09	1.48
Fe	1.45	Fe	2.81	0.12	2.81
Au	0.20	Au	1.37	0.17	1.37
O	39.45	O	22.01	0.13	22.01
<Total>	100.00		100.00		100.00

Figure 3.18. EDX spectrum of fly ash BFA1 and the corresponding SEM image

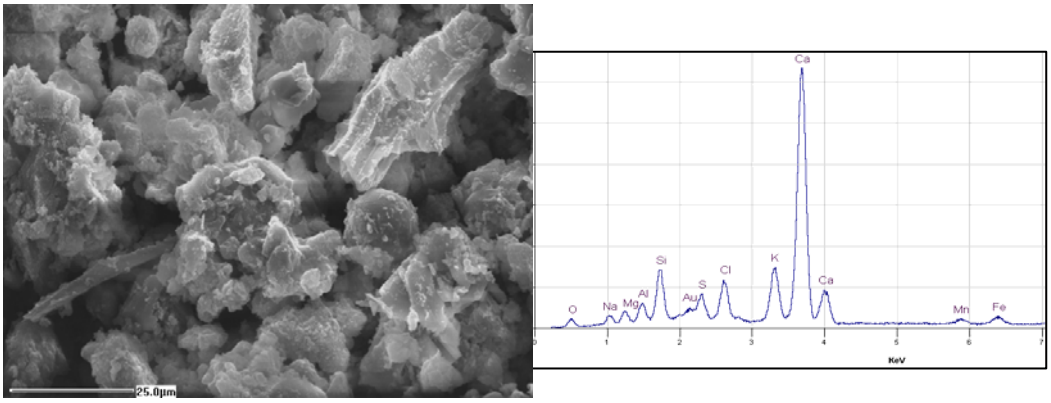

Element	Atoms%	Compound	Weight%	Error(±)	Norm%
Na	2.75	Na	1.78	0.07	1.78
Mg	5.38	Mg	3.68	0.09	3.68
Al	9.84	Al	7.47	0.11	7.47
Si	15.62	Si	12.35	0.14	12.35
P	3.84	P	3.34	0.10	3.34
S	3.92	S	3.53	0.12	3.53
Cl	5.65	Cl	5.64	0.15	5.64
K	8.63	K	9.50	0.22	9.50
Ca	38.39	Ca	43.31	0.41	43.31
Fe	5.97	Fe	9.38	0.37	9.38
<Total>	100.00		100.00		100.00

Figure 3.19. EDX spectrum of fly ash BFA2 and the corresponding SEM image.

Table 3.7. Summary of XPS analysis done on the surface of the cement and the fly ash samples.

sample	*(atomic %)*									
	C	O	Na	Mg	Al	Si	S	Cl	K	Ca
cement	23.5	38.8	0.4	0.9	2.4	6.3	2.0	1.5	1.6	22.8
BFA1	41.6	27.5	0.5	2.0	5.3	8.8	0.6	1.9	3.7	8.1
BFA2	38.7	29.0	1.0	2.5	3.6	6.9	0.9	3.0	2.2	12.1

3.3.7. Leaching

The two biomass fly ashes with the two fractions- 1) the ash in the as received condition which is labeled here as "raw"and 2) a fraction below 75 µm- were used for the leaching analysis. Each ash sample was subjected to two consecutive leaching cycles named as 1st leaching and 2nd leaching respectively. The pH of leaching solutions obtained from the biomass fly ashes was highly alkaline in nature ranging from 10.2 – 11.9 (Figure 3.20). The biomass fly ash BFA1 showed a slightly high pH value compared to BFA2. It was also noted that pH decreased in the second leaching cycle (each leaching cycle was using 1 liter of double distilled water for 100 g of fly ash sample). It can be noticed that the pH value did not decrease from the first to the second leaching of the biomass fly ash BFA2. There was a marked difference in the conductivity between BFA1 and BFA2 fly

ashes. The biomass fly ash BFA2 showed twice the conductivity compared to biomass fly ash BFA1. The conductivity measurements showed a significant decrease in conductivity from the first to the second leaching.

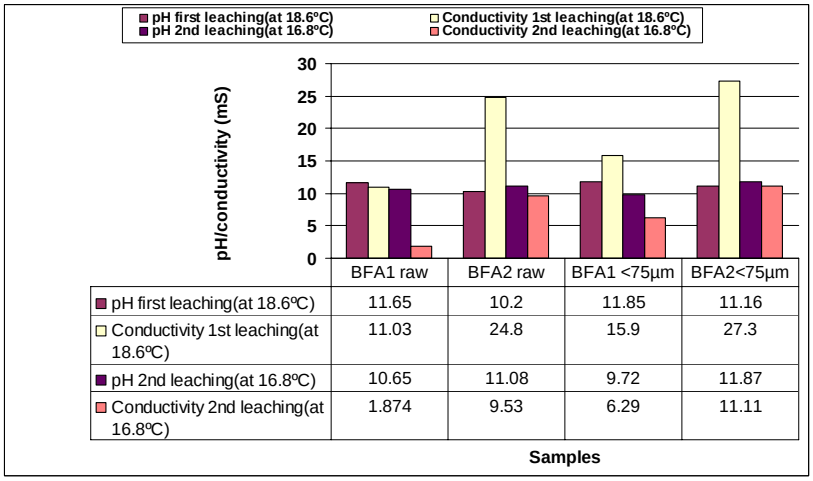

Figure 3.20. PH and conductivity of the leaching solution of the ashes samples, for the first cycle and second cycle of leaching.

The major elements in the fly ash leaching solutions obtained by ICP-MS method as the mass proportion by the dry residue sample (mg/kg) is shown in Figure 3.21. It was observed that K, Ca and Na with traces of Si are the most abundant elements in the leaching solutions of the ash samples. It can be observed that both fly ash leaching solution contained potassium (K) in a significant amount. The biomass fly ash BFA2 leaching solution contained more Na and potassium K content compared to biomass fly ash BFA1, which is the prime reason for its higher conductivity whereas the soluble sodium component was less in content in the biomass fly ash BFA1.

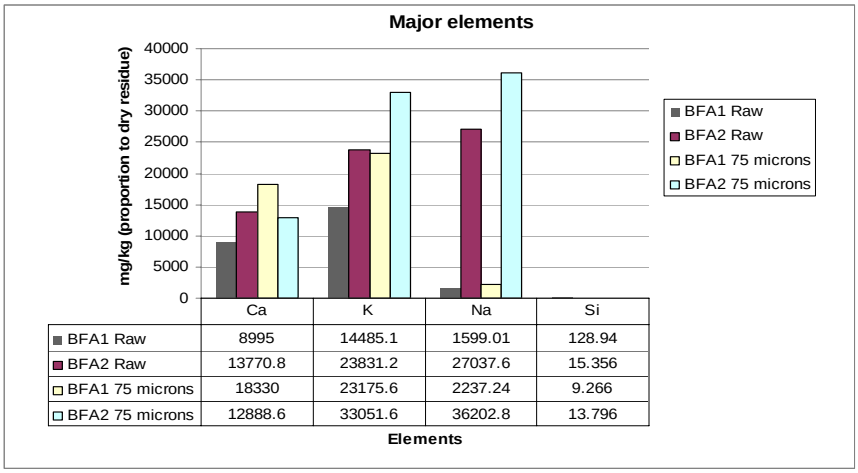

Figure 3.21 Major elements content in the leaching solution from the ash samples, for the total leached in the two cycles.

The ICP-MS values obtained for the trace element content in the leaching solution are shown in Figure 3.22. The Mg concentration in the solutions from leaching was below the detection level of the equipment for all the ash samples except for biomass fly ash BFA1 raw which contained around 4.57 mg Mg/kg dry ash in the sample. Al was also detected in the leaching solution of the biomass fly ash raw sample. An increased Cr content was shown in the biomass fly ash BFA2 leaching solution compared to BFA1 and a high content of Pb (5.805 mg/kg) and Zn (1.824 mg/kg) were determined in the leaching solution of the BFA1 fine fraction of the fly ash. Fe, Ni and P were below the detection level (limit:- Fe= 0.002 µg/l, Ni =0.002 µg/l and Pb=0.004 µg/l (dry basis)) in all the samples, though their presence were identified qualitatively.

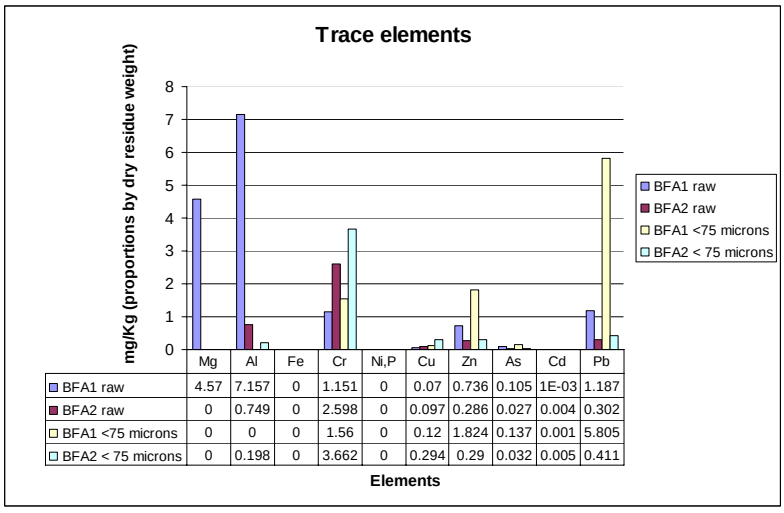

	Mg	Al	Fe	Cr	Ni,P	Cu	Zn	As	Cd	Pb
BFA1 raw	4.57	7.157	0	1.151	0	0.07	0.736	0.105	1E-03	1.187
BFA2 raw	0	0.749	0	2.598	0	0.097	0.286	0.027	0.004	0.302
BFA1 <75 microns	0	0	0	1.56	0	0.12	1.824	0.137	0.001	5.805
BFA2 < 75 microns	0	0.198	0	3.662	0	0.294	0.29	0.032	0.005	0.411

Figure 3.22. Trace elements content in the leaching solution from the ash samples, for the total leached in the two cycles (Mg, Al, Fe , P and Ni content obtained were below detection level)

Its clear from the literature that the ash particle properties are closely linked to its leaching behaviour (Skodras et al 1990). Table 3.8. shows the total weight of the elements in the samples and the weight proportions of the elements that were leached. The high surface area due to the continuous outer porous surface is enhancing the leachable efficiency of the biomass fly ashes.

The leaching characteristics of ashes were compared with the Portuguese legislation about acceptance of solid wastes in landfill [Decreto-Lei n.º183/2009]. According to it both the biomass flyes have a concentration of Cr above the allowed limit for material to be disposed in landfill for inert materials. So these biomass fly ashes are not inert materials for landfilling. Considering the parameters analyzed in this work the biomass fly ashes BFA1 and BFA2 can be considered as materials that can be landfilled as the nondangerous materials category.Similar observation was obtained for biomass fly ashes collected from some other biomass power plants also in Portugal. [Tarelho et al. 2011].

Table 3.8. Total weight of the element in the dry residue of the nonleached sample (w_{GT}) and the proportion by weight of the leachable amount (w_R)(%)

	BFA1 raw		*BFA2 raw*		*BFA1 <75µm*		*BFA2 <75 µm*	
Element	$(w_{GT})10^3$ (mg/Kg)	w_R (%)	$w_{GT}x10^3$ (mg/kg)	w_R(%)	w_{GT} $x10^3$ (mg/Kg)	w_R (%)	$w_{GT}x10^3$ (mg/Kg)	w_R (%)
Ca	109.3804	0.009764	249.5516	0.006633	157.4386	0.013617	345.9632	0.005192
K	56.99912	0.030174	44.44361	0.064449	61.20596	0.044286	57.96495	0.07947
Na	9.598611	0.01978	65.39751	0.049692	10.21665	0.025612	82.65686	0.061044
Si	221.1531	6.92E-05	159.0185	1.16E-05	195.0108	5.56E-06	96.51923	1.99E-05
Mg	17.50543	3.1E-05	26.5	0	22	0	35.4	0
Al	73.6085	1.15E-05	37.0009	2.43E-06	67.9	0	32.30028	8.55E-07
Fe	31.4		19.8		29.3		166.6	
Cr	0.07560137	1.81E-06	0.05610312	5.57E-06	0.07850182	2.32E-06	0.0563051	9.06E-06
Ni	0.037.8	0	0.0346	0	0.0426	0	0.0389	0
Cu	0.1240001	6.75E-08	0.04580012	2.56E-07	0.1510001	9.27E-08	0.04830041	8.48E-07
Zn	0.6530009	1.34E-07	0.1020003	3.36E-07	1.010002	2.11E-07	0.1250004	3.24E-07
As	0.08940012	1.39 E-07	0.009750033	3.37E-07	0.1440002	1.11E-07	0.01300004	3.38E-07
Cd	0.003500001	3.32E-08	0.001400004	3.18E-07	0.004900002	3.17E-08	0.001500007	4.36E-07
Pb	0.2070014	6.81E-07	0.06360036	5.71E-07	0.2570068	2.64E-06	0.04030057	1.42E-06

A comparison study was done on the values of oxides determined by ICP-MS method as well as the XRF method (Table 3.9). In both of the methods volatilisation of organic content happen during the analysis. It can be noticed that there is no much variation in the values when determined by both the destructive method and non-destructive method except for BFA2 <75 µm sample.

Table 3.9. Comparison between ICP-MS and XRF methods

Oxides	*BFA1 raw*		*BFA1 <75µm*		*BFA2 raw*		*BFA2 <75µm*	
	ICP-MS	XRF	ICP-MS	XRF	ICP-MS	XRF	ICP-MS	XRF
CaO	13.8	14	19.0	16	32.6	30	45.9	31
K_2O	4.8	5	4.1	5	1.9	2.4	1.4	2.6
Na_2O	1.0	1.1	1.0	1.3	4.4	4.4	4.4	3.4
SiO_2	47.3	52	41.7	50	34.0	23	20.7	24
MgO	2.9	2.7	3.7	2.9	4.4	3.9	5.9	4.5
Al_2O	13.9	11	12.8	12	7.0	4.1	6.1	5.9
Fe_2O	4.5	3.2	4.1	3.6	2.8	1.6	2.4	2.2

3.3.8. Pozzolanicity

The pozzolanic activity of fly ash is defined in terms of the reactions of its main components SiO_2 and Al_2O_3 with $Ca(OH)_2$ to form CSH and CAH phases. From the XRF analysis it was observed that both biomass fly ashes demonstrated the chemical compositions similar to a Class C fly ash according to the ASTM/EN standards. Figure 3.23 shows the Fratini pozzolanicity diagram of the biomass fly ashes. The saturation curve is that of cement without pozzolans. Fly ash BFA1 is positioned (marked as "x") significantly below the saturation curve indicating pozzolanicity, whereas fly ash BFA2 is positioned (marked as "x") closer to the saturation curve indicating its dominant hydraulic activity because of an increased quantity of CaO present in the fly ash.

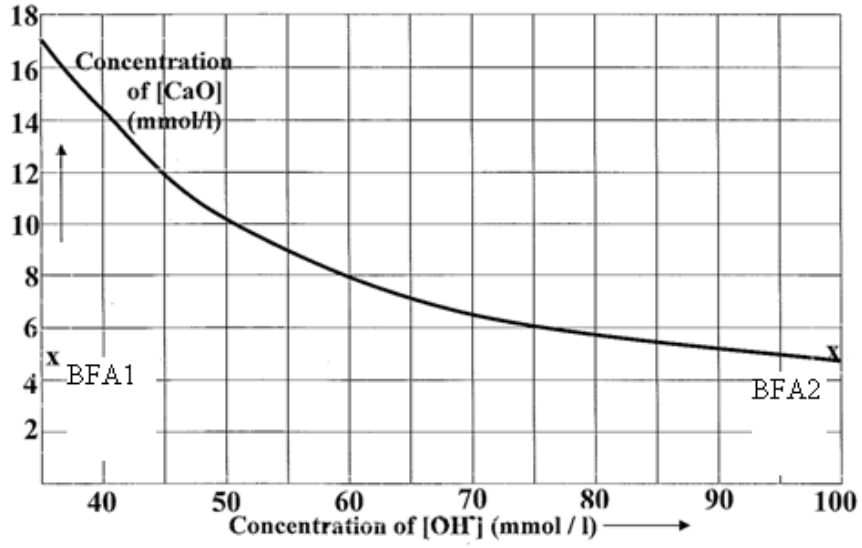

Figure 3.23. Pozzolanicty diagram of biomass fly ashes.

The pozzolanic index calculated by the strength measurements along with the Chapelle test results are shown in Table 3.10. The modified Chapelle test showed a CaO fixation of 618 mg/g and 701 mg/g for the biomass fly ashes BFA1 and BFA2, respectively, confirming their pozzolanic character. It can be noticed that the pozzolancity index value exceeds the minimum 70% specified by ASTM C618 for all classes of coal fly ash to be suitable as pozzolan. The tests give an estimation of the weak pozzolanic potential of the biomass fly ashes.

Table 3.10 Pozzolanic behaviour of the biomass fly ashes

Sample	*$Ca(OH)_2$ fixed Chapelle method g/mg*	*Pozzolanicity índex(28 days)*
BFA1	618	73
BFA2	701	80

3.4. Summary

The physical as well as chemical characterisation of the biomass fly ashes were investigated in detail. For the convenience of a detailed investigation, two types of biomass fly ashes available in Portugal were used based on the combustion processes that influence the physical chemical characterisitcs of the biomass fly ashes. These ashes were the representatives of biomass fly ash from 1) a grate furnace and 2) a fluidised bed furnace.

The biomass fly ash BFA1 was black whereas BFA2 was medium grey. The biomass fly ashes were heterogeneous mixtures of particles with varying shapes. The fly ash BFA1 consisted of coarse particles, which were unburned, or partially burned wood or bark particles. The overall particle size distribution of the ashes cut at 1mm were typically below 100 µm with a mean particle size 52.92 µm and 16.04 µm for biomass fly ash BFA1 and biomass fly ash BFA2 respectively. The surface of BFA1 fine fractions was 40 m^2/g where as BFA1 showed a value of 8 m^2/g. This is due to the irregular and porous nature of the biomass fly ash particle especially BFA1 that contained more unburnt material. However there was no much difference in the real density of the fly ashes. The variations in the organic content of the biomass fly ashes were mainly due to the difference in the burning efficiency of the furnaces. The fluidized bed furnace works more efficiently than the grate furnace reducing the unburned organic matter content in the biomass fly ashes.

The X-ray diffraction patterns indicated the presence of quartz (SiO_2) and Calcite ($CaCO_3$) as the major mineral components in both the biomass fly ashes. Portlandite ($Ca(OH)_2$), feldspar $K(AlSi_3O_8)$ and anhydrite ($CaSO_4$) were also present in biomass fly ash BFA1. In BFA2 a peak of calcium silicate (Ca_2SiO_4) was also observed. The TG/DTA analysis confirmed the presence of organic matter, and calcite.

From XRF values also it can be confirmed that Fly ash BFA1 contained pozzolanic material SiO_2, Al_2O_3 and Fe_2O_3. Fly ash BFA2 contained 25% CaO. Both fly ashes were similar to a class C material (EN 450) in terms of chemical composition. Inorder to monitor the trend of variation of the elements in the biomass fly ashes, a number of samples were collected with a periodicity of two months, during one year and were analysed for chemical composition using XRF, The variations were comparatively significant in SiO_2, CaO as they are the main oxides in the fly ashes. The difference can be attributed to the variation in the combustion conditions as well as the biomass fuels used for the combustion. Al_2O_3 was the third major oxide in both the fly ashes. A relative variation upto around 10% is observed in the overall distributiton of the oxides .

From the surface chemical analysis, significant amounts of Ca, Si, Al and Mg were present on the ash surfaces compared to that of cement. The carbon content was high for the fly ashes. The amount of chlorine as chloride was also high on the surface fly ashes: 1.9 % and 3.0 % for fly ash BFA1 and fly ash BFA2, respectively. A significant amount of alkali metals Na, K were also present in the fly ashes.

The organic content of the biomass fly ashes in the as received state were around 23% and 10% for BFA1 and BFA2 respectievly. In the finer fractions the organic content percentage was reduced to almost half in both the fly ashes. This indicates that the finer fractions have less carbon compared to the ashes in the as received state.

It was observed that K, Ca and Na with traces of Si are the most abundant elements in the leaching solutions of the ash samples. The high surface area due to the continuous outer porous surface enhances the leachable efficiency of the biomass fly ashes. It can be observed that both the fly ash leaching solution contained potassium (K) in a significant amount. The biomass fly ash BFA2 leaching solution contained more Na and K content compared to biomass fly ash BFA1 which is the prime reason for its higher conductivity where as the soluble sodium was less in the biomass fly ash BFA1. The Mg concentration in the solutions from leaching was below the detection level of

the equipment for all the ash samples except for biomass fly ash BFA1 raw which contained around 4.57mg/kg of Mg in the sample. Al was also detected in the biomass fly ash raw sample. An increased Cr content was shown in the biomass fly ash BFA2 leaching solution compared to BFA1 and a high content of Pb (5.805 mg/Kg) and Zn (1.824 mg/Kg) was determined in the BFA1 fine fraction of the fly ash. Fe, Ni and P were below the detection level in all the samples, though their presence was identified qualitatively. The leaching experiments indicate that these fly ashes can be considered as nontoxic solid wastes.

The pozzolanicity tests proved the pozzolanic nature of biomass fly ashes. The Frattini pozzolanicity diagram demonstrated the pozzolanic behaviour of BFA1 while the BFA2 exhibited an increased hydraulic activity. But the modified Chapelle test showed a CaO fixation of 618 mg/g and 701 mg/g for the biomass fly ashes BFA1 and BFA2, respectively. The pozzolanicity index values were promising to label these fly ashes as pozzolans as per the pozzolanicity index limit of ASTM 618.

CHAPTER 4. BIOMASS FLY ASH INCORPORATION IN CEMENT MORTARS

4.1. Outline

Not much work has been reported relating to the applications of biomass fly ash as an addition in construction materials, particularly in cement-based materials. Due to high carbon content in biomass ash, its use is limited to low and medium strength concrete materials. In Europe, biomass ash has also been used as a feedstock in the manufacture of Portland cement [Etiegni 1990]. Based on the measured physical, chemical, morphological properties, Naik 1999] reported that wood ash has a substantial potential for use as a pozzolanic mineral admixture and as an activator in cement-based materials. He further indicated that wood ash has significant potential for use in numerous other materials including controlled low strength materials (CLSM), low and medium strength concrete, masonry products, roller-compacted concrete pavements (RCCP), materials for road base, and blended cements.

In this chapter, an evaluation of the potential of biomass fly ashes available in Portugal as a substitute for ordinary Portland cement in mortar applications was carried out. The behaviour of biomass fly ash incorporated cement mortars was discussed in terms of impact on fresh as well as on the hardened properties. The overall testing design is listed in Figure 4.1. Cement pastes and cement mortars were prepared by replacing ordinary Portland cement with different amounts of biomass fly ashes (10%, 20% and 30% by weight of cement) in dry conditions. The two biomass fly ashes BFA1 and BFA2 were used for the evaluation procedure. The fresh properties of the mortars were investigated using various methods such as flow table, initial and final setting by Vicat, and rheological studies. The hydration behavior and phase analysis were studied using quasi adiabatic calorimetry thermal analysis, X-Ray diffraction and impedance spectroscopy. The hardened properties were studied using strength measurements and porosimetry methods. The microstructure of the cement pastes were evaluated using electron microscopy. The overall performance of biomass fly ash incorporated cement pastes and mortars for the duration of 2 years was evaluated and a discussion on the potential use of biomass fly ashes in the replacement of cement was made.

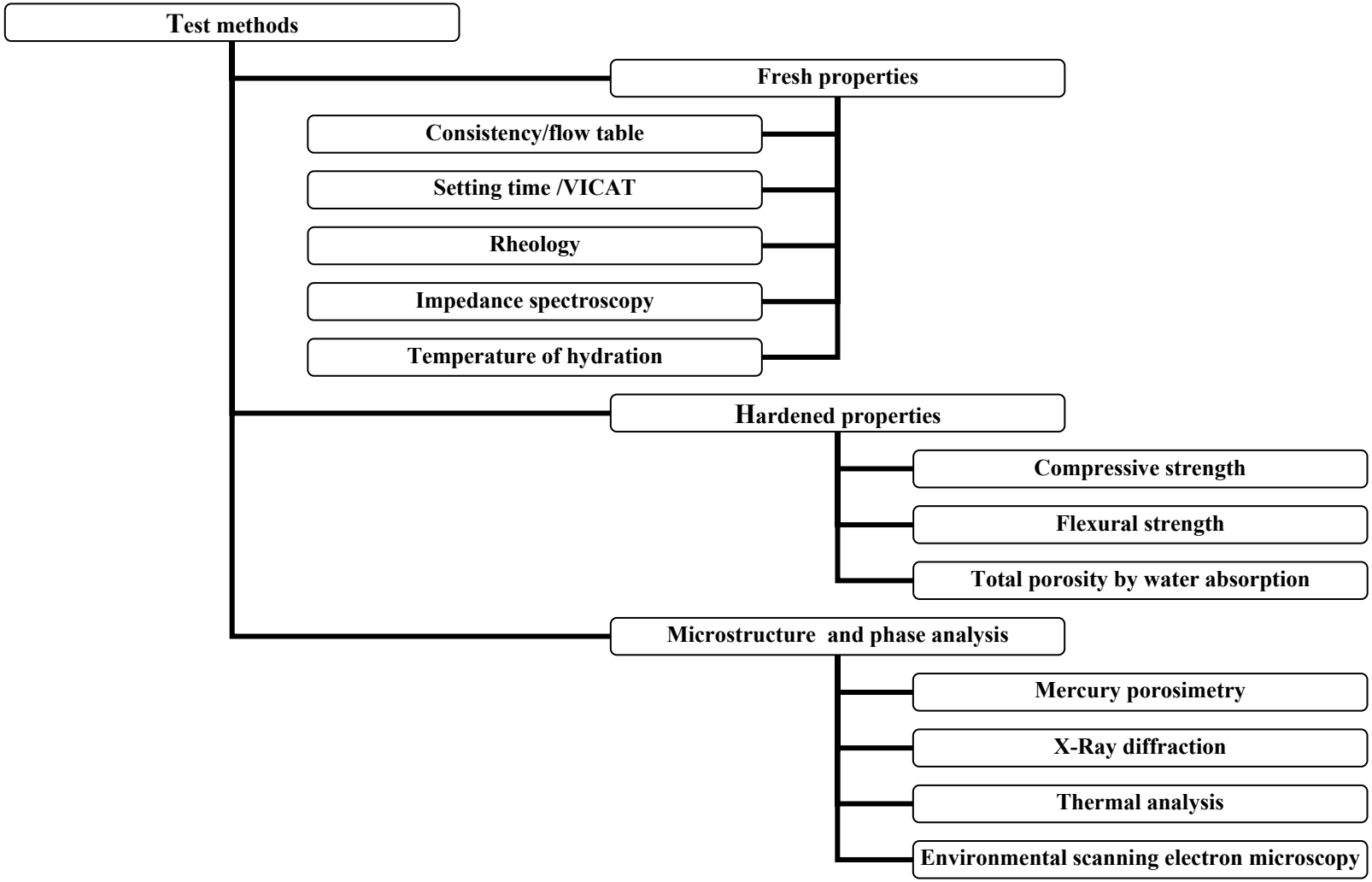

Figure 4.1. Experimental Design

4.2. Materials and compositions

4.2.1. Materials

Cement

An ordinary Portland cement (OPC) was used throughout the experiment. The Portland cement used was CEM I 42.5 R, certified in accordance with the NP EN 197-1:2001. Type I cement consists of 5% gypsum and 95% clinker. The chemical composition of the cement was determined by XRF analysis as stated in Table 4.1.

Table 4.1. Chemical composition of the cement determined by XRF analysis

Composition	*SiO_2*	*Al_2O_3*	*Fe_2O_3*	*CaO*	*MgO*	*SO_3*	*K_2O*	*Na_2O*	*L.I*
Cement (%)	19.74	4.74	2.69	63.54	2.42	3.11	1.02	0.19	1.66
Bogue calculated phases (%)	C_3 S	64.03							
	C_2S	8.30							
	C_3A	8.01							
	C_4AF	8.17							

Biomass fly ashes

The biomass fly ashes BFA1 and BFA2 were sieved at 75 μm and dried at 60 ºC before incorporated in the mortars. The chemical composition of the typical biomass fly ashes used in the tests was listed in chapter 3 (Table 3.3, Table 3.5 and Table 3.6).

Aggregates

The aggregate used in the tests was silicious sand for the purpose of making concretes and mortars. The sand was also dried previously at a temperature of 60 °C for 24 hours to control the moisture content and was sieved through a 2.36 mm mesh sieve. The gradation of the aggregates is shown in **Figure 4.2.**

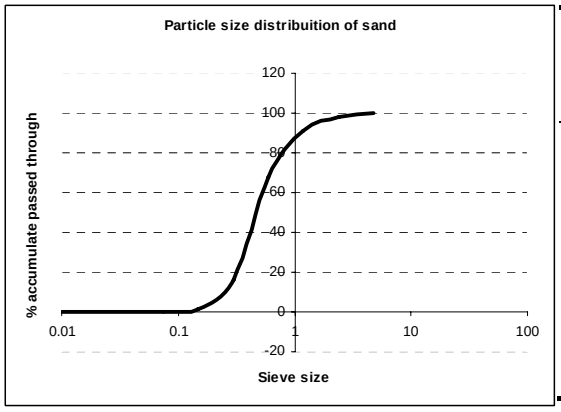

Sand grain size (mm)	*Fraction (%)*
4.75-2.36	1.64
2.36-1.18	7.28
1.18-0.60	23.30
0.60-0.30	51.45
0.30-0. 15	15.40

Figure 4.2. Particle size distribution of sand

Superplasticizer

The super plasticizer used in the composition of the mortar was Sikament 300 Plus, manufactured by Sika Portugal-Construction Products and Industry SA. This product, a mixture of organic polymers and additives, is a super plasticizer / high water reducer / retarder for mortar and concrete, according to the Standard NP 934-2:2003.

4.2.2. Mortar mix design

Cement pastes and cement mortars were prepared by replacing ordinary Portland cement (OPC) by different amounts of biomass fly ashes in dry condition. The researches conducted on various kinds of fly ashes (including the wood ashes) showed that the trend of behaviour of the supplementary cementing materials in cement formulations comes under the limit of 30% addition because of their lesser hydrating material content.[Udoeyo et al. 2006, Abdullahi 2006, Wang et al. 2008]. Therefore a test series of samples were considered by incorporating biomass fly ashes ranging from 10%, 20% and 30% by weight percentage of the binder.

The water content requirement was tested keeping the workability similar (120mm-160mm flow table. The cement mortars were prepared within the range of 0.55-0.65 water/binder (w/b) weight ratio considering the demand of water for higher amount of fly ash substitution. The cement to aggregate ratio was taken as 1:3, and for the reference mortar sample prepared with the cement alone, the w/b ratio was taken as 0.55). Superplasticizer was used to control the water requirement for further detailed tests. Once after determining the doage of the superplasticizer used the rest of the experiments were conducted in the same conditions of w/b 0.55. and curing parameters (at a temperature of 20 ºC and a relative humidity of 65% for 24 hours and then immersed in the tap water (20ºC)).

The components were weighed and mixed thoroughly in a laboratory mixer (CONTROLS, 65-LS). The mixing procedure includes: (i) addition of water to the dry powder mix; (ii) mixing for 1 minute at a low rotation speed of (~60 rpm); (iii) stopping for one minute to gather the mix into the centre; (iv) mixing again for 2 minutes at a higher rotation speed (~120 rpm). The mortar mixture compositions selected for the mortar preparations for strength measurements are listed in Table 4.2.

Table 4.2. Mix proportions used for biomass fly ash cement mortars with no superplasticizer (Each composition for 3 mortar bars of dimensions 4 cmx4 cmx16 cm)

Sample Code	*Composition(Binder)*	*Substitution (wt. %)*	*Biomass fly ash (BFA) (g)*	*Cement (CEM) (g)*	*w/b ratio*	*Sand (g)*
Ref 1	CEM 42.5 R Type 1	0	0	400	0.55	1200
10 BFA1	90% CEM+ 10 % BFA1	10	40	360	0.55	1200
20 BFA1	80% CEM+ 20 % BFA1	20	80	320	0.60	1200
30 BFA1	70% CEM+ 30 % BFA1	30	120	280	0.65	1200
10 B FA2	90% CEM+ 10 % BFA2	10	40	360	0.55	1200
20 BFA2	80% CEM+ 20 % BFA2	20	80	320	0.55	1200
30 BFA2	70% CEM+ 30% BFA2	30	120	280	0.60	1200

4.3. Experimental methods

4.3.1. Consistency of cement pastes and mortars

Consistence is a measure of the fluidity of the fresh mortar/cement paste and gives a measure of the deformability of the fresh mortar when subjected to a certain type of stress. The consistency of mortars is determined by using the standard EN 1015-3:1999. The flow value consists of the measurement of a mean spread diameter of a test sample of the fresh mortar after placed on a defined flow table disc (Figure 4.3) (diameter 250 mm) and suffered 15 vertical impacts by raising the flow table and allowing it to fall freely through a given height. The mould is placed centrally on the plate of the flow table and the mortar mix is introduced in two layers, each layer is compacted by at least 10 short strokes of a tamper to ensure uniform filling of the mould. The excess mortar is skimmed off using a palette knife and the free area of the disc is dried by wiping. The mould is slowly removed vertically and the mortar is spread out on the disc by jolting the flow table 15 times at a constant frequency of approximately one per second. The diameter of the mortar in the 4 directions at right angle to one another is noted and the mean value of the measurements was taken as the flow table spread result with a limit of error of 10% in two experiments.

The consistency of the cement pastes was determined by the VICAT consistency needle penetration method following EN 196.3, 2006 standard.

Figure 4.3. Flow table apparatus.

4.3.2. Setting time

There are two periods in setting. The first setting time is referred to the time between mixing and partial loss of plasticity and the final setting time is the time necessary to acquire enough hardening to withstand a certain pressure [Coutinho 1997]. The setting time of the mortar mixes were measured using the VICAT apparatus using the standard NP EN 196-3:2006.

The VICAT method is the commonly used method to identify the setting time. The method is applied by the penetration of needle with 1 mm diameter in a cylindrical mould full of mortar or paste weighing around 500 g performed.Tests were performed on the equipment Automatic Recording Vicat apparatus (Figure 4.4). The apparatus is programmed for the needle to penetrate at an interval of 10 min. The initial setting time is the elapsed time between time zero and the moment when the penetration depth of the needle is 5 ± 1 mm from the base of the mold. The final setting time is determined when the VICAT plunger makes only a mark on the surface of the mortar samples.

Figure 4.4. VICAT apparatus.

4.3.3. Rheology

Rheology is the science of flow and deformation of materials and is concerned with the interaction between shear stress, shear strain and time. As setting of cement formulations is concerned with the development of rigidity in an initially fluid material, it is also assumed to be part of rheology. The application of rheology to the workability of fresh concrete has been extensively documented and it has been applied to mortar more effectively [Banfill 2003, Chaira et al. 2001, Paiva et al. 2009, Luciano et al. 2009].

Cement mortar, defined as a fine grained material containing sand particle not greater than 2 mm size can also be considered to be model concrete. A knowledge of its rheology may contribute to an understanding of the behaviour of fresh concrete, which determines how easily this important construction material can be moulded and compacted and may ultimately lead to an ability to predict the flow properties of the latter from small scale tests on mortars. Cement based materials are classified within the non Newtonians liquids, where a two point measurement is sufficient to characterise the rheological parameters, based on the Bingham plastic model [Tattersall et al., 1983]. Therefore the flow of cement is characterised by its yield stress (below which the suspension displays a solid like behaviour) and its plastic viscosity.

The rheological behaviour of fresh mortars was evaluated in a Viskomat PC Rheometer (Figure 4. 5(a)). Torque gives an indication of flow resistance and it can be measured as function of time and rotation speed profile. This procedure allows to set up a relation between shear stress (or torque) and strain (rotation speed). This apparatus is internally limited to a maximum torque value of 300 N.mm. The rotation speed, time and torque data are sampled by a data acquisition system. The total testing time ranged from 15 to 60 min, depending on the biomass fly ash content. The rheometer maximum speed (N) used was 100 rpm and at every 15 min the speed was brought to zero, kept as that for 30 s, and after the speed was increasing during the 30 s until reach to 100 rpm. In all measurements the yield stress (*g)* and the plastic viscosity (*h)* related coefficients were obtained from Bingham's model and using the down curve, since it shows a more regular behaviour, as shown in Figure 4.5(b). The upper curve shows more irregular behaviour influenced by the preceding resting period where some restructuring exists. From the relation between torque and speed set up by the Bingham model (T = g + hN), the rheological parameters related to viscosity (h) and yield stress (g) were obtained.

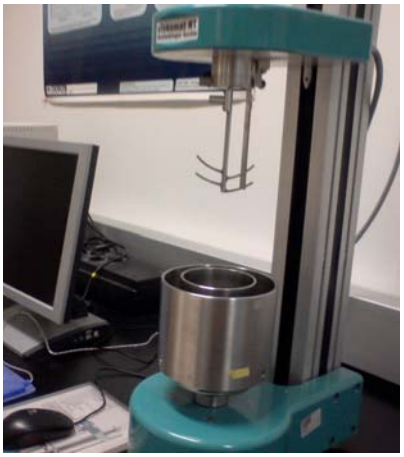

Figure 4.5.(a) Viskomat PC Rheometer

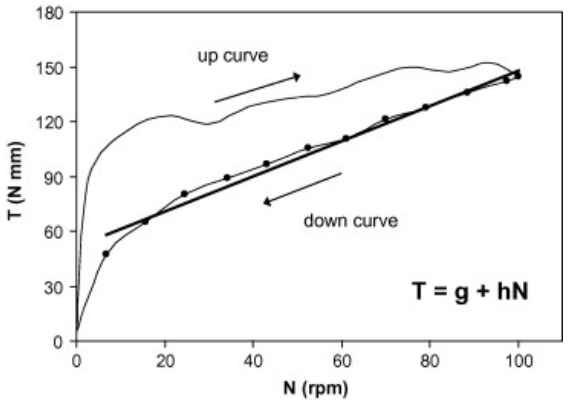

Figure 4.5 (b). Bingham's model.

4.3.4. Hydration

The hydration behavior of the biomass fly ash-cement mortars were analyzed using impedance analysis and measuring thetemperature of hydration using an adiabatic calorimeter.

4.3.4.1. Impedance spectroscopy

The electrical behaviour of the fresh cement-biomass pastes with time is studied using impedance spectroscopy. Samples were electroded with copper plates and their electrical measurements were conducted at room temperature in the experimental setup represented in Figure 4.6 (a) using a Hewlett-Packard 4284A bridge and changing the frequency between 20 and 10^6 Hz. The electrical response of the samples was then correlated with setting behaviour of the biomass fly ash cement pastes in order to study the ability of impedance spectroscopy to evaluate the hydration nature of the biomass fly ash cement pastes.

.

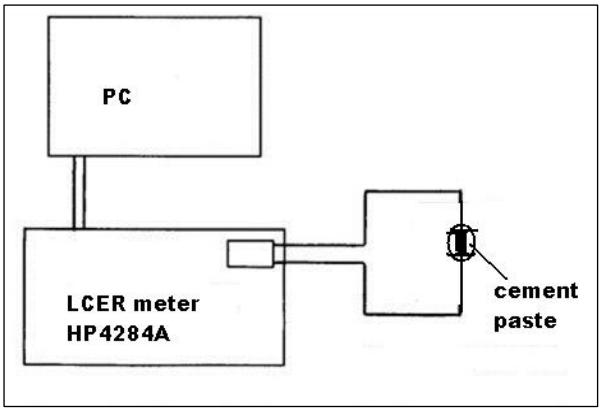

Figure 4.6 (a). Schematic diagram of impedance test apparatus.

Impedance spectra are generally recorded over a wide range of frequencies from MHz to Hz. A schematic impedance spectrum for a cement paste (two-point measurement configuration) plotted in the real versus imaginary plane is illustrated in Figure 4.6(b). Single arc in the high-frequency range and a small part of a second arc in a relatively low-frequency region are depicted. The high frequency arc (HFA) is attributed to the bulk paste impedance behaviour and the second arc is due to the cement paste-electrode surface capacitance. The intercepts R1 (at the high frequency end) and RI + R2 (at the minimum between the electrode arc and bulk arc) are important parameters providing information related to the cement paste and concrete microstructure. The HFA diameter (DHFA), is determined from equivalent circuit modelling (Figure. 4.6(b) b). Ideally, the value of R2 should be equivalent to DHFA if the HFA is a perfect semicircle. However, an ideal response is rarely observed. Most materials exhibit an inclined semicircle with the center depressed below the real axis by an angle Θ (Fiure. 4.6(b) c). DHFA is then equal to R2/cos Θ.

In this study, the bulk resistance of the cement pastes was determined from the intersection of low and high frequency arcs with the real impedance axis at around 7 kHz, which corresponds to the R1 + R2 value in the equivalent circuit model shown in the Figure 4.6 b (b).

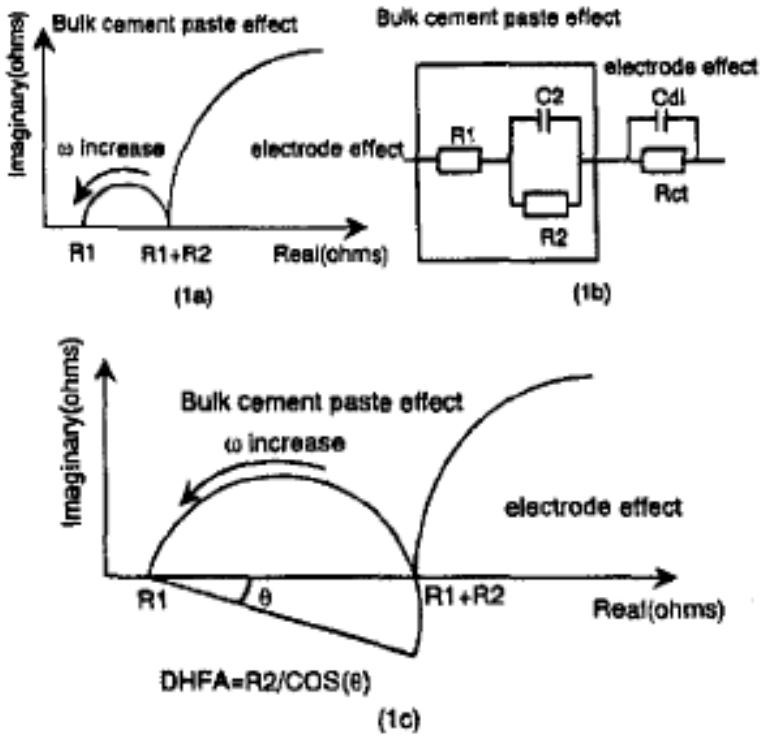

Figure 4.6 (b). Schematic plot of a high frequency in the impedance complex plane obtained for cement paste or concrete systems; (b) the corresponding electrical equivalent circuit and (c) an inclined semicircle whose centre is depressed below the real axis by an angle Θ. (Gu et al. 1995]

4.3.4.2. Temperature of hydration

The heat of hydration of pastes was measured in terms of the temperature using a quasi-adiabatic calorimeter. The calorimeter consists of cylindrical units which are polyvinyl based. Semi adiabatic conditions were assumed by insulating the internal cylinders with liner similar to that used in the furnaces. Type K thermocouples were used to monitor the temperature inside the cells. An external sensor placed at the surface of the polyurethane box that accommodates the cells can monitor the exchange of temperature with the surroundings. The measurements set up were placed in a curing chamber at 20ºC to maintain the temperature. The cement pastes were filled inside the cells with dimension of 3cm x 4cm and were then placed inside thermally isolated boxes. The temperatures of the mixes were recorded continuously at every 5 minutes with the help of thermocouples and computer aided data loggers (Compact Field point CFP-2100 data logger, NI instruments). The measurement started after 30 minutes with respect to the mixing time.

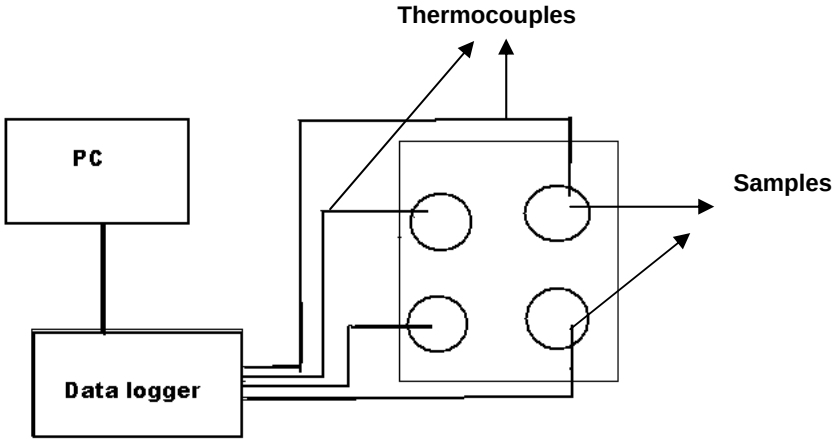

Figure 4.7. Schematic diagram of quasi adiabatic calorimeter

4.3.5. Hardened properties

4.2.5.1. Mechanical strength

The mortar samples for mechanical tests were prepared with the standard dimensions 16 cm x 4 cm x 4 cm. The moulds were covered well with plastic sheets to avoid water loss and stored in a curing chamber at a temperature of 20 ºC and a relative humidity of 65%. After 24 hours, the blocks were removed from the moulds and immersed in tap water for curing for 28 days. The mechanical strength was evaluated by compression and flexural tests carried out according to EN 1015-11:1999, on three samples of each composition, using a Standard Universal Testing Machine (Shimadzu) (Figure 4.8). The prisms were first mechanically tested in three-point bending mode, after which each part was tested in compression.

The flexural strength (in MPa) was measured using the equation

$$M = \frac{3\ F\ L}{2\ b\ d^{\ 2}} \qquad \longrightarrow \qquad \textbf{Eqn 4.1}$$

Where F is the flexural load of force (N), L is the length between the supports of the mortar bar (m) b is the width (m) and d is the height (m) of the mortar bar.

The compressive strength is obtained from the ratio between force and area of the mortar surface under test.

Figure 4.8. Mechanical strength determination

4.2.5.2. Porosity by water absorption

The determination of water immersion was carried out at atmospheric pressure, according to the LNEC procedure 394:1993 specification. The samples were immersed in water for 48 hours, removed from the water and its weight was recorded, with the dry surface (the surface is wiped with a cloth to remove any adsorbed water from the surface and weighed). The samples were then dried in an oven at temperature of 105 ± 5 °C and were weighed again. Water absorption by immersion or total water porosity is calculated using equation

$$Wi = \frac{m1 - m3}{m1 - m2} \times 100 \qquad \longrightarrow \qquad \textbf{Eqn.4.2}$$

where:

Wi- water absorption by immersion (%);
m1 - weight of water saturated sample with the surface dried (g)
m2 – weight of saturated specimen immersed in water;(g)
m3 - weight of specimen (g)

4.3.6. Microstructure evaluation

Several techniques were used to have a clearer picture of microstructure and its effects. Mercury intrusion porosimetry was used to assess the pore size distribution. Thermal analysis and X-Ray diffraction (XRD) were used as complementary techniques. Microstructure was also evaluated by ESEM (environmental scanning electron microscopy) and SEM/EDX (Scanning electron

microscopy with energy dispersive spectroscopy). These microscopical techniques are described in chapter 3.

4.3.6.1. Mercury intrusion porosimetry

The porosity of the cement mortars were calculated by mercury porosimetry. Pore Sizer model No. 9320, Micromeritics Instrument Corp., Norcross, GA) was employed to determine pore-size distribution. The principle of this technique (Lowel and Shields, 1991) is based on the fact that mercury does not wet most substances and, therefore, will not penetrate pores by capillary action, unless it is forced to do so. Liquid mercury has a high surface tension and also exhibits a high contact angle against most solids. Entry into pore spaces requires applying pressure in inverse proportion to the pore diameter. In mercury porosimetry, the sample is first evacuated, then surrounded with mercury and, finally, pressure is applied to force mercury into the void spaces whilst monitoring the amount of mercury intruded. Data of intruded volume of mercury versus applied pressure are obtained and the pressure values are converted in terms of pore sizes as per the equation

$$D = -4 \Upsilon \cos \theta / P \longrightarrow \text{Eqn.4.4}$$

Where D is the pore diameter (m), Υ is the surface tension (N/m), θ = Solid liquid contact angle and P is the pressure (Pa) applied to intrude the mercury into the sample.

4.4. Results and discussion

4.4.1. Fresh properties of biomass fly ash-cement mortars

4.4.1.1. Effect of biomass fly ash incorporation on the workability and setting

The water required for the consistency of the biomass cement pastes are shown in Figure 4.9. It was observed that water demand of biomass fly ash/OPC blended cement paste increases with the level of cement replacement by biomass fly ash expressed as a percentage of total binder's weight. The 10% substitution of biomass fly ashes did not influence the consistency of cement pastes visibly,but when substitution dosage of biomass fly ashes increased the water demand also increased. These results are in agreement with the findings of some researchers who used wood

ashes from other sources like saw dust ashes [Elinwa and Ejeh 2004, Elinwa and Mahmood 2002, and Abdullahi 2006]. The responsible factor for this trend is the specific physical parameters of the fly ashes mainly. The irregular shape, fineness, increased surface area and the organic content in the biomass fly ashes favours the adsorption of water by the fly ash particles on mixing. A similar trend is observed in the spread diameter values of flow table for the mortar compositions also (Figure 4.10).

.

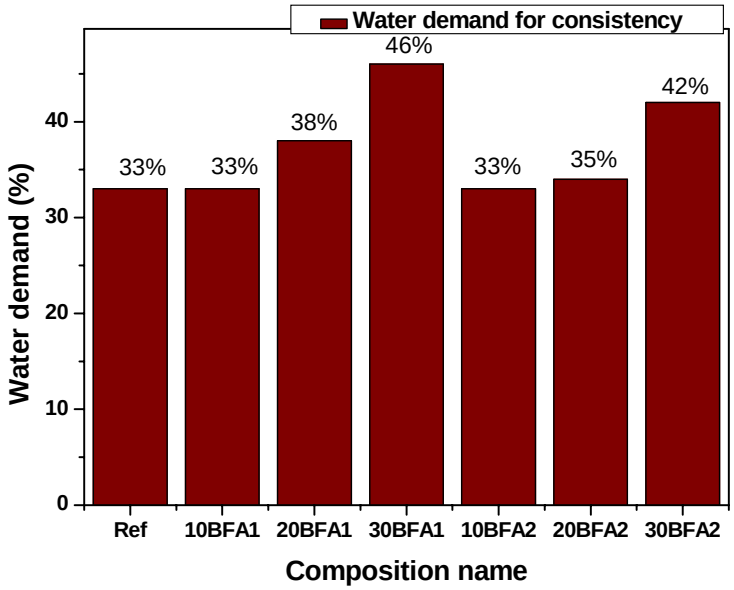

Figure 4.9. Biomass fly ash cement paste consistency.

The water requirement was decided considering a minimum requirement for a complete hydration of cementitious materials along with the desired workable condition for construction purposes. On increasing the amount of biomass fly ash in the compositions, the water requirement also increased. The irregularity in the shapes of the fly ash particles caused internal friction and reduced the fluidity of the mortars. It can also be noted that biomass fly ash BFA1 required more water compared to biomass fly ash BFA2. This is because BFA1 has a higher surface area (40.3 m^2/g) compared to BFA2 (7.9 m^2/g) though having similar fineness. Also BFA1 is having higher content of carbon which shows an affinity to water that reduces the free water availability during mixing. The spread diameter values obtained for different water to binder ratio (w/b) from 0.55 to 0.65 for the biomass fly ash cement mortars are shown in Figure 4.10. It could be seen that for a minimum spread diameter of 110 mm the fly ash 30 BFA1 required w/b ratio around 0.65. It was not possible to make a workable mix with 0.55 w/b water for 30BFA1 mortar. 30% BFA2 mortars behaved slightly better than 30% BFA1 mortars.

The setting time values of mortars containing fly ashes BFA1 and BFA2 are listed in Table 4.3. The fresh densities (apparent density) of the cement-fly ash mixtures were similar in all the

samples. The slight variations are influenced by the compactness degree obtained upon the sample preparation, and the different w/b ratios that were chosen considering the water requirement for a minimum workable condition for the mortars to be moulded.

The setting time varied with the different w/b ratio (Figure 4.11). The fly ash BFA1 absorbs more water, due to its higher surface area. The fly ash BFA2-cement mortar also required increased water content on substituting the higher amounts of fly ash, though less than that needed for the mixture containing fly ash BFA1. For 30% or more it was impossible to make a workable mortar without increasing the water content to beyond w/b 0.65-0.7. The chemical composition suggests that the biomass fly ash is less reactive than ordinary Portland cement. So the setting should be delayed in the biomass fly ash incorporated cement formulations because of reduced initial hydration. But the reduced setting times obtained for BFA1 mortars can be considered as the drying of the mortar mixture because of insufficient water content due to the water intaking nature of the biomass fly ash. The increased w/b ratio also did not help BFA1 from preventing the drying. For BFA2 the setting time followed the same trend when the w/b was kept constant. But for 30% BFA2 when the w/b was increased to 0.6 the setting time started delaying. It was because, the BFA2 biomass fly ash was saturated with water imbibing and thus excess water was oozing out from the ashes soon after moulding that prevented the sudden drying process.

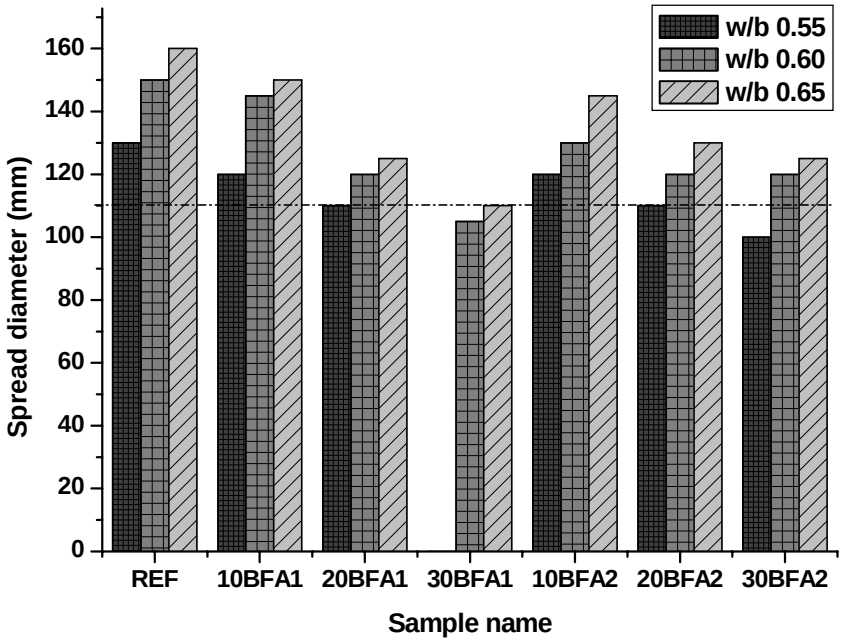

Figure 4.10. The flow table values of biomass fly ash-cement mortars for different w/b ratio

Table 4.3. Fresh properties of biomass fly ash –cement mortars without superplasticizer

Mortar compositions	*w/b ratio*	*Spread diameter (mm)*	*Setting time Initial (min)*	*Setting time Final (min)*	*Density*
Ref	0.55	130	180	520	3.17
10 BFA1	0.55	120	197	450	3.06
20 BFA1	0.60	110	150	360	3.10
30 BFA1	0.65	110	120	320	3.11
10 BFA2	0.55	120	212	600	2.94
20 BFA2	0.55	110	121	420	3.00
30 BFA2	0.60	120	221	650	3.17

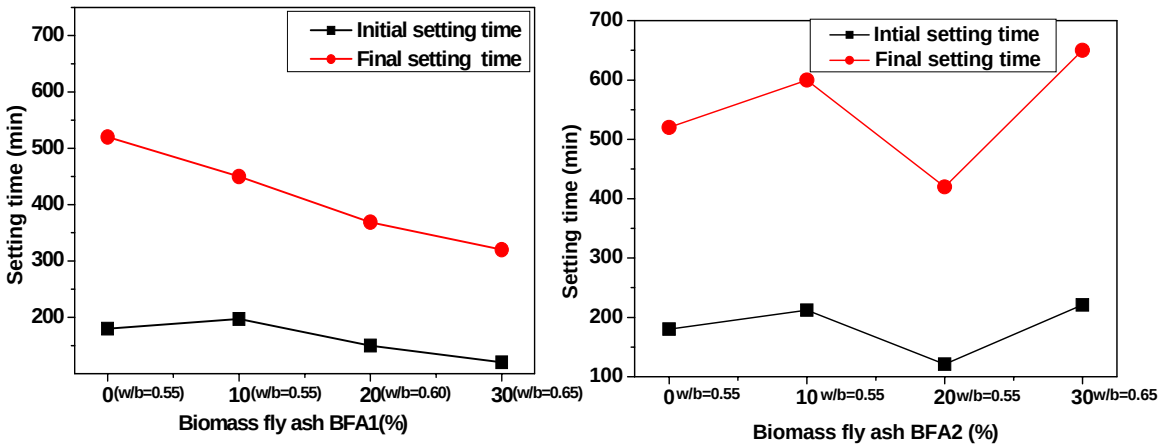

Figure 4.11. Setting time for biomass fly ash incorporated mortars without superplasticizer

4.4.1.2. Role of admixture on controlling the workability

Many important characteristics of mortars are influenced by the weight ratio of water to binder materials (w/b) used in the mixture. By reducing the amount of water, the cement paste will have higher density, which results in higher paste quality. An increase in paste quality will yield higher compressive and flexural strength, lower permeability, and increase in resistance to weathering, improve the bond of concrete and reinforcement, reduce the volume change from drying and wetting, and reduce shrinkage cracking tendencies [Komatska and Panarese 1988]. Reducing the

water content in a cement based mixture should be done in such a way so that complete cement hydration process may take place and sufficient workability of mortar or concrete is maintained for placement and consolidation during construction. The w/b needed for cement to complete its hydration process ranges from 0.22 to 0.25. Additional water in the mixture is to ease he mixtures placing and finishing. In the case of biomass fly ash incorporated mortars a minimum of 0.6-0.65 was needed for a moderate mixing of higher amount of biomass fly ash incorporated mortars (30%). In order to obtain a satisfying workable condition it is not advisable to use more water because of a later strength reduction in the mortars. So the biomass fly ashes require the use of a water reducer/superplasticizer for a replacement of more than 10% fly ash.

The superplasticizer used in the present work for studying the workability of the mortars was Sika. It is a super plasticizer / high water reducer / retarder for concrete, according to the Standard LST EN 934-2:2003. However, less than 1% addition the superplasticizer works as a high water reducer. Two dosages of superplasticizer were selected for the study, a minimum dosage of 0.35% (weight % of binder) to control the w/b to a value 0.55 and the spread diameter around 120-140mm and a moderate dosage of 0.75% (weight % of binder) keeping the same conditions of workability for comparison studies. The designations of samples with superplasticizer are listed in Table 4.4 and the corresponding mortar compositions are listed in Table 4.5 and Table 4.6.

Table 4.4. The designations of mortars with superplasticizer added in % (weight % of binder)

Ref 2	*CEM 42.5 R Type 1+0.35% SP*
0.35 SP 10 BFA1	90% CEM+ 10 % BFA_1 + 0.35%SP
0.35 SP 20 BFA1	80% CEM+ 20 % BFA_1+ 0.35%SP
0.35 SP 30 BFA1	70% CEM+ 30 % BFA_1+ 0.35%SP
0.35 SP 10 BFA2	90% CEM+ 10 % BFA_2+ 0.35%SP
Ref 3	CEM 42.5 R Type 1+ 0.75% SP
0.75 SP 10 BFA1	90% CEM+ 10 % BFA_1 + 0.75 % SP
0.75 SP 30 BFA1	70% CEM+ 30 % BFA_1+ 0.75 % SP
0.75 SP 10 BFA2	90% CEM+ 10 % BFA_2 + 0.75 %SP
0.75 SP 20 BFA2	80% CEM+ 20 % BFA_2+ 0.75 %SP
0.75 SP 30 BFA2	70% CEM+ 30 % BFA_2+ 0.75 %SP

Table 4.5 Mortar compositions with 0.35% SP and w/b 0.55

Mortar compositions	*w/b ratio*	*Super plasticizer (%)*	*Spread diameter (mm)*	*Setting time Initial (min)*	*Setting time Final (min)*	*Density (g/cc)*
Ref 2	0.55	0.35	150	232	600	2.26
0.35SP10 BFA1	0.55	0.35	140	440	740	2.25
0.35SP 20 BFA1	0.55	0.35	125	460	720	2.21
0.35SP 30 BFA1	0.55	0.35	120	460	750	2.23
0.35SP 10 BFA2	0.55	0.35	145	400	720	2.29
0.35SP 20 BFA2	0.55	0.35	135	330	550	2.26
0.35SP 30 BFA2	0.55	0.35	135	420	730	2.34

Table 4.6 Mortar compositions with 0.75% SP and w/b 0.55

Mortar compositions	*w/b ratio*	*Super Plasticizer (%)*	*Spread diameter (mm)*	*Setting time Initial (min)*	*Setting time Final (min)*	*Density (g/cc)*
Ref 3	0.55	0.75	160	250	600	1.93
0.75SP 10 BFA1	0.55	0.75	155	460	762	1.94
0.35SP 20 BFA1	0.55	0.75	140	460	745	1.93
0.35SP 30 BFA1	0.55	0.75	140	480	740	1.92
0.35SP 10 BFA2	0.55	0.75	160	420	712	1.94
0.35SP 20 BFA2	0.55	0.75	155	310	560	1.96
0.35SP 30 BFA2	0.55	0.75	155	420	760	1.94

The flow table values obtained for the cement biomass fly ash compositions are compiled in Figure 4.12 for different dosages of superplasticizer. On adding the superplasticizer the flow table values

increased though they also showed the similar trend of reduction in spread values on higher substitution of biomass fly ashes. The inhomogeneous particle sizes are also playing a part in it in both the fly ashes. The overall workability increased with an increase in the super plasticizer content. This makes possible the incorporation of the biomass fly ashes in the cement formulations with a controlled w/b ratio.

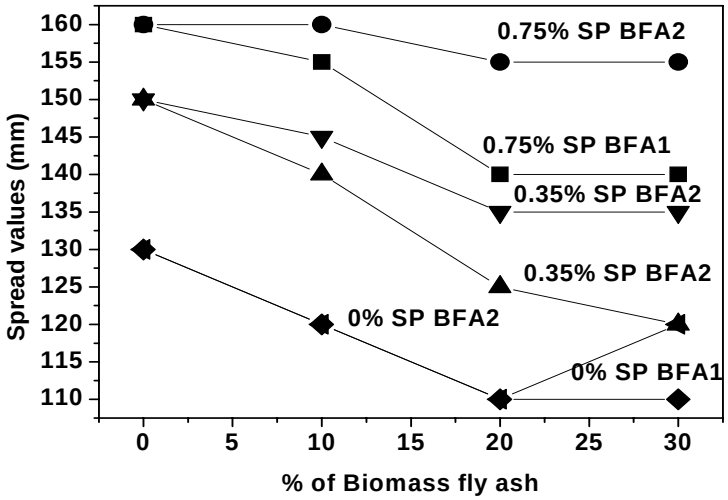

Figure 4.12. The influence of super plasticizer on the flow table measurements.

With the superplasticizer both the initial and final setting time also increased as shown in Figure 4.13. It can be observed that the setting time is almost double in the superplasticizer added mortars. The increase in setting time gives a clearer picture of fly ash reactivity in terms of hydration on deciding the setting behaviour. It was also noted that the setting time was also increased slightly on increasing the superlasticizer content. For higher content of biomass fly ash incorporation (more than 10%) a superplasticizer dosage of less than 1% is enough for a moderate spread diameter properties.

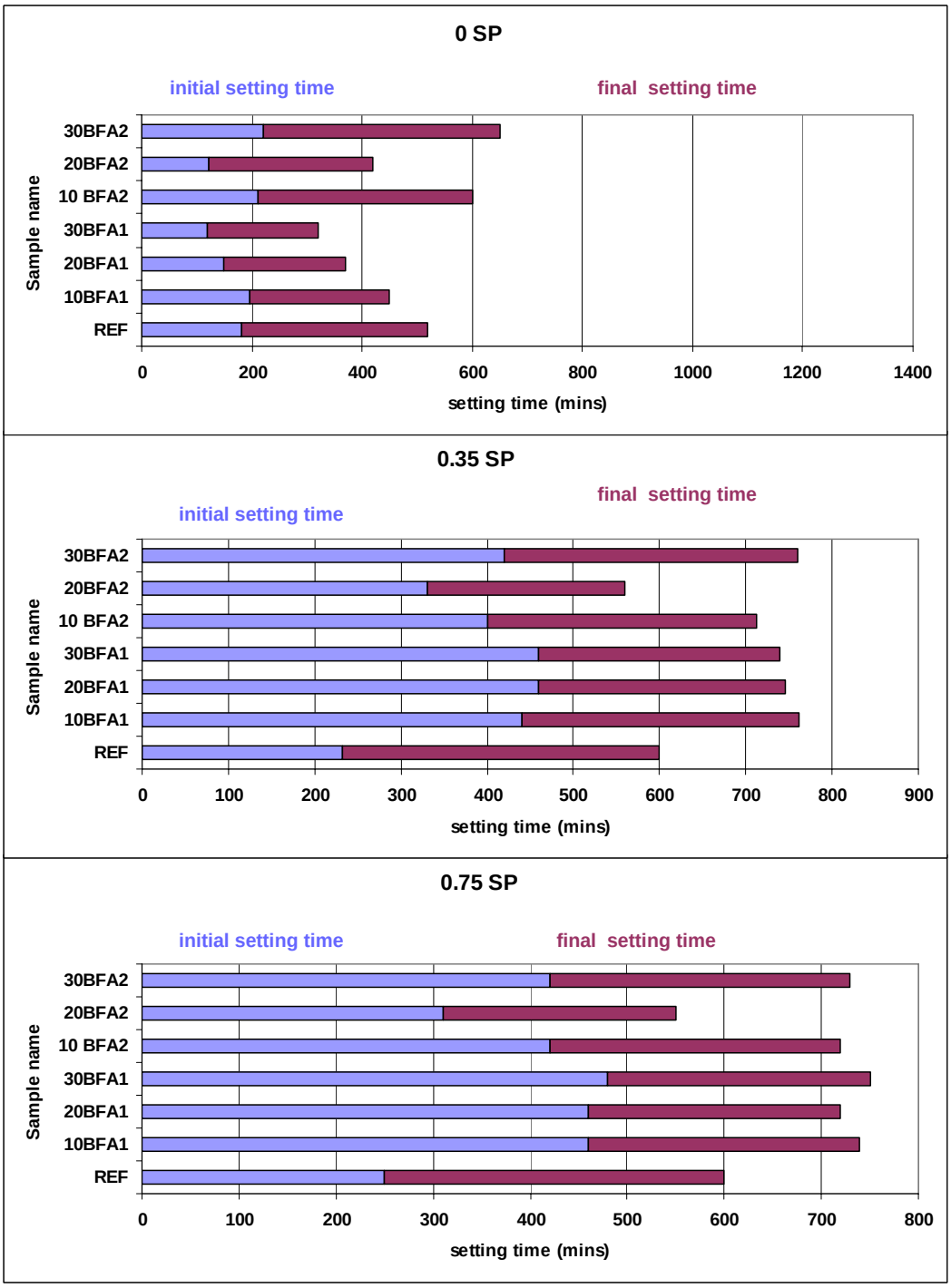

Figure 4.13. Setting of biomass fly ash cement mortars with and without superplasticizer

4.4.1.3. Effect of biomass fly ashes on the rheology of the biomass cement mortars

For a clear evaluation of the effect of biomass fly ashes on the workability of mortars rheological measurements are necessary. In Figure 4.14 the rheological measurements for the two biomass fly ashes at two different percentage of fly ash substitution (10% and 20%) are shown. The gradation and fineness of the sand, cement and admixtures content and the water/binder ratio of the mortar are the composition parameters that can affect the rheological behaviour. All tests were conducted at the same dosage of superplasticizer (0.75 %) with the same w/b ratio (0.55) to fulfill the minimum requirement of the plasticity, to start the rheology experiments and also to keep up all parameter constant except the binder components. Flow table spread values were used along with the rheometer data to study the influence of biomass fly ashes on the rheological properties of mortars. The flow table spread values and the Vicat setting behaviour showed that when Portland cement is replaced by biomass fly ashes, the workability of mortars changed significantly. Increasing the plasticizer content by more than 0.75 % did not provide any significant improvement in the workability. The fluidity of the less amount of biomass fly ash incorporated mortars increases beyond the measurement limit of the flow table on increasing the water content. Thus the substitution compositions were chosen to a limit of 20% biomass fly ash incorporated formulations in order to study the sole effect of biomass fly ash influence on the rheological properties in comparison with the flow table measurements.

From the rheological properties obtained, it can be seen that there is an increase in the torque of the mortar mix on increasing the biomass fly ash content (Figure 4.14, 4.15). The effect is the greater on 20BFA1 biomass fly ash incorporated mortars. The torque also increases by prolonging the measurements (Figure 4.15). Particle collisions, formation of the hydration products, and the corresponding reduction in free water available are the possible causes for that variation. The mixtures will show adequate fluidity only if the amount of water added is enough to fill in the porosity of the system and then keep the solid particles separated to avoid an intense friction. [Luciano et al. 2009]. As the biomass fly ashes are finer and have higher surface area than the cement grains, they reduce the amount of free water available to lubricate the solid particles. As a result the internal friction of the particles increases and the plasticity of the mixture diminishes. The irregular shape of the biomass fly ashes enhances the internal friction. Such mechanism is observed especially in mixtures with lower initial workability such as in 20 BFA1. In addition to this the fine particles in the solution have a stronger tendency to agglomerate, which hampers the adequate flow of the mixture.

The reference mortar as well as the 10% biomass fly ash substituted mortars showed a consistent plasticity where as 20BFA1 showed the least plasticity and the fitting of flow curves by the Bingham model was poorer after 15 min of testing. As a consequence the open test is shortened. BFA2 showed a greater plasticity than BFA1 indicating the higher surface area and the water adsorbing organic content in the biomass fly ash BFA1. The vertical variation on the torque line increases gradually in each stop time (15. 30, 45 and 60 minutes) (Figure 4.15). During this period, an intense structure formation is expected and the maximum torque required to turn back the movement of the mixtures is higher at each pause.

The evolution of plastic viscosity is shown in Figure 4.16. It can be observed that the plastic viscosity is higher for biomass fly ash BFA1 incorporated mortars and the biomass fly ash BFA2 showed a lower plastic viscosity trend comparable to the reference mortar. On looking at the yield stress values, g, [Figure 4.17 an increase can be observed along the test and with the biomass fly ash incorporation. The composition 20 BFA1 showed a faster loss of workability and the accuracy of fitting by the Bingham´s model became poorer. The plastic viscosity depends largely on the volume of solid particles and how densely they are packed. The microstructure that is mostly responsible for a high yield stress is the three dimensional network that often forms due to flocculation. The yield stress reflects the extent of this flocculation and the strength of the attractive inter particle forces responsible for flocculation [Leslie et al. 1995]. The observation of the figures confirms the agglomeration of fly ash particles as well as the low availability of the free water which in turn are responsible for the high yield stress and higher plastic viscosity in biomass fly ash BFA1 mortars. The BFA2 mortars show a similar trend in the yield stress values but the plastic viscosity was less compared to the all other compositions in the study.It is an established explanation that the hydration is known to increase both yield stress and plastic viscosity [Tattersall 1983] The increase in the yield stress and plastic viscosity along with time can be explained by this.

From the measurements of fresh properties it can be inferred that biomass fly ashes influence the properties in a greater measure because of its specific particle properties. Fineness, irregular shape and the organic content influence the workability of the biomass fly ash incorporated mortars in a prominent way.

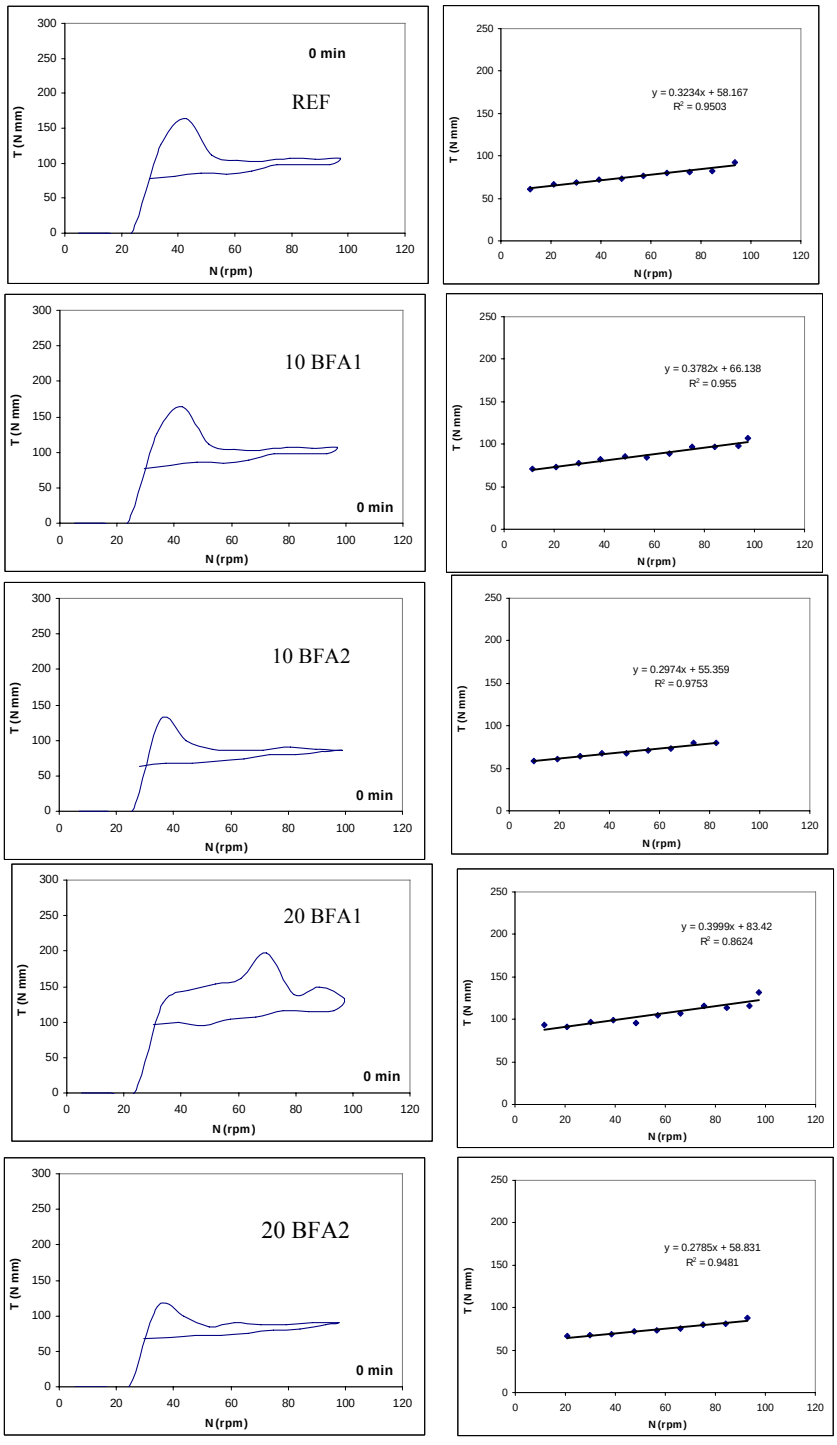

Figure 4.14 Flow curves (torque vs speed) of the biomass fly ash incorporated mortars at initial rotation about 10 minutes after the water addition.(with curresponding downcurve values)

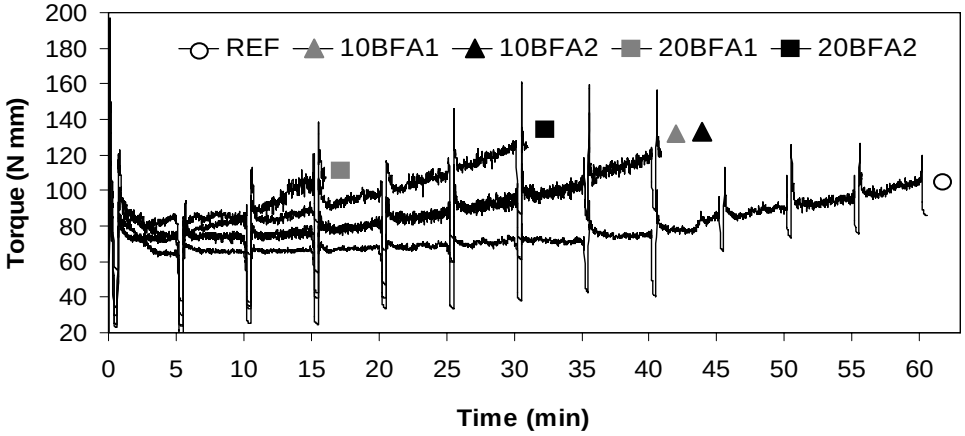

Figure 4.15. The evolution of torque of the biomass fly ash with time.

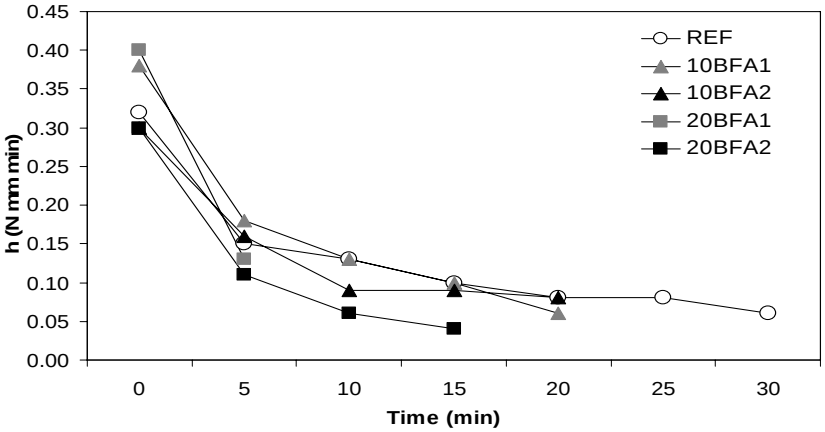

Figure 4.16. Evolution of plastic viscosity with time.

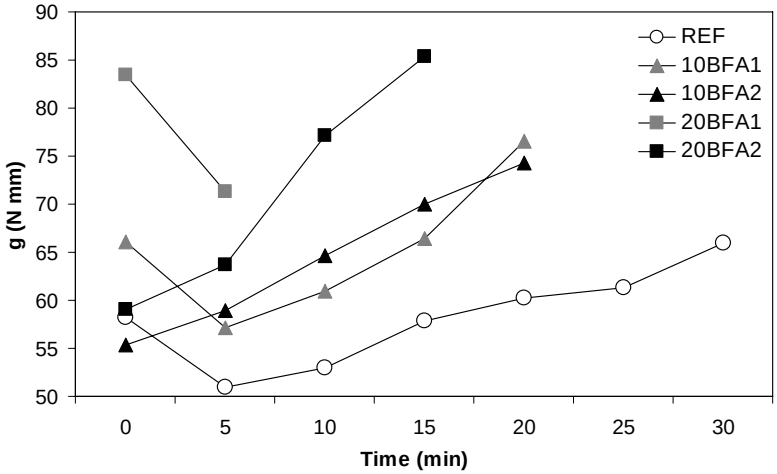

Figure 4.17. Evolution of yield stress value (g) with time.

4.4.2. Hydration of biomass fly ash cement pastes and mortars.

4.4.2.1. Electrical resistivity of hydrating biomass fly ash cement pastes

Resistivity is used to study and analyse the hydration process of cement based materials at early stages [He and Li 2004]. The impedance measurements of the biomass fly ash incorporated cement pastes are shown in Figure 4.18. Cement pastes with w/b ratio 0.55 and superplasticizer content 0.75% is used for this test. It can be observed that the rate of resistivity of the biomass fly ashes is slightly less than that of reference mortars. The main factors affecting the resistivity of the pastes are the free water content, the hydration products, the particle size and the surface area of the components. It can be observed that resistivity for each composition reached to a maximum and remained stable at the end of around 48 hours, indicating the reduced hydration rate with a peak of hydration that is achieved by the end of the first two days.

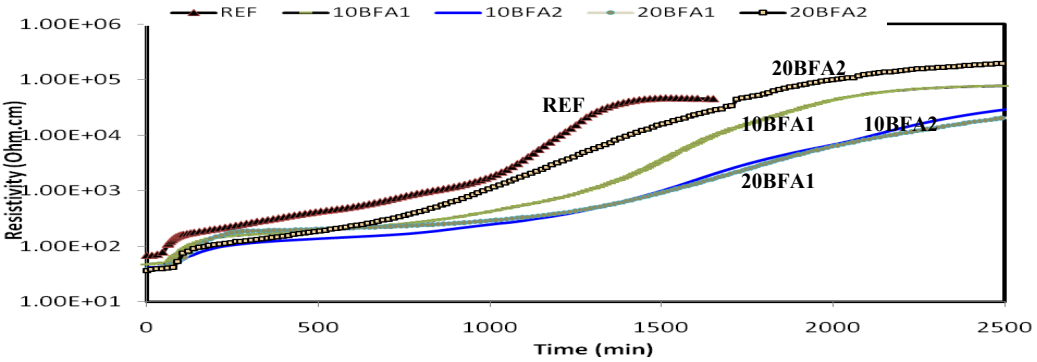

Figure 4.18. The resistivity curves of the biomass cement paste sample on hydration

The hydration products, especially the CSH gels are mainly responsible for the enhancement of the resistivity of the pastes. The cement paste is having the highest content of hydration products relative to the biomass fly ashes especially in the earlier stages of hydration. Obviously, the reference cement paste is showing the maximum rate of resistivity in the initial hours.

Figure 4.19 shows the change in bulk resistivity with time up to 1000 min for the biomass fly ash cement pastes taken with a w/b ratio 0.55 . This low resistivity region indicates a high ionic concentration and good ionic mobility. Here also the biomass fly ash incorporated cement pastes are having lesser resistivity compared to that of reference cement paste. This can be mainly due to the decrease in the cementitious phases and also the increase in the alkali ions level as the biomass fly ashes contain soluble alkalis richer than that of the ordinary Portland cement as per the leaching

experiments. The electrical resistivity of the cement pastes is very sensitive to the ions present in the mix.

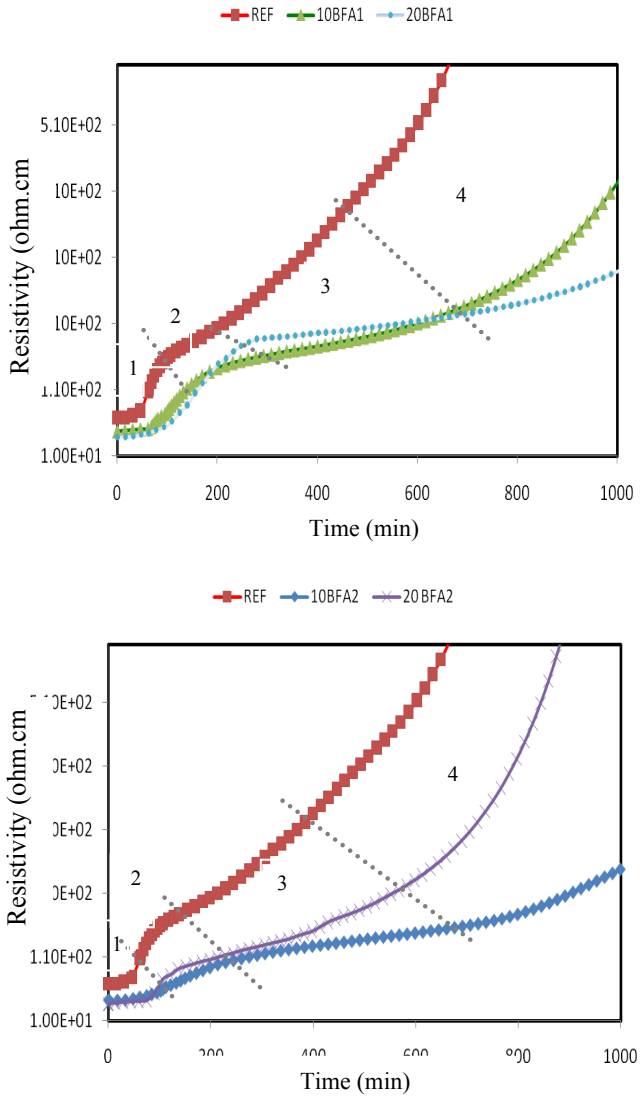

Figure 4.19. Setting behaviour from the electrical resistivity curves

To characterise the hydration process based on electrical resistivity, four periods are defined as shown in Figure 4.19. The period 1 is the period in which the resistivity is the minimum and is in the steady state. This is the dormant period where dissolution of ions is happening making the system the maximum conductive. After remaining in the steady state for a time the resistivity starts increasing in response to a competition balance between dissolution and precipitation of phases. In the third period which is in the range of setting period, the electrical resistivity is changed gradually over time indicating the decrease of porosity and increase of tortuosity. The final setting time

occurred during the third period. In the fourth hardening period the curve of electric resistivity continue to rise to a large electrical resistivity which existed after setting. This represents further decrease of porosity and water content.

The trend of setting behaviour in the third phase illustrated by the resistivity curves are in agreement with the Vicat measurements done on biomass fly ash cement mortars. The lower resistivity values as well as the flattened resistivity curves in the initial periods up to the phase 3 indicate that the setting of the biomass fly ash incorporated cement pastes were delayed compared to the reference mortar. Among the biomass fly ash cement pastes, 10BFA1 shows a higher resistivity compared to the remaining compositions. And 20 BFA2 shows comparatively lower resistivity. This can be mainly due to the difference in the chemical composition of the fly ashes. Fly ash BFA2 has more alkali content compared to fly ash BFA1 which makes the paste more conductive in the initial wet stage. Here also there was no indication of extra water consumption in the biomass fly ash incorporated cement pastes which can be indicated by a sudden increase in the resistivity during the first hour, if it happens. This confirms what was happening during the rheological experiment which indicated a loss of plasticity for the biomass fly ash cement mortars especially when the biomass fly ash BFA1was incorporated by an amount of 20%. In this case the increased surface area and irregular shape of the fly ash particle along with content of carbon are causing increased friction among the grains because of agglomeration and water adsorption leading to the loss of plasticity of the cement mortar samples in an earlier stage itself compared to the other cement paste formulations.

4.4.2.2. Temperature of hydration of biomass fly ash incorporated cement pastes/mortars

Results of calorimetric experiments conducted on the biomass fly ash cement pastes are shown in Figure 4.20. The highest temperature of hydration, ~40 ºC, was observed in the pure cement paste after a period of approximately 10 hours. The hydration process in all the samples reached a steady state temperature 22-24 ºC within 2 days. As the amount of fly ash content was increased, the heat of hydration decreased indicating a reduction in the hydrating phases in the ash replaced cements.. From Figure 4.20 it was also evident that the rate of hydration for fly ash BFA1 substituted cement pastes was less compared to that of fly ash BFA2 substituted cement pastes. The difference in the hydration rate and the shift in hydration peak are probably influenced by the alkalis and chlorine present in the fly ashes that regulate the hydration process.

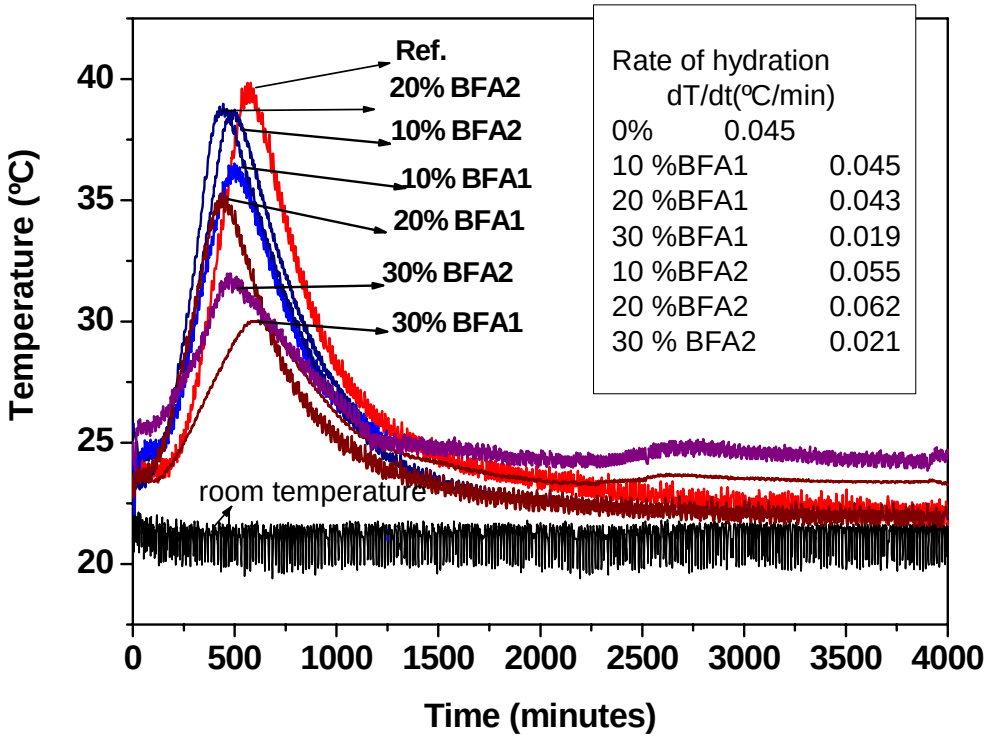

Figure 4.20. Temperature evolution upon hydration of the biomass fly ash -cement pastes

Figure 4.21 shows a comparative study with mortar samples in which superplasticizer was used keeping up the water content in the mixtures constant. There is no relative difference in hydration compared to the samples where no superplasticizer is used. The difference in temperature is due to the reduction in cement content. Only 1/3 of the cement is used for the mortar samples compared to the cement pastes in the first experiments.

From the graphs it is evident that there is no significant shift in the temperature peaks or a visible difference in the hydration evolution except that 10% BFA sample showed a slight increase in the temperature. So it can be concluded that the superplasticizer applied in this experiments acted as a water reducer only and does not make significant impact on the hydration behaviour**.**

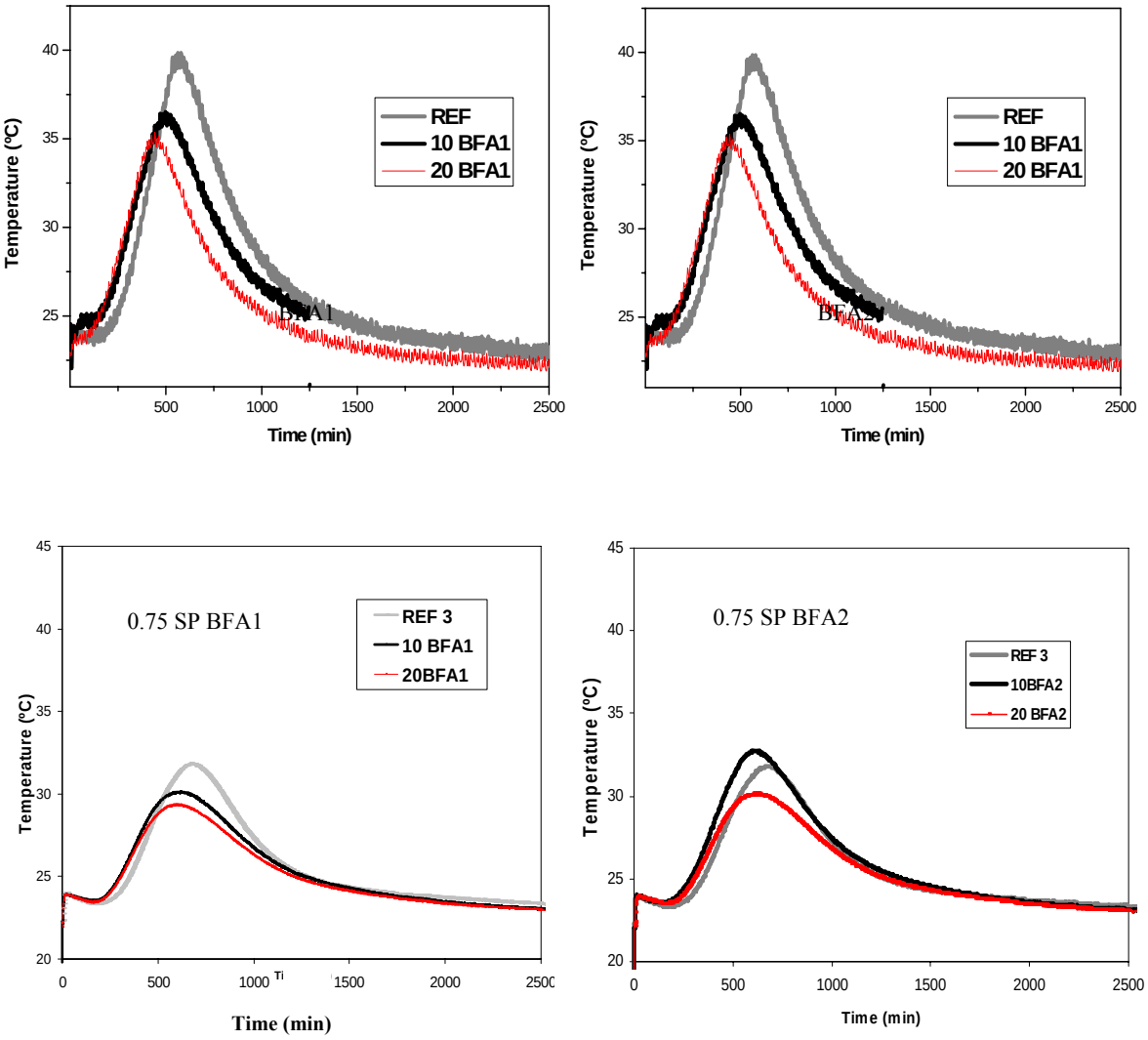

Figure 4.21.Effect of superplasticizer on hydration.

4.4.3. Effect of biomass fly ash incorporation on the hardened properties mortars.

The compressive strength of the biomass fly ash containing mortars up to the age 365 days under maximum hydration conditions (RH 100%, 22 ºC) is shown in Figure 4.22 and Figure 4.23. The w/b ratio was kept constant (0.55) through out the experiments with the help of 0.75% SP. It can be observed that on increasing the content of biomass fly ashes the strength was reduced. The reference mortar with 0% biomass fly ash incorporation showed the maximum strength value. The decrease in the strength on incorporating the biomass fly ashes is mainly due to the less hydrating

products in the mortar mix. As the density of the biomass fly ashes was slightly lower than that of cement, substituting the fly ashes by weight percentage will result into an increase of fly ash contribution to the total volume of the mortar mix.

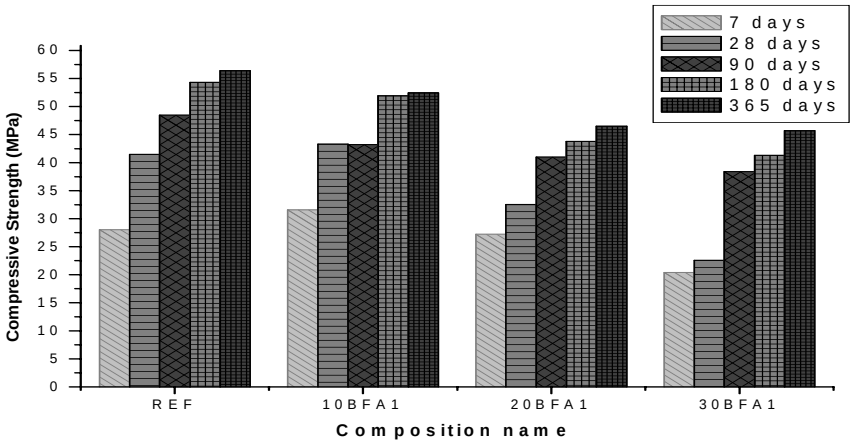

Figure 4.22. Compressive Strength values of biomass fly ash BFA1 cement mortars. (Standard deviation STDV range 1.07-2.24MPa)

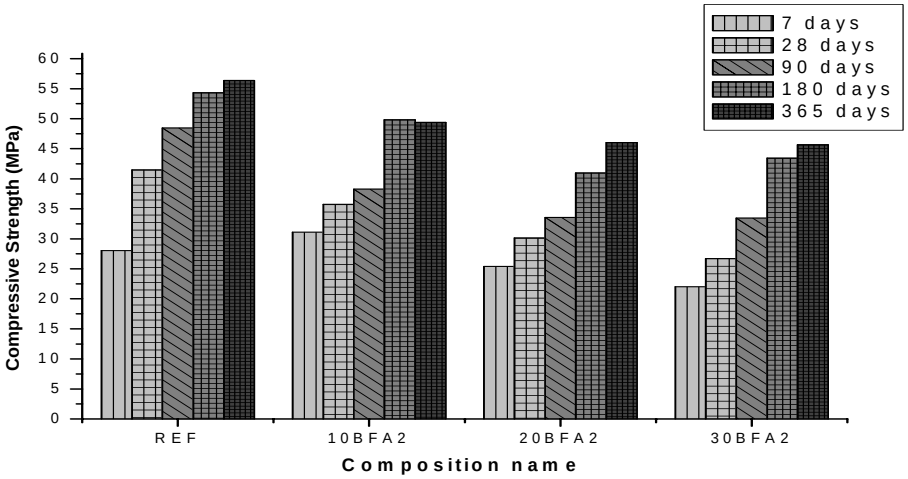

Figure 4.23. Compressive Strength values of biomass fly ash BFA2 cement mortars (Standard deviation STDV range=0.75-1.6 MPa)

Both the biomass fly ashes showed not much difference in strength development. The relative strength of biomass fly ash incorporated mortars with respect to the reference mortar strength is shown in Figure 4.24 and Figure 4.25. The reference strength for the comparison studies was assumed as the strength of reference mortar at the age of 365 days. In Figure 4.24 the strength graphs are plotted for early curing conditions such as 7 and 28 days. It can be noticed that the relative strength of 10% biomass fly ash incorporated mortars is similar to that of the reference mortar cured at the same ages. 10% BFA1 actually shows a slight increase in the compressive strength compared to the other mortars in both curing ages. 10% also followed the same trend of

biomass fly ash BFA1 but to a lesser extent. The strength increases on aging in all the samples. But there is a reduced relative strength development in the mortars with higher content of biomass fly ashes. With both fly ashes there is only a marginal difference in the strength of the mortars on incorporating 20% fly ashes. The same trend is observed for the 30% mortars also for both the biomass fly ashes. This indicates the low hydration rate in the 20% and 30% biomass fly ash composition on early hydration compared to the other compositions. However after 28 days of curing, mortars with 30% biomass fly ash incorporation could attain a strength of 40-50% compared to the 75% strength gain by the reference mortar.

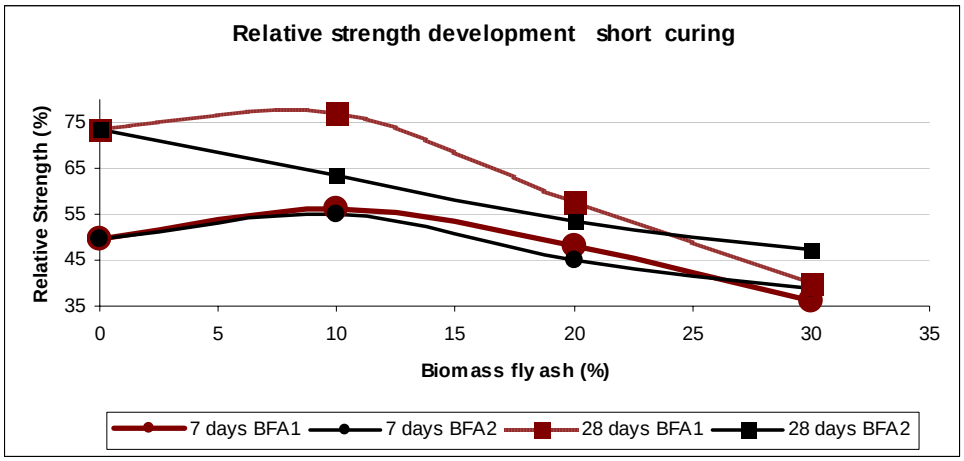

Figure 4.24. Relative strength development of biomass fly ash cement mortars at the age of 7 days and 28 days * The strength obtained for the reference mortar at 365 days is taken as the 100% reference strength for the comparison studies (Std. Difference 2%- 5%)

From the trend of strength development it can be inferred that up to 28 days of curing no visible contribution from the biomass fly ashes was observed in terms of accelerating the hydration process except that the biomass fly ashes acted more like a filler than as a binder.Thus, increasing the ash content led to an increase in the surface area of the concrete filler to be bonded by the same amount of cement as that of the control [Udoeyo et al. 2006].

In order to observe whether there is a contribution from the biomass fly ashes in later ages of curing the graphs were plotted with relative strength of the biomass fly ashes at the ages of 90 days and 365 days. From Figure 4.25 it is evident that the difference between the strength of the reference mortar and the 30% biomass fly ash incorporated mortars was around 25% and 15% for the biomass fly ashes BFA1 and BFA2 respectively. The graphs clearly show that the strength development rate is more in the higher content of biomass fly ash incorporated mortars compared to the reference mortar. When the strength difference between the 90 days and 365 days curing of the reference mortar is estimated as 15%, the 30% biomass fly ash BFA2 showed a strength

difference of 20% between its 90 days and 365 days strength values. 30% BFA1 also shows a strength increase of around 12%. The relative strength obtained at the age of 365 days; on 10% substitution were 95% and 90% for the biomass fly ash BFA1 and BFA2 respectively. In the case of 20% fly ash substitution the strength of the mortars were 82% and 80% for BFA1 and BFA2 respectively. All the more, the 30% biomass fly ash inclusion showed a relative strength of 80% for both types of biomass fly ash mortars compared to the reference mortar.

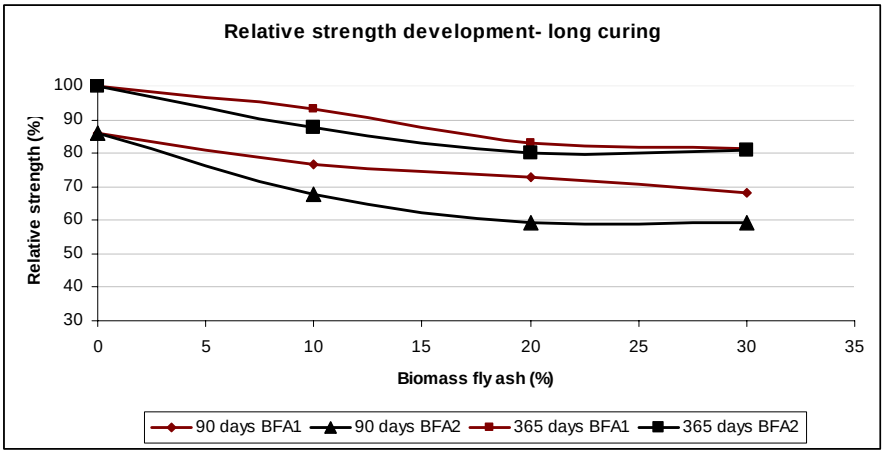

Figure 4.25. Relative Strength development of biomass fly ash cement mortars at the age of 90 days, 180 days and 365 days (* The strength obtained for the reference mortar at 365 days is taken as the 100% strength for the comparison studies).(std. 2%-5%)

The improvement in the later-age strength may be due to both the fine-filler effect and the pozzolanic or latent hydraulic property of the biomass fly ashes. The pozzolanic activity of fly ashes in the matrix enhances the formation of additional calcium silicate hydrate (CSH) binder, through the reaction of amorphous silica (SiO_2) content of the ash with the free lime ($CaOH_2$), from OPC hydration and from the chemical reaction of the high CaO content of the ash with water. The high Ca content in the biomass fly ash BFA2 can contribute in terms of hydraulic activity also. However there was no significant strength difference between both 20% and 30% substitution levels of the biomass fly ashes. It could be due to the inadequate water in the mix for the continuation of the weak pozzolanic activity of the ash in the concrete since self-desiccation may have taken place much earlier with such addition levels [Siddique 2008].

The results of the three-point bending tests on the biomass fly ash cement mortars for flexural strength evaluation are shown in Figure 4.26 and Figure 4.27. Three samples were used for each test. It can be seen that the difference between the samples cured up to 28 days were small in all the samples and the variations were seen from 90 days measurements onwards. From this point it was

observed visibly that the flexural strength also decreased according to the increase in the biomass fly ash content. The flexural strength development is also attributed to the hydration process in the cement matrix. Generally the 180 day strength measurements showed the maximum strength for the samples in the present work. But the flexural strength measured after 1 year showed a lower value. This may be due to the micro cracks developed in the samples. However it can be noticed that the variation in flexural strength is not enhanced much in the mortars with high biomass fly ash content. 20BFA and 30BFA did not show significant difference in the flexural strength development throughout the curing period. The reason can be the inhomogenous compostion of biomass fly ashes inside the cement matrix because of the reduced workability during the mixing time and higher porosity because of the irregular particle sizes of the biomass fly ashes.

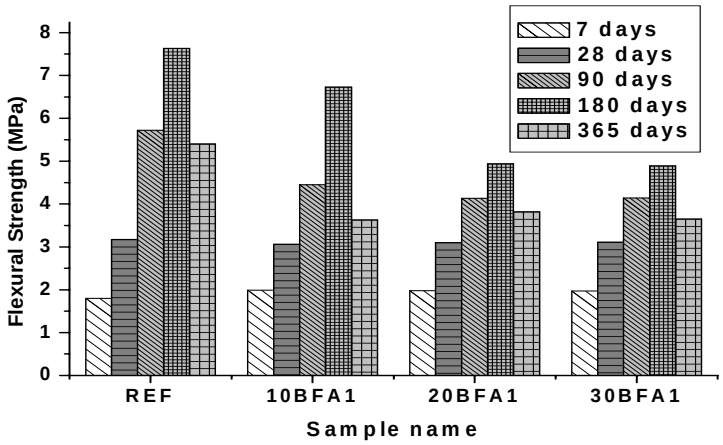

Figure 4.26. Flexural Strength values of biomass fly ash BFA1 cement mortars (Standard deviation STDEV range =0.03-0.4MPa)

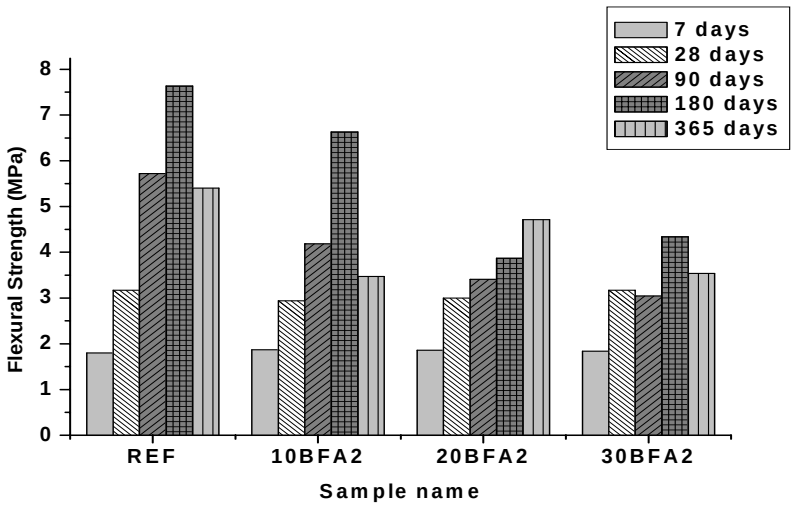

Figure 4.27. Flexural Strength values of biomass fly ash BFA2 cement mortars.

4.4.4. Microstructure Evaluation

4.4.4.1. Total porosity and pore size distribution

Total porosity determined by water immersion for mortars with and without biomass fly ashes is shown in Figure 4.28. The presence of biomass fly ash seems to increase the porosity level of mortars at any age (28, 90 and 720 days). This effect is predominant for 30% BFA2 biomass fly ash containing mortars. The porosity decreases with age for all mortars. However, the decrease is more important between 28 and 180 days for biomass fly ash containing mortars compared to the reference mortar. These variations in reactions are mainly due to the reduction of hydrated compounds content and to latent hydration of biomass fly ashes when reacting in the presence of calcium hydroxide. The pore diameter measured by the mercury intrusion porosimetry for 28 days cured mortars are shown in Table 4.6 and Figure 4.29. It can be observed that although total porosity increases with increasing fly ash replacement, the median pore diameter decreases. Similar results were reported for coal fly ash incorporated cement mortars [Li and Roy 1986). The mean diameter decreased because of the finer particle inclusion that in turn acted as a better packing filling effect. But the total porosity increased because of the net hydration was lesser in the fly ash incorporated mortars. But it can be noticed that by the end of 720 days the difference in the porosity for all samples dropped to a insignificant difference.

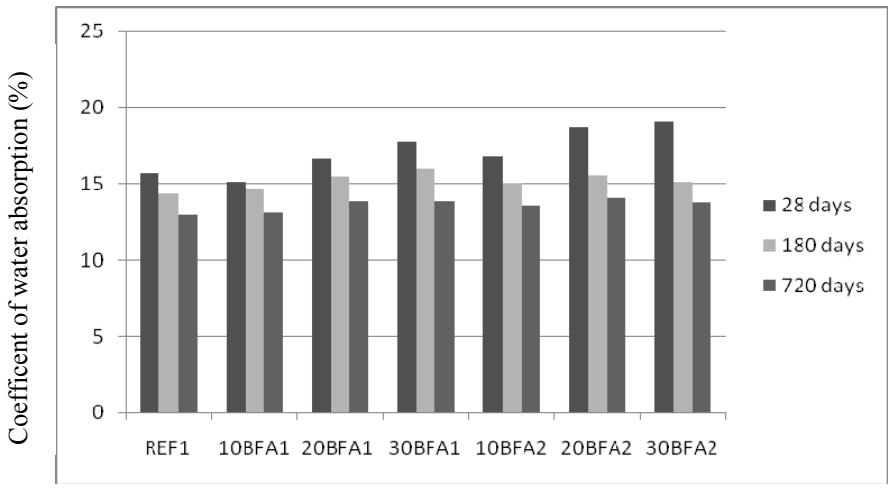

Figure 4.28. Porosity of the biomass fly ash cement mortars by water absorption

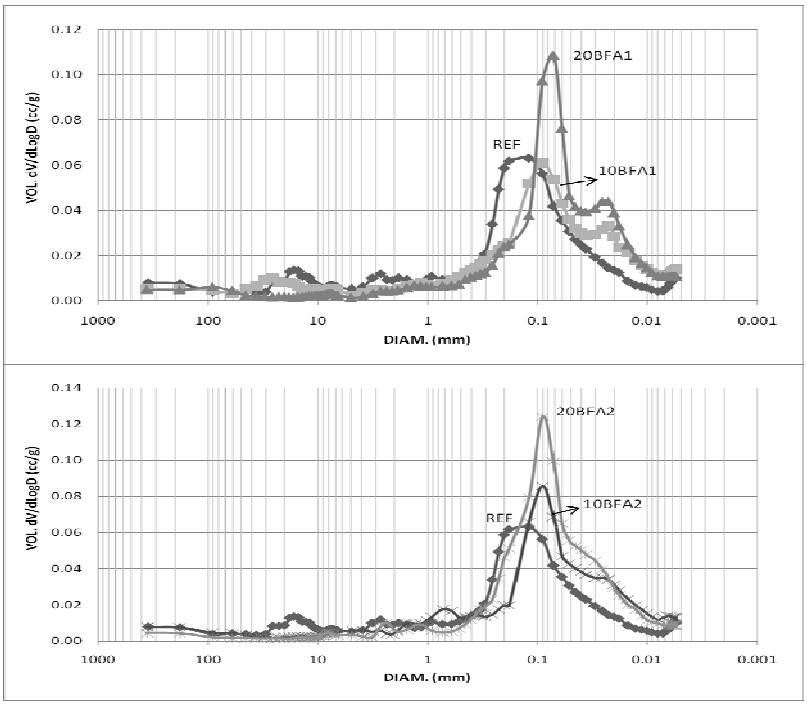

Figure 4.29. Pore size distribution of biomass fly ash cement mortars at the age of 28 days by mercury porosimetry intrusion

Table 4.6. Mercury porosimetry results of biomass fly ash cement at the age of 28 days

Sample name	*Total Intrusion volume ml/g*	*Total pore area (m^2/g)*	*Median pore diameter (volume) (μm)*	*Median pore diameter (area) (μm)*	*Average pore diameter (μm)*	*Bulk density (g/ml)*	*Apparent density (g/ml)*	*Porosity (%)*
REF	0.08	4.01	0.16	0.03	0.08	2.08	2.47	15,66
10BFA1	0.07	6.30	0.10	0.02	0.05	2.11	2.48	15.10
20BFA1	0.08	7.56	0.07	0.02	0.04	2.07	2.49	16.69
10BFA2	0.08	7.15	0.09	0.02	0.05	2.07	2.50	16.77
20BFA2	0.09	7.32	0.09	0.03	0.05	2.03	2.49	18.71

4.4.4.2. Minerals and Phases

The mineralogical composition of the fly ash cement pastes at 28 days, 90 days and 720 days of curing has been analyzed by means of the XRD method (Figures 4.30-32). The prominent peaks in all the diffraction patterns are quartz, calcite and calcium hydroxide. Peaks from ettringite, calcite

and silica were also found. The XRD patterns gave a preliminary idea of the fly ashes influence on the phase formation in the paste samples. The ettringite formation was enhanced in the cement-fly ash paste samples, specially on substitution of higher amounts of fly ash, due to the presence of alkalis and increased water content.

Diffraction patterns confirm the presence of the same phases after 720 days of curing as in the list of found compounds of reference mortar shown in the Table 4.7. The peaks for ettringite are also visible in the samples especially in 30% biomass fly ash incorporated cement pastes. It is also observed that the 720 days cured fly ash cement pastes were showing a reduced intensity level for the peaks and seemed to have less crystallanity.

Table 4. 7. Crystal phase compounds name and chemical formula.

Crystalline phase	*Chemical formula*
1. Calcium hydroxide	$Ca(OH)_2$
2. Calcium carbonate	$CaCO_3$
3. Calcium aluminate hydrate	$Ca_2Al(OH)_2.xH_2O$
4. Calcium silicate	Ca_2SiO_4
5. Ettringite	$(3CaO.Al_2O_3.3CaSO_4.32H_2O)$
6. Quartz	SiO_2

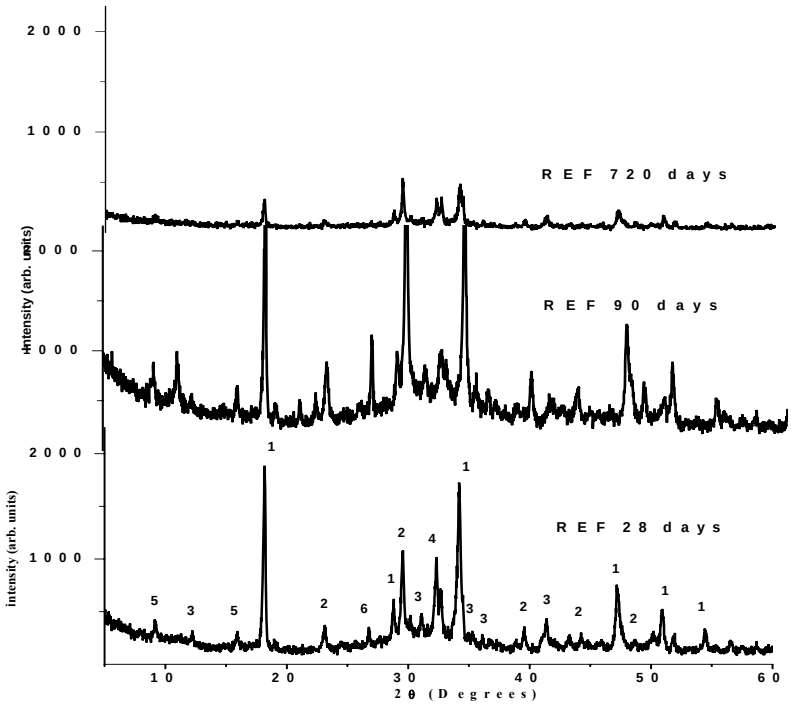

Figure 4.30 XRD pattern of the reference cement paste at different age of curing (28 days, 90 days, 720 days)

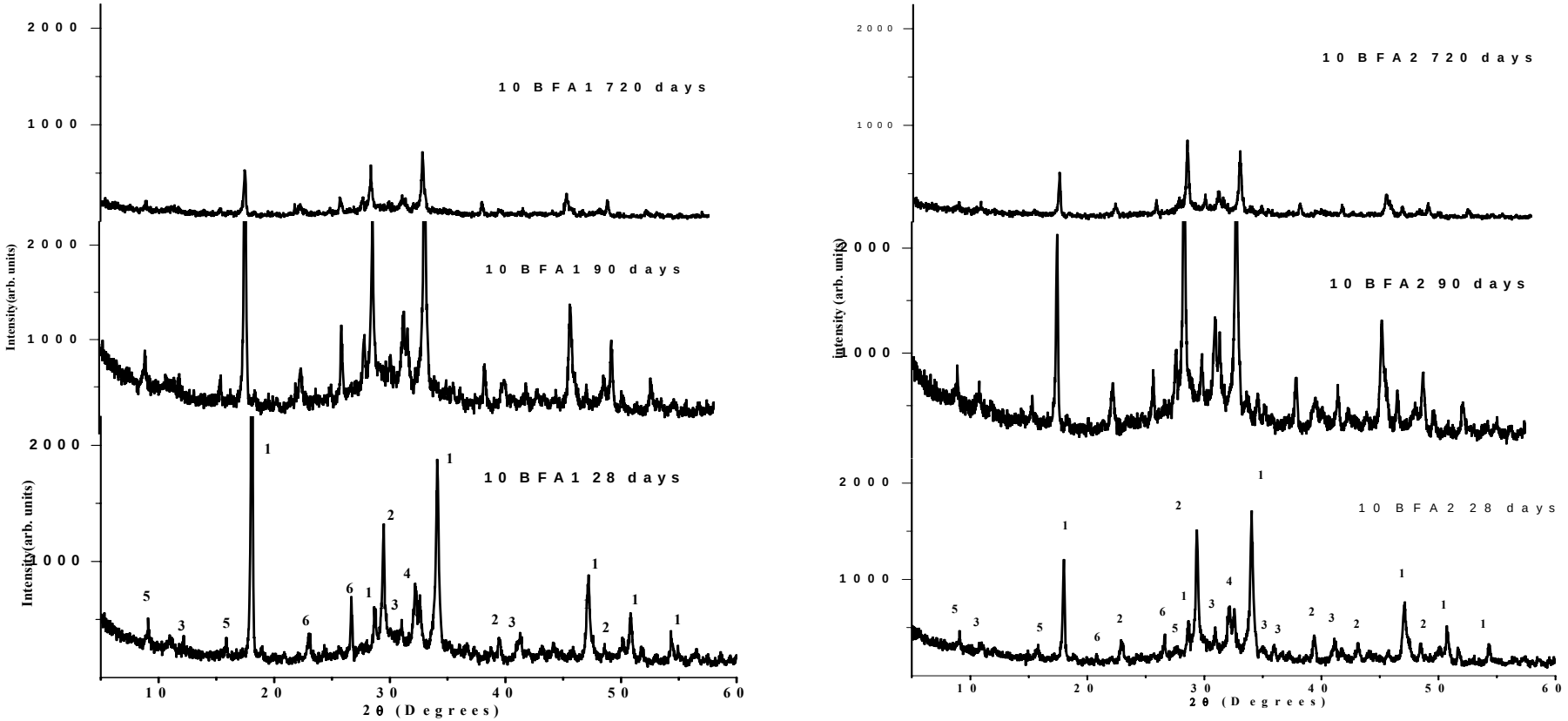

Figure 4.31 XRD pattern of 10% biomass fly ash cement paste at different age of curing (28 days, 90 days, 720 days)

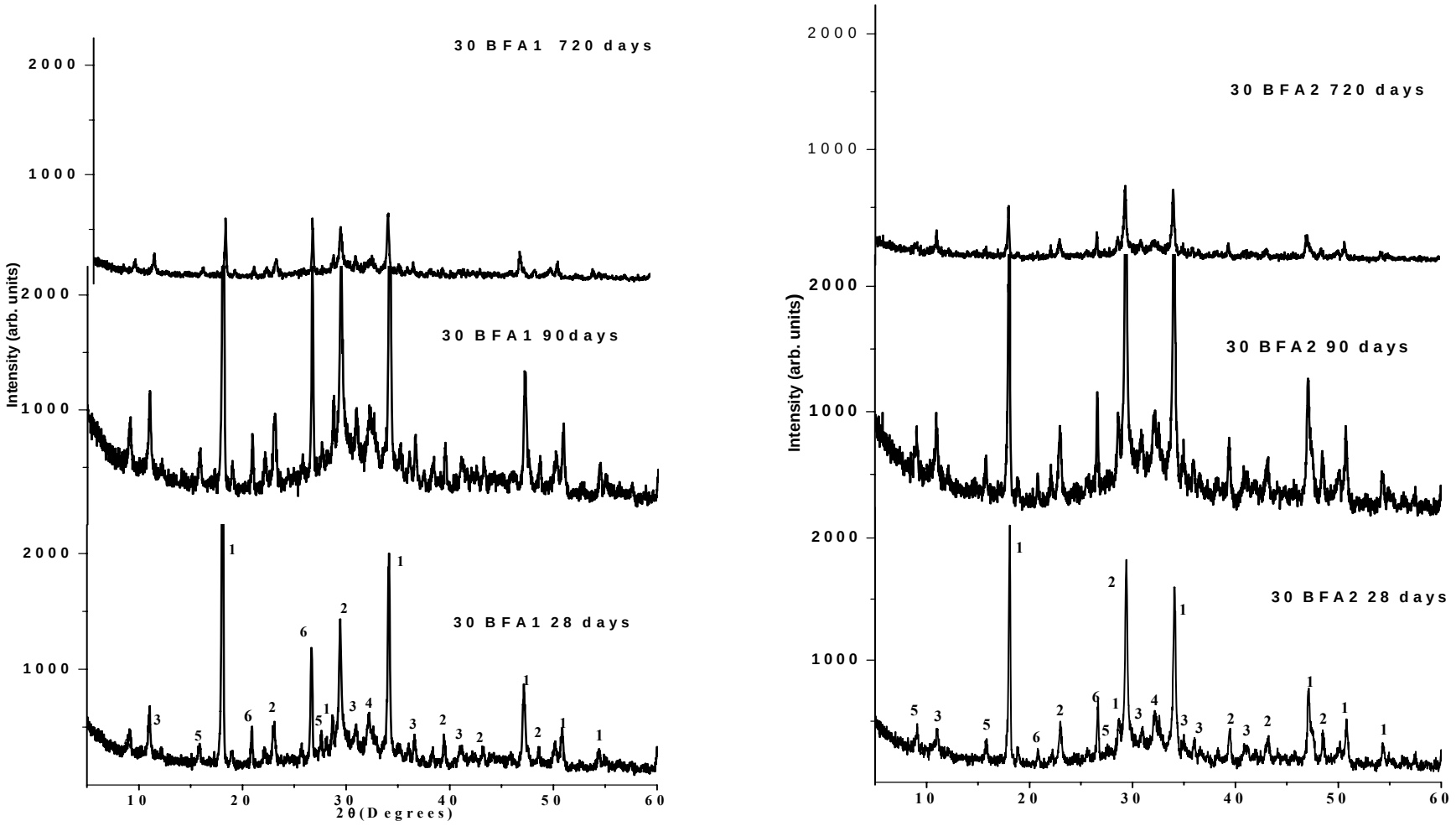

Figure 4.32. XRD pattern of 30% biomass fly ash cement pastes at different age of curing (28 days, 90 days, 720 days)

Figure 4.33-35 show the TG and DTA curves of the cement paste and of the cement-fly ash pastes after different curing time. There were 3 endothermic peaks in the DTA curves, located within the temperature ranges 135 ºC-185 ºC, 420-550 ºC and 620 ºC-780 ºC. The decomposition of calcium silicate hydrate and ettringite both occur within the temperature range 135 ºC-185 ºC. The peak at 525 ºC-575 ºC is due to calcium hydroxide (CH) decomposition. The TG curves show that the intensity of the CH peaks were reduced in the fly ash-containing pastes, compared to that of pure cement paste. Fly ash, BFA2-based pastes showed a higher amount of CH compared to fly ash BFA1. The peak after 800 ºC is related to the thermal decomposition of $CaCO_3$. The thermal analysis is in good agreement with the mineralogical characterisation obatined from XRD studies.

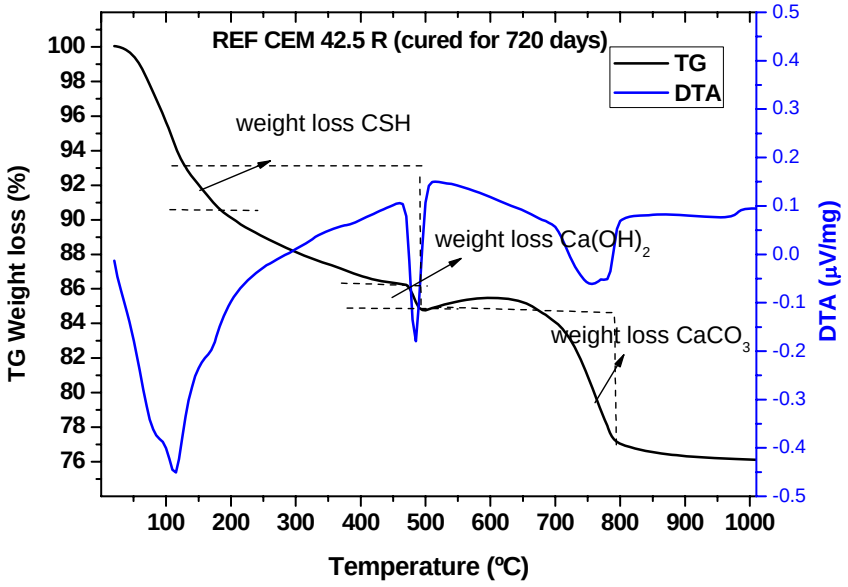

Figure 4.33. TG/DTA of the water cured cement paste for 2 year

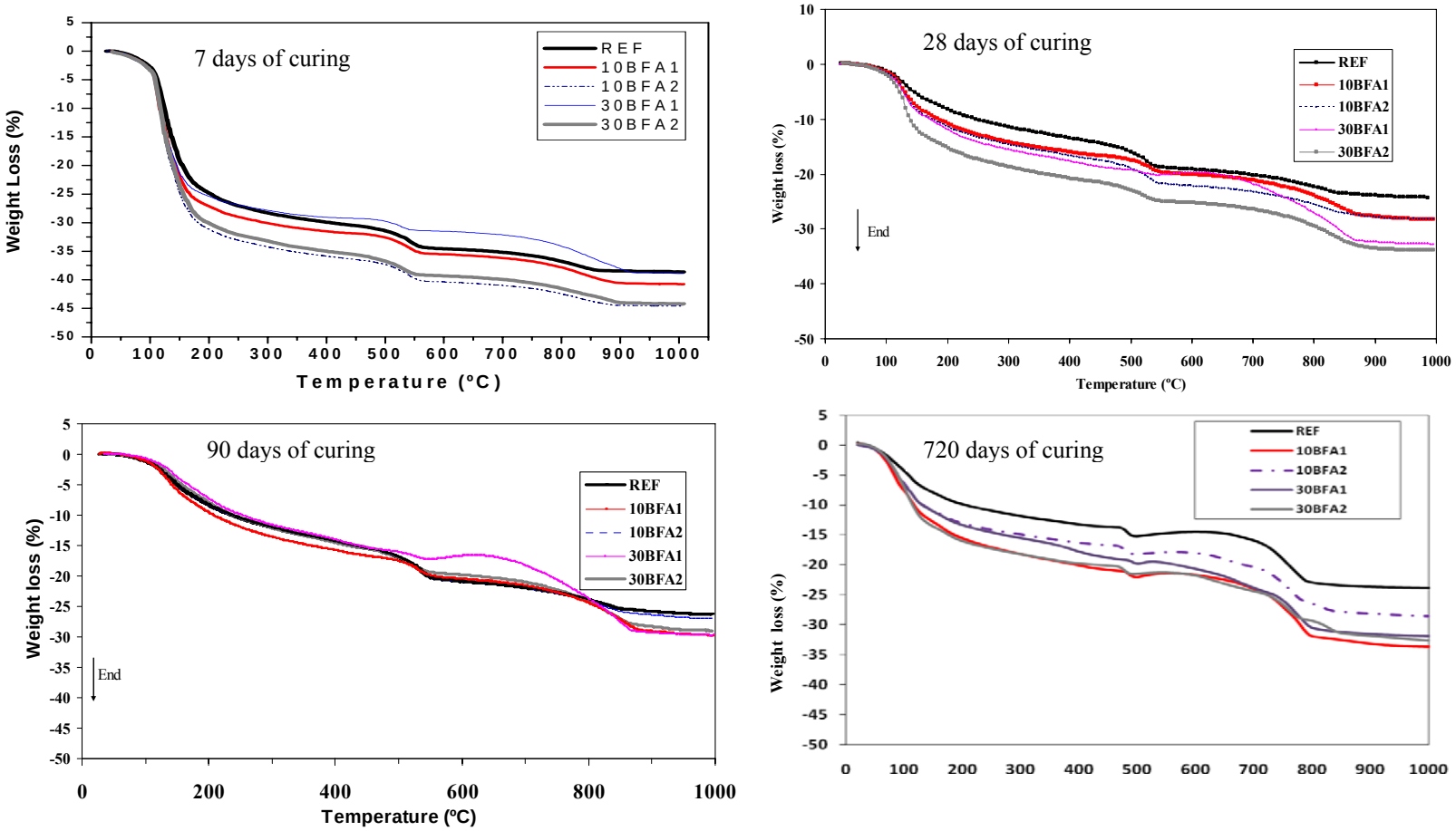

Figure 4.34. Thermogravimetric analysis curves of biomass fly ash substituted cement pastes at different curing ages

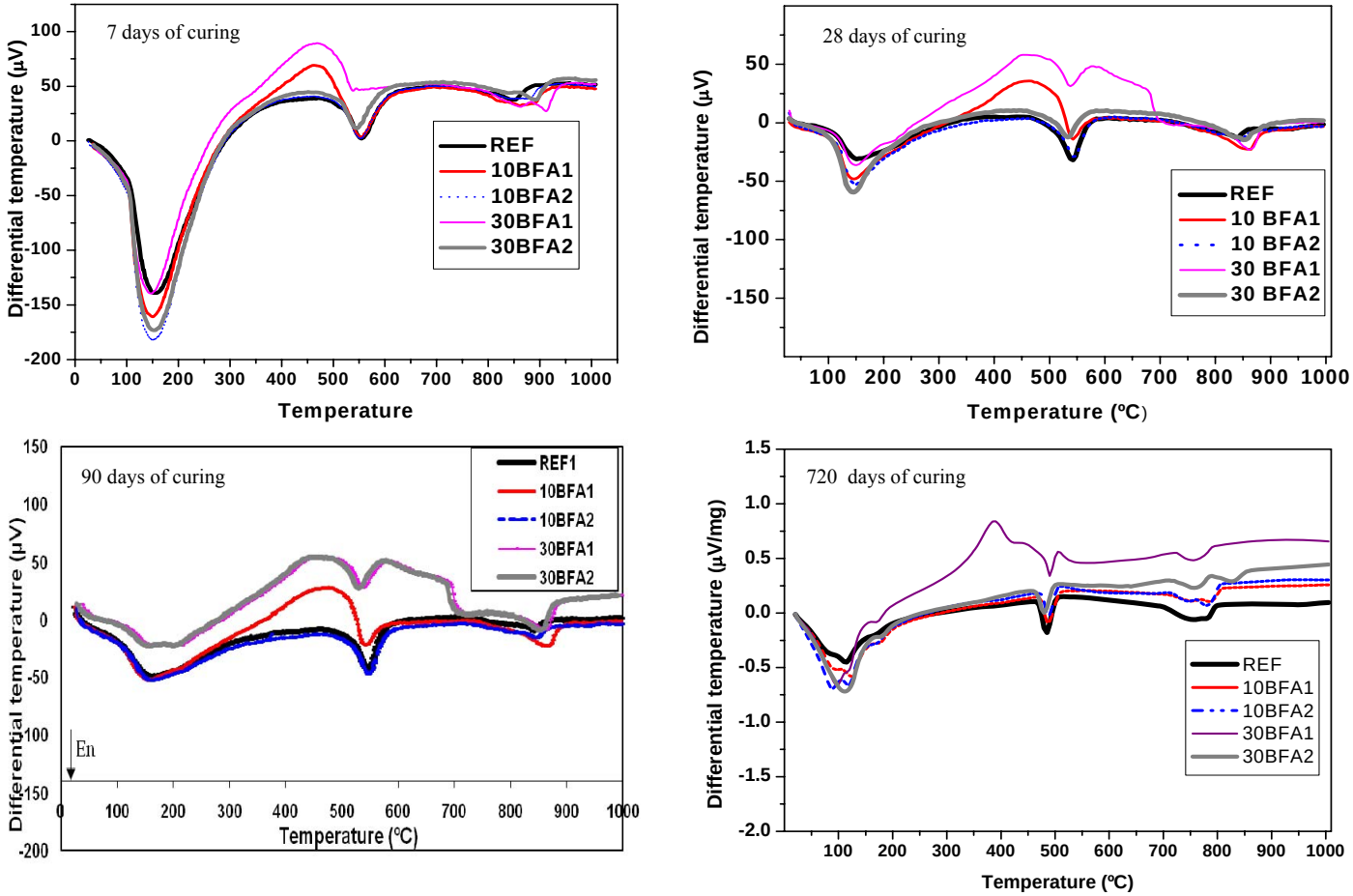

Figure 4.35. Differential thermal analysis curves of biomass fly ash substituted cement pastes at different curing ages

4.4.4.3. Content of calcium hydroxide

The amount of CH produced is a function of the relative amounts of alite and belite present in the cement. Therefore, it follows that the variation in CH indicates the amount of calcium silicate hydrate (CSH) gel formed. A contribution from the pozzolanic effect of fly ashes is also expected. The pozzolanic reaction primarily occurs between amorphous siliceous materials and CH, as a simple acid-base reaction between (CH), and silicic acid (H_4SiO_4) or $Si(OH)_4$, to form calcium silicate hydrate of general formula ($CaH_2SiO_4.2H_2O$) or CSH.

The thermogravimetry data were used to calculate the amount of Ca $(OH)_2$ in the pastes. The dehydration of $Ca(OH)_2$ occurs at a temperature in the range of 420-550ºC. The following chemical reaction usually takes place in this region:

$$\underset{(74\ g)}{Ca(OH)_2} \xrightarrow{420-550} \underset{(18\ g)}{CaO + H_2O} \longrightarrow \textbf{Eqn 4.5}$$

The equation indicates that the weight loss corresponding to one gram molecule of water (18g/mol) is originated from the dehydroxylation of one gram-molecule of calcium hydroxide (74g/mol). However, there is always possibility of some carbonation of the calcium hydroxide, even though if much care is taken during the preparation of specimens for testing, the reaction is shown in equation, [Cabrera and Lynsdale 1996]

$$\underset{(74\ g)}{Ca(OH)_2} + CO_2 \rightarrow \underset{(100\ g)}{CaCO_3} + H_2O\,(carbonation) \longrightarrow \textbf{Eqn 4.6}$$

Therefore the amount of $Ca(OH)_2$ is corrected using the amount of $CaCO_3$ detected in the TG output. Calcium carbonate decomposes as follows:

$$\underset{(100\ g)}{CaCO_3} \xrightarrow{600-780} \underset{(44\ g)}{CaO + CO_2\,(decarbonation)} \longrightarrow \textbf{Eqn 4.7}$$

Above equations show that one gram molecule of CO_2 is generated from the decomposition of one gram molecule of $CaCO_3$. However, the weight of calcium carbonate is generated, in first

place, from the carbonation of one-gram molecule of calcium hydroxide. Therefore, the weight loss of one gram molecule of CO_2 corresponds to one gram molecule of $Ca(OH)_2$ originally present in the cement paste. A reduction factor from the calcite present in the fly ashes (LOI $BFA_{calcite}$] were also applied. The total amount of $Ca(OH)_2$ in the sample is then calculated using the equation

$$\textbf{LOI } [Ca(OH)_2] = (\text{LOI}_{420\text{-}550\,^{\circ}C}) \times 74/18 + (\text{LOI}_{600\text{-}780\,^{\circ}C}) \times 74/44 - (\text{LOI } BFA_{calcite}) \quad \textbf{Eqn 4.8}$$

.

The amount of $Ca(OH)_2$ in the biomass fly ash pastes at different curing conditions was calculated by using the above method. The calculated $Ca(OH)_2$ content of the biomass fly ash cement pastes are shown in Figure 4.36. The biomass fly ash incorporated cement pastes showed lesser content of $Ca(OH)_2$ compared to that of the reference due to the lesser hydrating phases. It can be observed that the amount of $Ca(OH)_2$ formed increases with curing time. The formation of $Ca(OH)_2$ is the direct indication of the degree of hydration. [Cabrera and Lynsdale, 1995]. But In BFA2 samples it can also be observed that $Ca(OH)_2$ content decreases in the biomass fly ash cement paste after 90 days of curing. showing a pozzolanic behaviour-

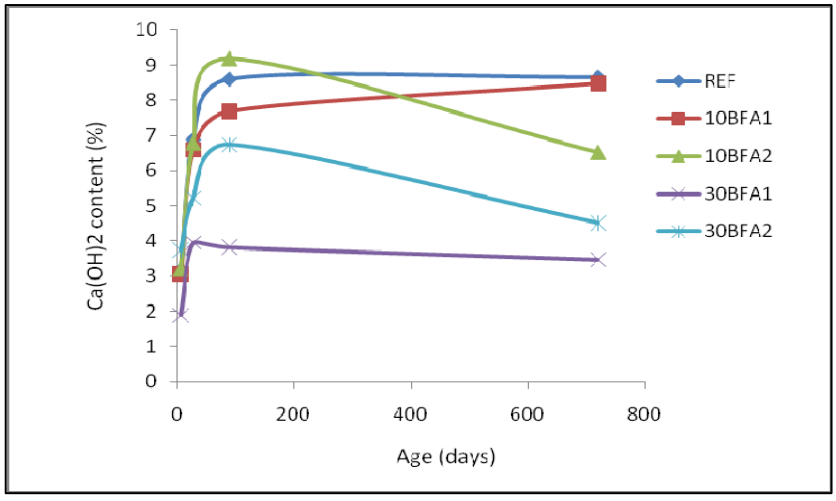

Figure 4.36. Content of $Ca(OH)_2$ of biomass fly ash cement paste at different curing period.

4.4.4.4. Microstructure evolution on hydration

When combined with water, cement undergoes a series of hydration reactions roughly expressed by the following equations (Jennings and Tennis 1994).

$$2\ C_3\ S + 10.6\ H \rightarrow C_{3.4}\ S_2\ H_8 + 2.6\ C\ H$$
$$2\ C_2\ S + 8.6\ H \rightarrow C_{3.4}\ S_2\ H_8 + 0.6\ C\ H$$

As these reactions occur, the cement and water mixture remains in a fluid stage for some hours, during which it can be easily transported and processed. This period of slow hardening, known as the induction period, is followed by a period of relatively rapid hardening. These materials, therefore, are first a fluid and then become hard at ambient temperatures. However the chemical mechanisms responsible for this induction period are not completely understood.

The ESEM images of the hydrating biomass fly ashes were taken at different curing periods to monitor the real time hydration behaviour of the biomass fly ash cement pastes. Figure 4.37 is the paste of 10 BFA1 incorporated cement that was monitored just after 1 hour of mixing. One can observe the hydroxylation of calcium compounds- the first step in the CSH formation.

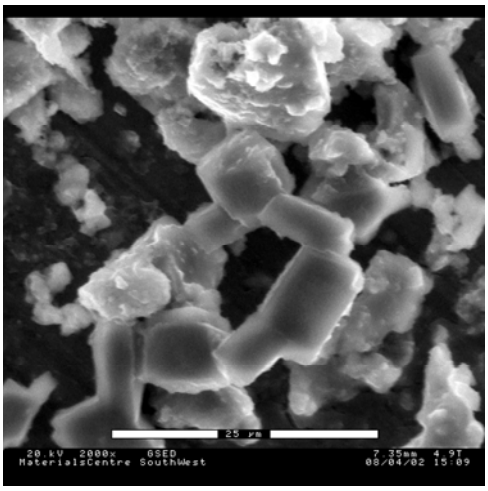

Figure 4.37. 10 BFA1 after 1 h of hydration

The ESEM images of pastes taken after 4 hours of hydration (Figure 4.38) were in the beginning of the acceleration period after the initial hydration of the C_3A phase. The C_3A phase reacted with water to form an aluminate rich gel and, following further reaction with sulphate ions within the water, ettringite in colloidal form with CH was formed. The CSH gel formation is visible in all the compositions. As the ESEM imaging is done at lower vacuum conditions.

The images seems blurry because of the amorphous surface layer of the gel forming, the beginning of CSH.

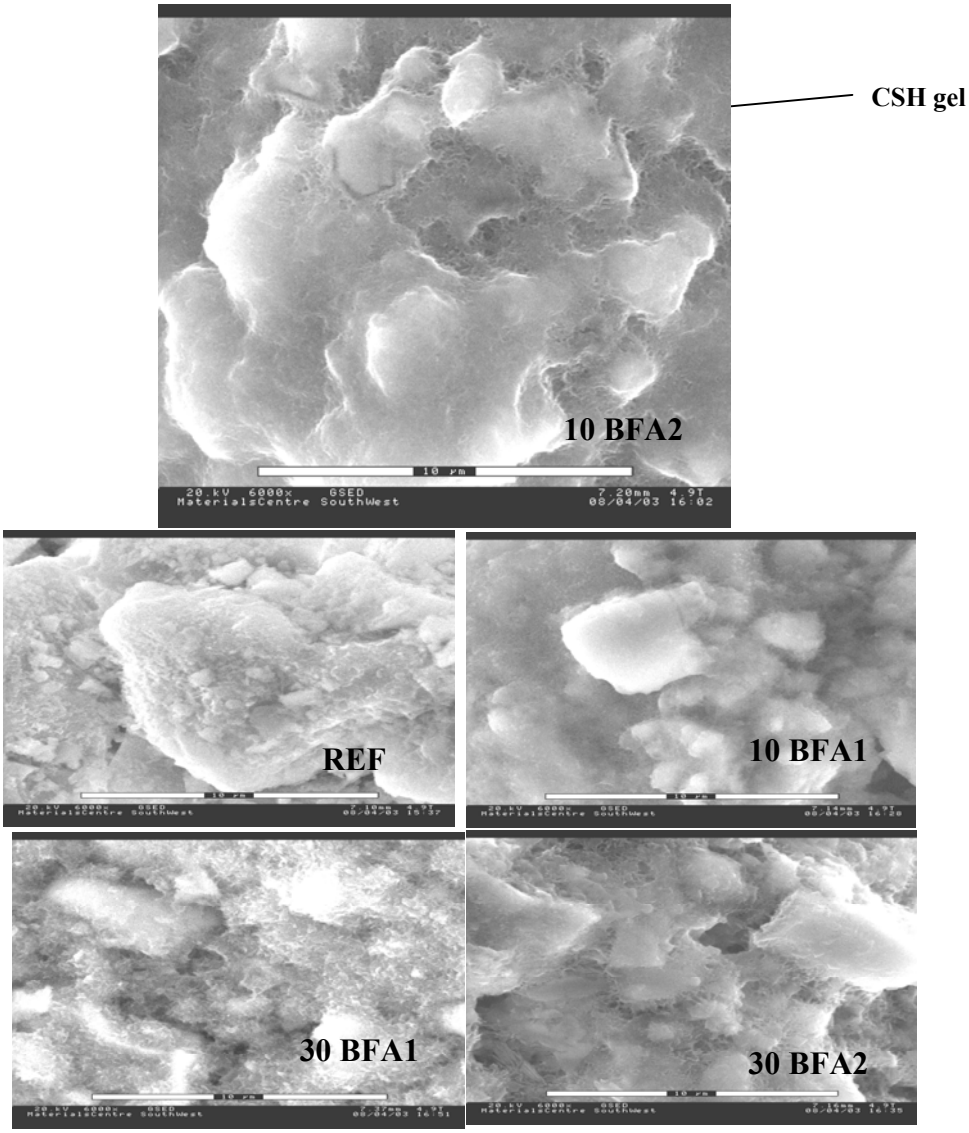

Figure 4.38. Microstructure of cement-biomass fly ash pastes after 4 hours of hydration: (a) 0% fly ash, (b) 10% fly ash BFA1, (c) 10% fly ash BFA2, (d) 30% fly ash BFA1, and e) 30% fly ash BFA2.

The ESEM images in Figure 4.38 show a gel-like structure around the cement grains identified as the amorphous CH gel.

The water content and the pH of the hydrating medium are the two major factors affecting the hydration mechanism in cements. The fly ash contained Na^{+} and K^{+} ions, together with Cl^{-} in amounts expected to influence the pH levelThese are the main factors affecting the hydration behaviour in the investigated samples. The Na^{+} ions decelerate hydration, whereas K^{+} and Cl^{-} ions accelerate the hydration process. [Lea´s chemistry of cement and concretes 2004]

After 24 hours of hydration the cement and 10% fly ash substituted pastes showed extensive CSH growth. At the same time the appearance of ettringite needles were comparatively dominant in 30 % fly ash BFA1 substituted cement paste (Figure 4.39).

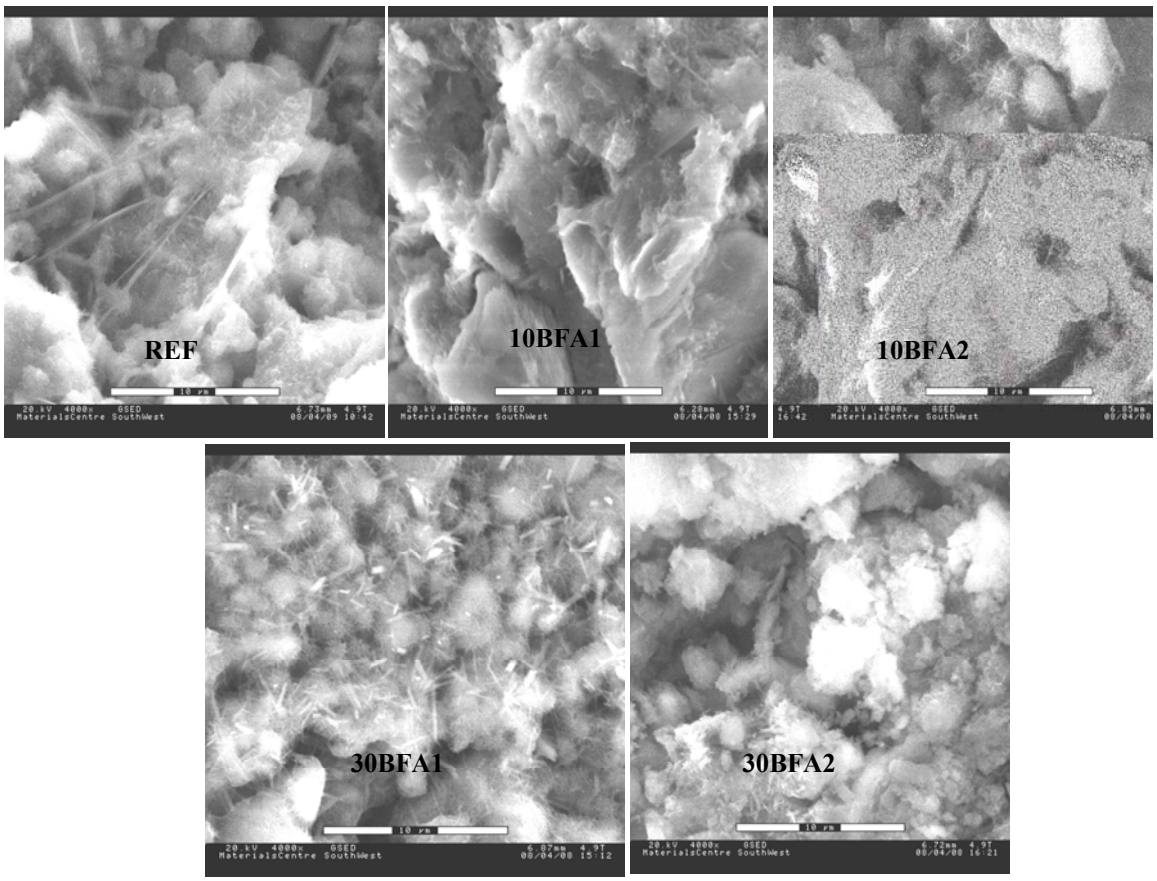

Figure 4.39. Microstructure of cement-biomass fly ash pastes after 24 hours of hydration:CSH formation (a) 0% fly ash, (b) 10% fly ash BFA1, (c) 10% fly ash BFA2, (d) 30% fly ash BFA1, and (e) 30% fly ash BFA2

After 7 days, a well-formed network of CSH crystals in the pastes covering the fly ash particles was visible (Figure 4. 40), in addition to large portlandite crystals. The CSH network was well-defined in the pure cement and 10% fly ash substituted pastes.

By 90 days the hydration is almost over and the very hardened structure is observed in the biomasss fly ash pastes. $Ca(OH)_2$ crystals were visible in the samples. Long ettringite needles were found in excess in the 30% biomass fly ash added pastes [Figure 4.42]. From these micro structural evaluation until 90 days, it could be convinced that the biomass fly ashes are not at all bringing up any deteriorating phase evolution that can cause the degradation of the biomass fly

ash included cement paste or mortars. And the mechanical strength values were backing up the durability of the biomass fly ash incorporated cements and mortars.

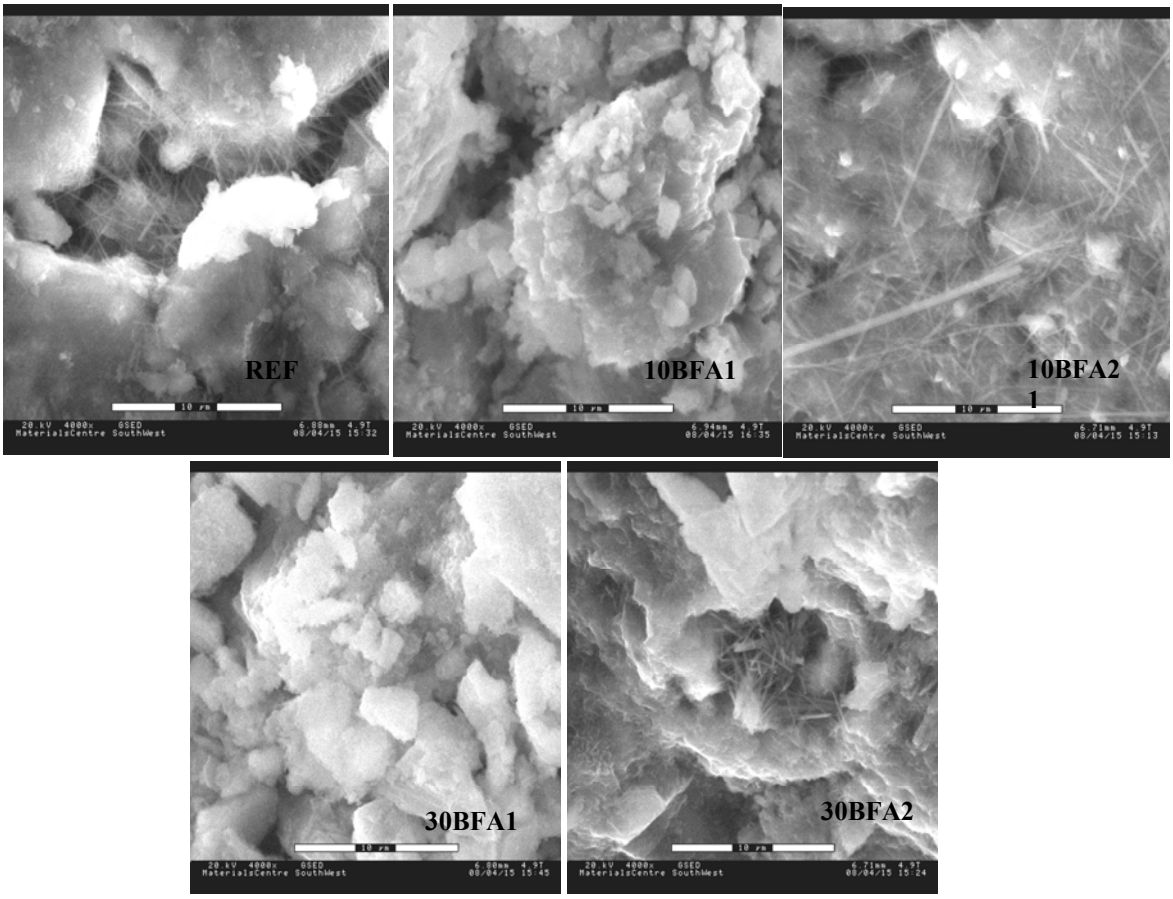

Figure 4. 40. Microstructure of cement-biomass fly ash pastes after 7 days of hydration: (a) 0%fly ash, (b) 10% fly ash BFA1, (c) 10% fly ash BFA2, (d) 30% fly ash BFA1, and (e 30%Fly ash BFA2

Analysis after 30 days of curing indicated that the hydration reaction was almost finished in the reference sample as well as the 10% biomass fly ash substituted pastes (Figure 4.41). The cement-fly ash pastes showed the silicate hardening phases and ettringite needles were observed in cements containing 30% fly ash substitution. This was attributed to the presence of sulphate ions in the fly ashes and the high water content of the pastes and also that the hydration process seemed to still going on while observing the fluffy nature of the CSH gels.

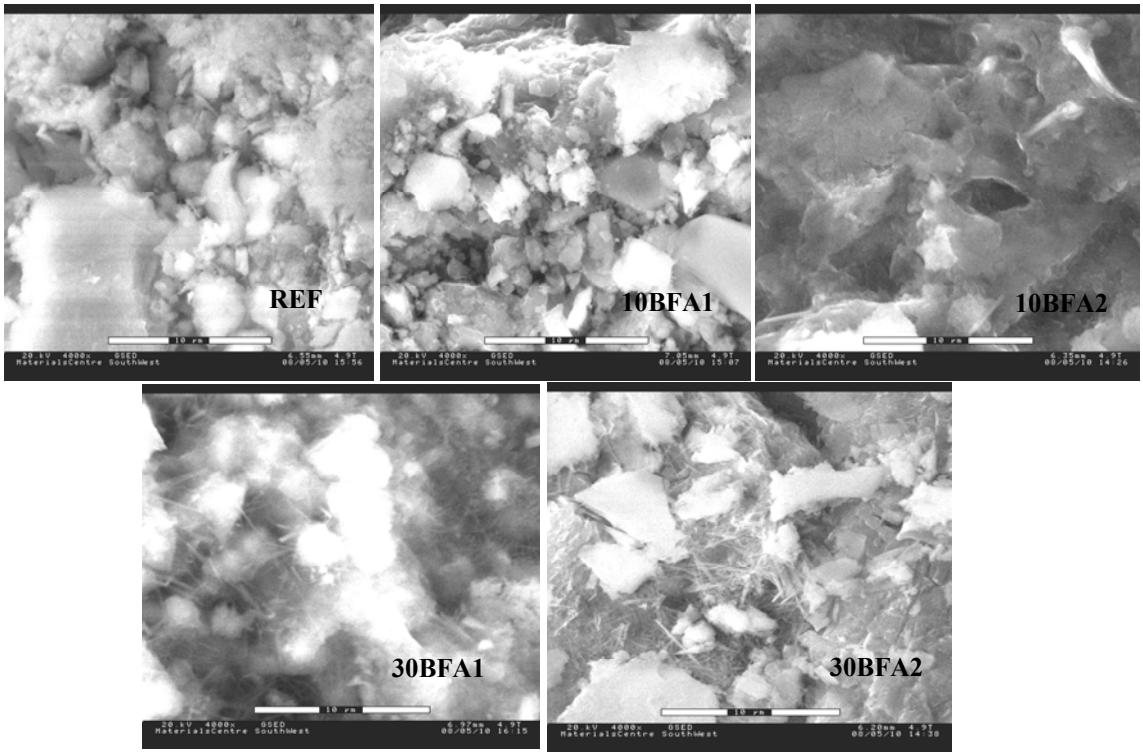

Figure 4.41. Microstructure of cement-biomass fly ash pastes after 30 days of hydration: (a) 0% fly ash, (b) 10% fly ash BFA1, (c) 10% fly ash BFA2, (d) 30% fly ash BFA1, and (e) 30% fly ash BFA2.

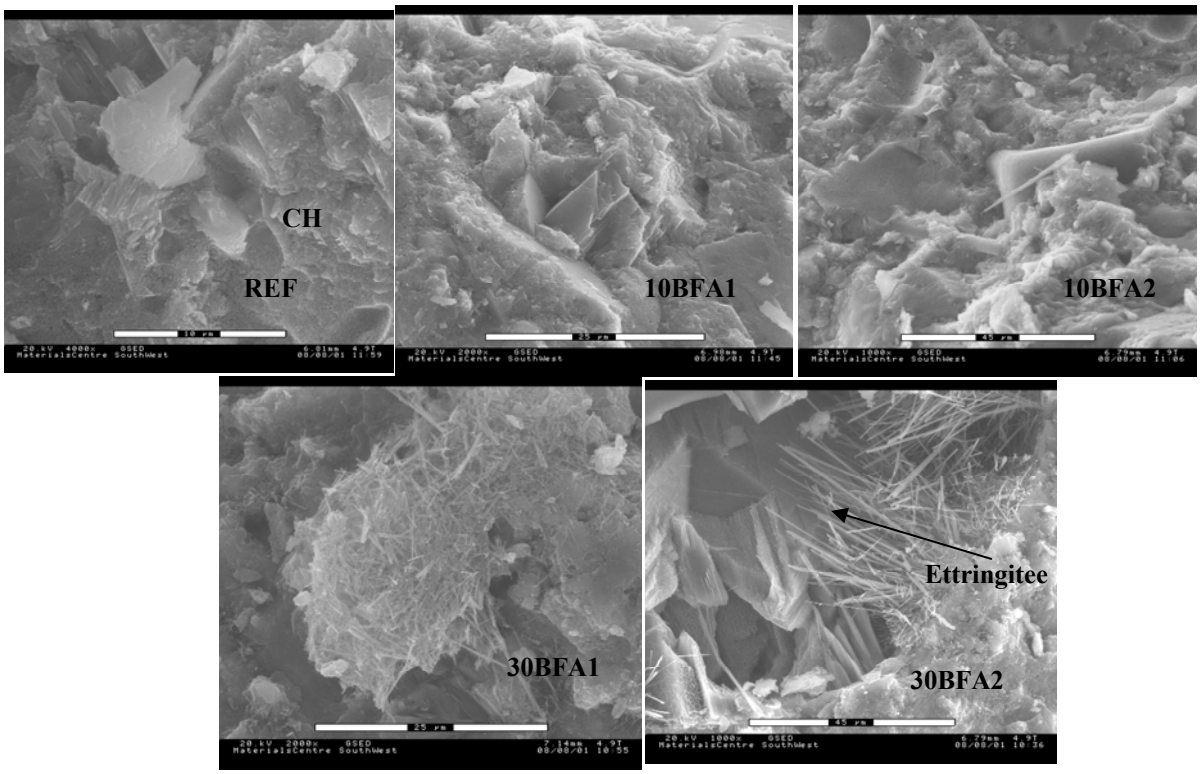

Figure 4.42. Microstructure of cement-biomass fly ash pastes after 90 days of hydration: (a) 0% fly ash, (b) 10% fly ash BFA1, (c) 10% fly ash BFA2, (d) 30% fly ash BFA1, and (e) 30% fly ash BFA2

It can be noticed after 180 days that all the biomass fly ash cement pastes got hardened – Portlandite precipitation is seen (the white parts of the SEM images) in all the samples. The matrix is very dense and pore structure is reduced. But micro cracks were also observed (in 30 BFA2) in the samples which leads to deterioration in flexural strength. In the overall monitoring of the biomass fly ash cement paste there was no much difference observed in the samples indicating that the biomass fly ash doesn't bring damaging effect to the cement matrix.

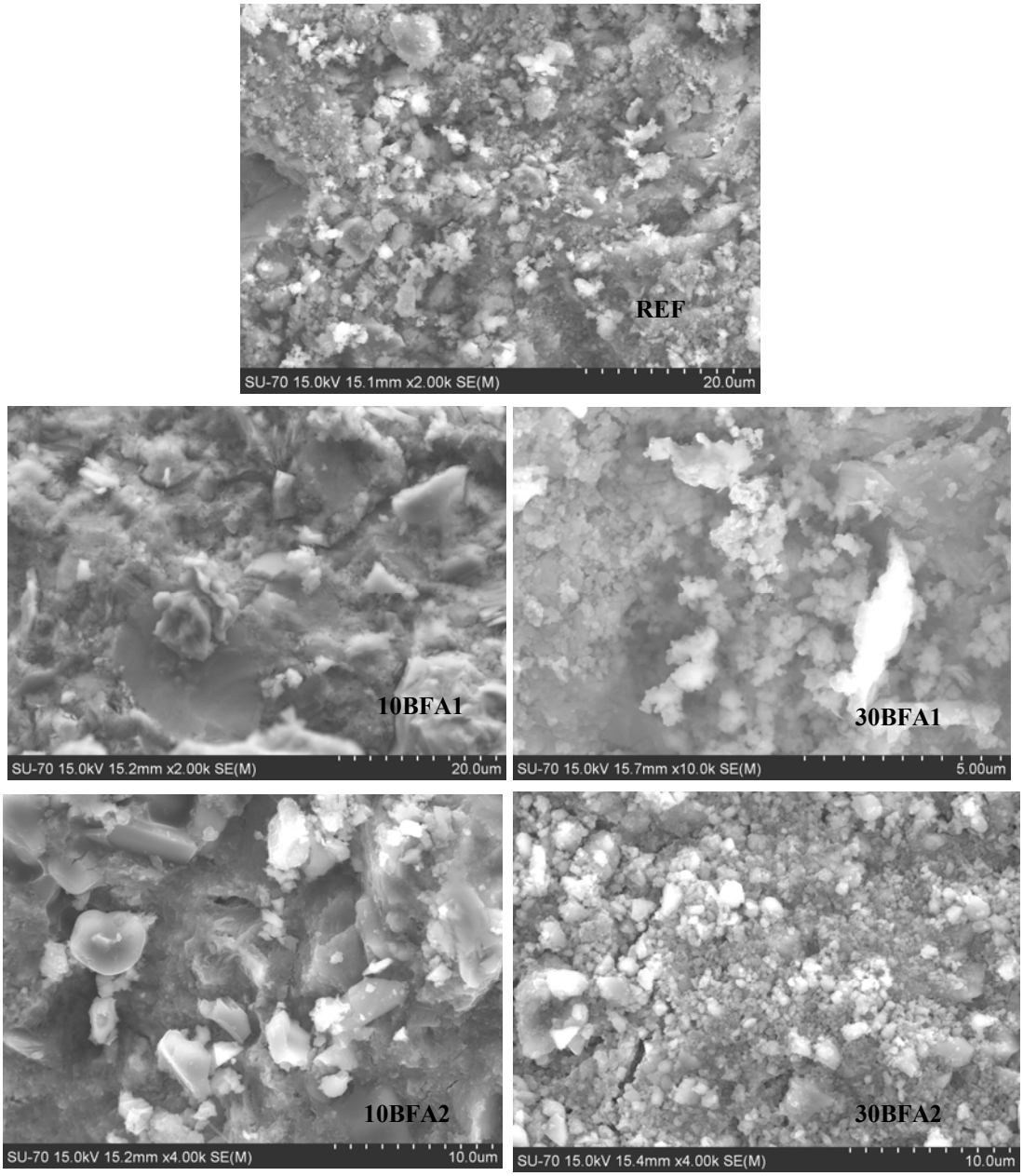

Figure 4.43. Microstructure of cement-biomass fly ash pastes after 180 days of hydration: (a) 0% fly ash, (b) 10% fly ash BFA1, (c) 10% fly ash BFA2, (d) 30% fly ash BFA1, and (e) 30% fly ash BFA2

4.5. Summary

1. Cement pastes and mortars were prepared by replacing OPC with different amounts of biomass fly ashes (10, 20 and 30% by weight of cement) in dry condition. On increasing the amount of biomass fly ash in the compositions the water requirement also increased. Generally, the introduction of more than 10% fly ash led to a decrease in setting time with the same w/b ratio because of the water adsorbing nature of the biomass fly ashes that reduces the water availability. But on adding water reducer setting was delayed for the biomass fly ashes incorporated mortars and the delay can be explained in terms of the reduced hydrating materials and alkali ions present in the biomass fly ashes. The fly ash incorporated mortars behaved similarly on increasing the fly ash content. Yet, the carbon content in the biomass fly ash BFA1 affected the workability in an increased manner.

2. The rheological behaviour was greater in the biomass fly ash incorporated mortars. It was observed that there is an increase in the torque of the mortar mix on increasing the biomass fly ash content. The effect greater in the 20BFA1 biomass fly ash incorporated mortars. The evolution of plastic viscosity showed that the plastic viscosity is higher for biomass fly ash BFA1 incorporated mortars and the biomass fly ash BFA2 showed a lower plastic viscosity trend compared to the reference mortar. On looking at the yield stress values, g, it can be observed that the yield stress increased along the test and with the biomass fly ash incorporation. The observations showed that the agglomeration of fly ash particles as well as the low availability of the free water which in turn are responsible for the high yield stress and higher plastic viscosity. The hydration caused increase of both yield stress and plastic viscosity
From the measurements of fresh properties it can be inferred that biomass fly ashes influence the properties in a greater measure because of their specific particle properties. Fineness, irregular shape and the organic content influencethe workability of the biomass fly ash incorporated mortars in a prominent way.

3. Impedance measurements of the biomass fly ash incorporated cement pastes were conducted. The resistivity of the biomass fly ash incorporated cements showed a lower value compared to the reference mortar during the hydration period confirming the hydration activity on biomass fly ash incorporation during the initial hydration time.

4. The temperature of hydration of the biomass fly ash incorporated cements and mortars were also measured using a quasi adiabatic calorimeter. As the amount of ash content was increased,

the heat of hydration decreased indicating a reduction in the hydrating phases in the ash replaced cements. However, 10 % BFA2 fly ash replaced cements showed a slight increase in the heat of hydration with respect to that of pure cement paste. The calorimeter values are in agreement with the impedance measurements.

5. Replacement of cement by both the fly ashes in mortars showed a gradual decline in strength, on adding higher amount of fly ashes. On adding 30% biomass fly ash the compressive strength was around 35- 45% of the reference mortar at the age of 28 days of curing. But the 10% and 20% replacement mixes showed comparable strength at the same time. In the initial phase of curing the biomass fly ashes acted more as a filler than a binder. On investigating the strength measurement unto a year of curing it was observed that the strength of the fly ash- replaced mortars increased at a higher rate during aging. This implies the biomass fly ash is contributes to the strength of mortars in later stages of curing due to its weak hydraulic/pozzolanic nature along with its filler contribution. At the age of 365 days the 30% addition showed around 80% of the strength of the reference mortars.

6. The porosity of the mortars increased with the increase in the biomass fly ash content in the matrix. But the mean pore diameter reduced on biomass fly ash mortars. The fineness of fly ashes helped in reducing the pore diameter though the overall porosity increased because of less hydrating materials in the fly ash mortars. But on aging the overall porosity decreased for all the compositions.

7. The hydration behaviour of hardened cement pastes were also studied using XRD and TG/DTA methods along with the ESEM analysis. The degree of hydration was measurement using the thermal method in terms of the calcium hydroxide content in the hydrated paste. It can be noticed that the content of calcium hydroxide was reduced on aging (after 90 days) in the biomass fly ash BFA2 cement paste, indicating its pozzolanic activity. BFA1 did not show pozzolanic behaviour but showed a hydraulic nature along with the cement.

8. The microstructure analysis of the biomass fly ash cement pastes from the early hydration to 90 days of hydration reveals that the biomass fly ashes behave as inert materials in the beginning of hydration. Ettringite crystals were formed in the 30% biomass fly ash incorporated mortars on analysing the sample cured at 90 days.

9. From the observations on the fresh and hardened properties of the biomass fly ash incorporated cement pastes and mortars it is conveyed that the biomass fly ashes demonstrate a

good potential as an additive in the cement pastes and mortars. The biomass fly ashes acted as filler as well as a binder in the matrix. The fineness of the ash particles was responsible for the filling contribution while the pozzolanic nature exhibited by the biomass fly ashes helped improving the binding capacity of the cement matrix in the later ages. However it was shown clearly throughout the experiments that the net binder content is reduced as the biomass fly ash content increased especially at the initial stages of curing. And also the workability results did not favour the addition of biomass fly ashes in higher amounts without the help of super plasticizer. More water was needed for the biomass fly ash addition to get a good workability. Considering the overall performance it could be wise to limit the use of biomass fly ashes to 20% incorporation to get a mortar/concrete mix with a moderate mechanical strength on casting.

CHAPTER 5. DURABILITY: EXPANSIVE REACTIONS: ALKALI SILICA REACTIONS AND SULPHATE REACTIONS

The occurrence of expansion reactions such as Alkali silica Reactions (ASR) and Sulphate Reactions that lead to the damage of concrete structures is widely reported in the last many decades. Cases were reported in Portugal too in the last decades in important structures such as dams and bridges. Several reinforced bridges in Portugal have gone through severe premature degradation [Silva et al. 2010]. The incorporation of supplementary cementing materials has proved to be useful in mitigating the expansion reaction. It is accepted that the alternative cementing materials react with $Ca(OH)_2$, to form compounds similar to those of hydrated cement products, such as hydrated calcium silicates (CSH), and reduces the alkalinity of the pore solution, thus avoiding the formation of expansive products. These supplementary cementing materials can be either pozzolanic (e.g. fly ash, metakaolin etc.) or latent hydraulic (e.g. ground granulated blast-furnace slag). In this chapter the efficiency of biomass fly ash in mitigating the ASR and the two types of sulphate reactions, External sulphate reaction (ESR) as well as Internal sulphate reaction (ISR) was investigated.

5.1. Alkali silica reactions

5.1.1. Introduction

Alkali-Silica reactions (ASR) are chemical reactions in concrete that can result in expansion, cracking and loss in durability of concrete structures affected. On aging, the micro pores in the matrix of hardened concrete are filled with a highly basic (i.e., pH ≥ 12.5) fluid that consists mainly of dissolved alkali hydroxides ($[K^+]$, $[Na^+]$—$[OH^-]$) with minor amounts of other elements (e.g., $[Ca^{+2}]$, $[SO_4^{-2}]$) [Diamond 1989]. In such high pH environment, the reactive silica within the coarse and (or) fine aggregates in concrete are chemically unstable and undergo reaction, sometimes inducing premature distress (i.e., internal expansion, cracking, loss in serviceability) of the affected element. This phenomenon is known as alkali-silica reactions (ASR). ASR related problems were first identified in the early 1940s in California (U.S.A.) [Stanton 1940]. By now, the ASR became a problem that has a well documented history worldwide.

ASR is one among the three types of Alkali Aggregate Reactions (AAR) found in concrete. The other two reactions are Alkali-Silicate Reaction and Alkali-Carbonate Reaction. Alkali-silicate reaction is the same as alkali-silica reaction except that in this case the reactive constituent is not

free silica but in the combined form of phyllosilicates. Alkali-carbonate reaction occurs in concrete when alkalis react with certain dolomitic lime stones containing clay. Reaction causes cracks, allowing water to enter, which causes the clay to swell and disrupt the aggregate. The majority of the structures affected by AAR is found due to alkali-silica reaction (ASR). Alkali-silicate and alkali-carbonate reaction are relatively rare.

Most of the structures reported as severely cracked by ASR were exposed to the weather or underground in contact with damp soil. This is because for significant expansion to occur sufficient presence of moisture is essential. ASR often occurs in old concrete hydraulic structures, where the problem was not detected or not properly treated before and during construction. Many concrete dams and other hydraulic structures worldwide have suffered from ASR [Charlwood 1994, Curtis 2000, Malvar 2001, Souma 2004, Santos Silva 2010]. Apart from the moisture, high content of alkali in the concrete is also essential.

In relation to ASR, alkali content is described as total mass of "equivalent sodium oxide", Na_2O_{eq}, which is determined from the following expression.

$$Na_2O_{eq} = Na_2O + 0.658\ K_2O \longrightarrow \textbf{Eqn.5.1}$$

The equivalent sodium oxide (Na_2O_{eq}) is conventionally used to indicate the alkalis content in the Portland cement, being normally limited in order to mitigate AAR to values lower than 0.6% (ASTM C150-02, 2003), even though some authors recommend lower limits, the most recent recommendations suggest that the control of Na_2O_{eq} content in concrete must be equal to the addition of Na_2O_{eq}, content and components, limited to 3 kg/m^3, except for vulnerable structures whose value is even lower (Miguel et al. 2009).

It is also observed that maximum expansion of concrete due to ASR occurs when the content and or the grain size of reactive minerals in aggregate is within a sensitive region, some refer to this as "pessimum" effect (Ichikawa, 2009). If the content or grain size of reactive minerals is below or above the pessimum value, ASR expansion reduces.

From the above details it can be concluded that for a damaging ASR expansion to occur, it is necessary to have

- sufficient moisture supply,
- pessimum amount of reactive silica in aggregate, and
- high content of alkali in concrete.

5.1.1.1. The reactive silica in aggregates

A form of reactive silica is an essential requirement for alkali silica reaction in concrete to take place though the volume required to produce deleterious effects needs to be only very small. As little as 2% of reactive component has been reported in certain cases where severe distress in the concrete has been observed (Swamy, 1992). Not all forms of silica are reactive in concrete. The reactivity depends on the crystal structure of the silica rather than its chemical composition. For example both quartz and opal are silica minerals and are predominantly composed of silica (SiO_2); i.e., they have similar composition (although opal has varying proportion of water, usually 3 to 9 percent). Quartz has a well-ordered crystal structure (Figure 5.1) and is very stable in concrete at normal temperatures. Opal, on the other hand, has an internal structure consisting of more-or-less densely packed aggregate of spheres of silica (cristobalite and/or tridymite) and is highly reactive in concrete.

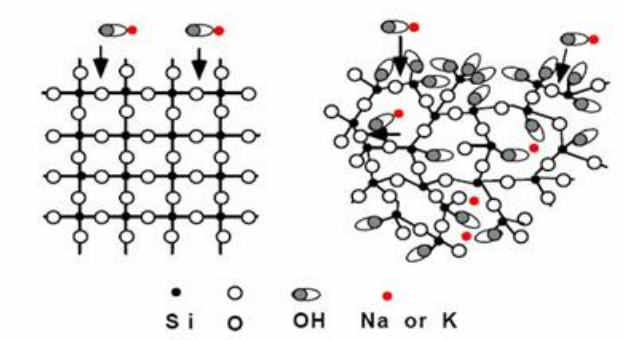

Figure 5.1. Schematic showing differences in crystal structure of quartz (left) and opal (right) [FHWA-HRT-06-133 2007].

Table 5.1 contains a list of reactive silica forms and the rock types. Not all sources of these rock types are reactive in concrete. Damaging reaction will only occur if these rock types contain sufficient quantities of the reactive silica. For example, many granites are not deleterious reactive in concrete and make excellent concrete aggregates. However, if the granite contains sufficient quantity of strained or microcrystalline quartz, the use of the rock may result in ASR when used in concrete; unless appropriate precautions are taken to control the reaction (sufficient alkali and moisture are also required to sustain the reaction).

Table 5.1. List of alkali-silica reactive minerals and possible rock types [FHWA-H RT-06-133 2007].

Rock Types		Reactive Minerals and Glass
Andesite	Hornfels	Cristobalite
Arenite	Quartz-arenite	Cryptocrystalline (or microcrystalline) quartz
Argillite	Quartzite	Opal
Arkose	Rhyolite	Strained quartz
Basalt	Sandstone	Tridymite
Chert	Shale	Volcanic glass
Flint	Silicified carbonate	
Gneiss	Siltstone	
Granite	Tuff	
Greywacke		

5.1.1.2. Sources of alkalis in concrete

Most alkali in concrete is supplied as sodium (Na) or potassium (K) ions. The other alkali metals may not contribute significantly to ASR damage. Alkali contents of mix constituents such as cement and water are therefore based on sodium and potassium contents. All ingredients of concrete may contribute to the total alkali content of the concrete, but the major source of alkali is from cement. The chemical composition of cement has great impact on regulating the ASR. Researches have proved that high alkali cement favours the ASR reaction in a faster rate than low alkali cements [Tosun et al. 2007]. Aggregates can contribute alkalis from two sources:

1. Release from minerals within the rock. For example, aggregate containing feldspars, some micas, glassy rock and glass may release alkali in concrete.

2. Marine salt contamination on the external surfaces of aggregate particles. Aggregates may be contaminated with sea salts, especially if they are derived from a marine source or stockpiled near the coast. The sodium chloride in the salt contributes reactive alkali to fresh concrete. For example, sea dredged sand, if not properly washed, may contain sodium chloride which can contribute significant alkali to concrete.

More over, some of the admixture chemicals contain sodium and potassium compounds which may contribute to the alkali content of concrete. Water may also contain a certain amount of alkali in the areas of cold weather, de-icing salt containing sodium compounds may increase

alkali content on the surface layer of concrete. Soils containing alkali may also increase alkali content on the surface of concrete.

5.1.1.3. The role of alkalis in ASR mechanism

The first stage of the alkali-silica reaction is the reaction between the hydroxyl ions (OH^-) in the pore solution and reactive silica in the aggregate; the silica is not directly attacked by the alkali metal cations (Na^+ and K^+).

The chemical attack of reactive silica by the highly basic pore fluid results in the formation of a hygroscopic "alkali-silica gel". Portlandite releases OH^- ions in the concrete pore solution in order to satisfy equilibrium between the cations (mostly alkali ions) and the anions (mostly OH^- ions). Differences in free energy between this gel and the pore fluid would then induce water and various ionic species in the pore fluid to flow into this gel. The Ca^{2+} ions also play a critical role in the process. Tensile stresses build up and microcracking occurs when the pressure generated at localized sites exceeds the tensile strength of the aggregate particles and of the cement paste. Concrete expansion develops with associated microcracking in the reactive aggregate particles and the cement paste. When poorly-crystalline hydrous silica is exposed to a strong alkaline solution, there is an acid-base reaction between the hydroxyl ions in solution and the acidic silanol (Si–OH) groups (Glasser and Kataoka, 1981) as follows:

$$\equiv Si–OH + OH– \rightarrow \equiv Si–O– + H_2O$$

And on further hydroxyl ions penetrating into the structure, some of the siloxane linkages (Si–O–Si) are also attacked as follows

$$: \equiv Si–O–Si\equiv + OH^- \rightarrow 2\equiv Si–O– + H_2O$$

The negative charges on the terminal oxygen atoms are balanced by alkali cations (Na^+ and K^+) that simultaneously diffuse into the structure. The disruption of siloxane bridges weakens the structure and, provided sufficient reserves of alkali hydroxide are available, the process continues to produce an alkaline silicate solution. The extent or rate of dissolution is controlled by the alkalinity of the solution and the structure of the silica. The concentration of alkali metal hydroxides in solution depends on a number of factors, particularly the alkali content of the cement, the water/cement ratio (w/c) and the degree of hydration, and typically ranges from about 0.15 to 0.85 mol/l, corresponding to pH values ranging from approximately 13.2 to 13.9 [Thomas and Folliard 2007]. In the absence of calcium the alkali and silica would remain in solution, however, abundant calcium is available as $Ca(OH)_2$ in Portland cement concrete, and an alkali-silica gel containing minor amounts of CaO forms as the initial reaction product. The gel that forms is hygroscopic and, as it imbibes water from the surrounding pore solution, it

swells causing volumetric expansion of the concrete which may ultimately lead to cracking. With time, the calcium content of the gel increases and a portion of the alkalis is released back in to the pore solution [Thomas 2001]. Figure 5.2 demonstrates the sequence of alkali-silica reaction (ASR) in concrete [FHWA 2007].

(a)

Concrete pore solution is dominated by Na,K, and OH (with minor amounts of Ca). If the silica in the aggregate is reactive the OH and then the Na and K will react with the SiO_2

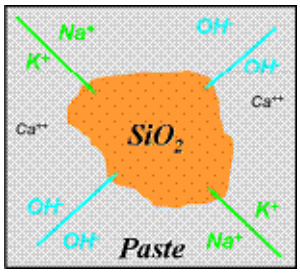

(b)

The product of the reaction is in alkali silica gel composed of Na, K, Ca, Si. The gel forms around and within the aggregate

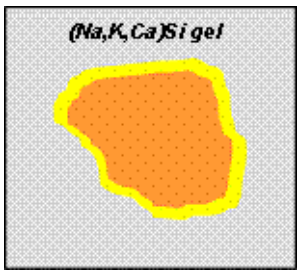

(c)

The gel imbibes water from the surrounding cement paste. The gel expands. Eventually the swelling pressures may exceed the tensile strength of the surrounding paste and cause expansion and cracking of the concrete

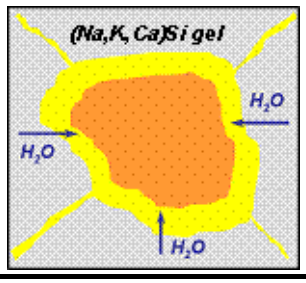

Figure 5.2 . The sequence of alkali-silica reaction (ASR) in concrete. (FHWA 2007).

Common symptoms of ASR in affected structures include [Joseph 2006] (Figure 5.3)

- Cracking which may be random in direction (i.e., map or pattern cracking) or may show preferred orientation if expansion is restrained in one direction.
- Discoloration around cracks.
- Gel exudation from cracks.
- Misalignment of adjacent sections.

- Closing of joints, extrusion of joint sealant and crushing/spalling of concrete around joints.
- Pop-outs over reactive aggregate particles.
- Operation difficulties (e.g., jamming of sluice gates in dams).

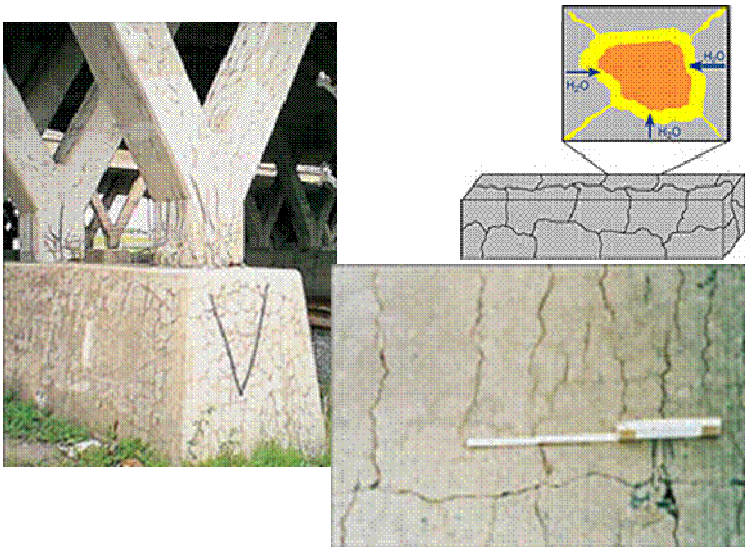

Figure 5.3. Cracks in a ASR damaged concrete structure [FHWA-HRT-06-133 2007].

5.1.1.4. Supplementary cementing materials (SCMs) as a solution to inhibit ASR

The amount of expansion and resulting damage that occurs in concrete affected by alkali-silica reaction depends on a number of parameters including the availability of alkalis in the system, the nature and amount of reactive silica in the aggregate, exposure conditions (temperature and moisture availability) and the degree of internal and external restraint to movement (e.g. amount and distribution of reinforcing steel). The parameters that can be influenced by the incorporation of supplementary cementing materials (SCMs) in the concrete are the availability of alkalis and the reactive silica contribution from the SCMs.

The use of SCMs, such as fly ash, slag, silica fume, and metakaolin has shown marked suppression of ASR-induced expansion in accelerated mortar bar test (AMBT, as in ASTM C 1260 and ASTM C 1567), concrete prism test (CPT, as in ASTM C 1293), and field exposure tests [Ballard et al. 2008, Thomas 2006, Silva et al. 2011, Silva et al. 2010].
The four possible mechanisms by which ASR is controlled when utilizing SCMs as replacement for cement are**: [**Robert et al. 2010].

(1) Formation of supplementary calcium silicate hydrates (C-S-H) and in the case of metakaolin, calcium aluminate and calcium aluminosilicate hydrates through reaction with the $Ca(OH)_2$ produced during Portland cement hydration. This results in lower permeability, thus limiting the ingress of external alkalis and moisture by densification of the paste fraction and interfacial transition zone.
(2) Formation of supplementary hydrates provides additional adsorption sites for the binding of alkalis, contributed by the materials used to produce the concrete or that may ingress from the environment, thus limiting ASR gel production.
(3) Replacement of cement with SCMs that have lower alkali contents results in a "dilution" effect — reducing the alkali loading (kg/m^3) in the cement matrix.
(4) Excess Ca^{2+} contributed by CH present in the pore solution may replace Na^+ and K^+ bound in the alkali-silica gel, initiating a complex interaction between "mature" and "immature" gel (i.e., gel which has or has not reacted with Ca^{2+}) which results in microstructural damage. The consumption of CH by pozzolanic reactions may limit ASR damage by reducing the amount of free calcium resent in the pore solution and thus limiting gel swelling.

Numerous works have shown that SCMs have a significant impact on the concentration of alkalis in the pore solution [Robert et al. 2010]. The incorporation of most SCMs leads to a reduction in the concentration of alkali-hydroxides in the pore solution of pastes, mortar and concretes, the scale of the reduction increasing with higher SCM replacement levels. The ability of SCMs to reduce the pore solution alkalinity is linked to their effect on the composition and alkali-binding capacity of the hydrates (especially C–S–H). Bhatty and Greening (1978) found that C–S–H with a low Ca/Si ratio was able to retain more alkalis (Na+K) compared to hydrates of higher lime to silica ratios. Uchikawa et al. (1989) showed that slag has a similar effect to low-calcium fly ash on hydrate composition. Glasser and Marr (1985) explain the differences in alkali absorption on the basis of the surface charge on the C–S–H which is dependent on the Ca/Si ratio. At high ratios, the charge is positive and the C–S–H tends to repel cations. As the Ca/Si ratio decreases the positive charge reduces becoming negative at low Ca/Si ratios, e.g. less than 1.3 [Glasser 1992]. Negatively charged C–S–H has an increased capacity to sorb cations, especially alkalis. Hong and Glasser (1999) confirmed the importance of the Ca/Si ratio on the alkali-binding capacity of synthesized single-phase C–S–H but subsequently showed that the binding capacity could be greatly increased by introducing alumina into the C–S–H to form C–A–S–H [Hong and Glasser 2002].

Silica fume is reported to be the most efficient SCM in this role, followed by metakaolin, low-calcium fly ash and slag [Thomas and Bleszynski 2001]. But it was noticed that on introducing

silica fume the OH^- concentration drops rapidly over the first 28 days but then starts to increase slowly with time beyond 3 months [Shehata and Thomas 2002]. And this long-term increase in the OH^- concentration seems to be prevented in pastes containing 5% silica fume by the addition of either slag (25%) or fly ash (15%). The use of aluminous SCM with regards to reducing pore solution alkalinity and the potential for ASR was reported by Hong and Glasser (2002). Studies on the effect of fly ash and slag on the pore solution of pastes have been reviewed by Thomas (1996). Current thought on the leading mechanisms for which fly ash controls expansion are that the fly ash dilutes the alkali content in the cement. Some of the alkalis are removed from the pore solution by binding them into CaO-silica hydrate gels. The fly ash reduces the concrete permeability and diffusivity by the silica reacting with the $Ca(OH)_2$ produced by the hydration of the cement to form calcium silicate hydrate. Since the calcium silicate hydrate takes up more space than the $Ca(OH)_2$ produced, the pore systems become finer and less continuous. The reduced porosity limits the ability of the alkalis to migrate and therefore reduces the ability of alkali-silica gel to form [Detwiler 2002]. Thomas (1996) indicated that several fly ash concrete samples show little or no expansion even when the available alkali content is relatively high. The amount of fly ash required for the effective mitigation depends on the reactivity of the aggregate, the quantity of alkalis contributed by the Portland cement, and the composition of the fly ash.

High calcium fly ashes classified as Class C by ASTM International (ASTM) C618 definition, are often excluded as a mean to mitigate alkali silica reactions (ASR) in concrete. This is because a relationship between high calcium content and expansion was often documented when class C fly ash was used at a 10% to15% replacement level in concrete. It is generally true that low replacement levels (<15%) of Class C fly ash may not offer ASR mitigation; however, it has also been demonstrated that Class C fly ashes can mitigate the effects of ASR even at the lowest replacement of 15% (Docter 2009).

5.1.2. Test Methods

The experiments conducted were of 2 types: mortar bar tests and tests on concrete prisms. The cement mortars were prepared meeting ASTM C 1260/ASTM C 1567 specifications. This method is used to test the reactivity of aggregates. This test was done in a 1 N NaOH soak solution. As the test conditions are accelerated in this method, it is also known as the "Accelerated Mortar Bar Test" (AMBT) method. The concrete prism tests were conducted according to the RILEM AAR-3 (RILEM 2000) and RILEM AAR-4 (RILEM 2007) test

methods. All of these test methods have been fairly recently adopted by ASTM (AMBT was first approved in 1989 (ASTM C 1260, 2001), but the use of SCMs in this test was approved much more recently (ASTM, C 1567 2008). The concrete prism tests, RILEM AAR-3 and RILEM AAR-4 test methodologies are broadly similar to ASTM C 1293.
Scanning Electron Microscopy (SEM) analysis was conducted on the samples after the tests for the microstructure evaluation. These tests were performed at LNEC, (National Laboratory of Civil Engineering, Lisbon, Portugal) and University of Aveiro facilities.

5.1.2.1. Standard ASTM C 1260 Test (AMBT) Method

In this test, the cement mortar bars (275 mm×25 mm×25 mm) were prepared meeting ASTM C 1260/ASTM C 1567 specifications with a water/binder (w/b) ratio of 0.47 and binder/aggregate (b/a) ratio of 0.44 (weight ratios). The different steps in the AMBT test are shown in Figure 5.4. A blend made of 20% of each biomass fly ash and 10% metakaolin was also tested. The components were weighed and mixed thoroughly in a laboratory mixer. Flow table measurements were done to check the workability. According to ASTM C 1567 the spread diameter of the mortar composition should be ± 7.5% of reference mortars, ie, around 115 to 133 mm.

The mortars were prepared with gauge studs at the ends for the length change measurement. The mortar bars were cast at an aggregate to cement ratio of 2.25. The mortar bars were cured in the moist room at 23±2 ºC and Relative Humidity (RH) >95% for the first 24 h, demolded and then kept in a storage container with sufficient amount of water in it. After removing from the moulds the initial expansion readings for the mortars were taken using a digital length comparator accurate to 1 μm. The ratio of the amount of soak solution used for the test to the volume of the mortar bars soaked in the solution is 4.5:1. After this the mortars were preconditioned for 24 h in water maintained at 80 ± 2ºC during 24 h. The length of the mortar bars was measured and then the bars were immediately transferred to storage containers filled with 1N NaOH solution maintained at 80 ± 2ºC. Length of the mortar bars was periodically measured over a 28 day period. The expansion value was calculated as the average percentage length change of 3 mortar bar samples based on length change since initial immersion in NaOH. The systematic approach is therefore to regard the accelerated test as a rapid screening method that provides a good indicator of the likely outcome of the longer term concrete prism test. The aggregate used is termed as innocuous or non-reactive, if the 14-day expansion is less than 0.1%. If the 14-day expansion is between 0.1 to 0.2%, the aggregate is termed as a potentially reactive aggregate and with an expansion higher than 0.2% it is termed as highly reactive.

Figure 5.4. Procedure of AMBT test.

5.1.2.2. Materials for ASTM 1260 Accelerated mortar bar test (AMBT)

Cement

The cement used was a Portuguese cement, CEM type I, 42.5 R. The alkali content of cement is expressed as 0.19% Na_2O, 1.02% K_2O and 0.86% $Na_2O_{eq.}$ The chemical composition of the cement determined by XRF analysis is stated in Table 5.2.

Table 5.2. Chemical composition of the cement determined by XRF analysis

Composition	SiO_2	Al_2O_3	Fe_2O_3	CaO	MgO	SO_3	K_2O	Na_2O	L.O.I
Cement (%)	19.74	4.74	2.69	63.54	2.42	3.11	1.02	0.19	1.66

Aggregate

The aggregate used was highly reactive in nature. The major component of the aggregate is siliceous quartz (obtained from Tramagal Rio Tejo, Portugal). The size distribution of the aggregates are listed in Table 5.3.

Table 5.3 Aggregate size distribution for AMBT test

Aggregate grain size (mm)	*Fraction (%)*
4.75-2.36	10
2.36-1.18	25
1.18-0.60	25
0.60-0.30	25
0.30-0. 15	15

Biomass fly ashes

The biomass fly ashes were subjected to a sieving and washing process before incorporating in the cement formulations. The coarse ash particles were removed by sieving at 75 μm mesh prior to incorporation in mortars. The fly ashes were subjected to a bulk washing process, to regulate its soluble compounds, like alkalis, chlorides and sulphates. Two batches of washed biomass fly ashes were selected. Single washed fly ashes and multiple washed (5 washes) fly ashes. They are represented as Batch 1 and Batch 2 respectively. A single wash is done by leaching 1 kg of biomass fly ash in 10 l distilled water. The leaching procedure of biomass fly ashes is explained in detail in chapter 3. The washed ashes were dried at 105 ºC to control the moisture content. The single washed ashes were represented as $BFA1_{B1}$, $BFA2_{B1}$. The multiple washed fly ashes are represented as $BFA1_{B2}$ and $BFA2_{B2}$. A blend of fly ashes with metakaolin is also used for the ASR studies. The metakolin used in this test was ARGICAL M 1000. The chemical composition of the fly ashes and metakaolin is shown in Table 5.4.

Table 5.4. Chemical composition of the biomass fly ashes and metakolin

Composition	*Biomass fly ash B FA1$_{B1}$(%)*	*Biomass fly ash BFA2$_{B1}$(%)*	*Biomass fly ash BFA1$_{B2}$ (%)*	*Biomass fly ash BFA2$_{B2}$(%)*	*Metakaolin (%)*
SiO_2	46.4	31	52.10	25.10	54.66
Al_2O_3	13.6	8.5	13.30	11.23	37.98
Fe_2O_3	5.18	3.0	5.30	5.18	1.22
CaO	18.9	24	15.90	40.10	0.01
MgO	3.85	4.8	3.31	6.63	0.05
SO_3	3.29	2.3	0.45	1.12	0.02
K_2O	4.77	2.7	4.14	2.07	0.01
Na_2O	1.01	6.6	1.05	3.61	0.01
$TiO_2 + P_2O_5$	2.769	1.61	2.57	2.64	---
Cl^-	2.45	1.34	0.10	0.25	---
Loss on Ignition			10.35	3.50	0.94
BET			28.56 m^2/g	1.74m^2/g	---
Particle size			<50 µm (mean diameter 17.15 µm)	< 50 µm (mean diameter21.32µm)	<45 µm (mean diameter 6.03 µm)
Pozzolanicty Chapelle test			618mg/g	701 mg/g	1466 mg/g

5.1.2.3. Mixture proportions for ASTM C 1260

The details of the compositions of mortars selected for the tests are shown in Table 5.5. The mixture proportions for the modified versions of ASTM C 1260/ASTM C 1567 tests are given in Table 5.6. All the proportions mentioned were for a batch of 3 bars. The aggregate to cement/cementitious materials ratio used in the mixes was 2.25:1 (990 g aggregates in total for each composition). A super-plasticizer Glenium 26 SCC was used to make the mortars in workable condition. The total water + superplastizer content remained constant (W/B 0.47) in all the experiments. The biomass fly ashes were substituted in the cement by 20%, 30% and 40%. These quantities were chosen considering the chemical properties of the fly ashes which have similar properties of those class C fly ashes. It was generally demonstrated that class C fly ash can mitigate ASR at high replacement level. [Dunstan et al 1981, Styron et al. 1997, Bruce 2009). A blend with metakaolin was also selected choosing a combination of 20% biomass fly ash and 10% metakaolin in order to determine its combined effect on the ASR mitigation.

Table 5.5 The compositions of the test mortars

Sample name	*Composition*
Ref	CEM 42.5 R Type 1
	Batch 1
20 F1$_{B1}$	80% CEM+ 20 % BFA1(1 time wash)
30 F1 $_{B1}$	70% CEM+ 30 % BFA1(1 time wash)
40 F1 $_{B1}$	60% CEM+ 40 % BFA1(1 time wash)
20 F2 $_{B1}$	80% CEM+ 20 % BFA2(1 time wash)
30F2 $_{B1}$	70% CEM+ 30% BFA2(1 time wash)
40F2 $_{B1}$	60% CEM+ 40 % BFA1(1 time wash)
	Batch 2
20 F1 $_{B2}$	80% CEM+ 20 % BFA1(5 times washes)
30 F1 $_{B2}$	70% CEM+ 30 % BFA1(5 times washs)
20F1 $_{B2}$ +10M	70% CEM+ 20 % BFA1(5 times washes)+10% MK
20 F2 $_{B2}$	80% CEM+ 20 % BFA2 (5 times washes)
30F2$_{B2}$	70% CEM+ 30% BFA2(5 times washes)
20F2 $_{B2}$ +10M	70% CEM+ 20 % BFA2(5 times washes)+10% MK

Table 5.6. Mortar formulations (W/B =0.47, B/A= 0. 44).

	Samples	*Substitution (wt. %)*	*Biomass fly ash (g)*	*Metakaolin (MK)(g)*	*Cement (g)*	*(Superplasticizer (ml)*[*2]	*Consistency (mm)*
	Ref	0	0	0	400	00	124
Batch 1	**20 $F1_{B1}$**	20	88	0	352	2.2	97*[1]
	30 $F1_{B1}$	30	132	0	308	2.2	64*[1]
	40 $F1_{B1}$	40	176	0	264	18.4	124
	20 $F2_{B1}$	20	88	0	352	00	64*[1]
	30$F2_{B1}$	30	132	0	308	00	33*[1]
	40$F2_{B1}$	40	176	0	264	30.8	102*[1]
Batch 2	**20 $F1_{B2}$**	20	88	0	352	4.4	131
	30 $F1_{B2}$	30	132	0	308	8.8	131
	20$F1_{B2}$ +10M	20+10M	88	44	308	8.8	125
	20 $F2_{B2}$	20	88	0	352	6.2	129
	30$F2_{B2}$	30	132	0	308	10.6	115
	20$F2_{B2}$ +10M	20+10M	88	44	308	17.6	137

**[1] – Not confirming to the requirement of ASTM C 1567 (flow table = ± 7.5% of reference mortars, ie, 115 to 133 mm of spread diametre)*
"2 The total water + superplastiziser remained 207ml throughout the tests.

5.1.2.4. RILEM 3 and RILEM 4 Concrete Prism Test (CPT)

Long-term concrete prism tests are respected internationally as the most definitive tests in the assessment of alkali reactivity (Sims and Nixon 2003). There are several variants of the test, but the differences are minor. A comparatively working composition 20 F2B2+10M was used for the confirmation for the AMBT test results. The test methods chosen for this study were RILEM AAR 3 and RILEM AAR 4 methods (Silva et al. 2010). The concrete specimens (75 x 75 x 250 mm) were cast using 440 kg/m^3 of cementicious material, a water/binder (w/b) ratio of 0.45, and with an alkali content of 5.50 kg of Na_2Oeq by cubic meter of concrete, calculated on the basis of available alkalis from the cement, additions and the added NaOH. During this test the concrete test prisms are stored in a closed plastic bag over water in sealed container at 38 ± 2ºC and a relative humidity > 95%.

For AAR 4 method the tests were conducted in an accelerated environment, at a temperature of 60ºC and the evaluation period is determined as 20 weeks [Ranc and Debray 1992]. The test has not yet been standardized by European standard organisations or ASTM, but researches are being done to present a reasonable correlation with RILEM AAR3. It has been observed by Fournier et al (2006). that the elevated temperature increases the rate of alkali leaching during the test period, and reduces the pore solution pH due to sulphate ions replacing some of the hydroxyl ions in solution. This results in a lower expansion rate in the accelerated test compared to the standard concrete prism test. The Table 5.7shows the tentative that criteria have been advanced for interpretation of expansion test results, applied to low- and normal-reactivity aggregates:

Table 5. 7.Classes of aggregate reactivity (ASTM C 1260, RILEM AA3)

Description of aggregate reactivity	*14-day expansion in AMBT (%)*	*One-year expansion in CPT (%)*
Non-reactive	≤ 0.10	<0.040
Moderately reactive	0.10 - 0.30	0.040 – 0.120
Highly reactive	0.30 - 0.45	0.120 – 0.240
Very highly reactive	> 0.45	> 0.240

This test methodology is broadly similar to ASTM C 1293 which uses a controlled alkali content of 5.25 kg Na_2Oeq/m^3 and a single expansion limit of 0.04% after 1 year the coefficient of variation for expansion measurements on three replicate specimens must be less than 0.02% at 90 days for effective ASR mitigation in the concrete expansion.

5.1.2.5. Mixture proportions for RILEM AAR-3 and RILEM AAR-4

The concrete compositions were prepared in accordance with RILEM AAR-3 (RILEM, 2000) and RILEM AAR-4 (RILEM 2007) test method for ASR are explained in Table 5.8. 1.6% Glenium 26 SCC superplasticizer is used to obtain an adequate workability (Figure 5.5). Cylinders of 10cm x 20cm were made for the mineralogical and chemical characterisation. The curing temperature was 38 ºC for RILEM AAR 3 and 60 ºC for RILEM AAR 4.

Table 5.8. Composition of Concretes - RILEM TC-106-3 (AAR-3 and AAR-4)

	Material	*% weight*	*Reference concrete*	*BAF2+10MK*
	Cimento CEM I 42,5 R, kg/m^3		440	308
Subsititution	Biomass fly ash BFA2	30%	0	88
Subsititution	Metakaolin		0	44
	Aggregate 10/20,(kg/m^3)	40%	692	692
	Aggregate 4/10,(kg/m^3)	30%	519	519
	Aggregate 0/4 (kg/m^3)	30%	511	511
	water (l/m^3)		200	200
	Na_2O eq./m^3 available		3.91	3.18
	Na_2O eq/m^3. to be required		1.59	2.32
	NaOH added /m^3		2.05	2.99

5.1.2.6. Scanning electron microscopy and energy dispersive analysis.

At the end of ASR tests, the microstructure of the sample mortars was studied by scanning electron microscopy (SEM) (Hitachi SU 70). The tests were run at a voltage of 20 KV. Samples were taken from mortar bars used for the AMBT expansion. The samples were cut using a masonry saw with relatively small dimensions to fit in the cylindrical molds. The cut samples were placed in an oven at 40 ºC to dry. After removal from the oven the cylindrical moulds were impregnated with resin using an impregnating machine (Logitech) in which vacuum is used to minimize the air voids during the impregnation of the samples with resin. The soaked samples in the moulds were kept for drying again for about 24h.

After drying and demolding the samples were cut superficially, to generate a new face of observation, using a precision cutting machine. After this surface was achieved, it was re-impregnated and finally placed an acetate film on the surface impregnated. Then the samples were polished very lightly, using machine polishing with silicon carbide grain size of 600 micrometers. This was done to remove the top layer of resin and straighten the sample, but without totally removing the layer of resin followed by polishing with aluminum oxide grain sizes 15:09 micrometers. Finally, the sample surface was again polished with diamond paste of 6, 3, 1 and 1 / 4 micrometers. After polishing is over the samples were washed and kept in oven at 40ºC to dry. After drying, the samples were covered with gold and were analyzed using the scanning electron microscope (SEM).

Figure 5.5: Preparation of Concrete prisms for ASR concrete test methods.

5.1.3. Results and discussion

5.1.3.1. Accelerated Mortar Bar expansion Test (AMBT)

According to the ASTM C 1260 test-method, an aggregate is considered reactive if the average expansion of the three bars of mortars at the end of 14 days of immersion in NaOH is greater than 0.20%. The expansion of the reference mortar prepared with the OPC CEM I type was 0.31% at 14 days and 0.51% at 28 days (Figure 5.6). This confirms the high reactivity of the aggregate used in these experiments.

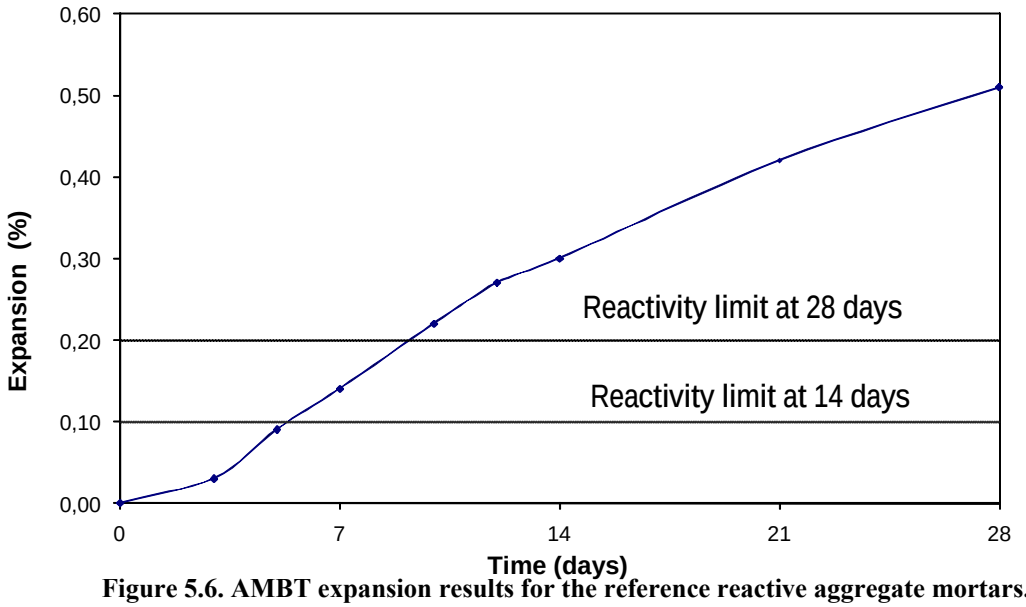

Figure 5.6. AMBT expansion results for the reference reactive aggregate mortars.

The first set of experiments was carried out with the Batch 1 (B1) cement formulations in which the single washed ashes were used. The accelerated expansion results are shown in Figure 5.7. An overall reduction in expansion is exhibited by the biomass fly ash substituted mortars. The ASR expansion is reduced on increasing the amount of biomass fly ash up to 30%. On substituting 30% biomass fly ash the expansion decreased to at least 0.14% and 0.17% for the biomass fly ash $BFA1_{B1}$ and $BFA2_{B1}$ respectively. However on further increase in the fly ash content, the expansion curve started rising and especially the 40% $BFA2_{B1}$ mortar bars gave an expansion of 0.32% while 40% $BFA1_{B1}$ mortar bars gave 0.18% in expansion. It may be due to the increase in the net soluble alkali content of the mortar formulations on the substitution of higher amount of biomass fly ash (Figure 5.8). From this observation the biomass fly ash content that should be incorporated in the concrete samples was fixed to a maximum limit of 30% for a safe ASR mitigation.

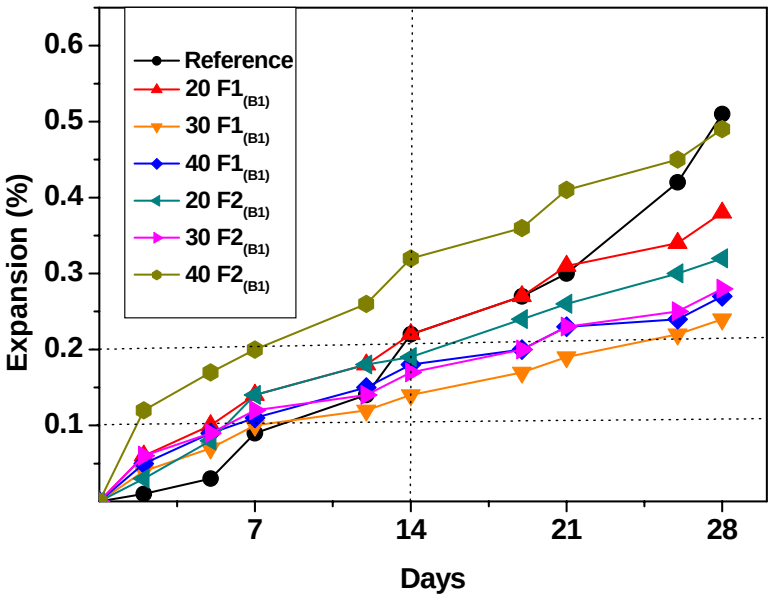

Figure 5.7. AMBT expansion results for single washed biomass fly ashes incorporated mortars

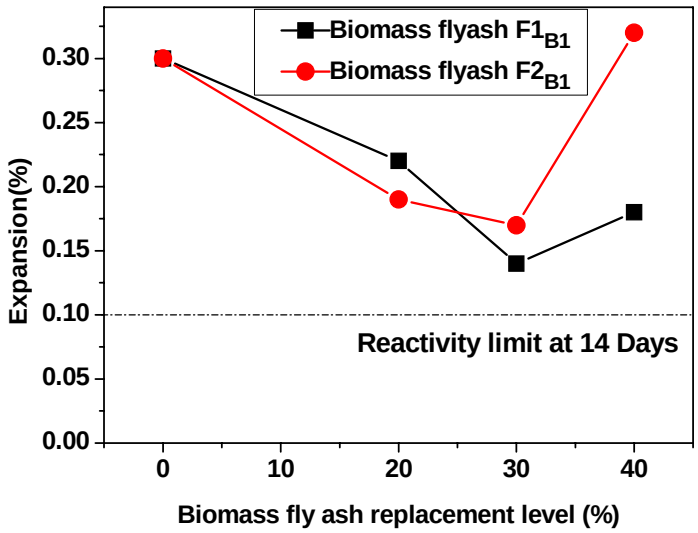

Figure 5.8. Expansion values of AMBT mortars on the14th day for different substitution compositions.

Soluble elements in the washed fly ashes

The fly ashes were tested for the soluble components after a washing processs. The ICP-MS test method was used for the quantification of the leached elements. Figure 5.9 shows the pH and conductivity of the leached solution of fly ashes of the 1st wash and 5th wash (batch B1 and and B2 respectively). The Na K and Ca solubility of biomass fly ash F2B1 is more than compared to that of F1B1. This could be the reason for the slight increase in the expansion values for F2B1 mortars.

From Figure 5.8 it can be noticed that the expansion values decrease on increasing the fly ash content up to 30% and then it changes adversely. This can also be explained in terms of the pessimum effect that high calcium fly ashes might show. High-calcium fly ash might have a pessimum effect, in which at low fly ash replacement levels, the expansion, meets or exceeds that with no fly ash, but at higher replacement levels the expansion decreases. The threshold fly ash fraction above which expansion decreases is specific to the fly ash. Occasionally, fly ash may have several pessimum replacement ratios (Farbiarz et al. 1986).

By the 5th wash the conductivity is minimized to a great extend indicating the decrease in the rate of solubility of alkalis. From the pH values it can be noticed that the alkalinity of the fly ashes also decreased. The similar solubility behavior of the fly ashes influences the behavior of the biomass fly ashes in the ASR mitigation as it is the soluble components which also govern the ASR reactions inside the cement matrix.

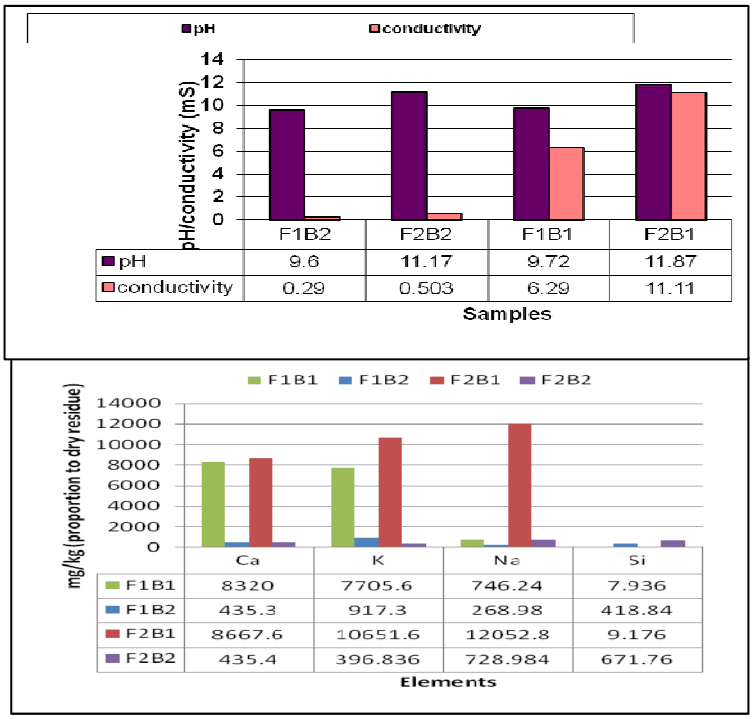

Figure 5.9 . pH, conductivity and the major elements of the leached solutions of the batch B1 .-one time washed, and batch B2. five time washed) biomass fly ashes.

Batch 2 biomass fly ashes were used for further detailed investigations where the alkali content was reduced to in an acceptable level compared to the Batch 1 compositions with the method of multiple washes using water. The expansion curves for the second batch of formulations are plotted

in Figure 5.10. The expansion curves followed a similar trend to that of the single washed fly ashes except there is a slight reduction in the expansion for the 30% $F2_{B2}$ substituted fly ash compared to that of 30% $F1_{B2}$ substituted fly ash. The 14^{th} day and 28^{th} day expansions of the tested mortars are shown in Figure 5.11. From the figure it is clear that the fly ashes substituted compositions have favoured the ASR mitigation in the mortar bar compared to that of the reference mortar. And the mortars containing a blend of 20% biomass fly ash and 10% metakaolin have mitigated the ASR expansion effectively.

From Table 5.9 it can be observed that the metakaolin substituted BFA2 biomass fly ash mortars have the highest ASR mitigation efficiency. Compared to the reference mortar, the biomass incorporated mortar expansion test showed an expansion reduction of 88% and 73% for $20F1_{B2}$+10M and $20F2_{B2}$+10M respectively. Among the biomass fly ash incorporated mortars 30BFA2 showed the maximum ASR mitigation efficiency; around 57% reduction in expansion compared to the reference mortar. 30 $F1_{B2}$ also showed a significant impact in the ASR reduction (by 31%). The 20% incorporation of the biomass fly ashes in the mortars showed a relatively lower efficiency. The lesser alkalinity favoures fly ash BFA1 substituted mortars compared to BFA2. For BFA2 the slight increase in pozzolanicity compared to BFA1 is an advantage in reducing the expansion. The contributions of these two factors favour a similar trend in the ASR mitigation in the biomass fly ash incorporated mortars though the fly ashes had noticeably different chemical compositions. However, among all the mortars combinations the metakolin incorporated biomass fly ash mortars alone satisfied the limit of expansion (0.1% at 14 days) to be considered as effective ASR mitigators.

The incorporation of biomass fly ash showed a high rate of expansion in the initial stages of the reaction, but the rate of expansion decreased after the initial stages of the test duration. (Table 5.9) This behaviour is likely a result of dilution effect at early ages (first half of AMBT) along with limited pozzolanic reactions, resulting in only a marginal reduction in expansion until pozzolanic reaction mechanisms start to influence the micro structural development and pore solution composition In the interaction between metakaolin and the biomass fly ash, the behavior of the mortars is quite different from that of biomass fly ash mortars. For the biomass fly ash metakaolin blend the reaction rate did not change significantly because of the effective pozzolanic nature of metakaolin and its vigorous reactivity in mitigating

the ASR even in the initial stages of the AMBT. The smaller particle size and the aluminosilicious chemical composition are the reasons for the greater relative effectiveness of metakaolin when

compared to the biomass fly ash. It is also researched and proved that t the metakaolin alone is working effectively in mitigating the ASR expansion when incorporated in 10% (Santos et al. 2011). So the reduction in expansion of $20F2_{B2}$+10M is rather a mixture of the behaviour of metakaolin and biomass fly ash. Biomass fly ash in not altering the mitigating efficiency of metakaolin rather it contributes a strong filler effect. Together, these should result in greater consumption of $Ca(OH)_2$, yielding lower permeability and decreased availability of calcium-containing reactants (e.g., solid CH, Ca^{2+} in pore solution) in biomass fly ash metakaolin blended cements.

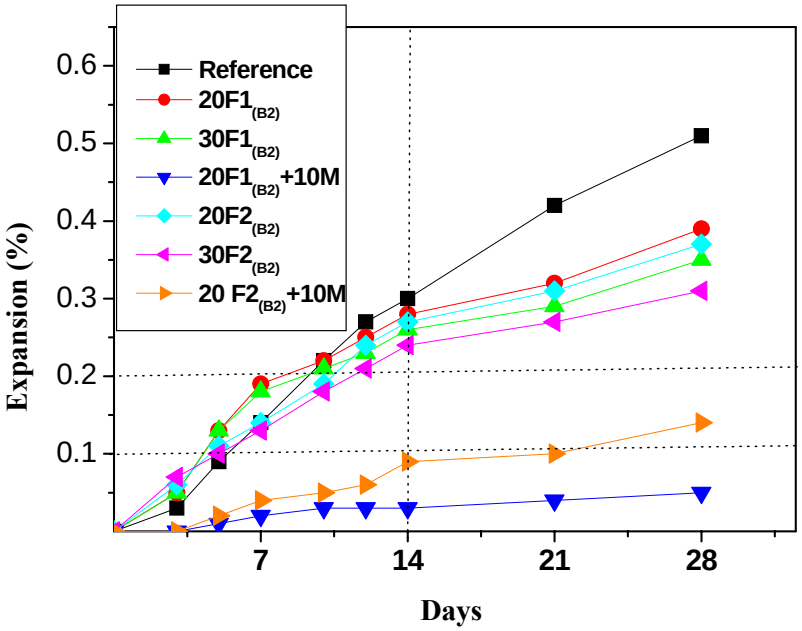

Figure 5.10. AMBT expansion results for the multiple washed fly ash compositions

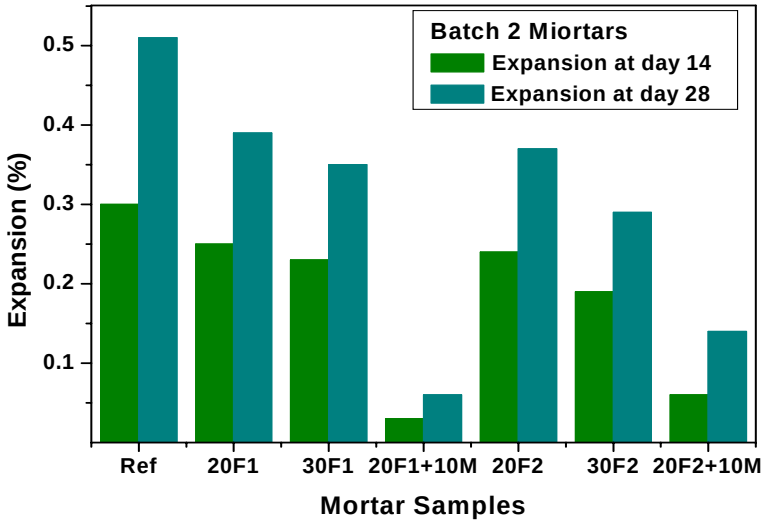

Figure 5.11. Expansion results at 14 and 28 days according ASTM C 1260/ASTM C 1567 method

Table 5.9. The ASR mitigating efficiency of the biomass fly ash mortars.

Sample	*Alkali content (%)*	*Expansion rate (%)*		*Increase in ASR mitigating efficiency compared to the Reference (%) at 28 days*
		0-14 days	14-28 days	
Reference CEMType 1 42.5	Na_2O:0.19 K_2O: 1.2	0.300	0.034	---
20 $F1_{B2}$	Na_2O:1.0	0.018	0.010	23.0
30 $F1_{B2}$	K_2O: 4.4	0.016	0.009	31.3
$20F1_{B2}$+10M		0.002	0.002	88.2
$20F2_{B2}$	Na_2O:3.6	0.017	0.009	27.4
30 F2	K_2O: 2.1	0.015	0.007	56.9
$20F2_{B2}$+10M		0.004	0.005	72.5

5.1.3.2. Concrete Prism expansion Test (CPT)

The CPT that results, RILEM AAR 3 and RILEM AA4 carried out for 20BFA2+10MK cement formulation, are shown in Figure 5.12& 5.13 and Figure 5.14 respectively. It is evident in the tests, the reference concrete with no added fly ash, gives the highest expansion. These results are confirm the test results obtained from the AMBT tests. In RILEM AA3 no expansion was observed in the 20BFA2+10MK till 196 days. Rather shrinkage occurred in the first 100 days (Figure 5.13). Both concretes did not exceedthe limit of expansion till 140 days. However a slight variation in weight happened in the concrete similar to the reference concrete. This could be due to either the hydrating products or the ASR gel. ASR-products are often called gels although some are precipitates or even crystals [BCrubC and Foumier 1986, Dron and Brivot 1996, Larive 1998]. They are also said to be "water-absorbent", i. e. to cause concrete destruction through their swelling (Dent Glasser 1979). The RILEM AA3 experiment is still going on and it tends to mirror the AMBT tests.

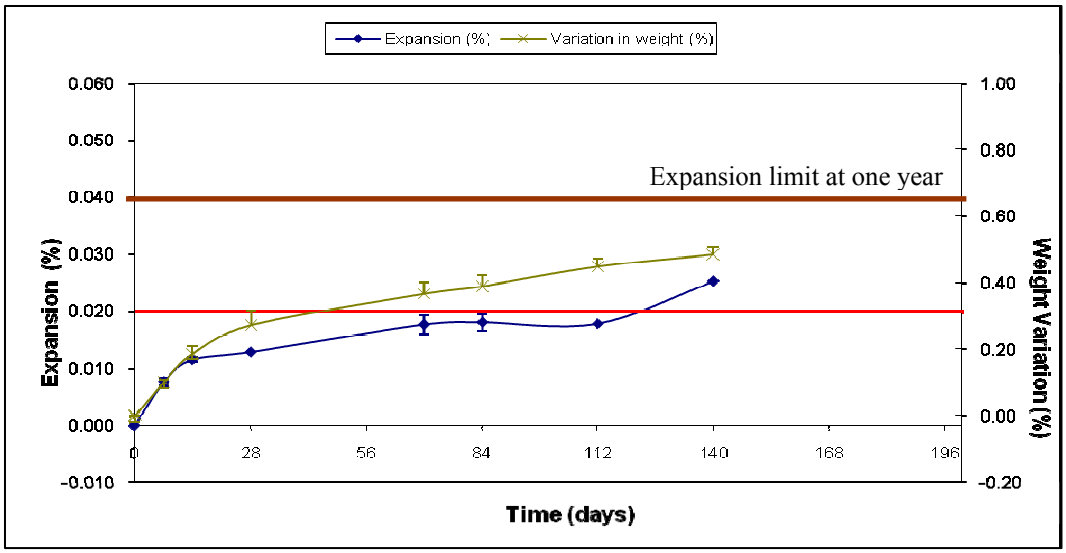

Figure 5.12. RILEM AAR 3 test results for the reference concrete.

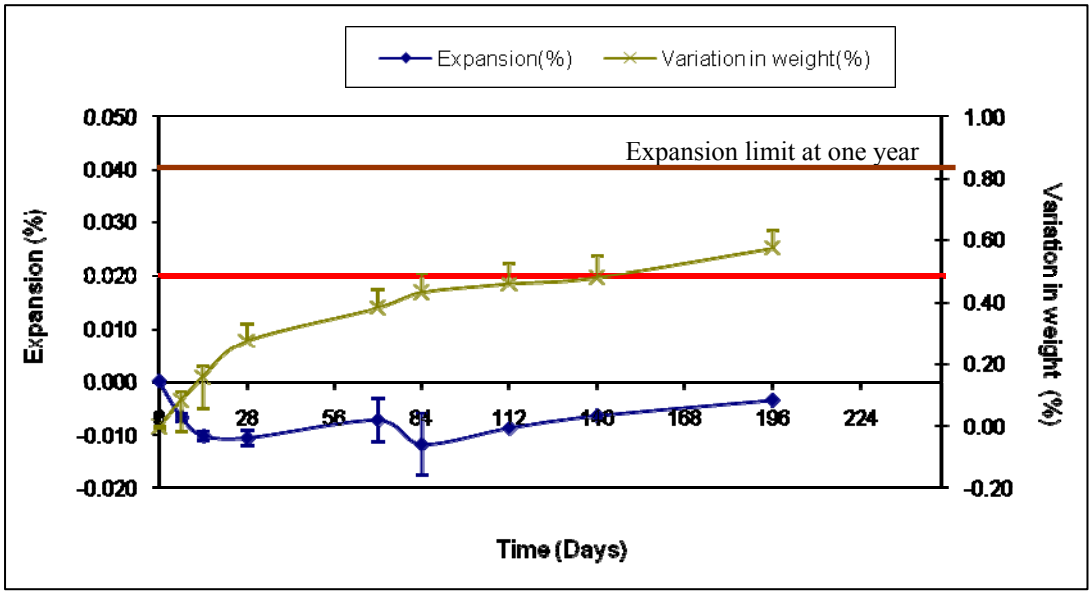

Figure 5.13. RILEM AAR 3 test results for the 20BFA2+10MK concrete.

The accelerated concrete prism mode, AAR 4 test was completed by 20 weeks. The expansion values were tolerable till the 12th week and it crossed the limit assigned (0.02%) slightly from 16th week onwards. This trend also confirms the previous results obtained from AMBT method where the expansion values started crossing the limit after of 28 days of curing.

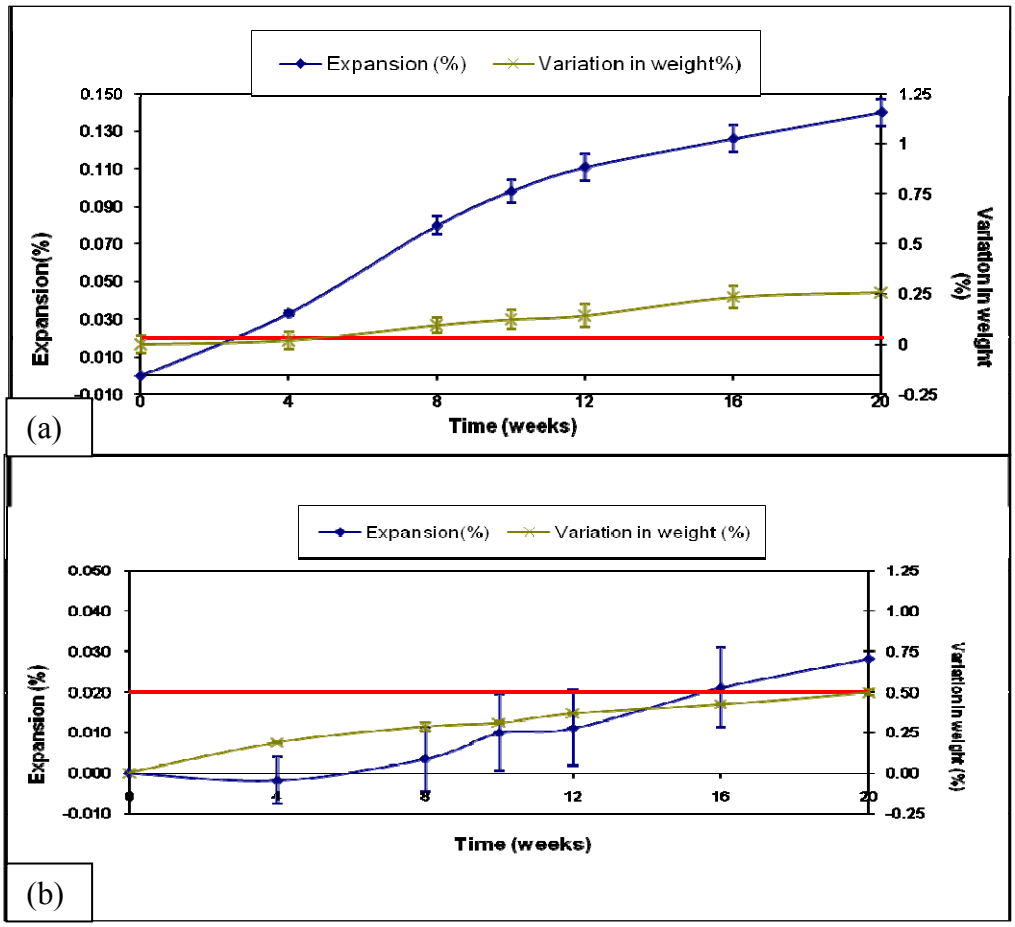

Figure 5.14. RILEM AAR 4 test results for the a) the reference and b) the 20BFA2+10MK concretes

5.1.3.3. Micro structural analysis of ASR products

The ASR gels formed in mortars at 28 days in ASTM C 1260 tests are shown in Figure 5.15, and Figure 5.16. ASR products can be identified within or near ASR cracks in concrete [Davies and Oberholster 1988; Shayan and Quick 1989]. SEM assisted with EDX (Energy Dispersive X-Ray Analysis) has been used to identify ASR gels as amorphous, semi organized, and crystalline products. Figure 5.15, a, b, c, d, and e show the morphology of ASR from nonpolished fractions of mortars. Figure 5.16 a, b, c and d shows the polished surface of mortar samples in order to approximate chemical composition of the ASR gels by EDX. ASR gels detected have significant amounts of Na compared to Ca. The crystalline products of ASR contain lamellar, acicular (fiber/filament) and rosette-like crystals, among which the rosette-like is most commonly detected (Figure 5:15.d). [Regourd and Hornain 1986, Reiset al. 1996].

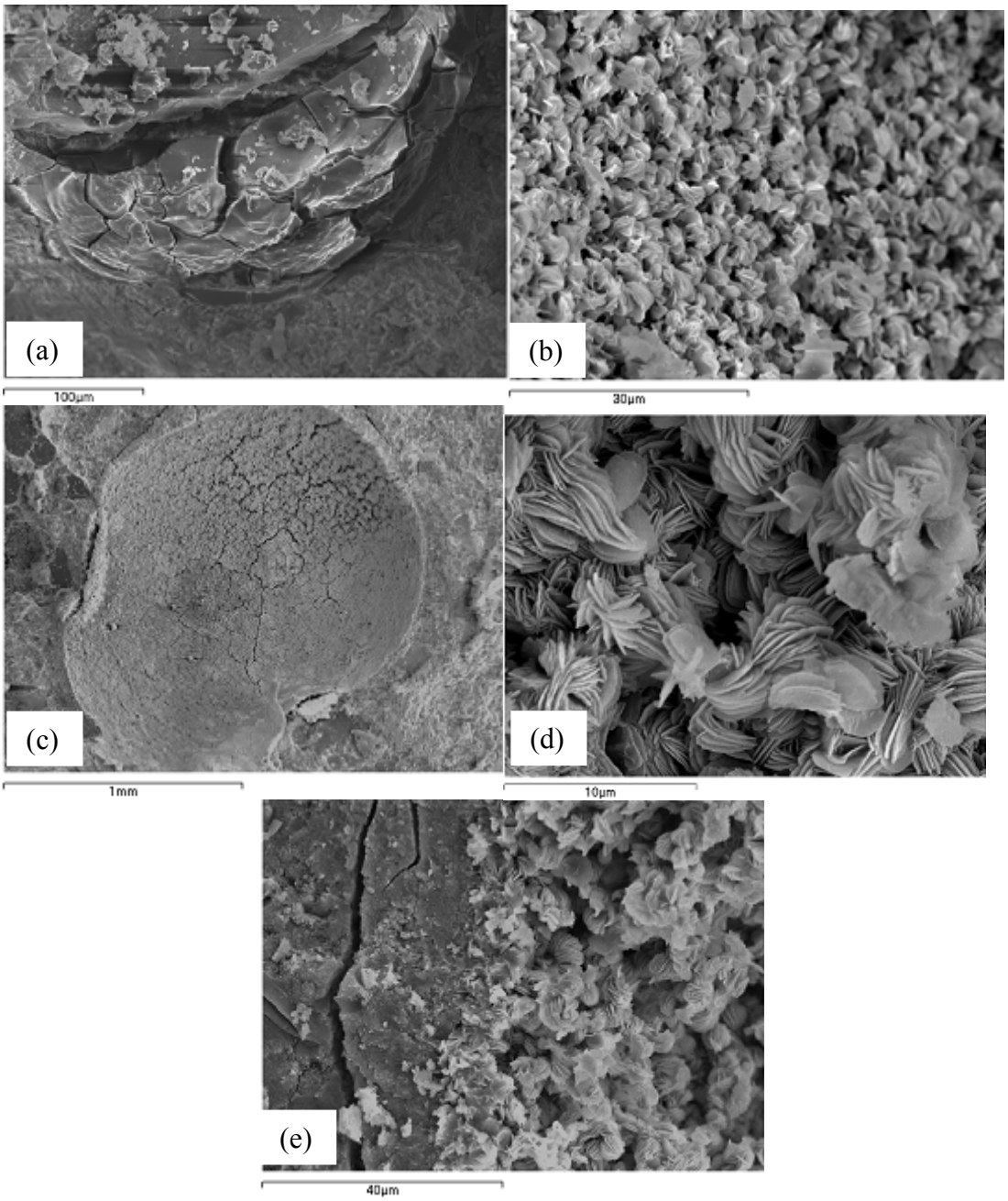

Figure 5.15. a) ASR amorphous gel in the 20 BFA1+10 MK mortar; (b) crystalline ASR in the 20 BFA1+10 MK mortar; (c,d) Crystalline ASR products inside air voids in the BFA2 mortar; (e) crystalline and amorphous ASR gel in BFA2 mortar.

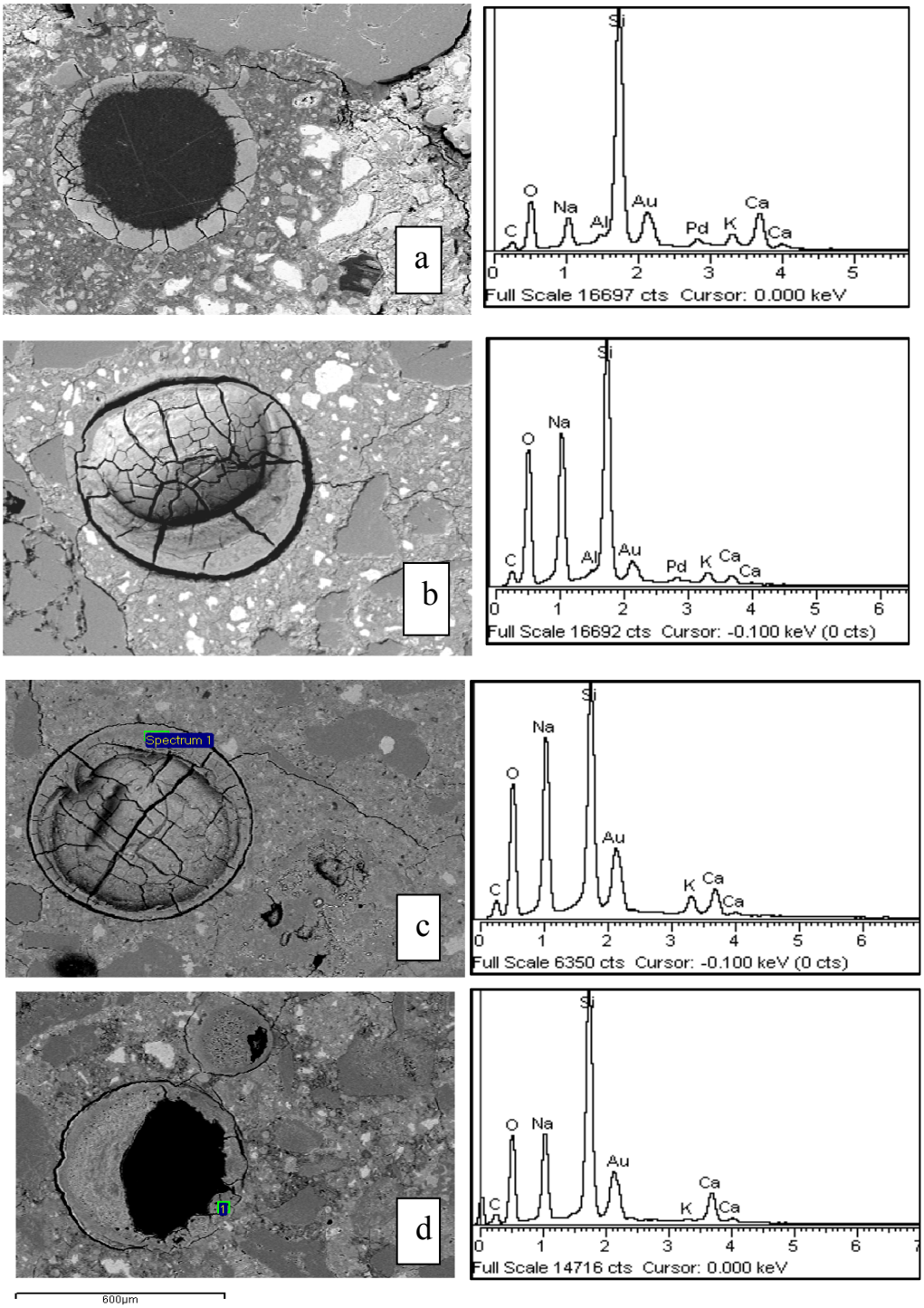

Figure 5.16. SEM/EDX of ASR gels formed in the polished mortars of a) 20F1+10M and b) 20F2+10M c) 20F1 and d) 20F2mortars at 28 days in ASTM C 1260 tests.

The Ca/Si ratio was determined from the quantitative EDX analysis from different points in the cement paste CSH gels during the micro structural analysis. The values are plotted in terms of expansion Vs Ca/Si ratio as in Figure 5.17. It can be observed that the expansion values and Ca/Si ratios are inversely proportional which confirms the earlier reports on the ASR mitigation effectiveness of SCMs that the CSH with a low Ca/Si ratio is able to retain more alkali (Na+K) compared to hydrates of higher lime to silica ratios (Bhatty and Greening 1978).

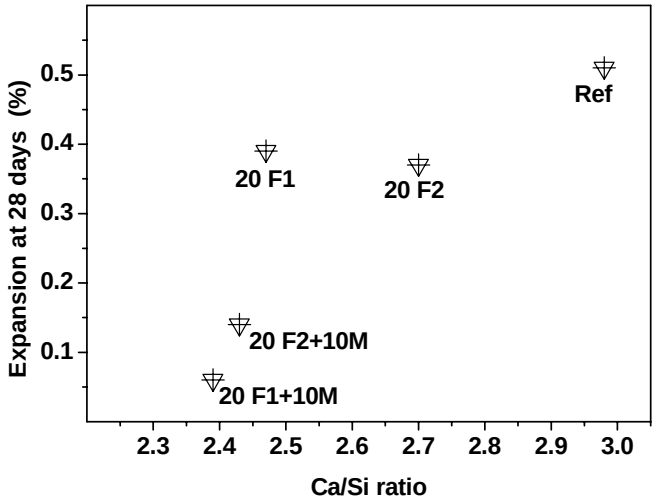

Figure 5.17. The expansion vs Ca/Si ratio of the biomass fly ash blended cement mortars of AMBT test after 28 days of curing.

5.2. Sulphate reaction

Sulfate attack is a chemical breakdown mechanism where sulfate ions attack components of the cement paste. The compounds responsible for sulfate attack are water-soluble sulfate-containing salts, such as alkali-earth (calcium, magnesium) and alkali (sodium, potassium) sulphates that are capable of chemically reacting with components of concrete. Sulfate attack processes decrease the durability of concrete by changing the chemical nature of the cement paste, and of the mechanical properties of the concrete. The sulfate combines with the C-S-H, or concrete paste, and begins destroying the paste that holds the concrete together. As sulfate dries, new compounds are formed, often called ettringite. These new crystals occupy empty space, and as they continue to form, they cause the paste to crack, further damaging the concrete.

Sulfate attack might show itself in different forms depending on

1) The chemical form of the sulphate

2) The atmospheric environment the concrete is exposed to

There are two types of sulphate attack named after the sources of sulfates causing the damage to mortar and concretes. They are 1) External sulphate Reaction (ESR) and 2) Internal Sulphate Reaction.

5.2.1. External Sulphate Reaction

5.2.1.1. Introduction

External sources of sulfate are more common and usually are a result of high-sulfate soils and ground waters, or can be the result of atmospheric or industrial water pollution. The general reactions involved in External sulphate reaction/external sulphate attack (ESA) have been described firstly by Cohen and Bentur (1988). It occurs due to penetration of sulphates in solution, in groundwater for example, into the concrete from outside. Other sources of sulfate which can cause sulfate attack include:

- Seawater
- Oxidation of sulfide minerals in clay adjacent to the concrete - this can produce sulfuric acid which reacts with the concrete
- Bacterial action in sewers - anaerobic bacteria produces sulfur dioxide which dissolves in water and then oxidizes to form sulfuric acid

The ESA-related damage manifests itself in several forms including cracking and spalling. The specific manifestation of the ESA-related damage depends on which one of the following three chemical processes is predominant:

i) Sulphate attack on CH and C-S-H to form gypsum:

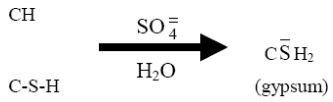

This process may cause expansion and spalling (Figure 5.18). However, its most important feature is the loss of strength and adhesion of the cement paste due to decalcification of *C-S-H* which is responsible for the binding capacity of the cement paste [Mehta et al. 1993]. This process may occur with all the sulphate salts (containing Na+, K+, etc.) except calcium or magnesium sulphate.

ii) Sulphate attack on calcium aluminate hydrates (C-A-H) and monosulfate hydrate (C3A·CS·H12-18) to form ettringite:

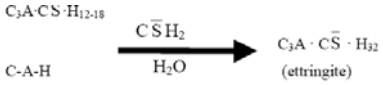

This process is mainly responsible for cracking and spalling as a result of expansion produced by secondary ettringite formation. This process may occur with all the sulphate salts (except $MgSO_4$) including calcium sulphate, produced according to the reaction (3) which acts directly on C-A-H and/or monosulfate hydrate.

iii) Sulphate attack on C-S-H and CH in the presence of carbonate ions to form thaumasite:

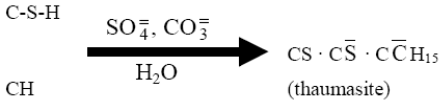

The thaumasite formation is accompanied by the most severe loss of strength and adhesion, which is able to transform hardened concrete into a pulpy mass, since a significant part of C-S-H can be destroyed according to reaction (5). This process may occur with every type of sulphate salts and is favoured by humid atmospheres and lowtemperature (<10°C) [Pauri and Collepardi 1989]

iv) Sulphate attack on C-S-H attack by magnesium sulphate (Mg SO_4) wich
is not directly related to ettringite formation:

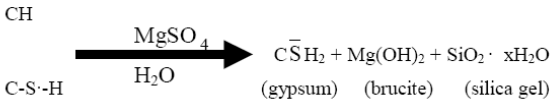

Even in this type of attack, without ettringite formation, there is loss of strength and adhesion of the cement paste due to decalcification of C-SH.

Figure 5.18. Deterioration in concrete due to sulphates[Collepardi 1999],

The ESA-induced damage, which is the traditional sulphate attack, is determined by the chemical interaction of a sulphate-rich soil or water with the cement paste. Soils containing sodium,

potassium, magnesium, and calcium sulphate are the main sources of sulphate ions in groundwater. For ESA to occur, the following three conditions must be fulfilled:

• high permeability of concrete;

• sulphate-rich environment;

• presence of water (Figure 5.19).

In the absence of one of these elements, the ESA-related damage cannot occur. For instance, in porous and/or micro-cracked concrete not exposed to water, the ESA-related damage does not happen, even if sulphate ions are present in the environment because, in the absence of water, these ions — for instance in dry soil — cannot migrate through the interconnected pores of the concrete.

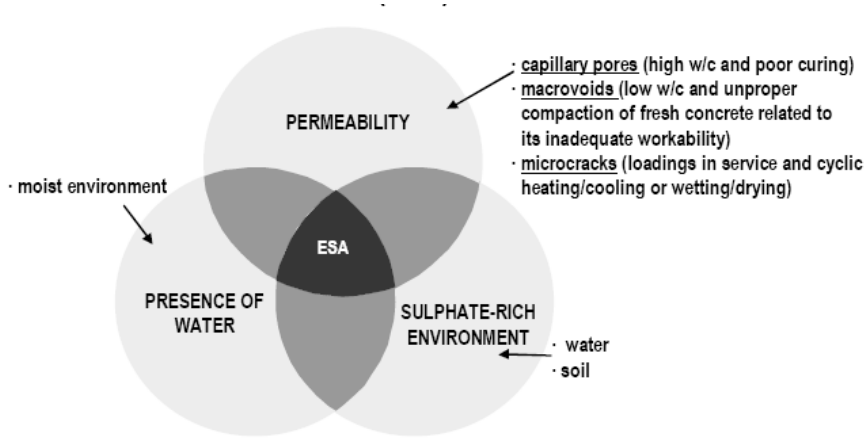

Figure 5. 19. Conditions for sulphate reactions [Collepardi 1999],

Assuming these conditions two factors will tend control the resistance of a given mortar/ concrete to sulphate attack: Chemistry of the cement and the permeability of the mortar/concrete.

To control cement chemistry, the content of C_3A in cement is reduced which in turn reduces the formation of CH, that leads to lesser formation of gypsum (Gypsum is the known to be the first step of formation of ettringite which can be considered as the principal cause of deterioration) [Sahmaran et al. 2007].

To control the permeability of concrete, lower w/c ratio and/or pozzolans are recommended. The effect of various pozzolans on the resistance of cements to external sulphate attack has been reported intensively in recent times. Pozzolans reduce not only the permeability but also the C3A amount if they are partial replacement of cement. Moreover, the use of pozzolans or of blended cements, in general, reduces the quantity of CH due to the pozzolanic reactions which would otherwise react with sulphates to form gypsum.

In this section the external sulphate reaction on the biomass fly ash incorporated cement mortars in severe conditions of sulphate environment were studied in order to evaluate the influence of biomass fly ashes against the external sulphate attack.

5.2.1.2. Experimental procedure

Mortar formulations ranging from 10 to 30% incorporation of biomass fly ashes were used for the mixes. (Table 5.10).The specimens (160 × 40 × 40 mm) were prepared with cement and sand (by weight) ratio of 1: 3, with the sand size < 2 mm. The workability of the mortars were kept in the flow table value of around 120 mm and w/c ratio was kept at 0.55 with a superplasticizer of 0.35%. Details of the materials used are described in chapter 4. The mortars were demolded after 24 hours and kept under water for another 28 days to get sufficient strength to cope with the severe sulphate environment.

The expansions were measured at the definite interval of 28 day, 90 days, 180 days, 280 days and 365 days. The average length was then recorded; results were expressed as a percentage of length change with respect to the initial length at day 28. At the end of the experiments the average weight was also recorded and is expressed as a percentage of weight change with respect to the initial mass value at 28 days. After the exposure period, the mortars were taken out for flexural compressive strength determination also, followed by SEM and EDS tests.

The exposure solutions were prepared by mixing reagent grade magnesium sulphate and sodium sulphate by 5% weight each in distilled water. This concentration represent very severe sulphate exposure conditions according to ACI 318-02 (Table 5.11). The concentration of the solutions was checked and adjusted periodically and the solutions were changed when needed to maintain the concentration.

Table 5.10. Mortar compositions for ESR tests (w/b ratio 0.55)

Sample Code	*Composition*	*Biomass Fly ash (g)*	*Cement (CEM) (g)*	*Super plastic izer (g)*	*Consistency (mm)*
REF	100% CEM Type 1 42. 5 R	0	400	1.4	150
10BFA1	90%CEM+10%BFA1	40	360	1.4	140
20BFA1	80%CEM+20%BFA1	80	320	1.4	125
30BFA1	70%CEM+30%BFA1	120	280	1,4	120
10BFA2	90%CEM+10%BFA2	40	360	1.4	145
20BFA2	80%CEM+20%BFA2	80	320	1.4	135
30BFA2	70%CEM+30%BFA2	120	280	1.4	135

Table 5.11 Classes of sulphate concentration in solid and water

Exposure	*Concentration of water-soluble sulphates in soil per cent*	*Concentration of water-soluble sulphates in water ppm*
Mild	<0.1	<150
Moderate	0.1 to 0.2	150 to 1500
Severe	0.2 to 2	1500 to 10000
Very severe	>2	>10000

5.2.1.3. Results and discussion

The mortar bars soaked in the sulphate solution made of 5% magnesium sulphate $MgSO_4$ and 5 % sodium sulphate (Na_2SO_4) were tested for expansion as well as variation periodically. The compressive strengths was determined using the standard method of strength measurements. The strength measurements of the chemically attacked mortars are summarized in Figures 5.20. It can be observed that that all blended cements exhibited no deteriorative performance in the severe sulphate environment as compared with that in the water cements. But an increase in strength in observed in the fly ash substituted mortars. From the physical analysis it could be observed that, flakes of reacted layers were appeared on the surfaces of the mortars. The chemical attack leading to the swellening and cracking of the hydrated phases existed only within the surface of the mortars for the biomass fly ash incorporated mortars and thus it did not affect the strength values much. The compactness of the mortar bars can be a reason for resisting the sulphate solution to interact to the interior of the mortars in the smaller curing periods. Another application for the relative increase in the compressive strength of the mortars on incorporation of biomass fly ashes in higher

amounts can be the $Ca(OH)_2$ deposits in the open pores of the mortar which in turn strengthens the mortar. The expansion of the mortars from Figure 5.21 indicates that the expansion values increases with the increase in the fly ash content. This can be mainly due to the porous nature of the biomass fly ash incorporated cement mortars. It was noticed that the workability poor for mortars with higher content of biomass fly ashes (>10%) thats leads to inhomogenous mixing and poroity

.

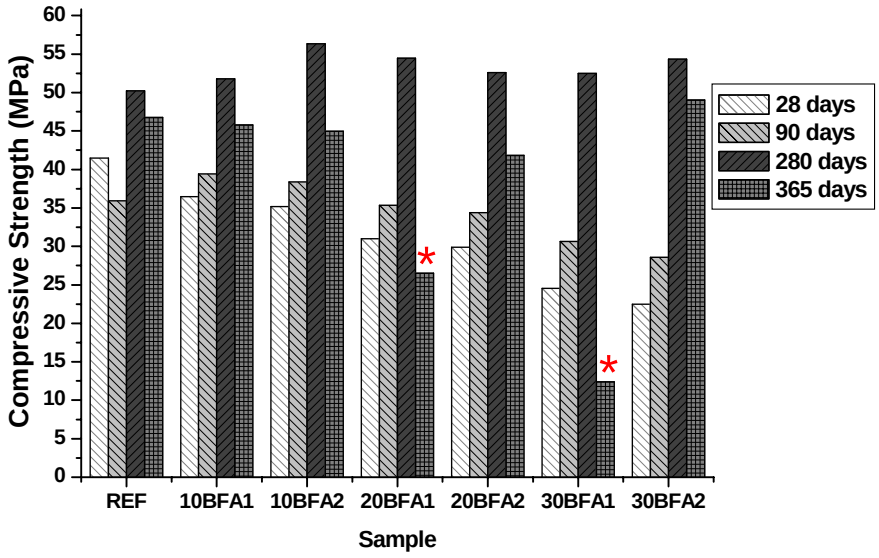

Figures 5.20. Compressive strength of chemically treated biomass fly ash mortars

(* the mortars were deformed).

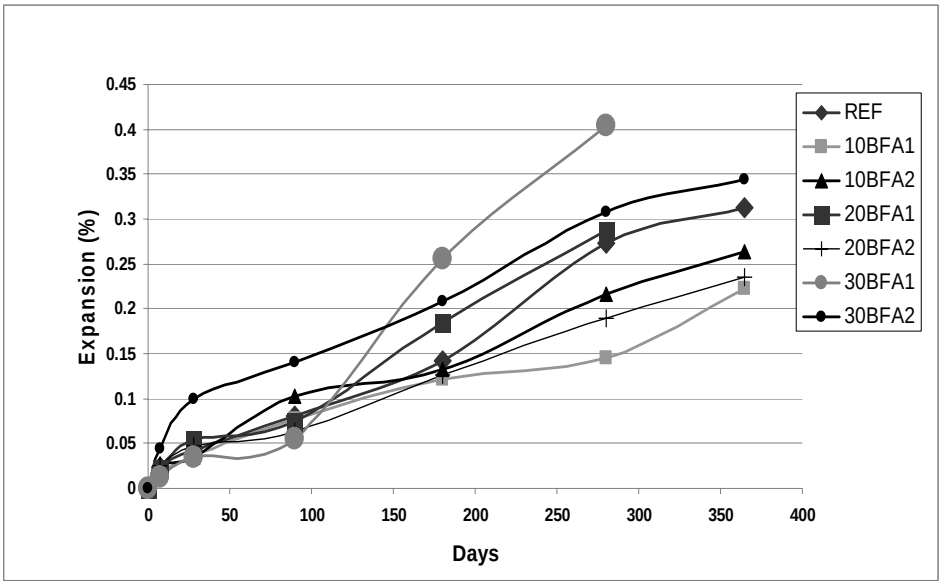

Figure 5.21. Expansion and variation in weight of mortars under ESR test

Cracks were noted in all the cement mortar specimen after an exposure of 1 year. (Figure 5.22) Disintegration of the edges and swelling was evident and also cracking of the surface skin, localized at the edges, was noted. In the case of the fly ash BFA1 mortars the deterioration was more severe compared to other specimens especially on 20% and 30% substitution of biomass fly ash.

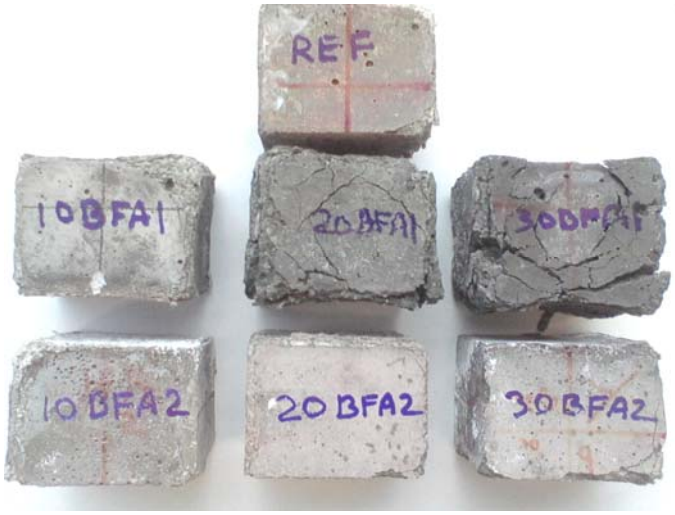

Figure 5.22. Mortar samples selected for strength measurements at 365 days of curing

The fly ash BFA2 mortars showed deterioration comparable to the reference mortars. The reason for this is the porosity of the mortars coupled with excess carbon content in the biomass fly ash BFA1 which disintegrate rapidly in the highly aggressive sulphate solution. After 1 year exposure the 20% and 30% BFA1 mortars were damaged completely. The weight loss of mortars at the end of experiment is shown in Figure 5.23. The external suphate attack is affecting adversely by increasing of the fly ash content. It could also be noticed that the net porosity increases with increase in biomass fly ash content in the mortars and it could be the major reason for the ESR expansion in biomass fly ash incorporated mortars. However 10% substituted mortars did not show any major deterioration that makes the samples disintegrate.

The SEM of the fractured sections of the biomass fly ash cement mortars cured in the sulphate solution are shown in Figure 5.24 and Figure 5.25. Well developed ettringite needles are visible in the 30BFA1 mortar at the sides of voids. .Gypsum crystals are evident in the 30BFA2 mortars.

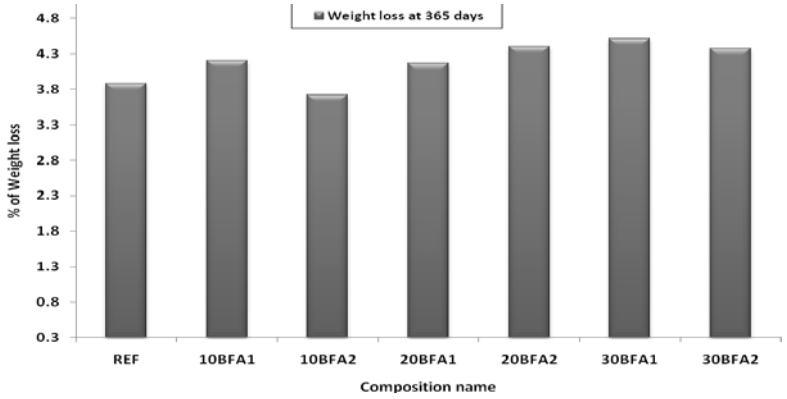

Figure 5.23. Weight loss (%) of the mortars at 365 days of curing

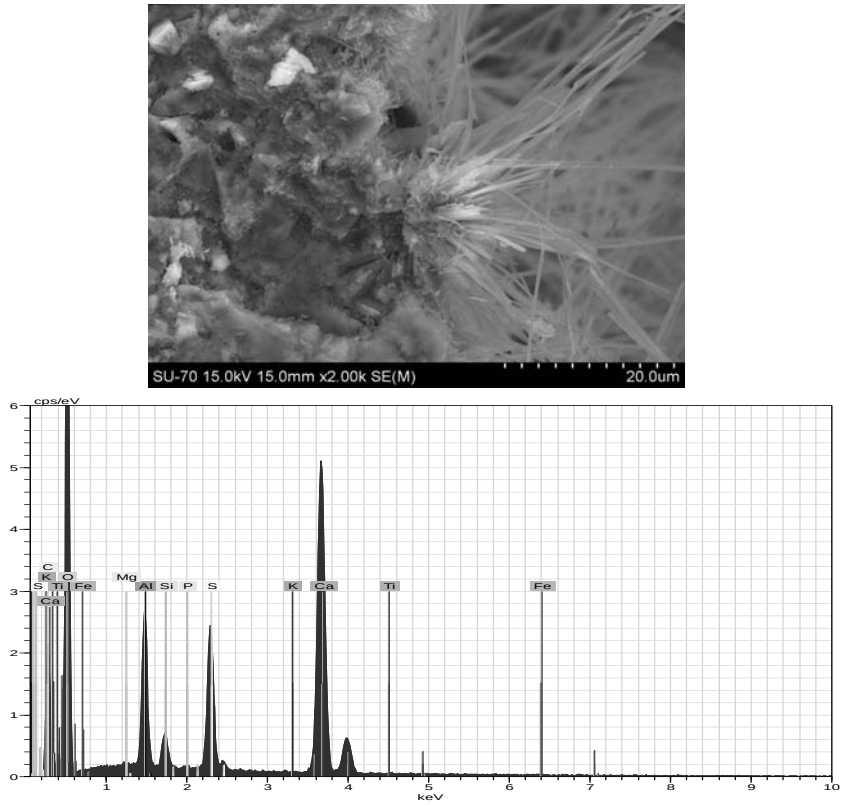

Figure 5.24. SEM/EDX of the sulphate attacked 30BFA1 mortar after 90 days of curing.

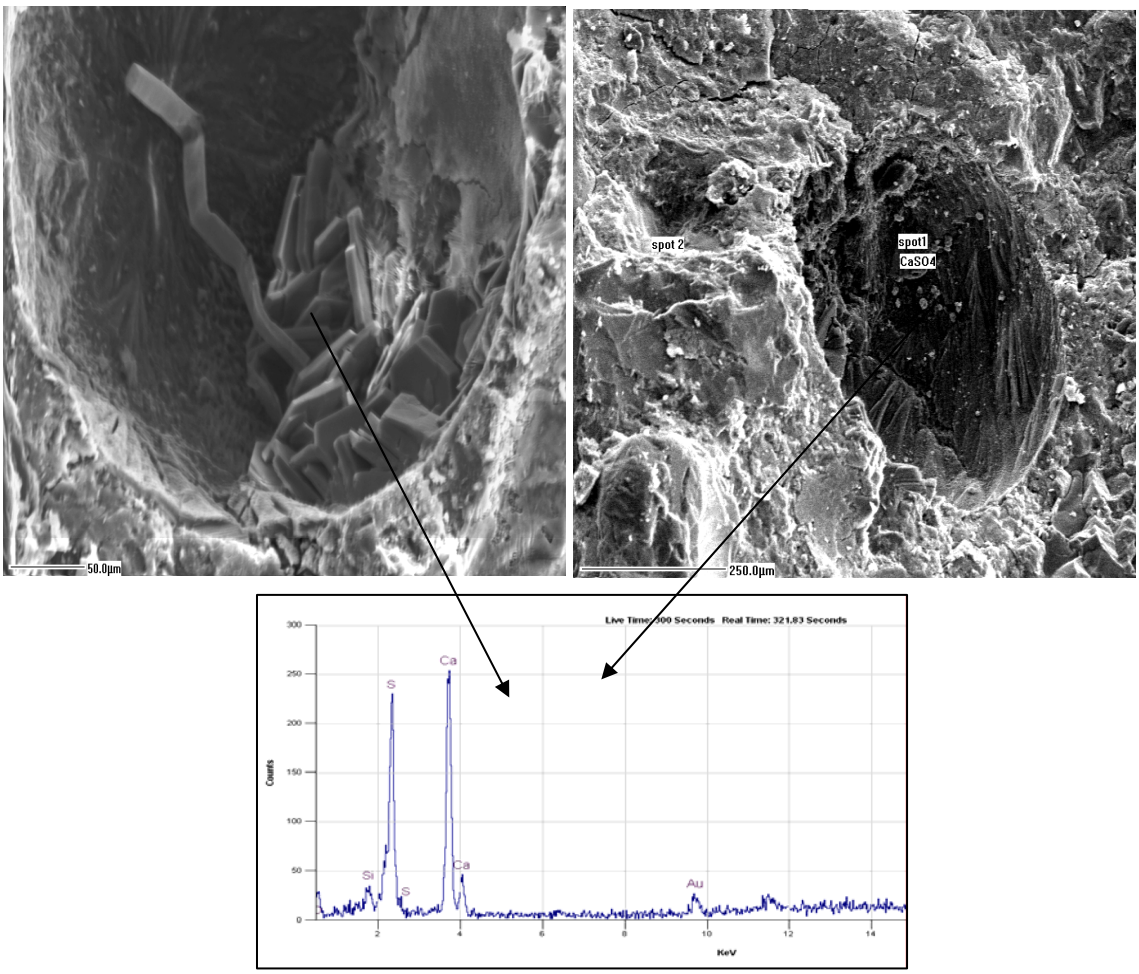

Figure 5.25. SEM of gypsum in the sulphate attacked mortar surface of 30BFA2 mortar after 90 days of curing.

5.2.2. Internal Sulphate Reaction (ISR)

5.2.2.1. Introduction

Internal sulphate attack occurs when there is deterioration of concretes caused by the sulfates that are introduced with the cementitious and/or aggregate materials. Delayed ettringite formation is one of the commonly known internal sulphate reaction. Delayed ettringite formation occurs when the ettringites that are formed during the early hydration are destroyed when the concretes undego heat curing and then reappear at a later age which causes the expansion in the concrete.

Ettringite formation in hardened concrete after heat-treatment is often traced back to temperatures in concrete above the stability limit of ettringite. With rising temperature there is a drop in the thermodynamic stability of ettringite in favor of monosulfate. Depending on the thermodynamic

data the theoretical transformation temperature from ettringite into monosulfate ranges between 70 and 90 °C. The stability limit of the ettringite falls with increasing alkali content in the pore solution. Concrete temperatures above the respective stability limit of the ettringite can lead to decomposition of the ettringite, e.g. with the formation of monosulfate and sulfate. With a subsequent drop in temperature the monosulfate becomes metastable so that, if there is sufficient water available (moisture effects) ettringite can be formed again.

According to current understanding, the majority of the SO_4^{2-} is adsorptively, i.e. physically, attached to the C-S-H and is therefore available as mobile sulfate which is available at later moisture storage of the concrete at lower temperatures. After heat-treatment ettringite is formed under service conditions (low temperature, elevated moisture) from monosulfate and C_3AH_6 both with the SO_4^{2-} from the alkali sulfates in the pore solution and with the SO_4^{2-} attached to the C-S-H. This delayed ettringite formation takes place unless sulfate is supplied from the outside.

Portland cements (apart from highly sulfate-resisting cements) always have excess C_3A relative to sulfate, so the sulfate governs the maximum quantity of ettringite that can be formed. This is the reason why the sulfate content is often held responsible for the occurrence of concrete damage. However, so far no clear connection has been proven between the normal sulfate levels in Portland cement and the expansion of the concrete, the occurrence of damage, and the degree of damage.

The alkali content in cement also has a role. The alkali content in cement affects not only the temperature dependent stability limit of the ettringite, but also the composition and the pH of the pore solution in concrete, which, according to Mehta (1993) affects the ettringite, whether forming fine or coarse crystals. The alkali levels in the range between 0.8 and 1.2 % Na_2O equivalents, which are normal in portland cements, always lead to pH values between 13.5 and 14 during the initial hydration with low water-cement ratios. The question arises whether the ettringite can be formed under these conditions or whether formed ettringite remains stable. If there is no carbonation or leaching while the concrete is in use, then these high pH values remain and the ettringite therefore retains its initial form.

The effect of DEF may be enhanced by the initial development of cracks due to alkali silica reactions (ASR) or by some other factor, with ettringite crystallizing in these cracks and leading to additional expansion of the concrete [Silva et al. 2010].

The development of ISR and/or DEF in concrete depends on several factors that influence not only the beginning of their formation, but also the progression of these reactions. For example some factors related to the composition of concrete, such as the aggregate nature, type of cement, water/cement ratio, and environmental conditions, including temperature and humidity [Silva et al 2011]. The prevention of these internal expansive reactions is normally carried out having in mind the elimination of at least one of the factors that promote them, namely, by the control of

1) the alkali reactivity of the aggregates; the alkali content of the concrete;
2)the maximum temperature of the concrete;
3) the aluminates and the sulphates of the binder;
4)the humidity (the maintenance of the concrete in a relatively dry state;
5)and the calcium hydroxide content of the concrete.

Another way of prevention is through the use of mineral additions in replacement of one part of cement. It is believed that additions have the ability to react with $Ca(OH)_2$ forming hydrated compounds similar to those of cement hydration, like CSH (calcium silicate hydrate), and control the alkalinity of the medium thus inhibiting the formation of the expansive products. The additions may be classified into two types: type I, "almost inert" additions (e.g. limestone filler – LF) and type II, pozzolanic (e.g. fly ash – FA, metakaolin – MK and silica fume – SF) or latent hydraulic additions (e.g. ground granulated blastfurnace slag – GGBS). [Silva et. al 2010].

In this work the performance of biomass fly ash incorporated concrete performs against internal sulphate reaction is investigated.

5.2.2.3. Materials and mix proportions

From the two biomass fly ashes, the fly ash BFA_2 was selected for the ISR tests as an ideal candidate to test the effect of biomass fly ash in the internal sulphate reaction. A 30% incorporation of biomass flyash- the maximum possible content for a moderate strength- was selected for the experiment. The mix proportions used for the concrete specimens are shown in Table 5.12. A superplasticizer Glenium 26 was used by 1.6% for the concrete preparation for an adequate workability.

Table 5.12. Mixture Proportions of 30% BFA2 concrete for ISR test

Components		*Ref. Concrete*	*30 BFA2*
Cement (kg/m^3)		442	310
Substitution (kg/m^3)		0	133
Water (l/m^3)		200	200
Water /Binder (w/b)		0.45	0.45
Aggregate(kg/m^3)	Coarse	1191	1191
	Fine	522	522
Binder/Aggregate ratio		0.26	0.26

5.2.2.2. Experimental procedure

The experimental procedure is conducted in accordance to the French concrete performance test-MLPC No. 66 test method, for DEF accelerated concrete performance (Pavoine et al., 2003). This is applicable in concretes susceptible to temperature elevation at young age (T > 65°C) and then exposed to be a wet environment.

Concretes with cylindrical dimensions of 110 x 220 mm were used for the experiments. In order to promote the occurrence of DEF immediately after casting the cylindrical casts were sealed and placed in a climatic chamber with controlled temperature and humidity, and the concretes were heat-cured using a heat curing cycle (Figure 5.26). It was based on a temperature core rise obtained during setting of a massive cast-in-place concrete with 14 m length, 3.5 m width and 1.5 m high. The concrete reached a maximum temperature of 80ºC after 15 hours and was maintained at temperatures above 70ºC during 3 days. This cycle was computed by the TEXO program part of the CESAR-LCPC finite element design code [Divet et al. 1998].

After that the concrete specimens were kept permanently immersed in water for long-term storage at 20 ± 2ºC. Length and mass measurements were taken periodically in accordance to the accelerated concrete performance French test MLPC nº 66 [LCPC 2007]. Modulus of elasticity and compressive strength were measured for the samples periodically and thermal analysis of the specimens were also done at the time interval 28 days , 90 days and 180 days.

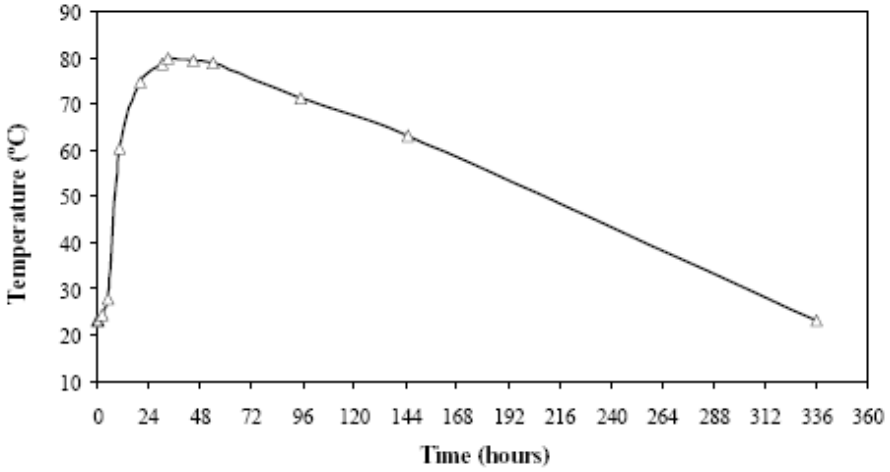

Figure 5.26. Concrete heat curing cycle to promote the occurrence of DEF [Silva et al. 2011].

5.2.2.4. Results and discussion

5.2.2.4.1. Expansion and weight variation

Figures 5.27 and 5.28 show the expansion curves of specimens tested according to the DEF test method, for the reference and the 30BFA2 concrete respectively. In these concrete compositions the content of binder and water/binder ratio is the same of the concrete mixes with cement volume replacement.

According to the test method, the concrete mixes are considered as being suitable in DEF control, if one of two criteria is met. In the first criterian the average longitudinal deformation of the three samples must be less than 0.04%, and no individual value must be greater than 0.06% at 12 months of testing. According to the second criteria the test should be extended up to 15 months if the longitudinal deformation of the three individual specimens is between 0.04% and 0.07% at 12 months of testing [Pavoine and Divet 2007].

At 1 year, the expansion of the control mix is 0.43%. For the biomass fly ash incorporated concrete the expansion tests are still going on, but the results up to now gave a conclusion that the 30 BFA2 substitution has a strong effect in the inhibition of the expansion due to DEF compared to the reference concrete (Figure 5.29). At 112 days the expansion in 30BFA2 concrete was 0.038% and after that the expansion was slightly crossing the limit. By the end of 252 days the expansion is measured as 0.155%.

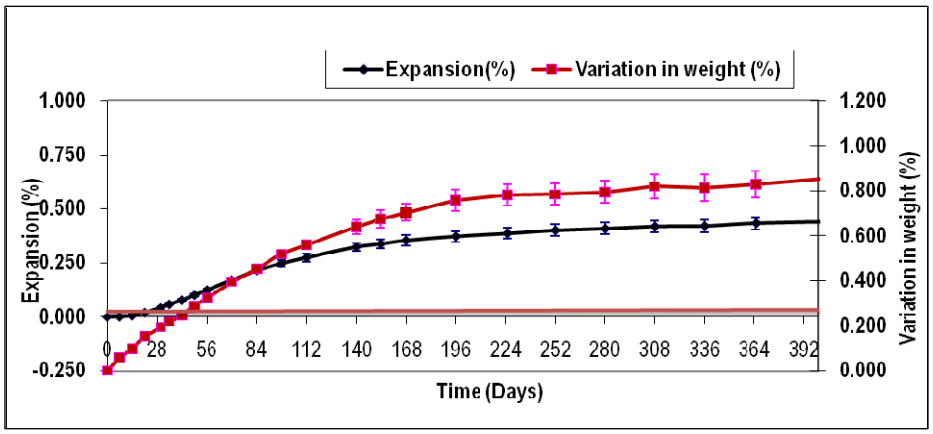

Figure 5.27. Effect of expansion due to DEF on the reference concrete

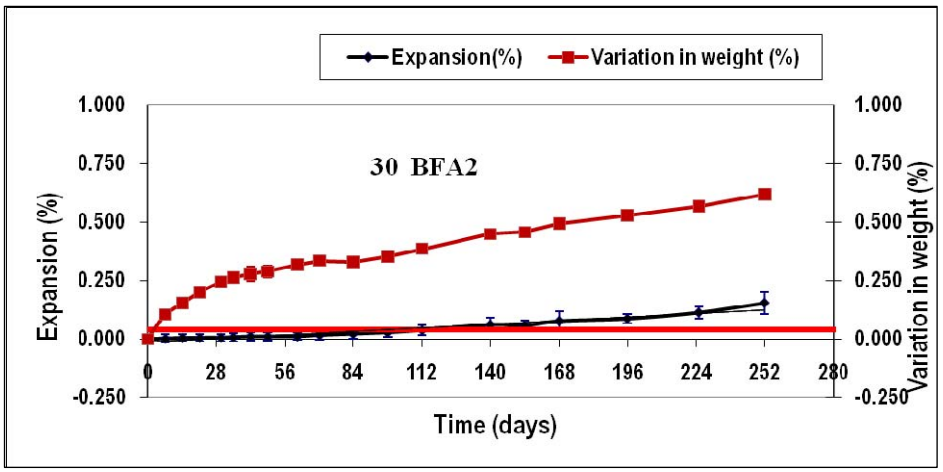

Figure 5.28 Effect of expansion due to DEF on the 30 BFA_2 concrete

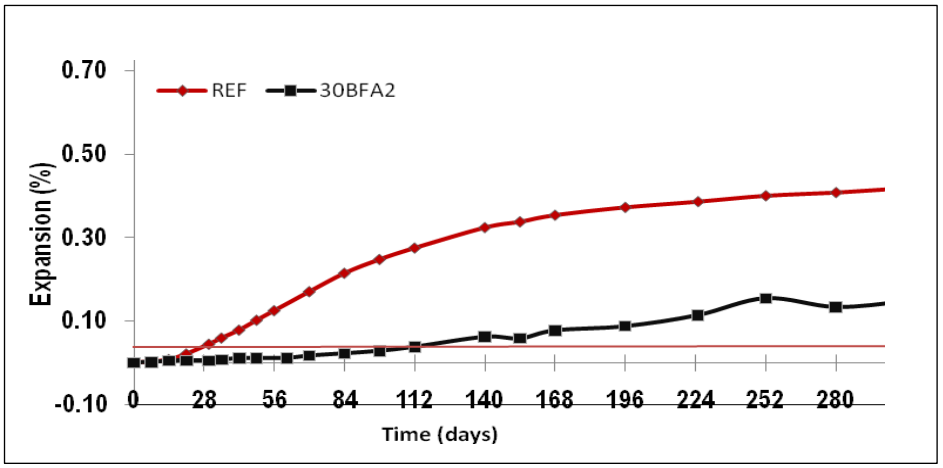

Figure 5.29. Effect of expansion due to DEF comparison

5.2.2.4.2. Strength measurements

Figure 5.30 and Figure 5.31 show the modulus of elasticity and compressive strength measurements of the concrete specimens measured at the interval of 28 days, 90 days and 180 days respectively. There is only a slight difference between the modulus of elasticity values for the reference concrete and 30BFA2 concrete. The compressive strength properties are slightly reduced in 30BFA2 concrete compared to the reference concrete as expected because of the less binding nature of the biomass fly ashes. It can also be observed that there was no deterioration in compressive strength till 180 days of test.

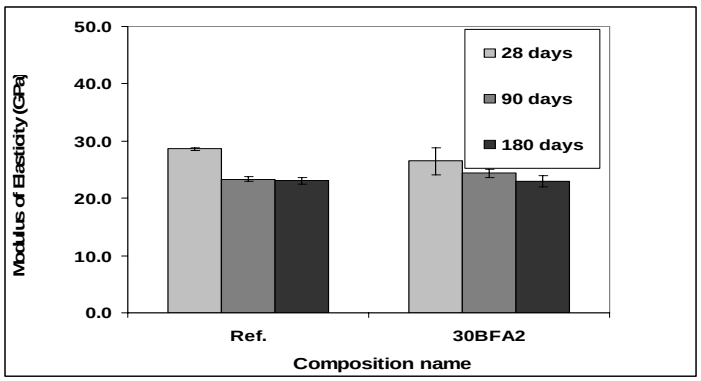

Figure 5.30 modulus elasticity of the concrete specimens.

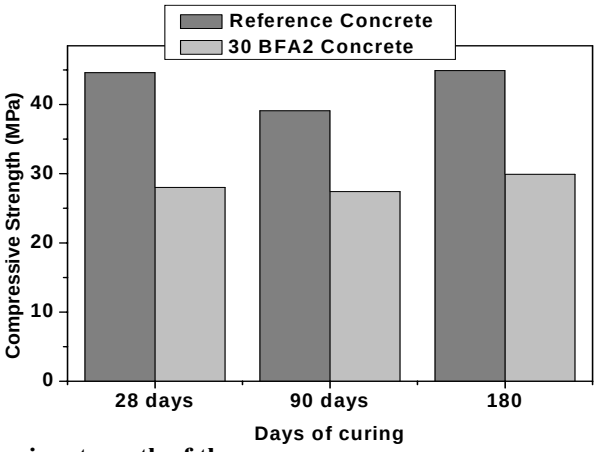

Figure 5.31. Compressive strength of the concrete specimens.

5.2.2. 4. 3. Consumption of calcium hydroxide $Ca(OH)_2$

The weight loss of the concrete samples under different temperature upto 1000ºC were determined by TG/DTA analysis and the results are plotted in Figure 5.32 and the corresponding thermal decomposition values are shown in Table 5.11. The amount of $Ca(0H)_2$ present in the specimens were determined by the equation

$$LOI\ [Ca(OH)_2] = (LOI_{400\text{-}500^oC}) \times 74/18 + (LOI_{500\text{-}620^oC}) \times 74/44$$

It can be noticed that in 30BFA2 concrete there is a reduction in the $Ca(OH)_2$ level. This can be due to the latent or pozzolanic reaction of the biomass fly ashes. $Ca(OH)_2$ is then consumed with the formation of additional calcium silicate hydrate, reducing the pore volume and consolidating the microstructure, especially in the regions around the aggregates. This restricts the damage promoting transport of moisture and phase-forming components in the concrete**.**

Table. 5.11. TG/DTA analysis of the ISR tested concrete specimens

Samples	***Temperature range***							
	upto 80ºC	80ºC-120ºC	120ºC-220ºC	220ºC - 400ºC	400ºC - 500ºC	500ºC - 900ºC	Total loss on ignition(%)	$Ca(OH)_2$ (%)
				28 days				
Ref-0.45		1.51		0.80	0.85	0.83	4.04	4.90
30BFA2-0.45	0.21	0.49	0.85	0.97	0.56	1.59	4.80	5.00
				90 days				
Ref-0.45		1.94		1.01	1.11	0.76	4.86	5.80
30BFA2-0.45	0.26	0.46	0.76	0.89	0.49	1.48	4.40	4.50

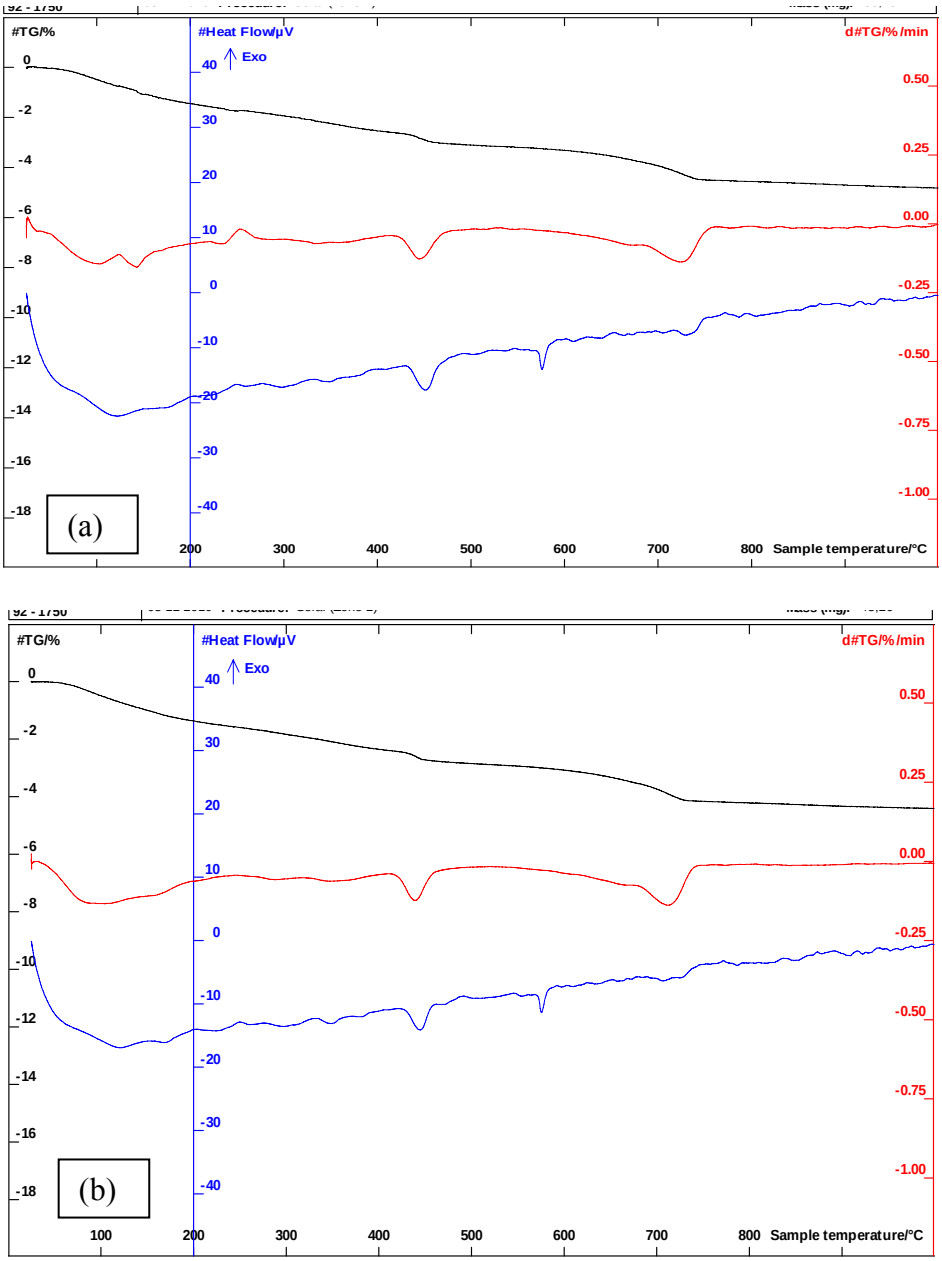

Figure 5.32. The TG/DTA of the (a) reference and (b) 30BFA2 concretes.

5.3. Summary

The biomass fly ashes BFA1 and BFA2 were examined for their ability to resist damage by ASR using the AMBT and RILEM AAR 3 & RILEM AAR 4 methods where a highly reactive fine aggregate was incorporated in the mortas. From the data it was observed that the biomass fly ash incorporation is useful to resist the alkali silica reaction, in concretes. A considerable reduction in expansion was observed on the biomass fly ash incorporated mortars and concretes. The less alkalinity is favouring fly ash BFA1 substituted mortars compared to that of BFA2. For BFA2 the slight increase in pozzolanicity compared to BFA1 results into reduction in the reaction rate. The use of metakaolin was significantly effective in limiting the AMBT and CPT expansion when used together with biomass fly ashes. The relative effectiveness of metakaolin incorporated biomass fly ash cement formulation is primarily due to the smaller particle size, higher degree of reactivity, and chemical composition. It may also be proposed that contributions to lower permeability and increased alkali binding also play a role in mitigating ASR. It was observed that the reaction rate decreases by a significant value after the substitution of the biomass fly ashes and also the rate of expansion was less after 14 days indicating the lesser availability of the alkalis for the expansion reaction. For the biomass fly ash metakaolin blend reaction rate did not changed significantly because of the effective pozzolanic nature of metakaolin and its vigorous reactivity in mitigating the ASR even in the initial stages of the AMBT and CPT. The biomass fly ash metakolin blend shows a mixture contribution in resisting the ASR expansion.

It is also pointed that in real situations, the concrete that is proportioned to have a low intrinsic alkali content will typically not be exposed to a significant concentration of alkalis from external sources until well into the service life when hydration reactions have ceased and concrete properties have fully developed. While this will not affect faster reacting metakaolin, it would undoubtedly have a large influence on the early-age expansion of mixtures incorporating slower reacting biomass fly ash which may take weeks to months to fully react under the 38 °C storage conditions of CPT specimens [Robert et al. 2010]. Additional research in the form of time dependent permeability and CH content measurements will be required to better understand these mechanisms and their influence on expansion throughout the test duration of the AMBT and CPT.

The external sulphate reaction studies showed the sulphate reaction affected BFA1 mortars severely after 1 year of testing. BFA2 mortars could withstand the attack till 1year , showing similar properties to those of the reference mortar. The higher porosity of the mortar specimens and

the organic content in the BFA2 decomposed over the time in the high sulphate solution making it deformed.

The results on Internal Sulphate Reaction (ISR) clearly show that the 30 BFA2 substitution has a strong effect in the inhibition of the expansion due to DEF. The fly ash was behaving pozzolnaically with the reduction in the content of calcium hydroxide in the matrix. The expansion tests are still ongoing, but the results obtained until now show that substitution of 30% BFA2 has diminished DEF considerably.

CHAPTER 6 ALTERNATIVE APPLICATIONS OF BIOMASS FLY ASHES

6.1. Introduction

In this chapter some other applications alternative to the ones discussed before are reported. There are many reasons for finding diverse applications for the use of biomass fly ashes. (i) costs and disposal area are minimized, thus enabling other uses of the land and decreasing disposal permitting requirements; ii) there may be financial returns from the sale of the by-product or at least an offset of the processing and disposal costs; iii) and, the by-products can replace some scarce or expensive natural resources. Utilization of biomass fly ashes can be in the form of an alternative to another industrial resource, process, or application. Significant research interest is being put in the investigation of biomass fly ashes that can be used in the place of coal fly ashes in various applications. The applications in which the researches were performed so far included, usage as an industrial catalyst, for improvement of soil alkalinity, as a pollution control agent, usage in road sub base, as a binding material in mortar/concretes etc [Vinod et al. 2003, Kastner et al. 2009, Rejini et al. 2009, Naylor and Schmidt 1986, NCASI 1993].

In this chapter, two possibilities were studied. They were 1) Addition in lime mortars and 2) synthesis of alkali activated binders (geopolymers).

6.2. Biomass fly ash in lime based mortars

For several centuries, lime-based mortars were used as binding materials in monuments. As a consequence, now a broad variety of mortars can be found in historical buildings. Nowadays, these traditional mortars have been replaced by cement mortars [Arandigoyen and Alvarez 2007, Moropoulou 2000 and Papayianni 2006] because of the characteristics of lime-based mortars: such as (i) slow setting that hinders and delays restoration work; (ii) lime mortars present lower strengths than cement mortars, and take longer to reach them. Cement-based mortars have therefore displaced lime-based mortars because of their faster setting, higher mechanical strength and advanced industrial development and affordable cost. But their unsuitability in repairing the

historic buildings has led the intensive researches in lime mortars to develop mortars of better performance.
The use of a reactive pozzolan as an addition to lime produce mortars, similar to historic ones, that exhibit an advanced durability to severe climate and moisture conditions and high values of mechanical strength (aqueducts, thermal baths, foundations of buildings, bridges, and so on) [Bakolas et al. 2008] .

Two types of pozzolans have been used in the past: natural, usually of volcanic origin and artificial like ceramic powder. Another artificial pozzolana that has been used is metakaolin and is being researched recently and results suggest that, in adequate proportions, they produce an increase in mechanical strength and durability of mortars, meeting water intake and drying requirements. [Fortes-Revilla 2006, Velosa 2006, Eleni et al. 2001]. In this context, the binding/pozzolan effect of biomass fly ash in the lime mortars is a matter of interest.

6.2.1. Materials, composition design and sample preparations

Lime mortars were prepared by replacing lime with different amounts of biomass fly ashes (5%, 10%, 15% and 20% by weight of binder). Hydrated lime was used for the mortar preparation. Biomass fly ash BFA2 was chosen for this investigation. The mortar bars were prepared with 20%(% of total solid weight) water content. The lime to aggregate ratio was taken as 1:3 in all the compositions and 1% of a superplasticizer (Sika) was used to maintain the workability. A fine sand with particle size < 2mm was used as aggregate (a description of the sand characteristics is listed in chapter 4, section 4.2.1). The components were weighed and mixed thoroughly in a laboratory mixer (CONTROLS, 65-LS). The mixing procedure includes: (i) addition of water to the dry powder mix; (ii) mixing for 1 minute at a low rotation speed of ~60 rpm; (iii) stopping for one minute to gather the mix into the centre; (iv) mixing again for 2 minutes at a higher rotation speed (~120 rpm). The mixture proportions used for the experiments are shown in Table 6.1.

Mortar workability was measured with the flow table method and expressed as spread diameter in mm. The flow table measurements were performed according to EN 1015-3 European standard. The mortar sample spread diameter measured before and after 15 strokes (1 stroke per second) represents the flow table values. The density was obtained from geometrical measurements. The fresh state relative density was evaluated through the weight determination of a specific mortar volume. The standard dimensions of 16 cm x 4 cm x 4 cm were used for the preparation of mortar samples for mechanical tests. The mortars were demoulded after 7 days of curing in the moulds at

room temperature and then moved to a curing chamber at a temperature of 20 ºC. The strength measurements were done on the cured samples aged from 28 days onwards. The mechanical strength was evaluated by compression and flexural tests carried out according to EN 1015-11:1999, on three samples of each composition, using a Standard Universal Testing Machine (Shimadzu). Porosimetry studies were carried out using water absorption and mercury porosimetry techniques. Capillarity absorption test was also carried out in the cured samples.

Table 6.1. Mix proportions for biomass fly ash lime mortars

Composition	*Biomass fly ash (g)*	*Lime(g)*	*Spread diamater (mm)**	*Fresh desnity(g/cc)*
0 % BFA_2	0	400	180	1.98
5% BFA_2	20	380	180	1.97
10% BFA_2	40	360	180	1.89
15% BFA_2	60	340	175	1.92
20% BFA_2	*80*	*320*	*175*	*1.94*

**** Water 20% (320g) , Superplasticizer 1% (4g) , Binder: Aggregate =1:3***

6.2.2. Results and discussions

6.2.2.1. Mechanical strength

It was observed that the substitution of biomass fly ashes in high amounts decreased the flow table spread diameter. The water content in the mixes were kept the same by the addition of 20% water (% of solid weight) along with 1% super plasticizer (% of binder weight). In Figure 6.1 the strength measurements obtained up to a curing time of 180 days are plotted. It can be noticed that the flexural as well as the compressive strength decreased on incorporation of the biomass fly ashes. But on the long term curing, the biomass fly ashes contributed to the strength development significantly compensating the initial loss of strength. By the end of 180 days of curing the compressive strength properties were comparable with the reference mortars up to 15% of incorporation of biomass fly ash. This indicates the secondary hydration effect of biomass fly ash that was exhibited upon a long term curing. But for 20% replacement of biomass fly ashes the strength was again in the declining side compared to the other compositions. This can be attributed to the excess decrease in the lime content as well as the morphology of the biomass fly ashes such as irregularity which in turn reduces the overall homogeneity of the mixture.

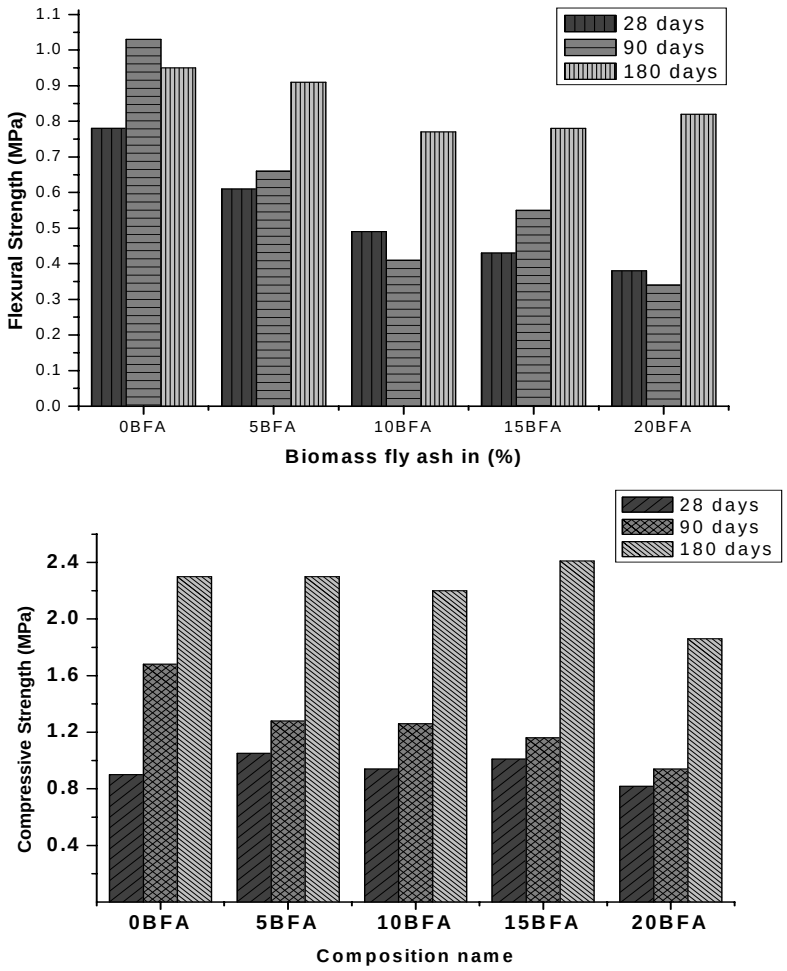

Figure 6.1 Strength properties of biomass fly ash incorporated lime mortars.

6.2.2.2. Microstructure

The total porosity in terms of coefficient of water absorption is shown in Figure 6.2. The absorption coefficient shows a slight increase on the incorporation of the biomass fly ash. On aging, the porosity measured by water immersion slightly increases. This result is a bit contradictory when comparing with the strength values obtained. The mechanical strength showed a significant increase on the substitution of biomass fly ashes after long curing time. This is seen visibly from 5% of incorporation onwards. So this variation in porosity can be due to the presence of some hydrating phases like gypsum that alters the packing effect resulting into an increase in the porosity though it increases the strength of matrix as well [Sivapullaiah and Arif 2011].

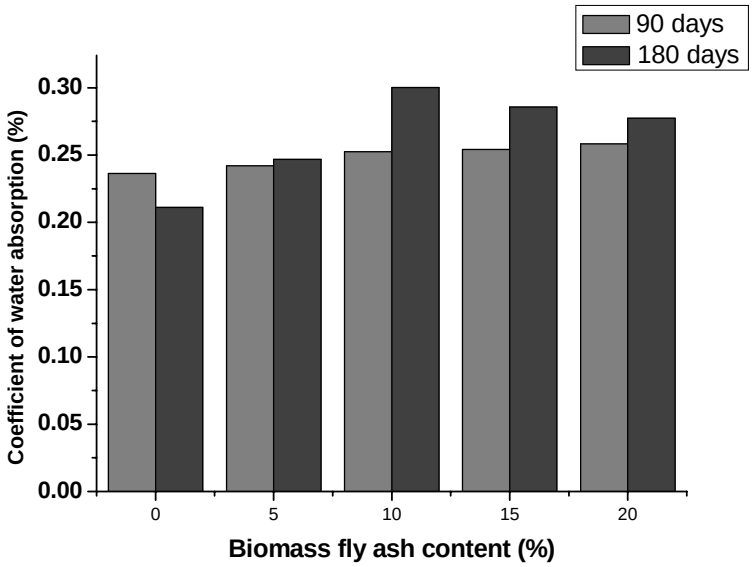

Figure 6.2. Coefficient of water absorption for the biomass fly ash incorporated lime mortars

The mercury intrusion porosimetry carried out on the biomass fly ash lime mortars at the age of 6 months are shown in Table 6.2. The average pore diameter also showed a small increase with the increase in the biomass fly ash content. The pore size distribution curves showed a clearer picture (Figure 6.3). It can be noticed that on incorporating biomass fly ashes there is a slight shift in the pore size distribution in mortars both in terms of small pores and the large pores. The smaller pores (0.1µm - 1µm) shifted towards the higher pore size direction and the bigger pores (1µm -100 µm) shifted towards the lower pore size distribution. This clearly indicates the redistribution of matrix structure due to the biomass fly ash particles and the secondary hydrating phases that it contributes.

Table 6.2. Mercury Intrusion Porosimetry data summary

Composition	***0BFA***	***10BFA***	***20BFA***
Total Intrusion Volume mL/g	0.8	0.9	0.2
Total pore area (m^2/g)	2.1	1.9	1.5
Median Pore Diameter (Volume)(µm)	0.4	0.7	0.8
Median Pore Diameter (Area) (µm)	0.9	0.9	0.2
Average pore diameter (µm)	0.3	0.4	0.5
Bulk Density (g/mL)	1.8	1.7	1.8
Apparant Density (g/mL)	2.5	2.5	2.5
Porosity (%)	29.5	31.1	29.9

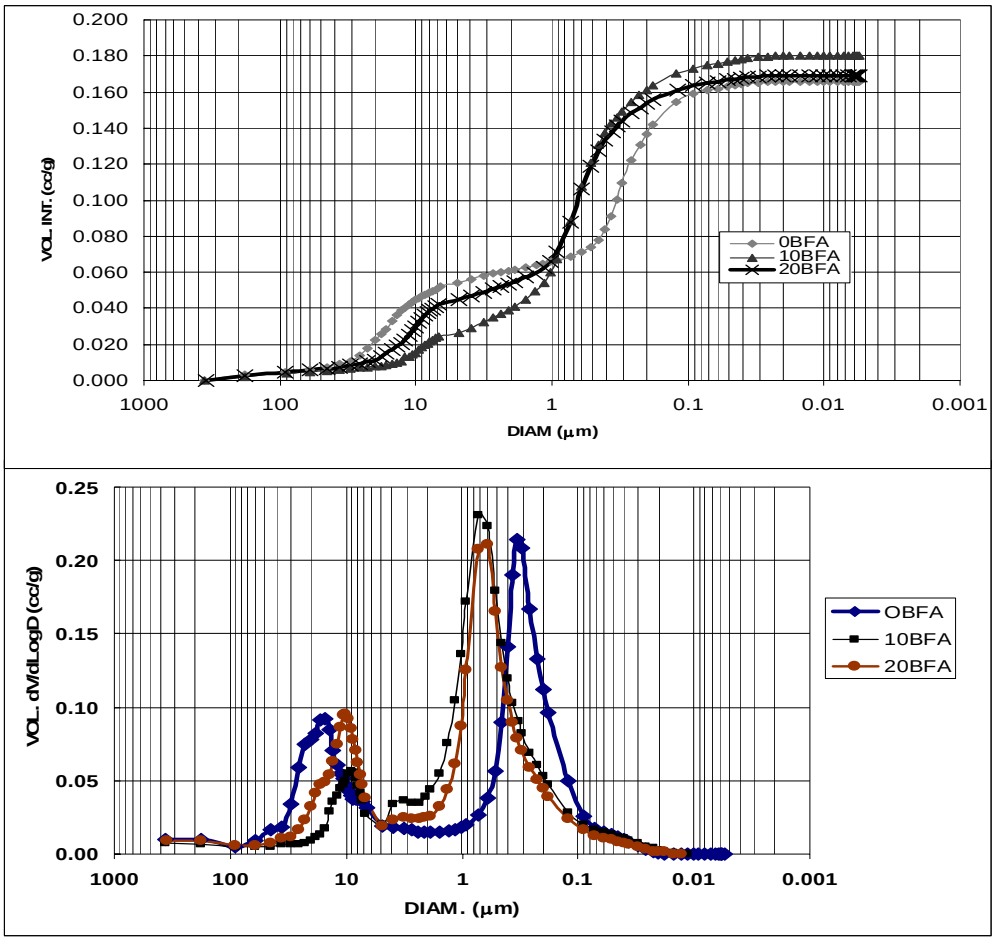

Figure 6.3. Pore size distribution of the biomass fly ash lime mortars at the age of 180 days

The capillarity absorption curves are shown in Figure 6.4. It was observed that the capillary coefficient values were higher for the biomass fly ash incorporated lime compared to the reference mortar when determined at the age of 90 days. But the capillary coefficients had similar values on 180 day measurements (Table 6.3). This also indicates the influence of biomass fly ashes on later ages of curing by its secondary hydration. However, the overall capillarity coefficient increased with increase in time for all the mortars. The extent of carbonation is checked by the application of phenolphthalein solution. Figure 6.5 shows the biomass lime mortar bars cured for a duration of 6 months checked by phenophthalein. The spot size of noncarbonated regions in the mortar with 15% and 20% BFA was smaller/insignificant compared to the reference mortar as well as 10% BFA incorporated mortar. This indicates the pozzolanic nature of BFA which causes secondary hydration.

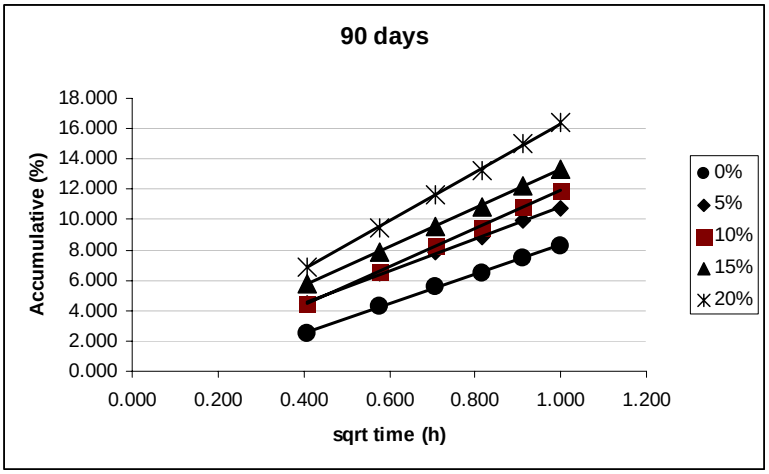

Figure 6.4(a). Curves of capillary absorption for biomass fly ash substituted lime mortars cured for 90 days.

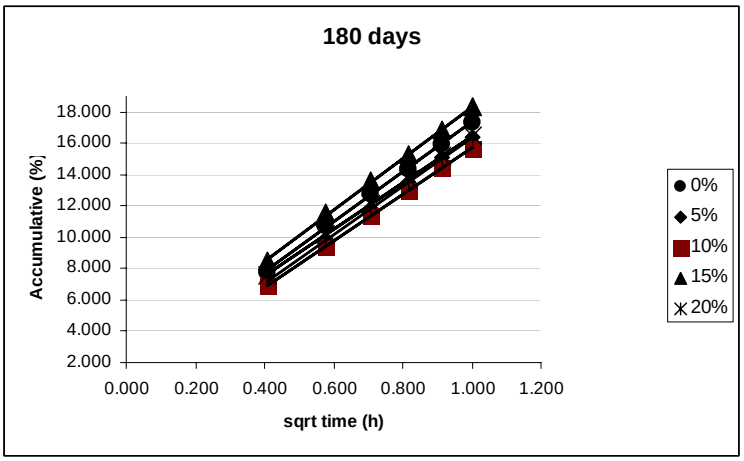

Figure 6.4(b). Curves of capillary absorption for biomass fly ash substituted lime mortars cured for 180 days.

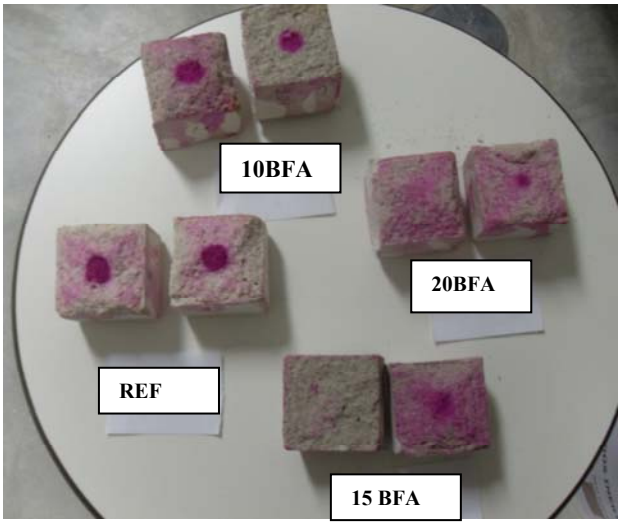

Figure 6.5. Carbonation in BFA lime mortars cured for 180 days.

Table 6.3. Capillary coefficient values of biomass fly ash-lime mortars

biomass fly ash (%)	*capillary coeffcient (90days)*	R^2	*capillary coeffcient (180days)*	R^2
0	9.70	0.9993	15.98	0.9999
5	10.51	0.9992	15.54	0.9991
10	12.60	0.9995	14.78	0.9997
15	12.79	0.9991	16.48	0.9992
20	16.10	0.9994	14.97	0.9992

A more detailed investigation is to be carried out in terms of micro structural evolution of the fly ash incorporated lime mortars in a long duration basis to get a clearer picture of the influence of biomass fly ashes in lime. The fly ashes could help improving the properties, when subjected to long time curing. However the properties such as water absorption coefficient are negatively affected in the biomass fly ash incorporated lime as long as it is not proved that the expelling capacity of absorbed moisture is overtaking its intake capacity [Velosa 2001]. And also it should be mentioned along with that the difference between the capillary coefficients of the biomass fly ash incorporated mortars were decreased by 180 days. From the data until now it can be concluded that the biomass fly ash can be considered for lime mortars as a new candidate of pozzolan additive.

6.3. Alkali activation of biomass fly ashes

Studies of alkali activated cements have a long history in the former Soviet Union, Scandinavia, and Eastern Europe, but they had an exponential increment after the research results of Joseph Davidovits who developed and patented binders obtained from the alkali-activation of metakaolin and termed it as geopolymer. Alkali-activated complex binders (AACBs) are a developing field of research for utilizing solid wastes and by-products. Geopolymers, a type of AACB, are materials analogous to organic materials that react at ambient temperature to form solid polymers. The prefix “geo” refers to the inorganic nature of the material. Geopolymerization is a chemical process that provides a rapid transformation of some geopolymeric structures to create products that are either partially or totally amorphous and/or meta-stable. In general, two types of cementitious raw materials can be used for geopolymerization:- those based on Si and Ca or those based on Si and Al. Coal fly ashes are effectively proved to have geopolymer properties on alkali activation.

Geopolymers can best be viewed as the amorphous equivalent of certain synthetic zeolites. Davidovits (1994) proposed that geopolymers consist of a polymeric Si–O–Al framework, with SiO_4 and AlO_4 tetrahedra linked alternately by sharing all the O atoms. The fact that Al is 4 co-ordinated with respect to O creates a negative charge imbalance and therefore the presence of cations such as K+, Na+ and Ca^2+ is essential to maintain electric neutrality in the matrix. The geopolymerisation reaction route can be classified as an inorganic polycondensation reaction and may be compared to the formation of zeolites. Most zeolite syntheses are performed under basic conditions using OH- as a mineralising agent [Van Bekkum et al. 1991]. According to Van Jaarsveld et al. (1998) it also appears that an alkali metal salt and/or hydroxide is needed for dissolution of silica and alumina to occur as well as for catalysis of the condensation reaction. The exact mechanism by which geopolymer setting and hardening occures is not fully understood. Most proposed mechanisms consist of dissolution, transportation or orientation, as well as a reprecipitation (polycondensation) step. Hua and Van Deventer (1999) presented the mechanism schematically as follows:

$$n(Si_2O_5, Al_2O_2) + 2nSiO_2 + 4nH_2O + NaOH/KOH \rightarrow$$

(Si–Al materials)

$$Na+, K^+ + n(OH)_3-Si-O-Al^- -O-Si-(OH)_3$$

$$(OH)_2$$

(Geopolymer backbone)

(1)

$$n(OH)_3-Si-O-Al^- -O-Si-(OH)_3 + NaOH/KOH \rightarrow$$

$$(OH)_2$$

$$(Na^+, K^+)-(-Si-O-Al^- -O-Si-O-) + 4nH_2O$$

$$O \quad O \quad O$$

(Geopolymer backbone)

(2)

Davidovits (1999) proposed the possible applications of the geopolymers depending on the molar ratio of Si to Al, as given in Table 6.4.

Table 6.4. Applications of geopolymers (Davidovits 1999)

Si/Al	*Application*
1	Bricks, ceramics, fire protection
2	Low CO_2 cements, concrete radio actives , toxic waste encapsulation
3	Heat resistant composites, fibre glass composities, foundry equipments,
>3	Sealants for industry
20<Si/Al<35	Fire resistance, heat resistance fibre composites

Investigations about alkali-activated binders have deserved increased attention by the research community mainly due to its environmental performance and superior durability over ordinary Portland cement. Recent papers have reported [Alonso and Palomo 2001, Yip et al. 2005, Palomo et al. 2007a] that the alkaline activation of blends of aluminosilicate (kaolinitic clay or fly ash) and calcium silicate (Portland cement or blast furnace slag) materials in proportions of around 70-80% / 30-20% generate binder systems with mechanical strength values similar to the figures recorded for Portland cement. Such cementitious properties may be inferred to be due to the formation in these systems of mixes of alkaline aluminosilicate (N-AS-H) and C-S-H gel (main reaction product in Portland cement hydration or blast furnace slag activation). The two gels would only co-exist at specific ranges of alkaline concentration (OH ion concentration). Earlier experiments seem to indicate that moderate calcium contents in alkaline systems may improve mechanical strength and durability. The role that this element may play in the microstructural development of cementitious phases is yet to be determined. The mechanical strength developed depends on the "hydrating" solution used. When the soluble solutions contain soluble silicates, the strength values rise substantially. A mix of different gels (C-A-S-H and (N+C)-A-S-H) is obtained when alkaline solutions are used (Alonso and Palomo 2001, Palomo et al 2007]

The objective of the alkali activation of biomass fly ashes in the present work is to formulate a binder with 0% Portland cement.

6.3.1. Materials

Theoretically, any material composed of silica and aluminium can be alkali-activated [Fernando et al. 2008]. The suitability of various types of fly ash to be geopolymer source material has been studied by Fernández-Jimenez and Palomo (2003). These researchers claimed that to produce

optimal binding properties, low CaO content, the low-calcium fly ash should have the percentage of unburned material (LOI) less than 5%, Fe_2O_3 content should not exceed 10%, the content of reactive silica should be between 40-50%, and 80-90% of particles should be smaller than 45 μm. On the contrary, Van Jaarsveld et al (2003) found that fly ash with higher amount of CaO produced higher compressive strength, due to the formation of calcium-aluminate-hydrate and the calcium compounds, especially in the early ages. The other characteristics that influenced the suitability of fly ash to be a source material for geopolymers are the particle size, amorphous content, as well as morphology and the origin of fly ash.

The fly ash used in this test is biomass fly ash BFA2 which is a class C type fly ash in terms of chemical composition. Metakaolin (ARGICAL 1200) was also used for making blends with the biomass fly ash. The major oxides in the precursor materials obtained by XRF method is shown in Table 6.5.

Table 6.5 The major oxides in precursor materials

Material	***Oxides wt %***								
	SiO_2	Al_2O_3	Fe_2O_3	CaO	MgO	Na_2O	K_2O	SO_3	TiO_2+P_2O_5
Biomass fly ash	31	8.5	3.0	24	4.8	6.6	2.7	2.3	2.77
Metakaolin	54.66	37.98	1.22	0.01	0.05	0.01	0.01	0.02	--

The SiO_2/ Al_2O_3 atomic ratio is 6.1 for biomass fly ash and it is higher than the one suggested by Davidovits of about 2 for making cement and concrete. However, the final SiO_2/Al_2O_3 atomic ratio in the hardened binder depends mainly on the reactivity of Al–Si because not all the silica and alumina are reactive. So one cannot expect the same Si/Al ratio in the final hydration product as the one present in the original precursor material. Indeed, most of the Al–Si materials cannot even supply sufficient Si in alkaline solution to start geopolymerization. This explains why they need extra silica provided in solution by waterglass, which influences the Si/Al ratio of the hardened binder [Fernando et al. 2008].

6.3.2. Alkaline activators

The most common alkaline activators used in geopolymerisation are a combination of sodium hydroxide (NaOH) or potassium hydroxide (KOH) and sodium silicate or potassium silicate [(Davidovits 1999; Palomo et al. 1999; Barbosa et al. 2000; Xu and van Deventer 2000; Swanepoel and Strydom 2002; Xu and van Deventer 2002]. Reactions occur at a high rate when the alkaline liquid contains soluble silicate, either sodium or potassium silicate, compared to the use of alkaline hydroxides alone. Xu and van Deventer (2000) confirmed that the addition of sodium silicate

solution to the sodium hydroxide solution as the alkaline liquid enhanced the reaction between the source material and the solution.

The alkali activators used in the present work were selected considering the above reports. A mixture of sodium hydroxide (NaOH) and sodium silicate or water glass ($Na_2SiO_2(OH)_2 \cdot 4H_2O$)) solution was used as the alkaline activator. In order to test the effect of sodium hydroxide and sodium silicate solution, different molar proportions of sodium hydroxide and sodium silicate solutions were used. The concentration of NaOH selected were 8 M, 10 M, 12 M and 18 M. The sodium hydroxide and sodium silicate solution proportions were taken in different ratios ranging from 0.5 to 2.5. Distilled water was used to dissolve the sodium hydroxide flakes to avoid the effect of unknown contaminants in the mixing water. Soon after the mixing of sodium hydroxide flakes with water the vessel containing the mix is cooled by keeping in a water bath to avoid the bioling of the solution. The alkaline mixes were made one day prior to use in order to have a homogenous solution at the time of paste/mortar preparation.

6.3.3. Compositions

The biomass fly ashes were sieved at 75 μm in order to remove the coarse particles. The metakaolin was used in the as received form. The mixes were prepared by weight proportions (Table 6.6). The different mixtures of biomass fly ash and the combination of biomass fly ash with metakaolin were moulded into small cylindrical polyethylene containers as the moulds (diameter x height = 3 cm x 4 cm). Three specimens of every mixture were prepared for the tests. After weighing the materials the solid components were added into the alkali solution slowly while keeping the mixing process by hand mixing using a palate knife. For biomass metakolin compositions the raw materials were mixed thoroughly before adding into the alkali activator. The amount of alkali activator solution and binding materials was selected in order to have sufficient workability for the mixes to be poured into the containers. After the mixtures were filled into polyethylene containers, they were sealed to avoid water loss, and were cured at 60 ºC for the first two days in a curing chamber with a RH 95% and then at 20 ºC for the rest of the curing time. The initial curing temperature was selected as per the previous reports on the curing temperature effect on the alkali activated fly ash materials [Detphan et al. 2009] and it was also reported that most of the strength achievement occurred in the geopolymer in the first 7 days. No fine sand was used for these pastes preparations. The mechanical strength was determined after 10 days curing. XRD and SEM/EDX analyses were also done to investigate the mineral and micro structural properties of the alkali activated biomass fly ashes.

Mortar bars were also prepared by selecting a combination of biomass fly ash with metakaolin by replacing biomass fly ash with metakaolin (0%, 20%, 40%). The sand used as aggregate was the same sand used in the mortar preparation for cement and lime compositions but the finer portion alone was used here. The sand was sieved at 600 μm and was dried at 60ºC overnight prior to incorporation in the matrix. The mixture proportions used for the mortar preparations are shown in Table 6.7. The sand and the binder components were dry mixed before adding to the activator, which is the mixing option that leads to the best results [Fernando et al. 2008]. The binder alkali activator ratio was chosen as 3:2 for the experiments. The binder to aggregate ratio was taken as 1:3 in all the compositions. To produce a workable mix extra water has been added along with a superplasticizer by 1% of the binder content. The water used as a percentage of the total solid content was 3.7-6% in the compositions.

An alkali solution with a sodium hydroxide and water glass ratio 1:2 was selected as the activation liquid composition for the mortars. Two different concentrations of NaOH solution (10 M and 18 M) were tested to verify the effect of NaOH in the mechanical properties. The components were weighed first and mixed thoroughly in a laboratory mixer (CONTROLS, 65-LS). The mixing procedure includes: (i) addition of alkali solution to the mixer; (ii) pouring the dry mix into the solution while mixer is at a low rotation speed of ~60 rpm, iii) finally, addition of superplasticiser and water. The addition of water was varied in the samples according to the requirement of workability. When it seemed that the mix became homogenous and in workable condition, the mixing was stopped and poured into the moulds quickly. The time for total mixing waskept always within less than 5 minutes because of the quick setting nature of the mix. All the mixes showed similar setting behaviour and got stiffened within 20-30 minutes from when mixing was started.

Table 6.6. Mixture compositions of alkali activated biomass fly ashes

Sample name	*NaOH concentration (M)*	*Na_2SiO_3: NaOH*	*Biomass fly ash (g)*	*Metakaolin (g)*	*Alkali activator (g)*	*workability*
8M100BFA	8	2:1	150	---	100	Stiff
10M100BFA	10	2:1	150	--	100	moderate
12M100BFA	12	2:1	150	--	100	moderate
10M100BFA	10	1:0.5	150	---	100	Stiff
10M100BFA	10	1:1	150	--	100	Stiff
10M100BFA	10	1:1.5	150	---	100	moderate
10M100BFA	10	1:2.5	150	---	100	moderate
18M100BFA	18	2:1	150	---	100	moderate
10M60BFA+40MK	10	2:1	90	60	100	moderate
10M80BFA+20MK	10	2:1	120	30	100	moderate
18M60BFA+40MK	18	2:1	90	60	100	moderate
18M 80BFA+20MK	18	2:1	120	30	100	moderate

Table 6.7. Mixture proportions for biomass fly ash metakaolin mortar blends

Sample name	*NaOH (M)*	*Na_2SiO_3: NaOH*	*Biomass fly ash(g)*	*Metakaolin (g)*	*Alkali activator solution (g)*	*Sand (g)*	*Water (g)*	*Workability (g)*
10M 100BFA	10	2:1	450	0	300	1350	75	moderate
18M 100BFA	18	2:1	450	0	300	1350	68	moderate
10M 80BFA	10	2:1	360	90	300	1350	80	moderate
18M 80 BFA	18	2:1	360	90	300	1350	92	moderate
10M 60BFA	10	2:1	270	180	300	1350	109	moderate
18M 60BFA	18	2:1	270	180	300	1350	91	moderate

6.3.4. Results and discussions

6.3.4.1. Compressive strength measurements

The workability was decided by checking the behaviour of the mix fluidity through observation while mixing. The workability was not able to be measured using flow table because of the quick setting nature of the mixes. It could be noted that when the amount of both sodium hydroxide and sodium silicate decreased the workability also decreased. An increase in the concentration of the alkali activator especially the content of sodium silicate in the activator solution favoured the fluidity of the mixes. Table 6.8. shows the mechanical properties of the alkali activated biomass fly ash compositions. Figure 6.6 shows the samples of alkali activated biomass fly ashes made for the mechanical strength measurements. It can be observed that strength of the biomass fly ash compositions increases with the increase in NaOH content. However for NaOH addition greater than 10 M the compressive strength tends to decrease (Figure 6.7). This is because of the fast setting on adding more alkali which does not give room for a homogenous mixing resulting into weak polymerisation. An increase in the amount of sodium silicate solution in the composition also favours the strength of the compositions. From the listed properties 10M NaOH can be considered as an optimum quantity for obtaining a good strength compared to the other compositions in Table 6.8. The metakaolin incorporated samples improved the strength values. It was noticed that an increase in the highly reactive metakaolin content leads increase in the strength values.

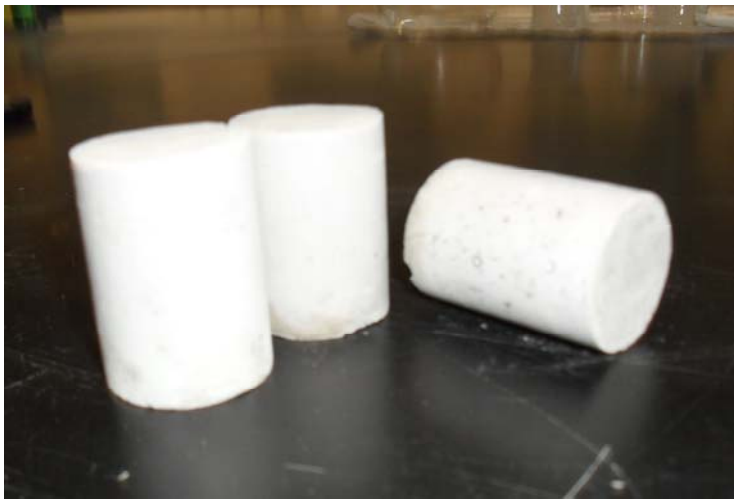

Figure 6.6. Alkali activated biomass fly ashes.

Table 6.8. Mechanical properties of alkali activated biomass fly ash.

Sample name	*NaOH concentration (M)*	*Density (gm/cc)*	*Compressive strength (MPa)*	*Na_2SiO_4: NaOH*
8M100BFA	8	1.54	8.59	2:1
10M100BFA	10	164	11.69	2:1
12M100BFA	12	1.67	11.50	2:1
10M100BFA	10	1.63	6.65	1:0.5
10M100BFA	10	1.64	10.89	1:1
10M100BFA	10	1.78	10.68	1:1.5
10M100BFA	10	1.67	8.16	1:2.5
10M60BFA+40MK	10	1.48	15.97	2:1
10M80BFA+20MK	10	1.47	14.37	2:1
18M60BFA+40MK	18	1.48	12.13	2:1
18M80BFA+20MK	18	1.46	13.10	2:1
18M100BFA	18	1.73	10.77	2:1

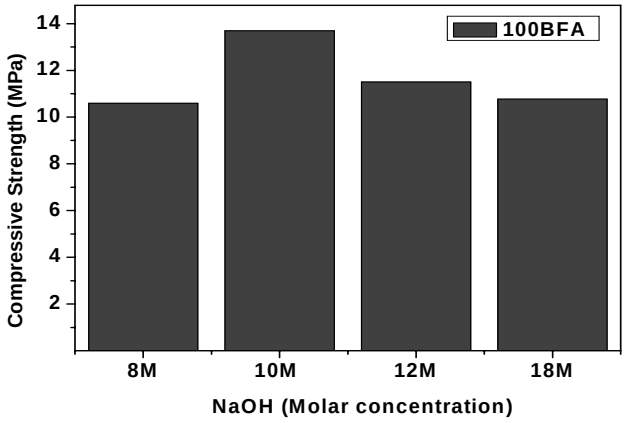

Figure 6.7. NaOH molar concentration Vs compressive strength of alkali activated biomass fly ashes(Na_2SiO_4: NaOH =2:1)

The mortars made with biomass and sand showed more strength to the geopolymer mixes (Figure 6.8). The biomass fly ashes gave a compressive strength of 18 MPa and 14 MPa for
10 M and 18 M NaOH concentration. The highest value was obtained for 40% metakaolin incorporated mortars where it got around 38 MPa for 10 M NaOH concentration. The 20% metakaolin incorporated mortars samples showed an intermediate value of 30MPa. This clearly shows that the metakaolin incorporation had behaved well with the biomass fly ashes in the alkali activated complex.

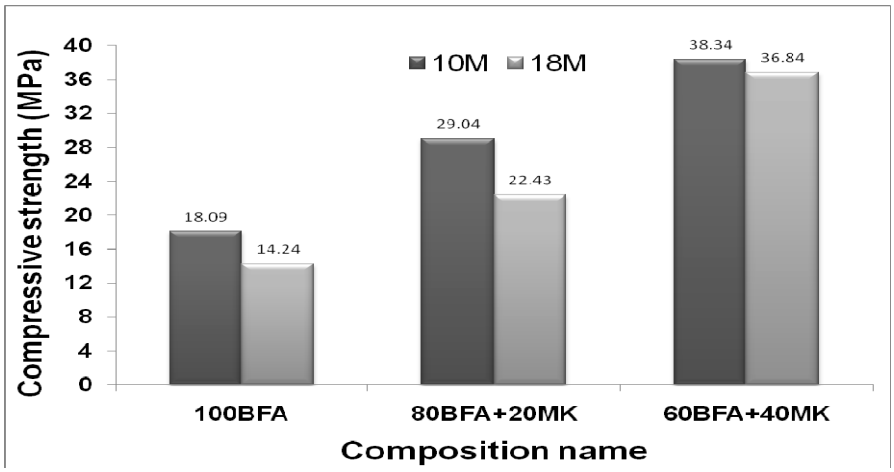

Figure 6.8. Compressive strength values of biomass fly ash metakaolin mortars

*** Average of 3 mortars (standard deviation ranging from 0.88 MPa-3.48 MPa)**

Concerning the components, four basic factors seem to be relevant in the development of the geopolymerization reaction: mineralogy, the relative percentage of silica and alumina, specific surface for reaction and morphology [Jaarsveld et al. 1997]. Some oxides (mainly SiO_2 and Al_2O_3) must follow some particular ratios in order to achieve the best results (Fernandez-Jimenez et al. 2004). Some researches consider that the ratios of the principal components, in the solid precursor, must be situated between 3.3 and 4.5 (SiO_2/Al_2O_3), 0.20 and 0.48 (Na_2O/SiO_2) and 0.8 and 1.6 (Na_2O/Al_2O_3) [Palomo et al. 2007, Lee & Van Deventer 2002, Carvalho et al. 2007]. Relative molar ratios of the mixture compositions tested are shown in Table 6.9. It can be noticed that the strength measurements increased when the SiO_2/Al_2O_3 ratio fell towards the middle of the suggested values agreeing with the earlier reports. The SiO_2/Al_2O_3 ratio of the 60BFA40MK was 3.39 and for 80BFA20MK the value was around 4.21 and the strength measurements increased values corresponding to it. However the ratio of Na_2O was lower in all the compositions though the biomass fly ash contributed a big portion in it. But this can be easily overtaken by the addition of sodium hydroxide and sodium silicate solution in the mix and it is the prime aim of adding alkali activators [Carvalho 2007].

Table 6.9. Relative molar mass ratios of the mixture compositions

Composition	*SiO_2/Al_2O_3*	*Na_2O/SiO_2*	*Na_2O/Al_2O_3*
100BFA	6.19	0.20	1.28
80BFA20MK	4.21	0.14	0.60
60BFA40MK	3.39	0.10	0.32

The formation of the three-dimensional amorphous geopolymeric gel with a general formula of $(Na/K)_m$–[[–Si–O_2]$_z$–Al–O]$_n$·$w$$H_2O$ (m is the alkaline element, z is 1, 2, or 3 and n is the degree of polycondensation) is often argued to be the phase that contributes to the binding property of geopolymeric gels. It is anticipated that if enough Ca is added to a geopolymeric system, some forms of C-S-H gel will be obtained instead. If the products are aluminosilicate network geopolymeric materials, the ratio of Si/Al should be 1, 2 or 3. The Si/Al ratios of 100BFA 80BFA20MK and 60BFA40MK are 6.18, 4.21 and 3.38 respectively. The products in these specimens could be not only geopolymeric gel but also hydrated products. Ca may have precipitated as $Ca(OH)_2$, bonded in geopolymers to obtain charge balance, or reacted with dissolved silicate and aluminate species to form C-S-H gel.

6.3.4.2 Microstructure and phase analysis

The X-ray diffraction patterns of the 10M 100BFA and 10M 60BFA40MK compositions with a alkali activator ratio of 2:1 (Na_2SiO_3: NaOH) after 10 days of curing are shown in Figure 6.9. The major components are Quartz and Calcite. A hump is observed around 20-35 º indicating the presence of the amorphous phases. Traces of calcium alumina silicates ($CaAl_2Si_2O_8.4H_2O$) and CSH were observed. It can be inferred from the X-ray Diffraction spectrum that the alkali activated biomass fly ash is a mixture of reacted and unreacted materials. Some of the soluble alkali silicates can react with the glassy phase of the fly ash to form poorly crystalline zeolithic phase too.

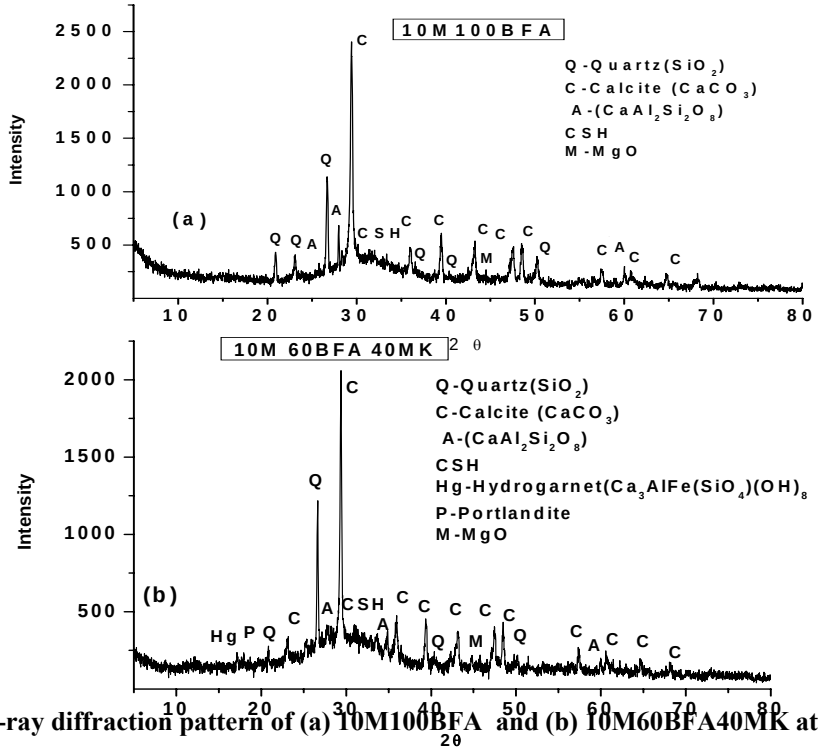

Figure 6.9. X-ray diffraction pattern of (a) 10M100BFA and (b) 10M60BFA40MK at 10 days of curing

Figure 6.10 shows the TG/DTA curves of the alkali reacted pastes of biomass fly ash and biomass fly ash –metakaolin blend after a heat treatment at 60 ºC. The main weight loss of the hydrated samples occurs between about 80 ºC and 250 ºC, corresponding to sodium aluminosilicate hydrates.

The activated high calcium fly ashes exhibit two more peaks in the relative weight loss curve up to 500°C. The second one is due to water loss of portlandite, that has formed in the pastes by hydration of free lime and the third peak can be observed above 500ºC, referring to CO_2-loss of calcite. On comparing the TG curves it could be seen that as the metakaolin increased the weight loss due to sodium aluminium silicate hydrate decomposition also increased, which in turn causes the strength increase. The strength determining phases are more abundant in the biomass fly ash – metakaolin blend because of the higher reactivity of metakaolin. The mechanical strength measurements done on the biomass fly ash –metakaolin samples confirm the same.

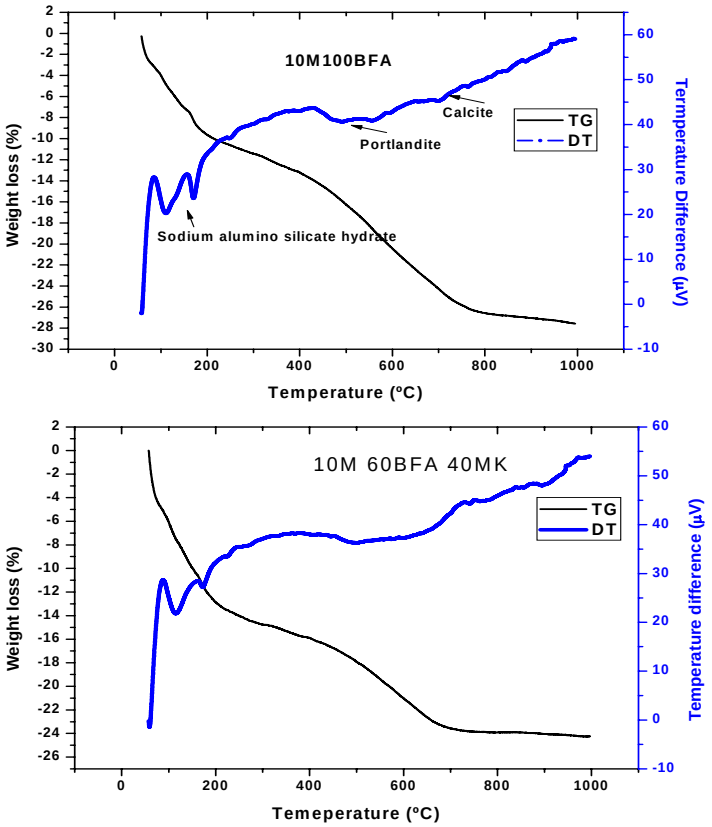

Figure 6.10 (a). TG/DTA curves of alkali activated biomass fly ash and biomass fly ash –metakaolin geopolymers.

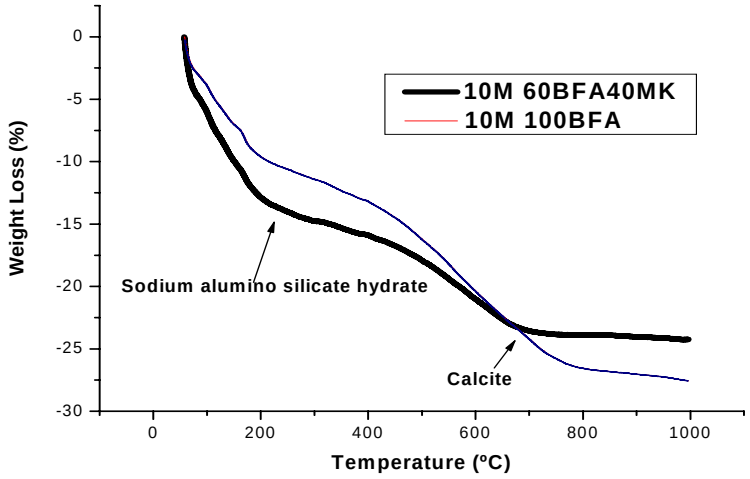

Figure 6.10 (b). TG curves of alkali activated biomass fly ash and biomass fly ash –metakaolin geopolymer-a comparison

Figure 6.11 lists the SEM images of freshly fractured surfaces of activated biomass fly ash and biomass fly ash metakaolin blend pastes. The structure of the activated 100% biomass fly ash system exhibits a loose connection of poorly dissolved fly ash particles compared to the biomass fly ash metakaolin blends. The comparatively poorly dissolved fly ash particles leading to high porosity of the gel-like matrix and the lacking connection is the reason for the low strengths of the activated biomass fly ash system where 100% biomass fly ash is used. In the case of biomass fly ash- metakaolin blends the matrix appears denser. The fly ash particles are well embedded and connected to the matrix. The SEM also demonstrates the good blending of biomass fly ash and metakaolin in the activated matrix which in turn leads to mechanical strength contribution.

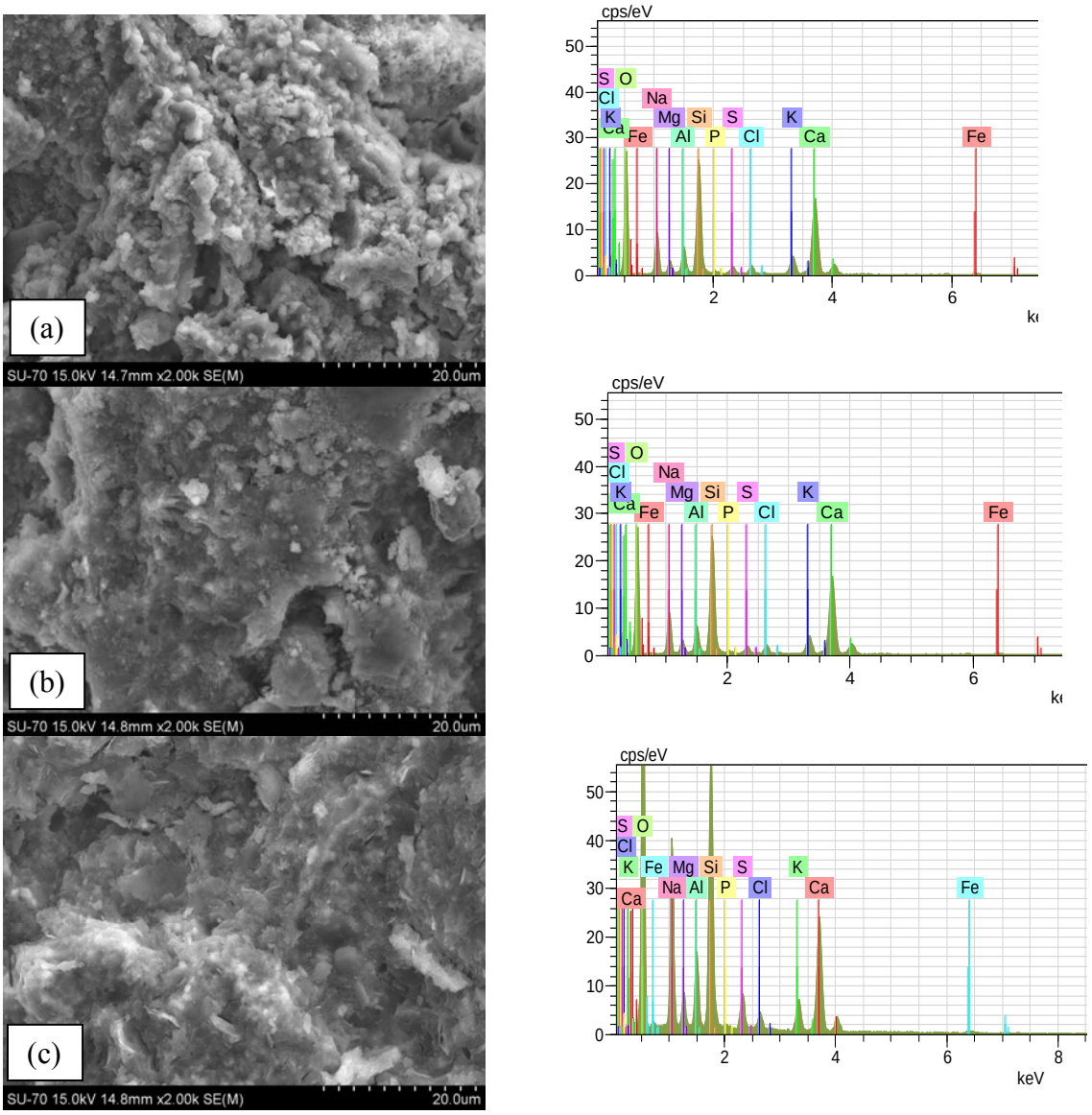

Figure 6.11. SEM picture of (a) 10M100BFA (b) 10M80BFA20MK and (c) 10M60BFA40MK

6.4. Summary

Lime mortars were prepared by replacing OPC with different amounts of biomass fly ashes (5%, 10%, 15% and 20% by weight of cement). It was observed that substitution of biomass fly for ashes in large amount in the system required more water. It was also observed that the mechanical strength decreased slightly with the increase in fly ash content. The pozzolanic effect of the biomass fly ashes was not significantly visible till the 28th day in the strength properties of the mortars. The strength measurement showed improvement on longer curing period, indicating the

secondary hydration of the biomass fly ashes inside the lime matrix. The porosity of the mortar specimens increased with increase in the substitution of biomass fly ashes. But the average pore diameter decreased with increase in the biomass fly ash content. Capillarity also decreased with increase in curing time.

Biomass fly ashes were subjected to alkali activation to observe their geopolymeric properties. Mortar samples were also prepared with fine sand to give structural stability. Different molar volumes of NaOH and sodium silicate solution were used for the preparation of alkali activators. Biomass fly ashes and mixtures of biomass fly ashes BFA2 and commercially available metakaolin ARGICAL 1200 were used as solid components. The biomass fly ashes were sieved at 75 μm in order to remove the coarse particles. It can be observed that strength of the biomass fly ash compositions increases with the increase in NaOH content. An increase in the amount of sodium silicate solution in the composition favours the strength of the compositions. The metakaolin incorporated samples showed a higher strength. The biomass fly ashes gave a compressive strength of 18MPa. The highest value was obtained for 40% metakaolin incorporated mortars where it got around 38 MPa. The biomass fly ash metakolin blend is working well in the geopolymeric application resulting in the contribution of both zeolithic and hydrated phases formation.

Possibilities are yet to be explored in a more detailed way to seek methods to use up the chemical richness of biomass fly ashes to the maximum. From current data it can be proposed that these complex binders can be widely utilized in various applications such as in building materials and solidification/stabilization materials.

CHAPTER 7. CONCLUSIONS AND FUTURE WORK

The present work has been conducted aiming at widening the knowledge of potential applications of biomass fly ash wastes (from forestry wood wastes) available in Portugal. The main objective was to study the possibility of using the biomass fly ashes in common building materials as an additive to mortars and concrete. The specific conclusions and the recommendation for the future work are listed below.

Conclusions from the characterization of biomass fly ashes.

1. Considering the variation in the physical chemical nature of the biomass fly ashes at different particle size ranges it was determined to sieve the biomass fly ashes through a 75 microns mesh for incorporating in cement matrix.
2. From the difference in the content of organic matter in the biomass fly ashes it could be concluded that the fluidized bed combustion appeared to be more efficient than the grate combustion.
3. Biomass fly ashes consisted of calcite and silica as the major minerals. Alkali salts, chlorides and sulphates were also present and the fly ashes showed weak pozzolanicity. They were similar to class C coal fly ashes. The leaching experiments proposed that these biomass fly ashes can be landfilled as nondangerous materials.

Conclusions from the biomass fly ash incorporation in cement based mortars and the durability tests.

1) Biomass fly ashes containing mixtures demanded more water to attain the desirable workability. The use of superplasticizer is necessary for controlling the water requirement.
2) The setting time was delayed on increasing the biomass fly ash content in the mortars.
3) The amount of hydrating materials decreased with the increase in the biomass fly ash content in cement mortar matrix.
4) Mortars incorporating 10% and 20% biomass fly ashes exhibited around 90-95% of mechanical strength with respect to the reference mortar at an age of one year of curing.
5) The $Ca(OH)_2$ evolution determined up to a curing age of 2 years in the biomass fly ash cement pastes indicated the pozzolanic/latent hydraulic character of the ashes.
6) It is recommended that biomass fly ashes should be used in lesser amount (<20 wt%) in replacing cement for the production of quality cement based materials.

7) ASR mitigation test proved that the biomass fly ash incorporated mortars lowered the expansion reaction in cement/concrete mortars compared to the reference mortar properties. Blending of biomass fly ash with metakaolin (20%BFA + 10%MK) resulted into the effective mitigation of ASR.

8) Formulations containing <10 wt% biomass fly ashes showed lower expansion values due to the external sulphate reaction in comparison to the reference cement mortar.

9) 30 wt% BFA2 replaced concrete showed an effective lower expansion in the internal sulphate reaction test.

Conclusions from the alternative applications of biomass fly ashes

1) The specific characteristics of biomass fly ash particles are not favouring the application in lime mortars. The use of biomass fly ash did not affect the mortar properties, namely the mechanical strength, in the initial curing period although improved them at longer curing ages. However, the carbonation was enhanced in 15-20 wt% biomass fly ash replaced lime mortars.

3) The alkali activation of biomass fly ashes and metakaolin blends produced high strength mortars with no OPC cement. This achievement was observed in a very preliminary study, a deeper investigation should be conducted in the future to explore this promising finding.

Future work on the characterization of biomass fly ashes.

1) On the basis of characterization tests, a guideline in terms of combustion conditions is to be recommended to the thermal power plants in order to enhance the quality of the production of biomass fly ashes for applications in construction materials in a cost effective and environmentally friendly way. Collection and sampling the fly ashes in a representative and constant manner should also be detailed.

Future work for the biomass fly ash incorporation in cement based mortars and the durability tests.

1) The durability tests need to be expanded to the areas of drying shrinkage, permeability, carbonation reactions for biomass fly ash incorporated cement mortars.

2) Biomass fly ash incorporated concretes are to be investigated in the real time scenario to verify the effect of biomass fly ashes against expansive phenomena.

3) It is recommended to explore further the possibility of using biomass fly ashes with other pozzolanic materials (in terms of binary, ternary blends), in order to explore the scope of using these biomass fly ashes in enhancing the mortar/concrete quality.

Future work on the alternative applications of biomass fly ashes.

1) The applications in lime and alkali activated binders should be investigated in detail in terms of microstructural analysis to expand the knowledge of the actual contribution of biomass fly ashes.
2) Considering the specific physical characteristics (high surface area, fine particle size distribution etc) of the biomass fly ashes, it is recommended to try these ashes for other alternative applications such as in industrial catalysts and adsorbents.

All the more, the incorporation of fly ashes in the construction material shows definitive advantages in the environment and contributes to different parameters of sustainability. The potential of biomass fly ashes in terms of CO_2 reduction and the cost effectiveness that benefits the cement production and the nation should be estimated based on the studied recycling ways applied on the biomass fly ashes.

REFERENCES

Abdullahi M., "Characteristics of Wood ASH/OPC Concrete", *Leonardo Electronic Journal of Practices and Technologies*, 89-16, 2006.

Aberg A., Kumpiene J., Ecke H., "Evaluation and prediction of emissions from a road built with bottom ash from municipal solid waste incineration (MSWI)". *Sci. Total. Environ.* 355, 1-12, 2006.

Ahmaruzzaman M., "A reviewon the utilization of fly ash", *Progress in Energy and Combustion Science*, 36, 327–363, 2010.

Aiqin Wang, Chengzhi Zhang and Wei Suna, "Fly ash effects: II. The active effect of fly ash", *Cement and Concrete Research*, 34(11), 2057-2060, 2004.

Akhmad Zaenia, Sri Bandyopadhyaya, Aibing Yua, John Ridera, Chris S. Sorrella, Stephen Dainb, Daryl Blackburnc and Chris Whitec, "Colour control in fly ash as a combined function of particle size and chemical composition", *Fuel*, 89,2, 399-404, 2010.

Alonso S. and Palomo A., "Alkaline activation of metakaolin-calcium hydroxide solid mixtures: Influence of temperature, activator concentration and metakaolin /$Ca(OH)_2$ ratio", *Materials Letters*, 47, 55-62, 2001.

Andrea Johnson, Lionel J.J. Catalan, Stephen D. Kinrade "Characterization and evaluation of fly-ash from co-combustion of lignite and wood pellets for use as cement admixture", *Fuel* 89, 3042–3050, 2010.

Anjan K. Chatterjee, "Indian Fly Ashes: Their Characteristics and Potential for Mechanochemical Activation for Enhanced Usability*" J. Materials in Civ. Eng*. 23, 783, 2011.

Antiohos S.K., Papageorgiou A, Papadakis V.G., Tsimas S. "Influence of quicklime addition on the mechanical properties and hydration degree of blended cements containing different fly ashes", *Constr Build Mater*, 22, 1191–200, 2008.

Arandigoyen, M. and Aalvarez, J.I., "Pore structure and mechanical properties of cement-lime mortars", *Cement and Concrete Research*, 37, 767-775, 2007.

Athene M. McDonald : *Materials World*,6 (7), 99-401, 1998.

Aubert J.E., Husson B., Sarramone N., "Utilization of municipal solid waste incineration (MSWI) fly ash in blended cement. Part 1: Processing and characterization of MSWI fly ash," *J. Hazard. Mater.*, 136, 624-631, 2006.

Aubert J.E., Husson B., Vaquier A., "Use of municipal solid waste incineration fly ash in concrete", *Cem. Concr. Res*., 34, 957-963, 2004.

Badogiannis E., Kakali G.and Tsivilis S., "Metakaolin as supplementary cementitious material: Optimization of kaolin to metakaolin conversion", *Journal of Thermal Analysis and Calorimetry*, .81, 457–462, 2005.

Bakolas A., Aggelakopoulou E. and Moropoulou A., "Evaluation of pozzolanic activity and physico-mechanical characteristics in ceramic powder-lime pastes", *J. Therm. Anal. Calorim.* 92 (1), 345–351, 2008.

Banfill P.F.G., "The rheology of fresh cement and concrete – a review", *Proc 11th International Cement Chemistry Congress*, Durban, May 2003.

Barbosa V.F., MacKenzie K.J., Thaumaturgo C., "Synthesis and characterisation of materials based on inorganic polymers of alumina and sı´lica: sodium polysialate polymers", *Int J Inorg Polym*; 2:309–17, 2000.

Barry E. Scheetz, and Russell Earle, "Utilization of fly ash, Current Opinion in Solid State and Materials Science", 3-5,510-520,1998.

Bentur A.,"Cementitious Materials-Nine Millennia and A New Century: Past, Present and Future", *Journal of Materials in Civil Engineering*, 14, 1-22, 2002.

Bhatty M.S.Y., Greening N.R., "Interaction of alkalis with hydrating and hydrated calcium silicates., *Proceedings of the Fourth International Conference on the Effects of Alkalis in Cement and Concrete*, Purdue, 87–112, 1978.

Bijen J., "Benefits of slag and fly ash", *Construction and Building Materials,* 10, 309-314,1996.

Biricik H., Akoz F., Berktay I., Tulgar A.N., "Study of pozzolanic properties of wheat straw ash", *Cem Concr Res.* 29, 637– 43, 1999.

Bouzouba N., Zhang M.H., and Malhotra V.M., "Mechanical properties and durability of concrete made with high-volume fly ash blended cements using a coarse fly ash", C*ement and Concrete Research*, 3:1393-1402.2001.

Bridgeman T.G, Darvell L.I., Jones J.M., Williams P.T., Fahmi R., Bridgewater A.V., "Influence of particle size on the analytical and chemical properties of two energy crops", *Fuel*, 86,60–72, 2007.

Bruder-Hubscher C., Lagarde F., Leroy M.J.F., Couganowr C., Enguehard F., "Utilisation of bottom ash in road construction: Evaluation of the environmental impact", *Waste Manag. Res.*, 19:545-556, 2001.

Bui D.D., Hu J, Stroeven P, "Particle size effect on the strength of rice husk ash blended gap-graded Portland cement concrete". *Cement & Concrete Composites,* 27,357–366, 2005.

Cabrera J.G., and Lynsdale C.J., "The effect of superplasticisers on the hydration of normal Portland cement", *Proceedings of the international conference on Advances in Concrete Technology*, Las Vegas (USA),741-751. 1995.

Campbell A.G., "Recycling and disposing of wood ash". *TAPPI Journal* 73 (9), 141–143, 1990.

Chandrasekhar S., Satyanarayan K.G., Pramada P.N. and Raghavan P. "Review processing, properties and applications of reactive silica from rice husk—an overview". *Journal of Materials Science (Norwell)*, 38(15),3159 – 3168, 2003.

Charles H.K. Lam Alvin W.M. Ip, John Patrick Barford and Gordon McKay, "Use of Incineration MSW Ash: A Review", *Sustainability*, 2, 1943-1968, 2010.

Charlwood R.G., “A Review of Alkali-Aggregate Reaction in Hydro Plants and Dams”, *International Journal on Hydropower and Dams*, 73-80, 1994.

Cheah Chee Ban and Mahyuddin Ramli, “The implementation of wood waste ash as a partial cement replacement material in the production of structural grade concrete and mortar: An overview”, *Resources conservation and recycling* 55, 669-685, 2011.

Cheerarot R., and Jaturapitakkul C., “A study of disposed fly ash from landfill to replace Portland cement”, *Waste Management*, 24, 701-709, 2004.

Chiara F. Ferraris, Karthik H. Obla, Russel Hill, “The influence of mineral admixture on the rheology of cement paste concrete”, *Cement and Concrete Research*, 31, 245.255, 2001.

Chiaverini, J., “Metakaolin–lime mortars: a replica of Genoese ‘porcellana’ as amortar for restoration”. *Proceedings of the second Swiss Geoscience Meeting*, Laussanne. 2004.

Chopra S.K., Ahluwalia S.C., Laxmi S., “Technology and manufacture of rice-husk ash masonry (RHAM) cement”, *Proceedings of ESCAP/ RCTT Workshop on Rice-Husk Ash Cement*, NewDelhi, 1981.

Christoph T. W., “Influence of Lecithin on Structure and Stability of Parenteral Fat Emulsions”,PHD thesis, Department of Pharmaceutics at the University of Erlangen-Nuernberg.

Chu, S.C. and Kao, H.S. “A Study of Engineering Properties of a Clay Modified by Fly Ash and Slag,” *Fly Ash for Soil Improvement-Geotechnical Special Publication*, 36, 89-99. 1993.

Cockrell C.F. and Leonard J.W. “Characterization and Utilization Studies of Limestone Modified Fly Ash,” *Coal Research Bureau*, 60., 1970.

Collepardi M., "A Holistic Approach to Concrete Durability - Role of Superplastiziers", Infrastructure Regeneration and Rehabilitation. Improving the Quality of Life through Better Construction. A Vision for the Next Millennium, Sheffield,15-25. 1999.

COM, Communication from the commission, Biomass Action Plan 628, 2005.

Cook J.E., “Research and application of high strength concrete using class C fly ash”, *Concrete International* 4, 72–80,1982.

Cordeiro G.C., Toledo Filho R.D., Tavares L.M., Fairbairn E.M.R. “Pozzolanic activity and filler effect of sugar cane bagasse ash in Portland cement and lime mortars,” *Cem. Conc. Comp,* 30, 410–8, 2008.

Curtis D.D., “A Review and Analysis of AAR-Effects in Arch Dams”, P*roceedings of the 11th International Conference on Alkali-Aggregate Reaction*, Centre de Recherche Interuniversitaire sur le Beton, Universite Laval, Quebec, Canada, 2000.

Davidovits J., “Chemistry of geopolymeric systems. Terminology”, *Proceedings of 99 geopolymer conference*, 1, 9–40. 1999.

Davidovits J., “Geopolymer chemistry and sustainable development. The poly(sialate) terminology: a very useful and simple model for the promotion and understanding of green chemistry.” Proceedings of 2005 geopolymer conference, 1, 9–15, 2005.

Davies G. and Oberholster R.E., "Alkali-Silica Reaction Products and Their Development."*Cement and Concrete Research,* 18, 621-635.

Delgado Rodrigues, M. Erdik, I. Siotis and S. Zoppi, Editors, Compatible Materials for the Restoration of European Cultural Heritage, Pact 58, 81–103m, 2000.

Decreto-Lei n.º183/2009. Portuguese legislation about waste in landfill.

Della V.P., Kuhn I., Hotza D., "Rice husk ash as an alternate source for active silica production". *Materials Letters*, 57, 818–821, 2002.

Demirbas A., "Potential applications of renewable energy sources, biomass combustion problems in boiler power systems and combustion related environmental issues", *Prog. Energy Combust. Sci*. 31,171–192. 2005.

Dent Glasser L.S. and Kataoka N.,"The chemistry of alkali-aggregate reactions." *Proceedings of the 5th International Conference on Alkali-Aggregate Reaction*, Cape Town, S252/23., 1981.

Detphan P Chindaprasirt, "Preparation of fly ash and rice husk ash geopolymer", *International Journal of Minerals Metallurgy and Materials* 16, 6, 720-726, 2009.

Detwiler R.J, "Substitution of fly ash for Cement or Aggregate in concrete: Strength Development and suppression of ASR", *Portland Cement Association Research and Development Bulletin*, RD 127, 2002.

Dhir R.K., Jones M.R. "Development of chloride-resisting concrete using fly ash", *Fuel*, 78:137–42, 1999.

Diamond S., "The utilization of fly ash Cement and Concrete Research", 14, 4, 455-462, 1984.

Diamond S. "ASR-Another look at mechanism." *Proceedings of the 11th International Conference on Alkali-Aggregate Reaction*. I<yoto (Japan), K. Okada, S. Nishibayashi, and M Kawamura, Editors, 83-94, 1989.

Diamond S., Barneyback R.S. & Struble L.J., "On the physics and the chemistry of alkali-silica reaction". *5th ZCAAR*, Cape Town, South Africa, S 252122, 1981.

Dias A.C., Carvalho C., "Composting as a process of material valorisation of industrial and forest wastes", Licentiate Thesis in Environmental Engineering (in Portuguese), Department of Environment and Planning, University of Aveiro, Portugal, 2008.

Docter B.C, "Using Class C fly ash to mitigate Alakli Silica Reactions in concrete", *2009 World of Coal Ash (WOCA) Conference*, Lexington, KY, USA, 2009.

Donatello S., Tyrer M., Cheeseman C.R, "Comparison of test methods to assess pozzolanic activity", *Cement & Concrete Composites*, 32,121–127, 2010.

Dunstan E.R., "Possible Method of Identifying Fly Ashes That Will Improve Sulfate Resistance." *Cement, Concrete, and Aggregates*. 2(1). PA, 1980.

Eleni Aggelakopouloua, Asterios Bakolasa, and Antonia Moropouloua, "Properties of lime metakaolin mortars for the restoration of historic masonries", *Applied Clay Science*, 53(1), Pages 15-19, 2011.

Elinwa A.U., Ejeh S.P., "Effects of incorporation of sawdust incineration fly ash in cement pastes and mortars", J *Asian Architecture Build Eng*, 3(1),1-7, 2004.

Elinwa A.U., Mahmood Y.A., "Ash from timber waste as cement replacement material", *Cem.Concr Composites*, 24,219-22, 2002.

Etiegni L., Campbell A.G., "Physical and chemical characteristics of wood ash", *Bio resource Technology, Elsevier Science Publishers Ltd*., 37 (2), 173–178, 1991.

Etiegni L, Wood ash recycling and land disposal. Ph.D. Thesis, Department of Forest Products, University of Idaho at Moscow, Idaho, USA, 174, 1990.

European List of Wastes, Commission Decision 2000/532/EC of 3 May 2000,amended by the Commission Decision 2001/118/EC, Commission Decision 2001/119/EC and Council Decision 2001/573/EC.

Fallot A. and Girard P., "Spatial assessment of biomass potentials for energy scenarios", *Proceedings of the 14th European Biomass Conference & Exhibition*, *October 2005*, Paris, France, ETA-Renewable Energies, Italy,104–107, 2005.

Farbiarz J., Carrasquillo R., et al., "Alkali-Aggregate Reaction in Concrete Containing Fly Ash", *7th International Symposium of Alkali Aggregate Reaction in Concrete,* Ottawa, Canada, 1986.

Federal Highway Administration (FHWA). Long-Term Plan for Concrete Pavement Research and Technology - The Concrete Pavement Road Map: Volume II, Tracks. HRT-05-053. FHWA, Washington, DC. 2005.

Fehrs J.E, "Ash from the combustion of treated wood: characterization and management options". "The National Bioash Utilization Conference", Portland, ME, 20. 1996.

Fernandez-Jimenez A., Palomo A., "Characterisation of fly ashes Potential reactivity as alkaline cements", *Fuel*, 822259–65. 2003.

Fortes-Revilla, Martinez-Ramirez S. and Blanco-Varela M.T., "Modelling of Slaked lime–metakaolin mortar engineering characteristics in terms of process variables", *Cem. Concr. Comp*. 28 (5) , 458–467, 2006.

Forteza R., Far M., Seguí C., Cerdá V., "Characterization of bottom ash in municipal solid waste incinerators for its use in road base", *Waste Management*, 24: 899-909. 2004.

Fournier B., Nkinamubanzi P.C., Lu D., Thomas M.D.A., Folliard, K.J., and Ideker J.H. "Evaluating potential alkali-reactivity of concrete aggregates: how reliable are the current and new test methods?" In: Fournier, B (editor): Marc-André Bérubé Symposium on alkali-aggregate, 2006.

Francois D. and Pierson K., "Environmental assessment of a road site built with MSWI residue", *Sci. Total. Environ.* 407, 5949-5960, 2009.

Ganesan K., Rajagopal K., Thangavel K., "Evaluation of bagasse ash assupplementary cementitious material", *Cem Concr Comp* , 29,515–24, 2007.

Gao P., Lu X., Lin H., Li X., Hou J., "Effects of fly ash on the properties of environmentally friendly dam concrete", *Fuel*, 861, 208–11, 2007.

Ghassan Abood Habeeb, Hilmi Bin Mahmud, **"**Study on Properties of Rice Husk Ash and Its Use as Cement Replacement Material", *Materials Research.*; 13(2): 185-190, 2010.

Glasser F.P., "Chemistry of the alkali-aggregate reaction", in: SwamyR.N. (Ed.), *The Alkali-Silica Reaction in Concrete*, Blackie, London, 96–121, 1992.

Glasser F.P., Marr J., "The alkali binding potential of OPC and blended cements", *Cemento*, 82, 85–94, 1985.

Gómez-Barea, A., Vilches, L.F., Leiva, C., Campoy, M., Fernández-Pereira, C. "Plant optimisation and ash recycling in fluidised bed waste gasification", *Chemical Engineering Journal*, 146,227-236, 2009.

Good, J., Nussbaumer, T., Delcarte, J. and Schenkel, Y. "Methods for efficiency determination for biomass heating plants and influence of operation mode plant on efficiency", in *Proceedings of the 2nd World Conference and Exhibition on Biomass for Energy, Industry and Climate Protection*, May, Rome, Italy, Volume II, ETA-Florence, Italy 1431–1434, 2004.

Górecka, H., Chojnacka, K., Górecki, H. "The application of ICP-MS and ICP-OES in determination of micronutrients in wood ashes used as soil conditioners", *Talanta*, 70,950-956, 2006.

Hardjito D, "The use of fly ash to reduce the environmental impact of concrete", *Proceedings of EnCon2007,* 1st Engineering Conference on Energy & Environment, Kuching, Sarawak, Malaysia, ENCON2007-101, December 27-28, 2007.

Hasan Biricik, "Resistance to magnesium sulfate and sodium sulfate attack of mortars containing wheat straw ash", Fevziye Aköz, Fikret Türker and Ilhan Berktay, *Cement and Concrete Research*, 30, 8, 1189-1197, 2000.

Haslinger W., Padinger R., Wörgetter M. And Spitzer J. "Austrian research and development of novel solid biofuels and innovative small-scale biomass combustion systems", *2nd World Conference and Exhibition on Biomass for Energy, Industry and Climate Protection*, 10–14 May, Rome, Italy, 2004.

He Z. and Li Z.J., "Non-contact resistivity measurement for characterisation of the hydration process of cement-paste with excess alkali", *Advances in Cement Research*, 16(1), 29–34, 2004.

Helmuth, Richard A., "Fly ash in cement and concrete", *SP040T*, Portland Cement Association.203, pages, 1987.

Hong S.Y., Glasser F.P, "Alkali sorption by C–S–H and C–A–S–H gels Part II Role alumina", *Cement Concr. Res.*, 32, 1101–1111, 2002.

Huang, W.J.; Chu, S.C. "A study on the cementlike properties of municipal waste incineration ashes", *Cem. Concr. Res.*, 33, 1795-1799. 2003.

Hwang C.L., Wu D.S., "Properties of cement paste containing rice husk ash", *American Concrete Institute* SP, 114, 733–765, 1989.

Hwang K.R., Noguchi T., Tomosawa F. “Effects of fine aggregate replacement on the rheology, compressive strength and carbonation properties of fly ash and mortar.” *ACI Special Publication* ,401–10. SP-178, 1998.

Jaarsveld J.G.S., Deventer J.S.J., Lukey G.C., “The characterisation of source materials in fly ash-based geopolymers”. *Mater Letts* 1272–80, 2003.

Jaturapitakkul C,, Roongreung B., “Cementing material from calcium carbide residue-rice husk ash”, *Journal of Materials in Civil Engineering* 15 (5) 470–475, 2003.

Jawed I., Skalny J., Bach T., Schubert P., Bijen J., Grube H., Nagataki S., Ohga H., and Ward M.A., “Hardened mortar and concrete with fly ash, RILEM Report, Fly Ash in Concrete: Properties and Performance”, Wesche, K (Ed.). 1991,

Johansson l.S., Leckner B., Gustavsson L., Cooper D., Tullin C., Potter A., and Berntsen, M “Particle emissions from residential bio fuel boilers and stoves – old and modern techniques’, *Proceedings of the International Seminar ‘Aerosols in Biomass Combustion’*, March, Graz, Austria, Volume 6 of Thermal Biomass Utilization series, bios bioenergie systeme, GmbH, Graz, Austria, 145–150, 2005.

Joshi R.C., Lothia R.P., “Fly ash in concrete: production, properties and uses. In: Advances in concrete technology”, vol. 2. Gordon and Breach Science Publishers, 1997.

Kastner JR, Miller J, Kolar P, Das KC., “Catalytic ozonation of ammonia using biomass char and wood fly ash”. *Chemosphere,* 75(6):739-44, 2009.

Komatska S.H. and Panarese W.C., “Design and Control of Concrete Mixtures”, PCA, 1988.

"Lea’s chemistry of cement and concrete. 4th ed. Peter C. Hawlett, Elsevier science and technology books; 2004.

Leslie J. Strublea, and Wei-Guo Leib, “Rheological changes associated with setting of cement paste”, *Advanced Cement Based Materials*, 2(6),224-230, 1995.

Lewandowski I., Clifton-Brown J.C., Scurlock J.M.O., Huisman W., Miscanthus:”European experience with a novel energy crop”, *Biomass Bioenerg*, 19, 209–217, 2000.

Loo S.V. and Koppejan J., “The Handbook of Biomass Combustion and Co-firing”, ISBN: 978-1-84407-249-1,22883, Quicksilver Drive, Sterling, VA 20166-2012, USA,2008.

Luciano Senff, João A Labrincha, Victor M Ferreira, Dachamir Hotza, Wellington L Repette, **“**Effect of nano-silica on rheology and fresh properties of cement pastes and mortars”, *Construction and Building Materials* 23(7), 2487-2491, 2009.

Luciano Senff , Pedro A. Barbetta , Wellington L. Repette , Dachamir Hotza , Helena Paiva , Victor M. Ferreira, João A. Labrincha, “Mortar composition defined according to rheometer and flow table tests using factorial designed experiments”, *Construction and Building Materials* 23, 3107–3111, 2009.

Lupu C., Jackson K. L, Bard S, Irene R, Barron A. R. “Control over cement setting through the use of chemically modified fly ash”, A*dv Eng Mater*, 8,576–80, 2006.

Malhotra V.M (Ed.), “Durability of Concrete, American Concrete Institute”, *Proceedings of the 2nd CANMET/ACI International Conference on Detroit*, 919–940, 1991.

Malhotra V.M. “Making concrete ‘greener’ with flyash”, *Concrete International.* Farmington Hills,21(5), 61-66, 1999.

Malvar L.J., et. al., “Alkali-silica Reaction Mitigation – State-of-the-art”, Technical Report TR-2195-SHR, Naval Facilities Engineering Service Centre, Port Hueneme, Calif., United States, 2001.

Martirena J.F., Middendorf B., Gehrke M., Budelmann H., “Use of wastes of sugar industry as pozzolana in lime-pozzolana binders: study of the reaction”. *Cem Concr Res*., 28:1525–36, 1998.

Marutzky R. and Seeger k. Energie aus holz und anderer biomasse“, drw-verlagWeinbrenner, Leinfelden-Echtlingen, Germany, 1999.

Masiá A.A.T, Buhre B.J.P., Gupta R.P.,. Wall T.F, “Characterising ash of biomass and waste”, *Fuel Processing Technology*, 88 1071–1081. 2007.

Mehta P.K. “Effect of fly ash composition on sulfate resistance of cement.” *J Am Concr Ins,.* 83(6). 994, 1986.

Mehta P.K., “Rice husk ash – a unique supplementary cementing material”, *Proceedings of the International Symposium on Advances in Concrete Technology*, Athens, Greece, 407–430, 1992.

Mehta P.K., “The chemistry and technology of cement made from rice husk ash”, *Proceedings UNIDO/ESCAP/RCTT*, Workshop on Rice Husk Ash Cements, Peshawar, Pakistan, January. Regional Centre for Technology Transfer, Bangalore (India), 113–22, 1979.

Mehta P.K., "Sulfate Attack on Concrete - A Critical Review", Materials Science of Concrete III, *The American Ceramic Society*, 105-130, 1993.

Mehta P.K., “Mechanism of Sulfate Attack on Portland Cement Concrete – Another Look”, *Cement and Concrete Research,*13(3), 401-406,1983.

Merckx B., Good J. and Delcarte, J., “Evaluation of uncertainties of a wood chips boiler yield”, *Proceedings of the 14th European Biomass Conference and Exhibition*, October, Paris, France, ETA-Renewable Energies, Italy, 1347–1348, 2005.

Mishra M.K., Ragland K.W., Baker A.J., “Wood ash composition as a function of furnace temperature”. *Biomass and Bioenergy*, Pergamon Press 4 (2): 103–116, 1993.

Mishulovich A., “Alternative materials”, *International Cement Review*, 59-62, 2003.

Mukherjee A. B., Zevenhoven R., Bhattacharya P., Sajwan K. S., Kikuchi R. “Mercury flow via coal and coal utilization by-products: a global perspective”. *Resour Conserv Recycl*; 52(4):571–91, 2008.′

Musil B., Hofbauer H., and SchiffertT., “Development and analyses of pellets fired tiled stoves”, *Proceedings of the 14th European Biomass Conference & Exhibition*, October, Paris, France, ETA-Renewable Energies, Italy, 1117–1118. 2005.

Naik T.R. , Ramme B.W., Tews J. H. “Use of high volumes of class C and class F fly ash in concrete”. *Cem Concr Aggreg,* 16:12–20., 1994.

Naik T.R., Singh S.S., Ramme B.W.” Mechanical properties and durability of concrete made with blended fly ash”, *ACI Mater* J 95:454–62, 1998.

Naik TR, “Tests of wood ash as a potential source for construction materials”. Report No. CBU-1999-09, UWM Center for By-Products Utilization, Department of Civil Engineering and Mechanics, University of Wisconsin-Milwaukee, Milwaukee, pp. 61,1999.

Naik T.R., Kraus R.N., Siddique R,. “CLSM containing mixtures of coal ash and a new pozzolanic material”., *ACI Materials Journal* 100 (3): 208–215, 2003.

Nair D., Fraaij A., Klaassen A. and Kentgens A. “A. structural investigation relating to the pozzolanic activity of rice husk ashes”, *Cement and Concrete Research* (Elmsford), 38(6):861-869, 2008.

NCASI, National Council for Air and Stream Improvement, Inc., “Alternative management of pulp and paper industry solid wastes”, Technical Bulletin No. 655, *NCASI*, New York, NY, pp. 44, 1993.

Nehdi M., Duquette J., Damatty A.E.l. “Performance of rice husk ash produced using a new technology as a mineral admixture in concrete. *Cement and Concrete Research* 33: 1203–1210, 2003.

Nuntachai Chusilp, Chai Jaturapitakkul , Kraiwood Kiattikomol, “Utilization of bagasse ash as a pozzolanic material in concrete”, *Construction and Building Materials*, 23, 3352–3358, 2009.

Nussbaumer T., (Verbrennung und Vergasung von Energiegras und Feldholz, Jahresbericht 1992 zum gleichnamigen Forschungsprojekt, Bundesamt für Energiewirtschaft, Bern, Switzerland. 1993.

Obernberger I, Biedermann F.,Widmann W., Riedl R., “Concentrations of inorganic elements in biomass fuels and recovery in the different ash fractions”, *Biomass and Bioenergy* 12, 211–224, 2007.

Obernberger I. and Thek G. “The current state of Austrian pellet boiler technology”, *Proceedings of the 1st World Conference on Pellets*, September, Stockholm, Sweden, Swedish Bioenergy Association, Stockholm, Sweden, pp45–48, 2002.

Obernberger I. Nutzung fester, „Biomasse in Verbrennungsanlagen unter besonderer Berücksichtigung des Verhaltens aschebildender Elemente“, Volume 1 of *Thermal Biomass Utilization series*, BIOS, Graz, Austria, dbv-Verlag der Technischen Universität Graz, Graz, Austria, 1997.

OECD/IEA publications, “Control and minimisation of coal fired power plant emission”, Rue André-Pascal, 75775 Paris Cedex 16, France, 2003.

Oner A., Akyuz S., Yildiz R. “An experimental study on strength development of concrete containing fly ash and optimum usage of fly ash in concrete” *Cem Concr Res*, 35:1165–71, 2005.

Oscar E. Manz, Coal Fly Ash: “A Retrospective and Future Look”, *Energia*, 9(2), 1998.

Ou E., Xi Y., and Corotis, R., M. ASCE, "The Effect Of Rice Husk Ash On Mechanical, Properties Of Concrete Under High Temperatures", *18th Engineering Mechanics Division, Conference (EMD 2007),* 2007.

Pacheco-Torgal, Joa˜o Castro-Gomes, Said Jalali, "Alkali-activated binders: A review. Part 2. About materials and binders manufacture" Fernando Construction and Building Materials 22 1315–1322, 2008.

Palomo A., Grutzek M.W., Blanco M.T. "Alkali-activated fly ashes. A cement for the future", *Cem Concr Res*; 29:1323–9. 1999.

Palomo A., Fernández-jiménez A., Kovalchuk g. ordoñez L.M.. and Naranjo M.C., "OPC-Fly Ash cementitious system. Study of the gel binders produced during alkaline hydration" *J. Materials Science*, 42, pp.2958-2966, 2007,

Paiva, H. Esteves, L.P,Cachim, B. FerreiraV. M.. "Rheology and hardened properties of single-coat render mortars with different types of water retaining agents", *Construction and Building Materials,* 23(2): 1141-1146, 2009.

Pan, J.R. Huang, C. Kuo, J.J. Lin, S.H. "Recycling MSWI bottom and fly ash as raw materials for Portland cement", *Waste Manag*. 28, 1113-1118, 2008.

Papayianni, "The longevity of old mortars", *Appl. Phys. A,* 83, 685–688,2006.

Pauri, M. and Collepardi M., "Thermo-hygrometrical Stability of Thaumasite and Ettringite", Il *Cemento*,.86, 177-184. 1989,

Paya J., Monzo J., Borrachero MV, Pinzon D.L., Ordonez L. M., "Sugarcane bagasse ash (SCBA): studies on its properties for reusing in concrete production", *J Chem Tech Biotech;*, 77(3):321–5, 2002.

Pengthamkeerati P., Satapanajaru T., Singchan O., "Sorption of reactive dye from aqueous solution on biomass fly ash", *Cement and Concrete Research* 13, pp. 401-406.1983.

Pierre Adamiec., Jean-Charles Benezet and Ali Benhassaine, "Pozzolanic reactivity of silico-aluminous fly ash", *Particuology*, 6, 2, 93-98, 2008.

Puvvadi V. Sivapullaiah1 and Arif Ali Baig Moghal, "Role of Gypsum in the Strength Development of Fly Ashes with Lime", *J. Mater. Civ. Eng.*, 197, 2011.

Ranc, R, and Debray, L, "Reference test methods and a performance criterion for concrete structures". In: Poole, AB (editor): *Proceedings of the 9th International Conference on Alkali-Aggregate Reaction in Concrete*. Concrete Society, Publication CS.104 (1): 110-116. 1992.

Rashid, R.A.; Frantz, G.C., "MSW incinerator ash as aggregate in concrete and masonry". *J. Mater. Civ. Eng.*, 4, 353-368, 1992.

Reis, M. O. B., A. S. Silva, et al. "AAR in Portuguese Structures. Some Case Histories". *10th International Symposium of Alkali Aggregate Reaction in Concrete*, Melbourne, Australia, 1996.

Regourd, M. and H. Hornain, "Microstructure of Reaction Products". *7th International Symposium of Alkali Aggregate Reaction in Concrete*, Ottawa, Canada, 1986.

Rejini Rajamma, Richard J Ball, Luís A C Tarelho, Geoff C Allen, João A Labrincha, Victor M Ferreira, "Characterisation and use of biomass fly ash in cement-based materials.", J*ournal of Hazardous Materials*, 172, 2-3, 1049-1060, 2009.

Remond S.P., Pimienta P. and. Bentz D.P, "Effects of the incorporation of municipal solid waste incineration fly ash in cement pastes and mortars. I. Experimental study", *Cement and Concrete Research* 32, 303–311, 2002.

Renewable energy in Portugal, Communication from the Portuguese Ministry of Economy and Innovation, 2007.

Ribeiro, A.S.M., Monteiro, R.C.C., Davim, E.J.R., Fernandes, M.H.V "Ash from a pulp mill boiler – Characterisation and vitrification", in: *Journal of Hazardous Materials*, in press, 2010.

Robert D. Moser, Amal R. Jayapalan, Victor Y. Garas, Kimberly E. Kurtis, "Assessment of binary and ternary blends of metakaolin and Class C fly ash for alkali-silica reaction mitigation in concrete", Cement and Concrete Reserarch, 40, 1664-1672, 2010.

Roland F. Bleszynski and Michael D.A. Thomas, "Microstructural Studies of Alkali-Silica Reaction in Fly Ash Concrete Immersed in Alkaline Solutions", A*dvn Cem Bas Mat*;7:66–78, 1998.

Sahmaran M. Kasap O., Duru K. Yaman IO, "Effect of mix composition and water cement ratio on the sulfate resistance of blended cements", *Cement and concrete composits*, 29,159-167. 2007.

Saikia N.; Kato, S.; Kojima T. "Production of cement clinkers from municipal solid waste incineration (MSWI) fly ash", *Waste Manag*., 27, 1178-1189. 2007.

Saouma, V., and Y.P. Xi, "Literature Review of Alkali Aggregate Reactions in Concrete Dams", *Report CU/SA-XI-2004/001*, Department of Civil, Environmental, & Architectural Engineering, University of Colorado, Boulder, Colo., United States, 2004.

Shayan, A. and G., "Quick Microstructure and Composition of AAR Products in Conventional Standard and New Acclerated Testing", *8th International Symposium of Alkali Aggregate Reaction in Concrete*, Hyoto, Japan. 1989.

Shehata M.H., Thomas M.D., "A Use of ternary blends containing silica fume and fly ash to suppress expansion due to alkali-silica reaction in concrete", Cem. Concr. Res. 32, 3341–349, 2002.

Shehata M.H., Thomas M.D.A., "The effect of fly ash composition on the expansion of concrete due to alkali-silica reaction", *Cem. Concr. Res.* 30,1063–1072, 2000.

Shi C., Qian J. "Increasing coal fly ash use in cement and concrete through chemical activation of reactivity of fly ash". *Energy Sources*; 25:617–28, 2003.

ShimodaT. & Yokoyama S. "Eco-cement: A New Portland Cement To Solve Municipal And Industrial Waste Problems" *Proceedings of International Congresson Creating with Concrete University of Dundee,* (ed. Dhir & Dyer) pp. 17 - 30., 1999.

Siddique R. “Performance characteristics of high-volume Class F fly ash” concrete. *Cem Concr Res* 34:487–93, 2004.

Silva A.S, D. Soares, L. Matos, L. Divet, M. Salta, “Inhibition of ASRand DEF: evaluation of the microstructure of concrete mixes with pozzolanic additions”, *13th Euroseminar on Microscopy Applied to Building Materials*, Ljubljana, Slovenia, 14-18 June 2011,

Silva, A.S. Soares, D. Matos, L. Salta, M.M. Divet, L. Pavoine, A. Candeias, A.E. Mirao, J. “Influence of Mineral Additions in the Inhibition of Delayed Ettringite Formation in Cement based Materials – A Microstructural Characterization”, *Materials Science Forum* Vols. 636-637 pp 1272-1279, 2010.

Sims I. and Nixon P., “RILEM Recommended Test Method AAR-0: Detection of Alkali-Reactivity Potential in Concrete-Outline guide to the use of RILEM methods in assessments of aggregates for potential alkali-reactivity”, *Materials' and Structures / Mat6riaux et Constructions*, 36, 472-479 ,2003.

Singh M, Garg M. “Cementitious binder from fly ash and other industrial Wastes”. *Cem Concr Res*, 29:309–14, 1999.

Singh N.B., Singh V.D., Rai S. “Hydration of bagasse ash-blended Portland cement,”*Cem Concr Res;*30:1485–8 2000.

Singh NB, Singh VD, Rai S, Chaturvedi S, “Effect of lignosulfonate, calcium chloride andtheir mixture on the hydration of RHA-blended Portland cement”, *Cem Concr Res*, 32: 387–392, 2002.

SkalnyJ. GebauerI. Odler (Eds.), “Materials Science of Concrete Special Volume on Calcium Hydroxide in Concrete”, *American Ceramic Society*, Westerville, OH, pp., 69–280, 2001.

Stanislav V. Vassilev, Rosa Menendez, Diego Alvarez, Mercedes Diaz-Somoano and M. Rosa Martinez-Tarazona, “Phase-mineral and chemical composition of coal fly ashes as a basis for their multicomponent utilization. 1. Characterization of feed coals and fly ashes”, *Fuel*, 82(14), 1793-1811,2003.

Stanton T.E., “Influence of cement and aggregate on concrete expansion”, *Eng. News Rec.* February 59–61, 1, 1940.

Steenari B.M., Lindqvist O., “Co-combustion of wood with coal, oil, or peat-fly ash characteristics”. Department of Environmental Inorganic Chemistry, Chalmers University of Technology, Goteborg, Sweden, Report No. ISSN 0366-8746 OCLC 2399559, 1372: 1–10, 1998.

Stratos E., Tavoulareas, “Fluidized-Bed Combustion Technology”, *Annual Review of Energy and the Environment* , 16, 25-57, 1991,

Swamy R.N., “The alkali Silica reaction in Concrete”, Blackie and Sons Ltd, 11, 1992.

Takemoto K., and Uchikawa H., “Hydration of pozzolanic cement”, 7th *International Congress on Chemistry of Cement sub-theme 4*, Principal reports. vol.l,pp 2/2-2/29, Paris, 1980.

Tangchirapat W., Saeting T., Jaturapitakkul C., Kiattikomol K. and Siripanichgorn A., Waste Management**,** 27, pp. 81–88, 2007.

Tarelho, L.A.C., Coelho A.M.S.L., Teixeira, E.R, Rajamma R, Ferreira, V.M., "Characteristics of ashes from two Portuguese biomass co-generation plants", *19th European Biomass Conference and Exhibition (EU BC&E)*, Berlin, Germany June 6-10, 2011,

Tattersall, G.H., Banfill, P.F.G. "The rheology of fresh concrete", Pitman, pp356, 1983.

Thek G., Obernberger I., Hirtenfellner J., "Investigation of woody biomass potentials in selected European countries and their allocation to potential applications for thermal utilisation", P*roceedings of the 14th European Biomass Conference & Exhibition*, October, Paris, France, ETA-Renewable Energies, Italy, 96–99, 2005.

Thomas, M.D.A., Hooton, R.D., Scott, A. and Zibara, H. "The Effect of Supplementary Cementitious Materials on Chloride Binding in Hardened Cement Paste." *Cement and Concrete Research,* In Press, Proof available online, March 2011

Thomas M.D.A., Bleszynski R.F., "The use of silica fume to control expansion due to alkali-aggregate reactivity in concrete—a review", in: S. Mindess, J. Skalny (Eds.), *Materials Science of Concrete VI,* American Ceramics Society, Westerville, OH, 377–434, 2001.

Thomas M.D.A., Folliard K.J, "Concrete aggregates and the durability of concrete", in: C.L. Page, M.M. Page (Eds.), Durability of concrete and cement composites, Woodhead, Cambridge, U.K, pp. 247–281, 2007.

Thomas M.D.A., Nixon P.J., Pettifer, K., "The effect of pulverized fuel ash with a high total alkali content on alkali silica reaction in concrete containing natural U.K. aggregate", *2nd CANMET/ACI International Conference on Durability of Concrete*, Vol. 2, American Concrete Institute, Detroit, 919-940,1991.

Thomas, M.D.A. "Review of the effect of fly ash and slag on alkali-aggregate reaction in concrete." *Building Research Establishment Report*, BR314, Construction Research Communications, Ltd, Watford, U.K, 1996.

Thomas, M.D.A., "The Role of Calcium in Alkali-Silica Reaction," *Material Science of Concrete – The Sydney Diamond Symposium* (edited by M. Cohen, S. Mindess, J. Skalny), American Ceramic Society, Westerville, OH, 325-337, 1998.

Tkaczewska E., Małolepszy J., "Hydration of coal–biomass fly ash cement*" Construction and Building Materials*, 23 (7) 2694-2700, 2009.

Tosun K., Felekoğlu B., and Baradan B., "The effect of cement alkali content on ASR susceptibility of mortars incorporating admixtures", *Building and Environment,* 42(9), 3444-3453, 2007.

Tsimas S., "Incorporation of CCPs in Cement and Concrete:the Hellenic Case", *Second international coference on sustainable construction materials and technologies*, Ancona, Italy 28-30, 2010.

Tsimas S., Vardaka G., Zervaki M,, "Composing cement raw mix by using fly and bottom high calcium ashes", *EuroCoalAsh*, Warsaw, 73-84, 2008.

Tsuneki Ichikawa, "Alkali–silica reaction, pessimum effects and pozzolanic effect", *Cement and Concrete Research*, 39(8) , 716-726, 2009.

Ubbriaco P., Calabrese D., "Hydration behavior of mixtures of cement and fly ash with high sulfate and chloride content". *J. Therm. Anal. Calorim.*, 61, 615-623, 2000.

Udoeyo F,F,, Inyang H,, Young D,T,, Oparadu E.E., "Potential of wood waste ash as an additive in concrete", *Journal of Materials in Civil Engineering* 18 (4): 605–611, 2006.

Van Dam J. et al- "Biomass production potentials and biofuel trade options of Central and Eastern Europe under different scenarios", *Proceedings of the 14th European Biomass Conference & Exhibition*, October, Paris, France, ETA-Renewable Energies, Italy, pp100–103,2005.

Velosa A.L. and Veiga R., "The use of pozzolans as additives in lime mortars for employment in building rehabilitation, Historical Constructions", P.B. Lourenço, P. Roca (Eds.), Guimarães, 2001.

Velosa A.L., Rocha F. and Veiga R., "Influence of chemical and mineralogical composition of metakaolin on mortars characteristics", *Acta Geodyn. Geomater.,* 6, 121–126, 2009.

Vinod K. Guptaa, C.K. Jainb, Imran Alib, M. Sharmaa, VK. Sainia, "Removal of cadmium and nickel from wastewater using bagasse fly ash—a sugar industry waste", *Water Research*, 37 4038–4044, 2003.

Wang K.S., Lin K.L.,. Lee T.Y. and Tzeng B.Y., "The hydration characteristics when C2S is present in MSWI fly ash slag", *Cement and Concrete Composites*, 26, 323–330, 2004.

Wang S, Baxter L, "Comprehensive study of biomass fly ash in concrete: Strength, microscopy, kinetics and durability", *Fuel Processing Technology*,88(11-12), 1165-1170, 2007.

Wang S., Baxter L., Fonseca F., "Biomass fly ash in concrete: SEM, EDX and ESEM analysis", *Fuel*, 87(3), 372-379, 2008(a).

Wang S., Llamazos E, Baxter L., Fonseca F., "Durability of biomass fly ash concrete: Freezing and thawing and rapid chloride permeability tests", *Fuel*, 87(3), 359-364, 2008(b).

Wang S., Miller A., Llamazos E., Fonseca F, Baxter L., "Biomass fly ash in concrete: Mixture proportioning and mechanical properties", *Fuel*, 87(3) 365-371, 2008(c).

Werther J., Saenger M., Hartge E.U., Ogada T., Z. Siagi, "Combustion of agricultural residues". *Progress in Energy and Combustion Science*, 26, 1-27, 2000.

Wiselogel A.E., Agblevor F.A., Johnson D.K., Deutch S., Fennell J.A., Sanderson M.A., "Compositional changes during storage of large round switchgrass bales". *Bioresour Technol*, 56:103–9, 1996.

Worrell E., Martin N., Price L., "Potentials for Energy Efficiency Improvement in the US Cement Industry", *Energy*, 25, 1189-1214, 2000.

Xu H., Deventer J.S.J., Jannie S.J., "Geopolymerisation of multipleminerals". *Min Eng*; 15:1131–9. 2002.

Xu H., Deventer J.S.J., "The geopolymerisation of alumino-silicateminerals". *Int J Miner Process*, 59,247–66, 2000.

Yeoh A.K., Bidin R., Chong C.N., Tay C.Y., "The relationship between temperature and duration of burning of rice-husk in the development of amorphous rice-husk ash silica", *Proceedings of UNIDO/ESCAP/ RCTT, Follow-up Meeting on Rice-Husk Ash Cement*, Alor Setar, Malaysia,1979.

Yin C., Rosendahl L.A. Kaer S.K., "Grate-firing of biomass fort heat and power production", *Progress in Energy and Combustion Science,* 34, 725–754, 2008.

Yip C.K., Lukey G.C., Deventer J.S.J., "The coexistence of geopolymeric and calcium silicate hydrate at the early stage of alkaline activation", *Cem. Concr, Res.* 35, pp.1688-1697, 2005.

Yu Q., Sawayama K., Sugita S., Shoya M., Isojima Y., "The reaction between rice-husk ash and $Ca(OH)_2$ solution and the nature of its product.", *Cement and Concrete Research* 29 (1): 37–43. 1999.

Yufen Y., Guosheng G. and Qingru C., "Preparation and characteristics of composite micro-bead particles", *Powder Handling Process* 17 (1), pp. 28–31, 2005.

Zerbino R., Giaccio G. and Isaia G.C., "Concrete incorporating rice-husk ash without processing", *Constr Build Mater,* 25 (1), pp. 371–378, 2011.

Zhang M.H., Lastra R., Malhotra V.M., "Rice-husk ash paste and concrete: some aspects of hydration and the microstructure of the interfacial zone between the aggregate and paste". *Cement and Concrete Research*, 26 (6): 963–977, 1996.

Zhang Y., Wang Z., Xu X., Chen Y., Qi T., "Recovery of heavy metals from electroplating sludge and stainless steel pickle waste liquid by ammonia leaching Method", *J Environ Sci.* China;11(3):381–4, 1999.

Zhang, M.H., Malhotra V.M., "High-Performance Concrete Incorporating Rice Husk Ash as a supplementary Cementing Materials", *ACI Materials Journal*, 93(6), 629-636,1996.

Online sources

Bushnell, D. J, Haluzok, C, Dadkhan-Nikoo, A. Biomass fuel characterisation: testing and evaluating the combustion characteristics of selected biomass fuels, Oregon, Departmnt of mechanical engineering, University of Oregon.

Feuerborn, H. J. "Coal ash utilization over the world and in Europe". www.coal-ash.co.il/sadna/ Abstract, Feuerborn.pdf , January, 2009.

Food and Agriculture Organization of the United Nations. World paddy production. 2008. Available http://www.fao.org/newsroom/en/news/2008/1000820/index.html.

HRC, Coal fly ash, Turner Fairbank, Highway Research cCentre, U. S. Department of transportation (US DOT). http://www.alf-cemind.com/cd/AF_and_ARM_fly_ash.htm

Jochen Stark, Katrin Bollmann, Delayed Ettringite Formation in Concrete, Bauhaus-University Weimar / Germany.http://www.faggruppeba.no/ikbViewer/Content/738949/doc-23-2.pdf

Nicolas Müller & Jochen Harnisch, Ecofys Germany GmbH, Nürnberg– Germany.(2007) "How to Turn Around the Trend of Cement Related Emissions in the Developing World. Report prepared for the WWF–Lafarge Conservation Partnership."(online)

TecEco Pty. Ltd. (TecEco), Eco-Cement. http://www.tececo.com/simple.eco-cement.php. TecEco Pty. Ltd., Tasmania, Australia. 2009.

Tracking industrial Energy efficiency and CO_2 emissions. OECD/IEA, 2007.

WBCSD,The Cement Sustainability Initiative Progress Report, June www.WBCSD.org. ,2005.

www.flyashaustralia.com.au/WhatIsFlyash.aspx

http://www.flyash.info

http://wwf.panda.org/about_our_earth/all_publications/?151621/A-blueprint-for-a-climate-friendly-cement-industry

Annex 1. Chapelle test calculations

Definition:

- V1 (ml) is the volume of 0,1N HCl necessary for the 25 ml of solution obtained by the blank sample
- V2 (ml) is the volume of 0,1N HCl necessary for the 25 ml of solution obtained by the reaction of the metakaolin

The titration reaction is:

$CaO + 2HCl \rightarrow CaCl_2 + H_2O$
$Ca(OH)_2 + 2\ HCl \rightarrow CaCl_2 + H2O$
Check of the blank reaction

56/2 x V1 must be under 1000 (blank solution value V1= 32.5 ml of HCl)

Trial with fly ash :

$$\text{Mg of } Ca(OH)_2 \text{ fixed} = 2 \times \frac{V1 - V2}{V1} \times \frac{74}{56} \times 1000$$

Results

The results are expressed in mg $Ca(OH)_2$ fixed by biomass flyash

Trial	Sample	HCL V2	Average V2	Ca(OH)2 fixing mg/g
1	BFA1	25.1	25.3	601.3
2	BFA1	25.5		
3	BFA2	23.8	23.9	718.2
4	BFA2	24.0		

Annex 2. Leaching test results by ICP. MS method

The ashes were dried to remove the moisture before the experiment, $W_{ES}=W_{ET}$

V_1=0.7 L, V_2= 1.19L,

	BFA1 as received			mg/Kg)		
		ß1	ß2	$W_{ES1(}$	W_{ES2}	Total W_{ES}
Ca(mg/L)	mg/L	1030	150	7210	1785	8995
K mg/L)	mg/L	1510	329	10570	3915.1	14485.1
Na mg/L)	mg/L	164	37.9	1148	451.01	1599.01
Si mg/L)	mg/L	0.74	10.4	5.18	123.76	128.94
Mg (µg/L)	µg/L	0	384	0	4569.6	4.5696
Al(µg/L)	µg/L	58.5	567	409.5	6747.3	7.1568
Fe(µg/L)	µg/L	0	0	0	0	0
Cr(µg/L)	µg/L	95.2	40.7	666.4	484.33	1.15073
Ni,P(µg/L)	µgL	<0.0001	<0.0001		0	0
Cu(µg/L)	µg/L	4.8	3.1	33.6	36.89	0.07049
Zn(µg/L)	µg/L	81.3	14	569.1	166.6	0.7357
As(µg/L)	µg/L	9.9	3	69.3	35.7	0.105
Cd	µg/L	0.14	0	0.98	0	0.00098
Pb	µg/L	165	2.7	1155	32.13	1.18713

V1=0.71L, V2= 1.08L

	BFA2 as received			mg/Kg)		
		ß1	ß2	W_{ES1}	W_{ES2}	W_{ES}
Ca	mg/L	662	846	4634	9136.8	13770.8
K	mg/L	2650	489	18550	5281.2	23831.2
Na	mg/L	2980	572	20860	6177.6	27037.6
Si	mg/L	1.7	0.32	11.9	3.456	15.356
Mg	µg/L	0	0	0	0	0
Al	µg/L	107	0	749	0	0.749
Fe	µg/L	0	0	0	0	0
Cr	µg/L	261	71.4	1827	771.12	2.59812
Fe,Ni, P	µgL	<0.0001	<0.0001			0
Cu	µg/L	4.2	6.3	29.4	68.04	0.09744
Zn	µg/L	23.2	11.4	162.4	123.12	0.28552
As	µg/L	3.9	0	27.3	0	0.0273
Cd	µg/L	0.36	0.11	2.52	1.188	0.003708
Pb	µg/L	24.8	11.9	173.6	128.52	0.30212

V1=0.7L, V2=1.28 L

	BFA1 75microns			mg/Kg)		
		ß1	ß2	W_{ES1}	W_{ES2}	W_{ES}
Ca	mg/L	1430	650	10010	8320	18330
K	mg/L	2210	602	15470	7705.6	23175.6
Na	mg/L	213	58.3	1491	746.24	2237.24
Si	mg/L	0.19	0.62	1.33	7.936	9.266
Mg	µg/L	0	0	0	0	0
Al	µg/L	0	0	0	0	0
Fe	µg/L	0	0	0	0	0
Cr	µg/L	127	52.4	889	670.72	1.55972
Ni,P	µgL	<0.0001	<0.0001			
Cu	µg/L	9.6	4.1	67.2	52.48	0.11968
Zn	µg/L	199	33.7	1393	431.36	1.82436
As	µg/L	12.1	4.1	84.7	52.48	0.13718
Cd	µg/L	0.19	0	1.33	0	0.00133
Pb	µg/L	555	150	3885	1920	5.805

V1=0.7 L,V2=1.24 L

	BFA2 75microns			mg/Kg)		
		ß1	ß2	W_{ES1}	W_{ES2}	W_{ES}
Ca	mg/L	603	699	4221	8667.6	12888.6
K	mg/L	3200	859	22400	10651.6	33051.6
Na	mg/L	3450	972	24150	12052.8	36202.8
Si	mg/L	0.66	0.74	4.62	9.176	13.796
Mg	µg/L	0	0	0	0	0
Al	µg/L	28.3	0	198.1	0	0.1981
Fe	µg/L	0	0	0	0	0
Cr	µg/L	330	109	2310	1351.6	3.6616
Fe,Ni, P	µgL	<0.0001	<0.0001	0	0	0
Cu	µg/L	7.1	19.7	49.7	244.28	0.29398
Zn	µg/L	14.9	15	104.3	186	0.2903
As	µg/L	4.5	0	31.5	0	0.0315
Cd	µg/L	0.21	0.26	1.47	3.224	0.004694
Pb	µg/L	33.7	14.1	235.9	174.84	0.41074

V1=0.7 L, V2=1.18 L

BFA1 washed (B2)						
		ß1	ß2	W_{ES1}	W_{ES2}	W_{ES}
Ca	mg/L	25.1	22	175.7	259.6	435.3
K	mg/L	71.2	35.5	498.4	418.9	917.3
Na	mg/L	21.4	10.1	149.8	119.18	268.98
Si	mg/L	27.3	19.3	191.1	227.74	418.84
Mg	µg/L	691	1550	4837	18290	23.127
Al	µg/L	215	158	1505	1864.4	3.3694
Fe	µg/L	0	0	0	0	0
Cr	µg/L	11.4	0	79.8	0	0.0798
Ni	µgL	0	0	0	0	0
Cu	µg/L	3.8	69.2	26.6	816.56	0.84316
Zn	µg/L	23.7	69.2	165.9	816.56	0.98246
As	µg/L	12.5	13.9	87.5	164.02	0.25152
Cd	µg/L	14	0	98	0	0.098
Pb	µg/L	13	11.8	91	139.24	0.23024

V1=0.7L, V2=1.24 L

BFA2 washed B2						
		ß1	ß2	W_{ES1}	W_{ES2}	W_{ES}
Ca	mg/L	69.6	35	487.2	435.4	922.6
K	mg/L	61.5	31.9	430.5	396.836	827.336
Na	mg/L	147	58.6	1029	728.984	1757.984
Si	mg/L	3.6	54	25.2	671.76	696.96
Mg	µg/L	268	274	1876	3408.56	5.28456
Al	µg/L	4640	3250	32480	40430	72.91
Fe	µg/L	0	0	0	0	0
Cr	µg/L	15	7.2	105	89.568	0.194568
Ni	µgL	<0.001	<0.0001	#VALUE!	#VALUE!	#VALUE!
Cu	µg/L	6	0	42	0	0.042
Zn	µg/L	11.9	13.9	83.3	172.916	0.256216
As	µg/L	0	0	0	0	0
Cd	µg/L	0	0	0	0	0
Pb	µg/L	32	0.42	224	5.2248	0.229225

Annex 3 Mehanical strength of biomass metakaoin mortars

Among the prepared compositions of the biomass fly ash metakaolin blended mortars, the 10% metakaolin cement mortar gave the maximum spread diameter value among the combination (Table 1). But it was observed that the blending of metakaolin with biomass fly ashes were more rigid and showed a lower flow table spread values despite of the addition of 1% superplasticizer. When 10% metakaolin substituted cement mortars showed a spread value of 160mm diameter, the biomass blended metakaolin mortars showed a spread value of 120 mm for 15 strokes. The diversity in the particle sizes and shapes of the metakaolin and biomass fly ashes can be the reason for the lesser workability.

Table 1 Mixture proportions for the biomass fly ash –metakaolin blended mortars w/b = 0.55. SP = 1%. Binder Aggregate ratio = 1:3

Sample Code	*Composition*	*Consistency (mm)*	*Fresh Density (g/cm^3)*
10MK	10 % MK+90% CEM	160	2. 21
$10BFA_1$+10MK	10% BFA1+10% MK+80% CEM type 1	140	2.30
$20BFA_1$+10MK	20% BFA1+10% MK+70% CEM type 1	120	2.25
$10BFA_2$+10MK	10% BFA2+10% MK+80% CEM type 1	120	2.21
$20BFA_2$+10MK	20% BFA2+10% MK+70% CEM	120	2.23

It can be inferred from this data that substitution of even 20% biomass fly ash along with a minimal amount of metakaolin retains the mechanical properties of the cement mortars with 100% efficiency. The mechanical strength was reduced with the increase in the content of the biomass fly ashes due to its relatively lesser binding effect, but not lesser than the reference cement mortar made of type I 42.5R, Portland cement. However these results are a clear indication for the scope of the use of biomass fly ashes in higher quantities as partial filler and binder when used with a minimum amount of highly reactive materials.

.

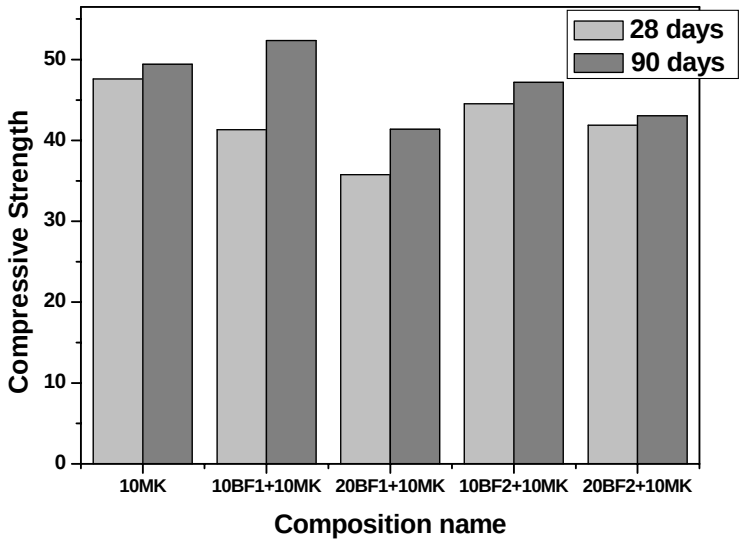

Figure 1. Compressive strength properties of biomass fly ash-metakaolin cement mortars after 28 days of curing at 100% RH

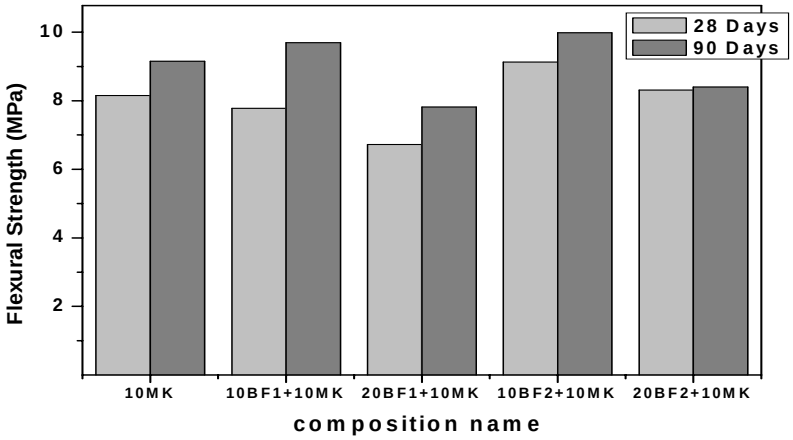

Figure 2 Flexural strength properties of biomass fly ash-metakaolin cement mortars after 28 days of curing at 100% RH

Appendix A. Standards

ASTM D5550 -06 Standard Test Method for Specific Gravity of Soil Solids by Gas Pycnometer

(ASTM) C-125. Standard terminology relating to concrete and concrete aggregates; American Society for Testing and Materials 2007.

ASTM C618 - 08 Standard Specification for Coal Fly Ash and Raw or Calcined Natural Pozzolan for Use in Concrete". ASTM International. 2008.

ASTM, C 1260 - Standard Test Method for Potential Alkali Reactivity of Aggregates (Mortar-Bar Method), American Society for Testing and Materials, West Conshohocken, PA, 2001.

ASTM, C 1293 - Standard Test Method for Determination of Length Change of Concrete Due to Alkali-Silica Reaction, American Society for Testing and Materials, West Conshohocken, PA, 2001.

ASTM, C 1567 - Standard Test Method for Determining the Potential Alkali-Silica Reactivity of Combination of Cementitious Materials and Aggregates (Accelerated Mortar BarMethod), American Society for Testing and Materials, West Conshohocken, PA, 2008.

ASTM) C-311, Standard test methods for sampling and testing fly ash or natural pozzolans for use in Portland-cement concrete; 2005.

British Standard (BS) 3892. Pulverised-fuel ash. Part 1: specification for pulverised fuel ash for use with Portland cement; 1997.

British Standard Euronorm (BS EN) 196. Methods of testing cement. Part 5: pozzolanicity test for pozzolanic cement; 2005.

CEN/TS 15290, Solid bio fuels- Determination of major elements.

CEN/TS 14775. Solid bio fuels, Methods for the determination of ash content.

CHLORIDE, 4500-Cl-; Argentometric Method, Standard Methods Committee, (1997)

DIN 38414-S4, German standard method for the examination of water, waste water and sludge-sludge and sediments (group S)- Determination of leachability by water (S4), 1984.

EN 197-1 (2000): “Cement - Part 1: Composition, specifications and conformity criteria for common cements.”,2000.
EN 450 European Standard for Fly Ash, 2007.

EN 1015-3. Methods of test for mortar for masonry-Part 3, Determination of consistence of fresh mortar (by flow table). 1999.

EN 1015-6, Methods of test for mortar for masonry, Part 6: Determination of bulk density of fresh mortar. 1998.

EN 196 Methods of testing cement .Part 3: Determination of setting times and soundness.

EN 1015-11, Methods of test for mortar for masonary - Part 11: Determination of flexural and compressive strength of hardened mortar,1999.

NF P 18-513, Annexe A Metakaolin - measuring the total quantity of fixed Calcium Hydroxide (Chapelle test modified), 2009.

RILEM Recommended Test Method AAR-3 (formerly TC-106-03) (2000), Detection of potential alkali-reactivity of aggregates: B - Method for aggregate combinations using concrete prisms. Materials & Structures (33): 290-293, 2000.

RILEM Recommended Test Method AAR-4 (2007): Detection of Potential Alkali-Reactivity - 60°C Accelerated Method for Testing Aggregate Combinations using Concrete Prisms -Committee Document RILEM/TC-ARP/06/15, 2007.

SULFATE, 4500-SO4-2; Gravimetric Method with Ignition of residue, Standard Methods Committee, 1997.

LST EN 934-2:2003, Admixtures for concrete and mortar.

Appendix B Acronyms

AAR- Alkali Aggregate Reaction
AMBT- Accelerated Mortar Bar Test
ASTM International, formerly American Society for Testing and materials
ASR Alkali Silica Reaction
BFA- Biomass Fly Ash
BFB Bubbling Fluidised Bed
Class C -fly ash from low rank coal, typically 50%<SiO2+Al2O3+Fe2O3<70%
Class F . fly ash from high rank coal, typically SiO2+Al2O3+Fe2O3>70%
CPT- Concrete Prism Test
EDX Energy Dispersive Xray
EN- European Norm
ESEM Environmental Scanning Electron Microscopy
ESR External Sulphate Reaction
DTA- Differential Thermal Analysis
ICP Inductively Coupled Plasma
ISR Internal Sulphate Reaction
LOI Loss on Ignition
MK- metakaolin
RILEM International Union of Laboratories and Experts in Construction Materials, Systems and Structures
SEM Scanning Electron Microscopy
SP SuperPlasticizer
TGA Thermo Gravimetric Analysis)
XRF X-Ray Florescence
XRD X-Ray Diffraction
XPS X-Ray Photoelectron Spectroscopy